STUDIES FOR RAIL VEHICLE TRACK STRUCTURES
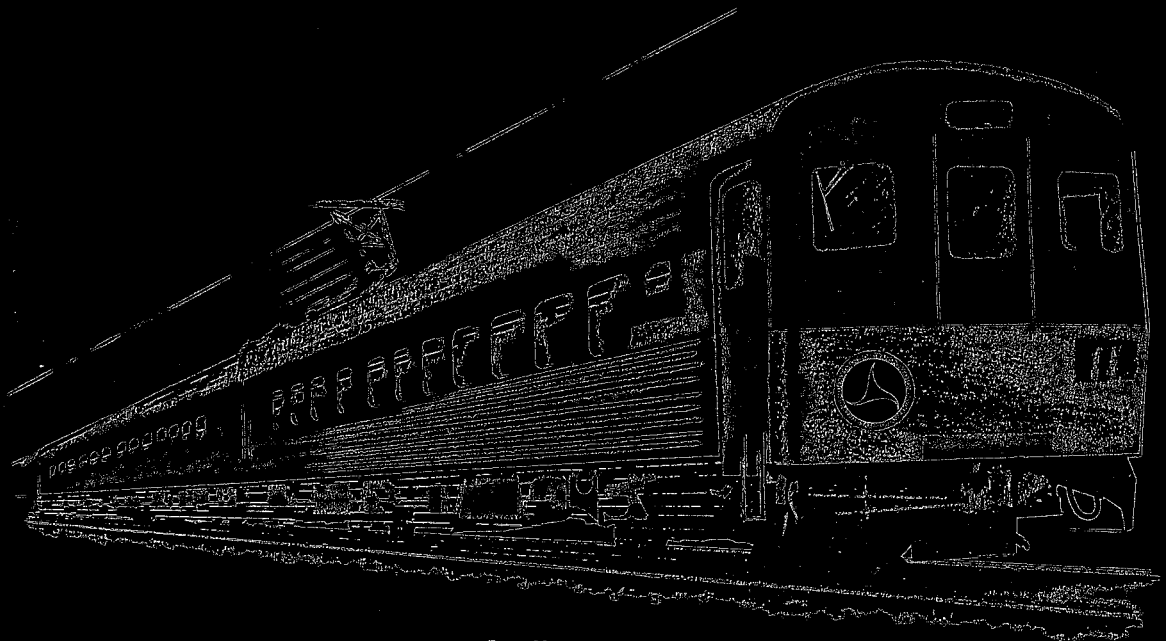
April 1970

FEDERAL RAILROAD ADMINISTRATION
OFFICE OF HIGH SPEED GROUND TRANSPORTATION

1. Report No. FRA-RT-71-45	2. Government Accession No.	3. Recipient's Catalog No.
4. Title and Subtitle Studies for Rail Vehicle Track Structures		5. Report Date April 30, 1970
		6. Performing Organization Code
7. Author(s) H. C. Meacham, R. H. Prause, D. R. Ahlbeck, and J. A. Kasuba		8. Performing Organization Report No. G-9172 Final Report
9. Performing Organization Name and Address Battelle Memorial Institute 505 King Avenue Columbus, Ohio 43201		10. Work Unit No.
		11. Contract or Grant No. Dot-FR-9-0021
12. Sponsoring Agency Name and Address Department of Transportation (FRA) Office of High Speed Ground Transportation 400 7th Street, S. W. Washington, DC 20591		13. Type of Report and Period Covered Final Report for period from Sept. 1966-April 1970
		14. Sponsoring Agency Code

15. Supplementary Notes This report covers Phases I, II, & III of the project. Phases I and II were each covered previously by final reports; therefore, Phase III work is covered in the most detail in this report.

16. Abstract Conventional (tie-type) and non-conventional rail vehicle track structures were studied, with the restriction that standard gage and rail-head contour be used. Computer programs were developed and used to analyze track response to both static and dynamic vehicle loading. The models of conventional track were validated by track, and on the Penn-Central high-speed track near Bowie, Maryland. The DOT research cars were used to obtain a series of controlled-speed passes at speeds up to 125 mph. Track response under Metroliner and regular freight traffic was also recorded, both at a joint and away from a joint. The measurements showed the lack of consistency of track characteristics at different locations and at different times, and indicated the computer results to be as accurate as the degree to which track parameters could be defined. The predicted presence of individual pressure pulses for individual axles on trucks with wheelbases exceeding 6' was verified by measured subgrade pressures 3' beneath the tie base, at speeds up to 125 mph.

A major philosophy in the development of improved track structures was to reduce the magnitude and number of pressure cycles transmitted into the roadbed, with the number of cycles reduced by using beam and slab type rail supports having substantial longitudinal bending stiffness. Following the analysis, performance specifications were written for rail fasteners and three types of reinforced concrete structures recommended for further evaluation in field tests: cast-in-place slab, cast-in-place twin beams, and precast twin beams.

17. Key Words track structures, concrete beams and slabs, rail fasteners, vehicle dynamics, track-structure dynamics, vehicle-track interaction, analog and digital computer studies, track costs, lateral track char.	18. Distribution Statement Availability is unlimited. Document may be released to the Clearinghouse for Federal Scientific and Technical Information, Springfield, VA 22151, for sale to the public	
19. Security Classif. (of this report)	20. Security Classif. (of this page)	21. No. of Pages	22. Price $3.00

Form DOT F 1700.7 (8-69)

ACKNOWLEDGEMENT

TABLE OF CONTENTS

TABLE OF CONTENTS

LIST OF TABLES

TABLE OF CONTENTS

LIST OF TABLES (Continued)

LIST OF FIGURES

TABLE OF CONTENTS

LIST OF FIGURES (Continued)

TABLE OF CONTENTS

LIST OF FIGURES (Continued)

STUDIES FOR RAIL VEHICLE TRACK STRUCTURES

by

H. C. Meacham, R. H. Prause,
D. R. Ahlbeck, and J. A. Kasuba

July 15, 1970

INTRODUCTION

In the fall of 1966, Battelle was awarded a contract for a study
of new track structure designs. The objective of this study was to generate
new ideas and designs for railroad truck structures which could (1) provide
an inherently more stable ride for a train, and/or (2) be more easily and
economically installed or maintained in alignment than existing track struc-
ture designs. The only design limitations were that standard gage and rail
head contour be maintained.

This study was completed in spring of 1967, and is now referred to
as Phase I. Phase II, a continuation of research relating to track struc-
ture analysis and development, covered the time period from November, 1967
to February, 1968. This phase included additional analyses of conventional
tie-type track structures, and more detailed studies of existing fasteners
designed mainly for concrete tie application.

Phase III was a further extension of this research program, cover-
ing the time period from September, 1969 to February, 1970. Emphasis during
the Phase III research was placed on validation of the computer programs
developed during the previous two phases, and on writing performance or
functional specifications for non-conventional track structures to be
included in a proposed DOT-Santa Fe test track somewhere in the Southwest.

Although separate summary reports were published for both the
Phase I and Phase II studies[1,2]*, DOT requested that the summary report

---

* Numbers refer to references listed in the back of this report.

written at the end of the Phase III research program be a comprehensive
document covering all three phases of the track study. Therefore, this
report covers all three phases of the study, although the Phase III work
is covered in more detail.

SUMMARY AND CONCLUSIONS

Early in this study of track structures, it was concluded that
a more stable track structure could be obtained by changing the "pressure
signature" of the track elements bearing on the ballast or subgrade. A
conventional track is very flexible longitudinally--having only the rail
itself to provide bending stiffness. Also, with conventional track, the
bearing area is only a portion of the tie base area, as the ballast usually
is purposely tamped to prevent "center-binding" which can cause tie breakage.
The net result is that cyclic pressures of relatively high magnitudes are
exerted on the ballast/subgrade support, and as speeds and loads of rail
traffic increase, the roadbed is unable to maintain dimensional stability.

In the Phase I studies of new designs, then, emphasis was placed
on those structures which would produce not only lower pressure pulses,
but fewer pulses as well. This was based on studies using passenger-type
vehicles, considering the Northeast Corridor as the most likely area of
application for nonconventional track structures. A "soil deterioration
factor" was defined, based on the settlement of soil under cyclic loading,
and this was used to define track structures that would support 160 mph
traffic with no greater roadbed settlement than conventional tie-type
structures with 60 mph traffic. These track structures were longitudinal
beam and slab type structures, constructed of steel or steel-reinforced
concrete.

An important component of such structures is the rail fastener
which supports the rail and is supported, in turn, by the beams or slabs.
Therefore, considerable analysis effort was devoted to fastener requirements,
particularly the effect of resilience in the fastener. The analysis included

2

an analog computer simulation in which the dynamic characteristics of the track structure as well as the vehicle were included. The conclusion drawn from this analysis was that wheel-rail impact loads generated by the inevitable imperfections in both rail profile and vehicle components can be greatly reduced by providing resilience in the rail support. Also, to minimize construction and maintenance costs, it was considered mandatory to include vertical and lateral adjustment capabilities in the fasteners themselves.

At the end of Phase I, then, four specific nonconventional track structures were recommended for serious consideration. Three nonconventional rail and fastener designs were included, though their use with the structures was not necessary. Being of relatively massive construction, (for example, twin beams each approximately 2 feet square in cross-section) the estimated initial costs of the four structures ranged from $385,000 to $514,000 per single track mile.

The Phase II studies covered various types of tie-type track, three types of longitudinal track structures, and a study of existing rail fasteners designed mostly for concrete ties. It was shown that the tie bearing area is a very important parameter, as the bearing pressures are nearly directly proportional to the bearing area per length of track. Any increase in stability expected from the use of concrete ties, with their larger bearing areas, can be lost if tie spacing is excessive. However, if bearing area per length is increased, the track structure becomes stiffer and impact loads will increase unless resilient rail pads are used. In the fastener analysis, it was also shown that a consistent clamping force on the rail is desirable, and that this objective is better achieved with typical foreign rail clips having lower spring rates, than with the relatively stiff clips normally used in domestic installations. A computer analysis of a particular clip, the English Pandrol, showed the potential of computer programs for analyzing rail fasteners; excellent correlation of computer and measured load-deflection characteristics were obtained for this complex three-dimensional clip.

3

The static load analysis of the longitudinal beam-type structures showed that the effects of joints in an otherwise continuous beam was surprisingly small, although a definite relative motion at the ends of adjacent beams occurred as the wheel passed over. The fact that longitudinal beams and slabs reduce direct bearing pressures significantly was again shown in the analysis of three other structures of this type.

Even more interesting were the results of the Phase III study, as this phase included field measurements of the track response on the C&O/B&O mainline track near Columbus, Ohio, and on the Penn Central-DOT high-speed track running between Washington, D.C., and New York City. In addition to controlled speed runs of the DOT test cars at speeds from 15-135 mph, track response was also measured under normal freight and passenger traffic, the latter including several Metroliners at speeds up to 115 mph. The measurement of a 33,000-pound individual tie plate load under a freight locomotive going over a newly-tamped tie, or a rail acceleration of 347 g's at a joint as a 115-mph Metroliner passed over, were extremely interesting, as was the verification that pressure pulses were transmitted by individual axles to the subgrade pressure cells buried three feet below the base of the tie.

However, perhaps the most important point emphasized by the measurements (and also by the computer studies) was that there is no such thing as a standard track to be used as a reference. This does not mean, however, that computer simulations or other analyses which assume some degree of uniformity in the physical systems cannot be used to advantage. On the contrary, the measurements showed that the computer programs which were developed and refined throughout the study produced results quite similar to those recorded. In the case of rail joints, the absence of the rail gap (5/8-inch) in the computer program was sufficient to change the response noticeably. However, now that this is known, it can be modified accordingly.

Throughout the Phase III program, the main emphasis was on the writing of performance specifications for nonconventional track sections, and associated rail fasteners. In a sense, then, the results of the track

4

structure study are included in the four sets of specifications included as Appendices to this report. These cover rail fasteners and reinforced concrete track structures of three types--precast twin beam, cast-in-place twin beam, and cast-in-place slab. The specification of bending stiffness was based on the Phase III studies devoted to reducing the cost of the track structures of the type suggested during Phase I, without seriously downgrading their stability. The success of these efforts can be judged only when structures are designed according to these specifications and tested in a field installation such as the proposed DOT-Santa Fe test track.

TECHNICAL WORK

Analysis of Conventional Tie-Type Structures

The basic function of any track structure is to support and guide trains. In order to perform this function, the track structure must withstand repeated vertical, lateral, and longitudinal loads which are developed at the wheel-rail interface during train passage. In addition to these loads imposed by the wheels, the track structures must withstand thermal expansion and contraction forces which act on it continuously.

The need for advanced track structures comes about because conventional tie-type track and roadbed deteriorate under the action of these loads. The definition of an advanced track structure, then, is one that is more stable, meaning it can withstand these loads for longer periods of time with less deterioration of vertical profile and lateral alignment.

To obtain more insight into the problems with conventional tie-type track, and to provide reference points for evaluating advanced track structures, an analysis of conventional track was undertaken as the first step of the research. During the Phase I concept study, then, an abbreviated force and stress analysis of conventional track was made, using a representation of the track structure as a continuous beam on an elastic foundation.

5

Calculations were made to determine forces imposed on the rail structure by a 180,000 pound passenger car (22,500 pound wheel load) representing the Budd cars ordered for the Northeast Corridor Demonstration. Of particular interest were the tie bearing pressure and ballast-subgrade dynamic pressures, since the ballast-subgrade support was assumed to be the "weak link" in the track structure, moving and shifting under the influence of the cyclic pressures produced by wheel loads. An approximation of the time-varying pressure at a point in the ballast directly beneath a tie is shown in Figure 1. The pressure increases to some maximum value as a wheel approaches and then decreases after the wheel has passed--this pattern being repeated for every wheel in the train. The frequency at which this rise and fall of pressure occurs is, of course, directly proportional to the train speed; at high train speeds the frequency of soil pressure cycles is proportionately higher.

The typical pressure curve shown in Figure 1 is quite fundamental to the development of advanced track structures. Consideration of this "pressure signature" indicated the importance of studying the ballast-subgrade properties under dynamic--rather than static--applied loads; it also led to the realization that the stability of the roadbed would be improved by reducing not only the pressure amplitudes, but also the number of pressure cycles.

Development of Mathematical Models

To facilitate the analysis of conventional tie-type structures, a more detailed model of the track structure was developed, with the end objective being a realistic representation of typical track structures. What was required was a procedure for converting track parameters--such as weight of rail, tie spacing and type, ballast depth and type, etc.--into mathematical models which could be used to determine track response to both static and dynamic loads.

6

90-ton car
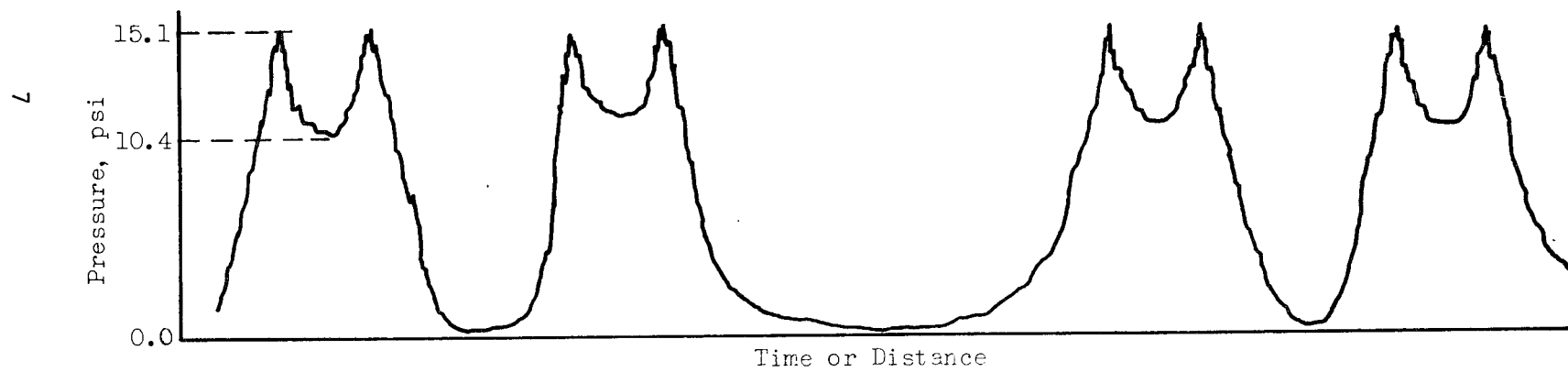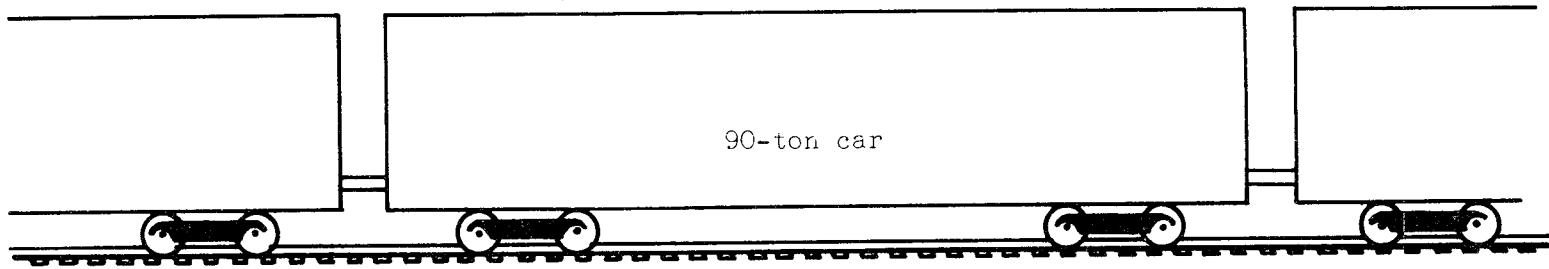
FIGURE 1.   TYPICAL DYNAMIC PRESSURE CURVE FOR PRESSURE DIRECTLY
            UNDER A TIE OF A CONVENTIONAL TRACK STRUCTURE

The models of conventional track structure which were developed were based on the classical beam-on-elastic-foundation theory that was originally developed to calculate stresses and deflections of railroad track[3,4]. In this theory the rail deflection y for a single wheel load P at a distance x from the wheel is

$$y = \frac{P}{K_r} e^{-\beta x}(\cos \beta x + \sin \beta x) \tag{1}$$

and the bending moment in the rail is

$$M_R = \frac{-P}{4\beta} e^{-\beta x}(\cos \beta x - \sin \beta x), \tag{2}$$

where K_r is the rail stiffness for a single point load given by

$$K_r = 2K/\beta , \tag{3}$$

$$\beta = (K/4EI)^{1/4} . \tag{4}$$

K is an overall foundation modulus representing a continuous elastic support under the rail, and EI is the rail bending stiffness.

The steps involved in this model development are indicated in Figure 2. For the track structures involving tie-supported track, the support for each tie can be represented as a spring whose spring rate is a function of the ballast and subgrade properties. As the calculation of this ballast-subgrade spring rate is not straightforward, a considerable effort was devoted to the development of a rational method for calculating the overall track stiffness from known properties of the ballast and sub-grade. Unfortunately, the area of soil mechanics is one where precise answers usually cannot be obtained, and this case was no exception.

The first step was to examine various methods of calculating the stiffness of the ballast and subgrade when loaded by a rectangular area such as a railroad tie. Three methods were considered:

8
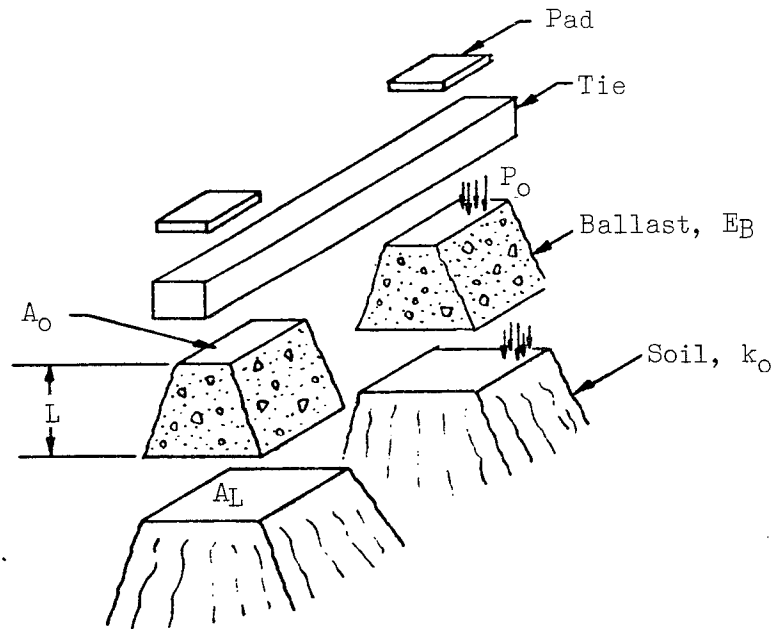
(a) Conventional Track Structure
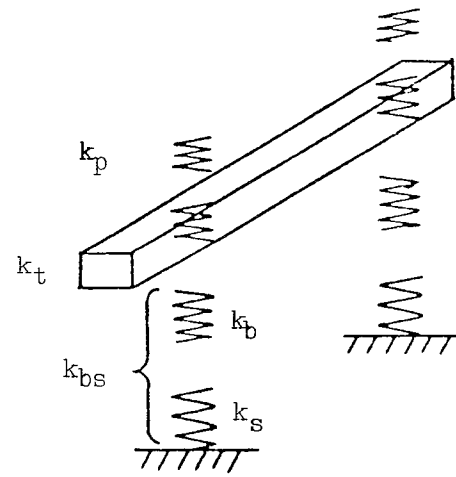
(b) Spring Rates of Track Components
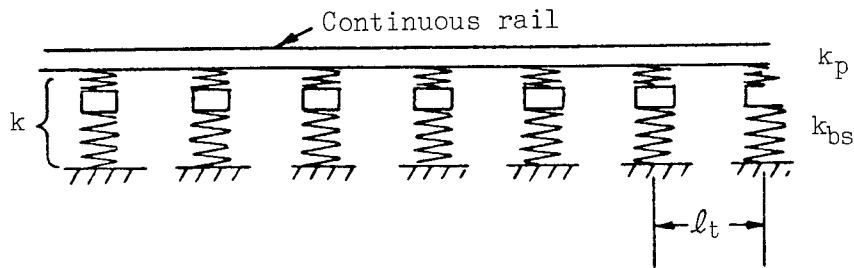
(c) Beam on Continuous Elastic Support
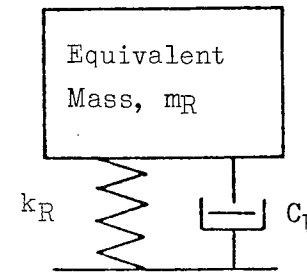
(d) Dynamic Equivalent of Beam on
     a Continuous Elastic Support

FIGURE 2.   PROGRESSIVE STEPS IN THE DEVELOPMENT OF STATIC AND DYNAMIC
            MODELS OF A CONVENTIONAL TRACK STRUCTURE

(1) Boussinesq equations

(2) Elasticity theory for plate loading

(3) Approximate method considering the affected volume of soil to be a pyramid of uniform pressure.

It was concluded that Boussinesq equations are not directly applicable for spring rate calculations because they assume point or line loading and yield infinite deflections under the point of load application. They are mainly useful for calculating stresses or pressures in the vicinity of a localized load.

Elastic theory predicts practically the same spring rates for two ideal cases of area loading: one case gives an average deflection of a uniform pressure-loaded area, and the other gives the uniform deflection under a rigid plate load. The main drawback of these equations is that two layers (ballast and soil) are not easily handled, and calculations based on a single layer yield results which do not agree with actual measured values. Equations accounting for two layers of different homogeneous materials or increasing stiffness with depth are more realistic, but are much too complex to be generally useful.

The pyramid approximation assumes uniform (but different) pressure at every depth to infinity and uniform deflection of the loaded area, and neglects the material outside the pyramid. The equation for stiffness is the same form as that given by the theory of elasticity, but is simpler and can account for two or more layers of different materials. The stiffness of the pyramid is highly dependent on the angle of its sides (the "angle of internal friction" of the soil), which determines the rate at which the load is assumed to spread out as it is transmitted downward (see Figure 2a). With a particular choice of this angle, the stiffness is the same as that predicted from the theory of elasticity; if a steeper angle is chosen, the stiffness will be less.

It was concluded that the pyramid method was the most applicable one. Figure 3 is a plot of the stiffnesses of the soil and ballast calculated by the pyramid method, for a given bearing area 9 in. x 25.5 in.,

10
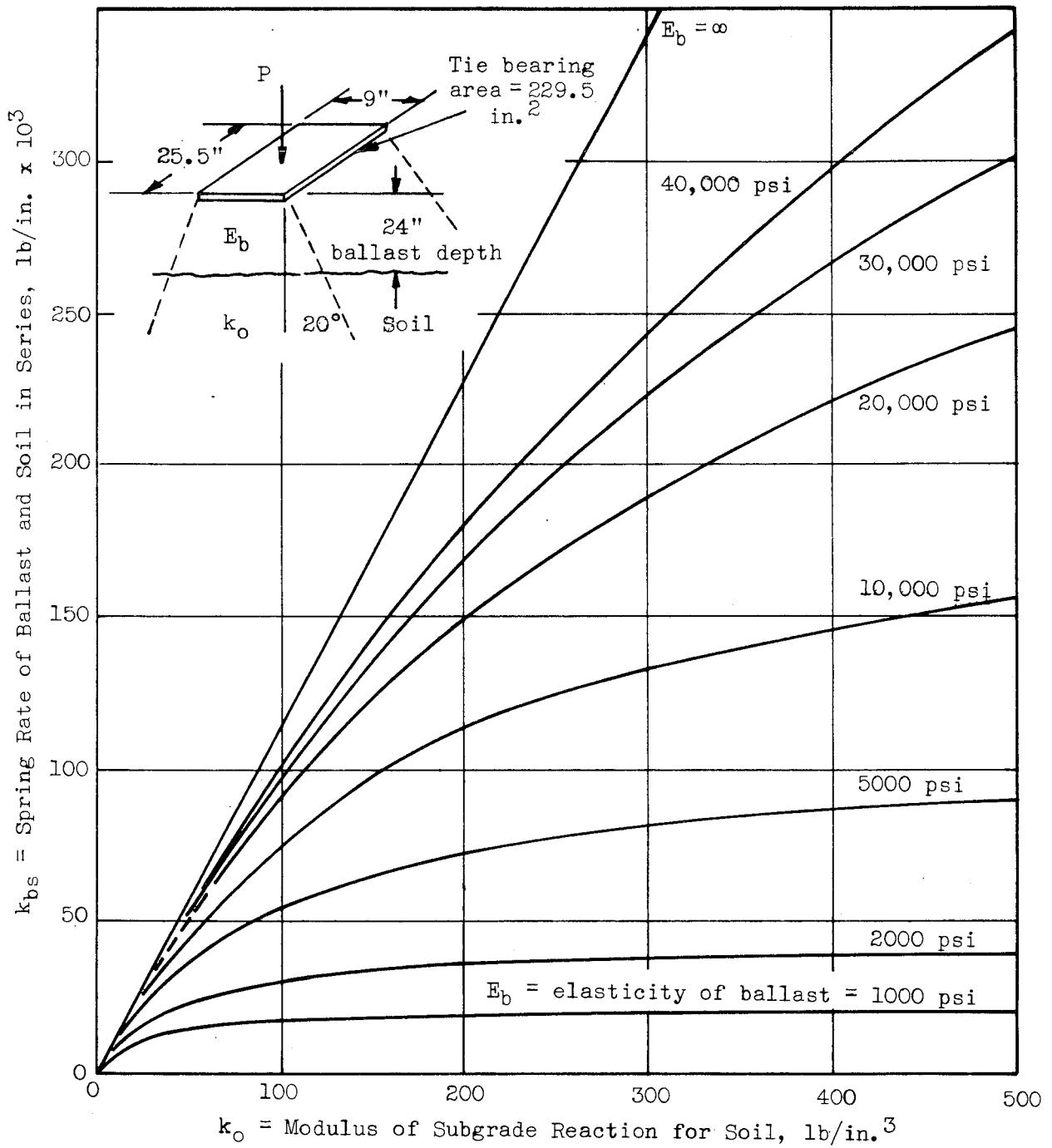
FIGURE 3. OVERALL VERTICAL SPRING RATE OF BALLAST AND SUBGRADE

11

corresponding to a conventional wood tie with half its area acting in bearing. (The spring rate is a function of the shape of the bearing area, as well as its size.) The depth of the ballast was assumed to be 2 feet, and the angle of internal friction was assumed to be 20 degrees. Using values of E_b and k_o in this figure, the overall spring rate of the ballast and soil in series may be found, based on the expression:

$$k_{bs} = \frac{k_b \, k_s}{k_b + k_s} \; .$$

(5)

The most uncertain factor involved in the determination of the overall spring rate is the so-called subgrade modulus of the soil beneath the ballast (k_o). It is affected by the size and shape of the area loaded, the moisture content and the degree of compaction of the soil, as well as the basic material, and so is not truly a material property. In general, however, it varies between 100 and 500 psi/in. for undisturbed earth, and for prepared subgrades such as those beneath new highways and railroads an average value is probably on the order of 150 psi/in. to 200 psi/in. Values of ballast E_b are generally on the order of 20,000 to 40,000 psi.

Values of ballast-soil stiffness obtained from the equation above can then be used in the representation of the track structure as a continuous beam supported on a continuous elastic foundation (Figure 2c). Straight-forward methods are then used to convert this distributed parameter system into a lumped-parameter system necessary for the analog computer representation (Figure 2d).

Considering the load on one rail, the spring rate of the half tie, tie plate, resilient pad, ballast, and soil in series is approximately

$$k = \frac{k_{bs} \, k_p}{k_{bs} + 2k_p} \; .$$

(6)

The factor of 2 is introduced in Equation (2) to account for the continuity of the ballast and soil deflection between adjacent loaded ties[4].

12

This continuity is neglected in the elastic foundation model and experiments indicate that each of the ties supporting a loaded rail is approximately twice as flexible as when it is loaded alone.

Knowing k_{bs}, the overall spring rate (k_R) of a rail supported on a row of these springs (Figure 2a) can be calculated. For example, Figure 4 shows overall spring rates for three different rails and four different tie spacings. The equations used for these calculations are given in Appendix A, and are based on the classical beam-on-elastic-foundation theory.

Response to Static Loading

To determine such factors as overall spring rate, rail stress, ballast pressure under ties, etc., the response of various tie-type track structures to a single wheel load of 22,500 pounds (single axle load of 45,000 pounds) was calculated. These track structures are shown in Figures 5, 6, and 7, and the values which are calculated are shown in Table 1.

Some observations can be made from this table. First, it is seen that the concrete tie track with resilient pads has a greater overall stiffness than the wooden tie track without pads, when the tie spacing is the same. The reason for this is not that the concrete ties themselves are very much stiffer than wooden ones, but that they have a larger bearing area, which results in a higher ballast-soil spring rate. Actually, considering only the ties themselves, a concrete tie with a typical resilient pad is much softer than a bare wooden tie. However, when the ties are placed on the same ballast and soil, the overall spring rate of the concrete-tie structure is higher due to its higher bearing area. The larger bearing area of the concrete tie results, of course, in lower ballast and soil pressures. Rail bending stresses are also lower due to the higher stiffness (and lower rail deflections). Note that this discussion assumes the spacing of wood or concrete ties is the same.

When the tie spacing is increased from 21 inches to 30 inches, the overall stiffness drops because there are fewer ties under the rail; the ballast and soil pressures increase because less total area must carry
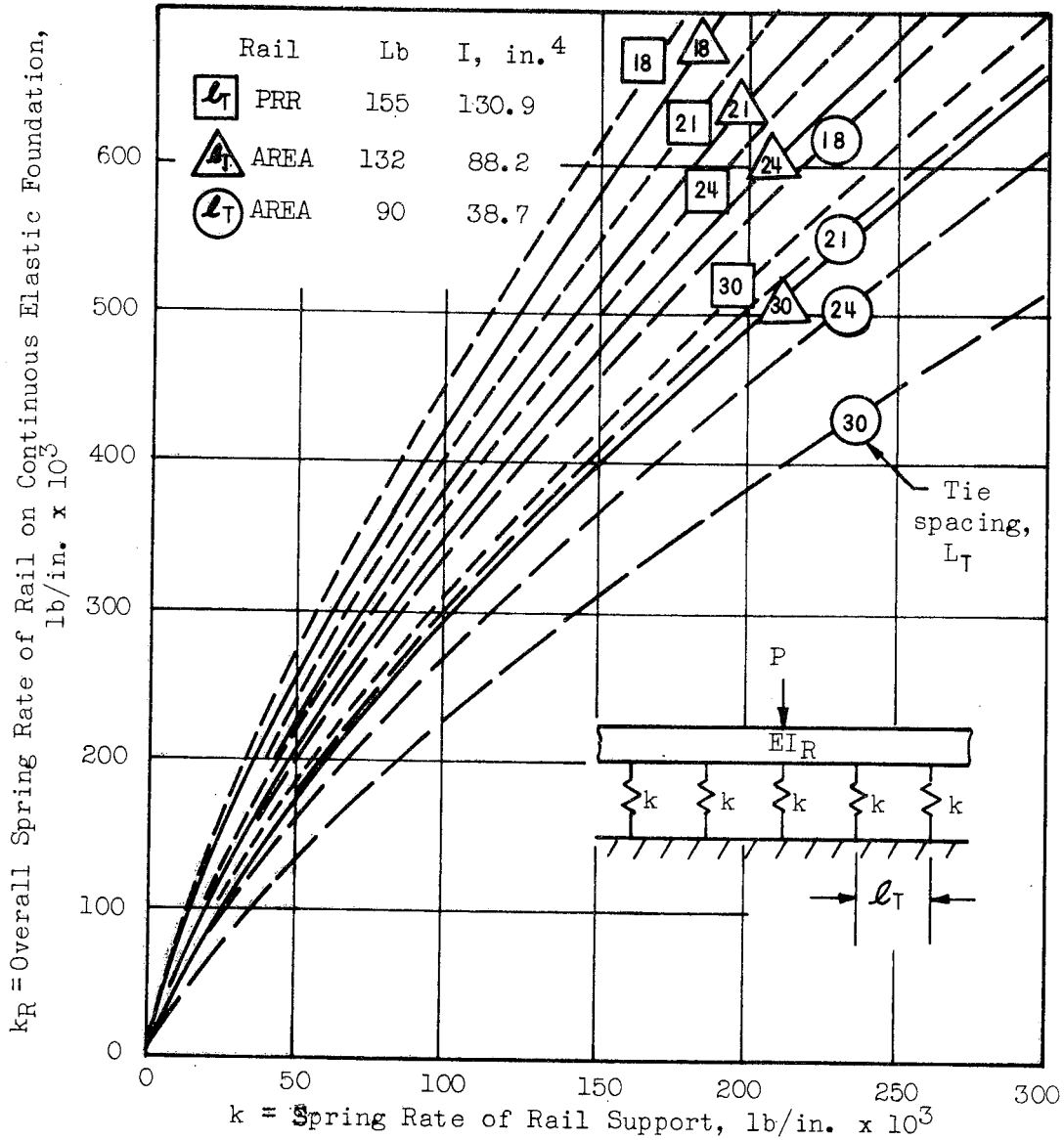
FIGURE 4. TRACK STRUCTURE SPRING RATE AS A FUNCTION OF RAIL, TIE, AND SUBGRADE CHARACTERISTICS

14

4' - 8½"

9" x 7" x 102" wood tie

26"

Bearing Length

2"

21"-30"
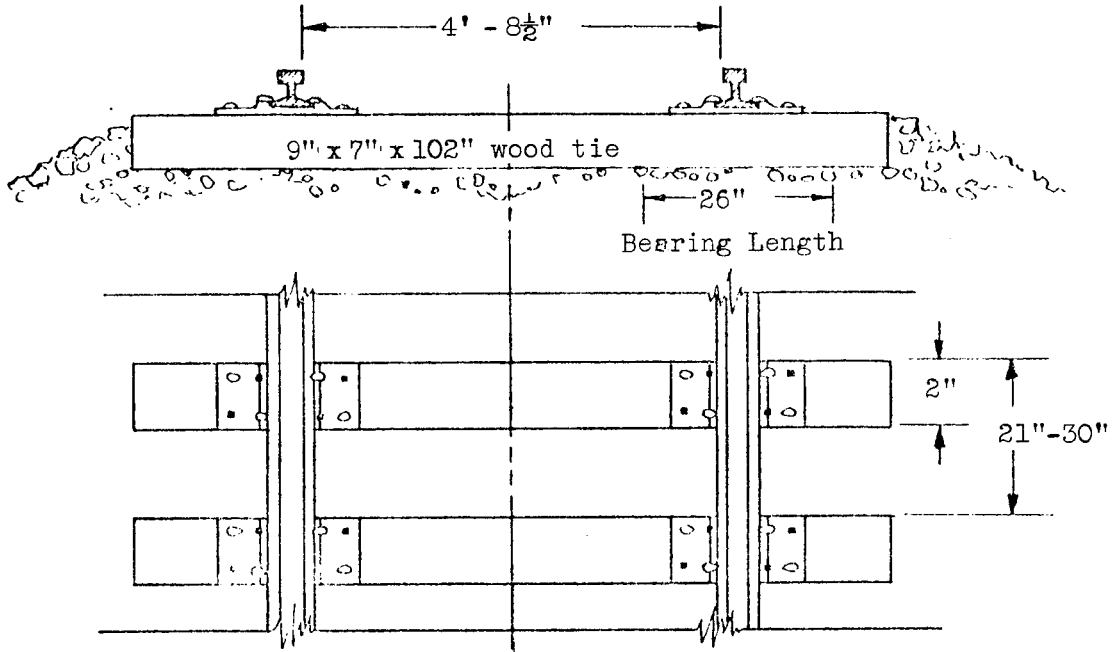
FIGURE 5.   CONVENTIONAL TRACK STRUCTURE WITH WOODEN TIES

8½'

MR-3 concrete tie

33"

Bearing Length

9" 12"

21" - 30"
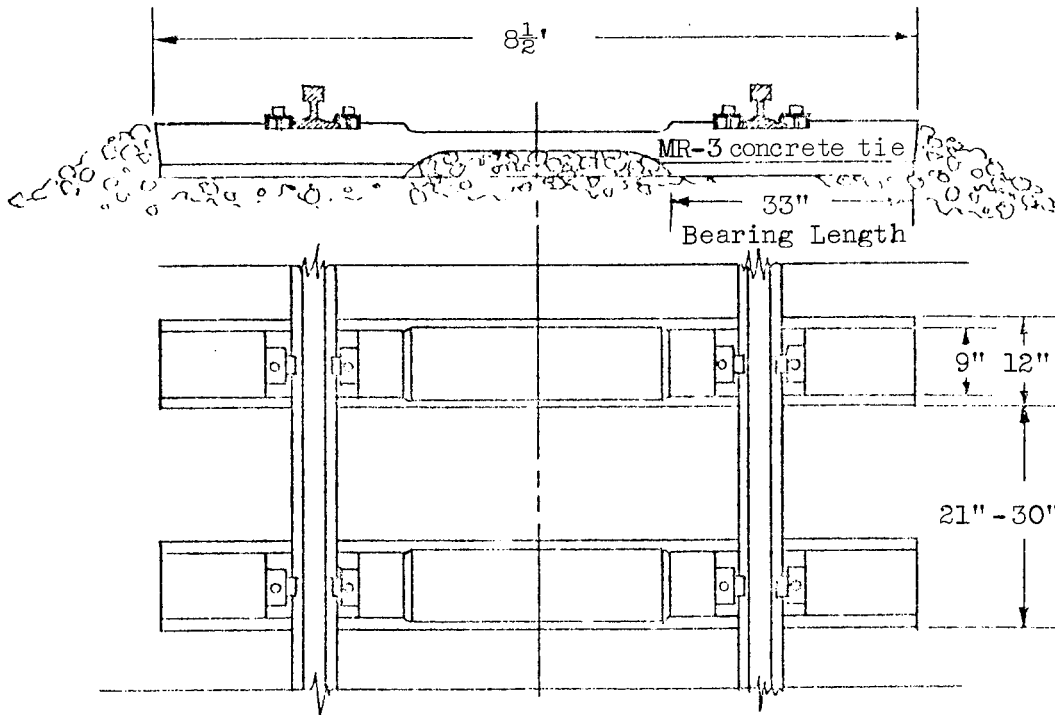
FIGURE 6.   CONVENTIONAL TRACK STRUCTURE WITH CONCRETE TIES
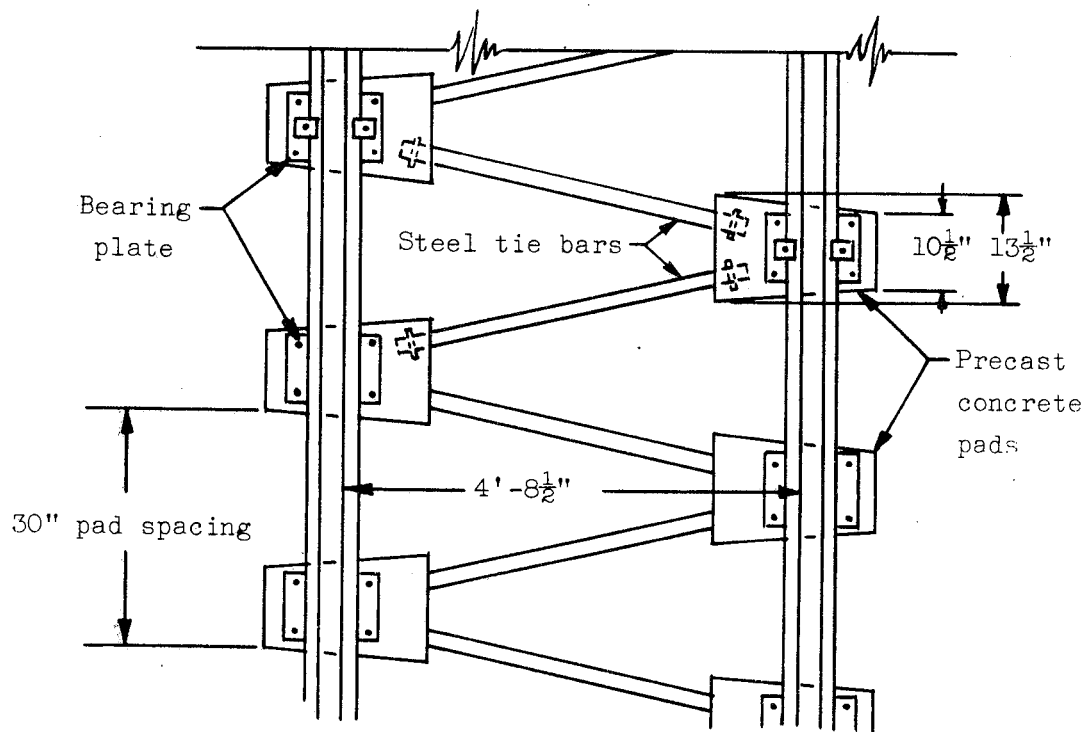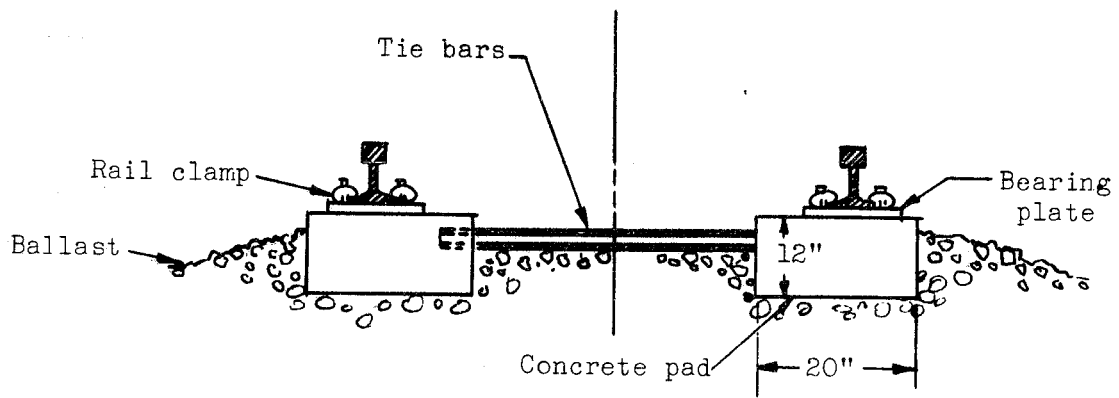
FIGURE 7. DUTCH "ZIG-ZAG" TRACK STRUCTURE

TABLE 1. RESPONSE OF SEVERAL TRACK STRUCTURES TO SINGLE AXLE LOAD*

Description	Pad Stiffness, lb/inch	Tie Spacing, inches	Subgrade Modulus, lb/inch^3	Overall Stiffness, lb/inch	Tie Bearing Pressure, psi	Rail Bending Stress, psi	Subgrade** Pressure, psi
Dutch Zig-Zag	∞	30	100	168,000	27	10,600	5.9
MR-3 Concrete Ties	700,000	30	100	200,000	17.2	10,100	4.6
MR-3 Concrete Ties	∞	30	100	212,000	17.6	9,800	4.7
9" x 7" x 102" Wood Ties	700,000	21	100	215,000	20.8	10,000	4.2
9" x 7" x 102" Wood Ties	∞	21	100	228,000	21.1	10,000	4.2
MR-3 Concrete Ties	700,000	21	100	263,000	13.0	9,300	3.5
MR-3 Concrete Ties	∞	21	100	280,000	13.4	8,500	3.6
MR-3 Concrete Ties	700,000	30	500	415,000	21.4	8,000	5.7
Dutch Zig-Zag	∞	30	500	422,000	35.4	8,100	7.7
9" x 7" x 102" Wood Ties	700,000	21	500	480,000	27.4	6,800	5.4
MR-3 Concrete Ties	∞	30	500	535,000	24.0	6,600	6.4
MR-3 Concrete Ties	700,000	21	500	540,000	16.6	7,300	4.4
9" x 7" x 102" Wood Ties	∞	21	500	562,000	28.8	6,600	5.8
MR-3 Concrete Ties	∞	21	500	700,000	18.2	6,300	4.8

* Axle load = 45,000 lb (22,500 lb/wheel), rail weight = 132 lb/yd.
** At base of 24-inch ballast depth.

17

the same load. The rail stress increases because the rail has to span a greater distance, and therefore, bends more under the same load.

A comparison of the conventional track structures with the Dutch "zig-zag" track design shows that the latter's combination of low bearing area and widely spaced tie blocks results in a system with the highest soil and ballast pressures, the highest rail stress, and the lowest spring rate, even though no resilient pad is used. Because of the high pressures and stresses, this structure appears to be inferior to conventional track from the standpoint of long-term stability.

During Phase III, the static analysis of conventional track continued, using new input data pertaining specifically to the proposed DOT-Santa Fe experimental track, rather than the Northeast Corridor application envisioned earlier. It was desired to define the response of conventional track specifically for the Santa Fe installation, thereby providing a quantitative reference for the design of "advanced" track sections to be installed in this track, along with conventional track sections.

To facilitate this analysis and enable the effects of different parameters of conventional track to be evaluated more easily, the equations describing conventional track (see Appendix A) were programmed for a digital computer, and a plotting routine was specified to give plots of rail vertical deflection versus distance along the rail as a direct computer output.

A series of computer runs was then made to define track response under the heavy freight traffic (35,000 pound wheel loads with six foot truck axle spacing) expected by the Santa Fe. These runs included wood ties and MR-3 concrete ties, with and without resilient tie pads. The range of values used for inputs and the results of the runs using the lower soil modulus, 100 lb/in.^{3}, are shown in Table 2. Typical computer plots are illustrated in Figures 8 and 9, for soil modulii of 100 and 500 lb/in.^{3}, respectively (note difference in vertical scales), and a condensed summary of results is shown in Table 3.

18

TABLE 2. RESPONSE OF TIE-TYPE TRACK STRUCTURES TO HEAVY FREIGHT-CAR LOADING*

	Input Data						Output Data			
	Ties			Ballast/Subgrade			Rail		Ballast/Subgrade	
Comp. Run	Type	Spacing, inches	Bearing Area, in.^{2}	Ballast Modulus E_B, lb/in.^{2}	Ballast Depth, inches	Overall Foundation Modulus, psi	Deflection, inches	Bending Stress, psi	Tie-Ballast Bearing Pressure, psi	Ballast-Subgrade Pressure, psi
1	Wood	30	2(229.5)	40,000	24	1675	0.275	12,000	60.0	12.1
2	"	18	"	"	"	2792	0.172	10,450	37.6	7.6
3	"	30	"	"	12	965	0.456	13,800	57.6	21.8
4	"	18	"	"	"	1609	0.284	12,100	35.9	13.6
5	"	30	"	20,000	24	1500	0.303	12,350	59.5	12.0
6	"	18	"	"	"	2500	0.190	10,750	37.2	7.5
7	"	30	"	"	12	922	0.476	14,000	57.4	21.7
8	"	18	"	"	"	1538	0.296	12,250	35.7	13.5
17	MR-3	30	2(396)	40,000	24	2223	0.211	11,100	35.5	9.5
18	"	18	"	"	"	3705	0.133	9,700	22.4	6.0
19	"	30	"	"	12	1381	0.327	12,600	34.3	15.7
20	"	18	"	"	"	2302	0.204	11,000	21.4	9.8
21	"	30	"	20,000	24	2015	0.231	11,400	35.2	9.4
22	"	18	"	"	"	3353	0.145	9,950	22.2	5.9
23	"	30	"	"	12	1325	0.340	12,700	34.2	15.6
24	"	18	"	"	"	2209	0.212	11,100	21.3	9.8

* Two 35,000# Wheel Loads at 6' Truck Axle Spacing, 136#/yd Rail, Subgrade Modulus = 100 lb/in.^{3}

19
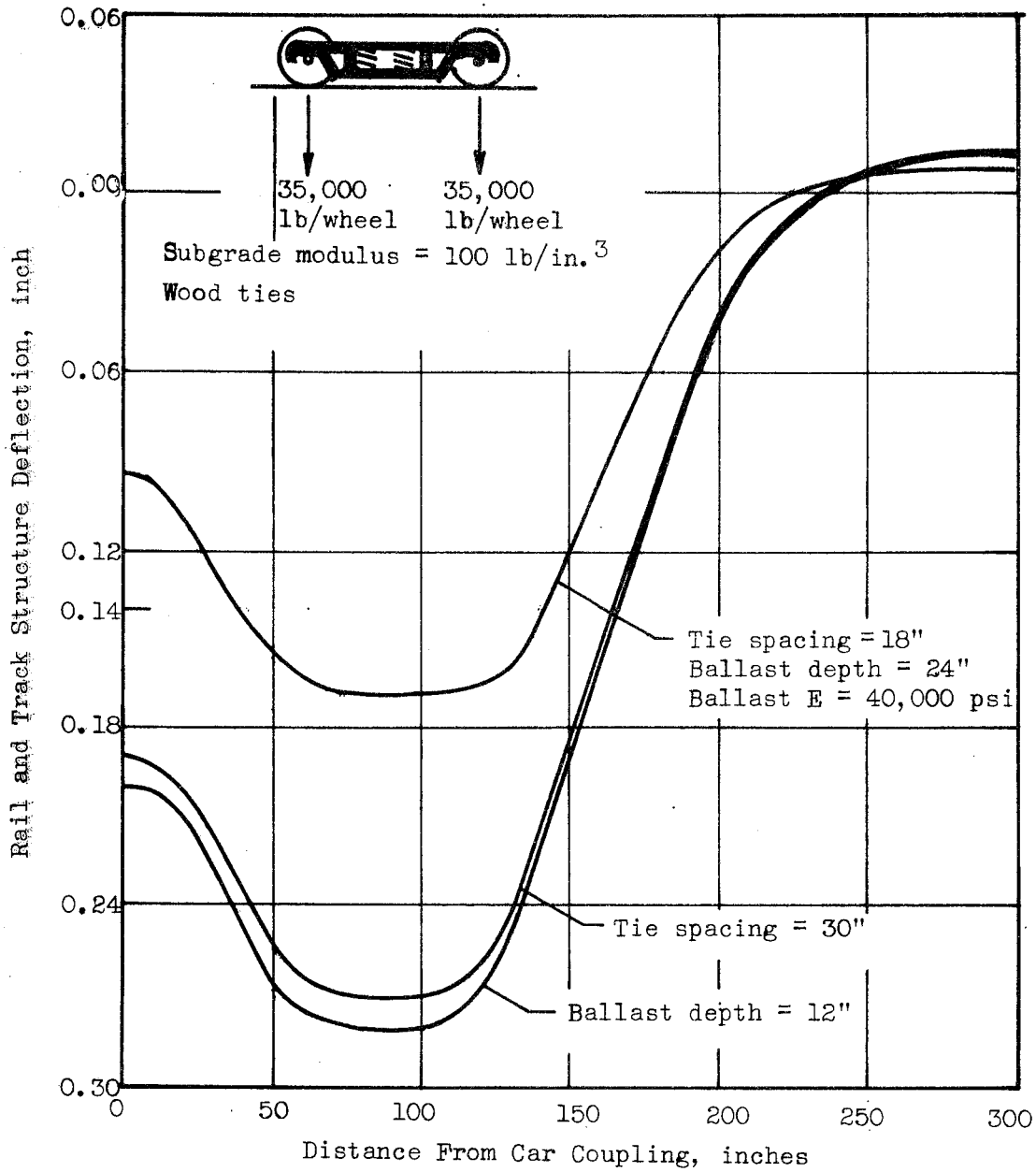
FIGURE 8. TRACK DEFLECTIONS FOR WOOD-TIE STRUCTURES
WITH LOW SUBGRADE MODULUS
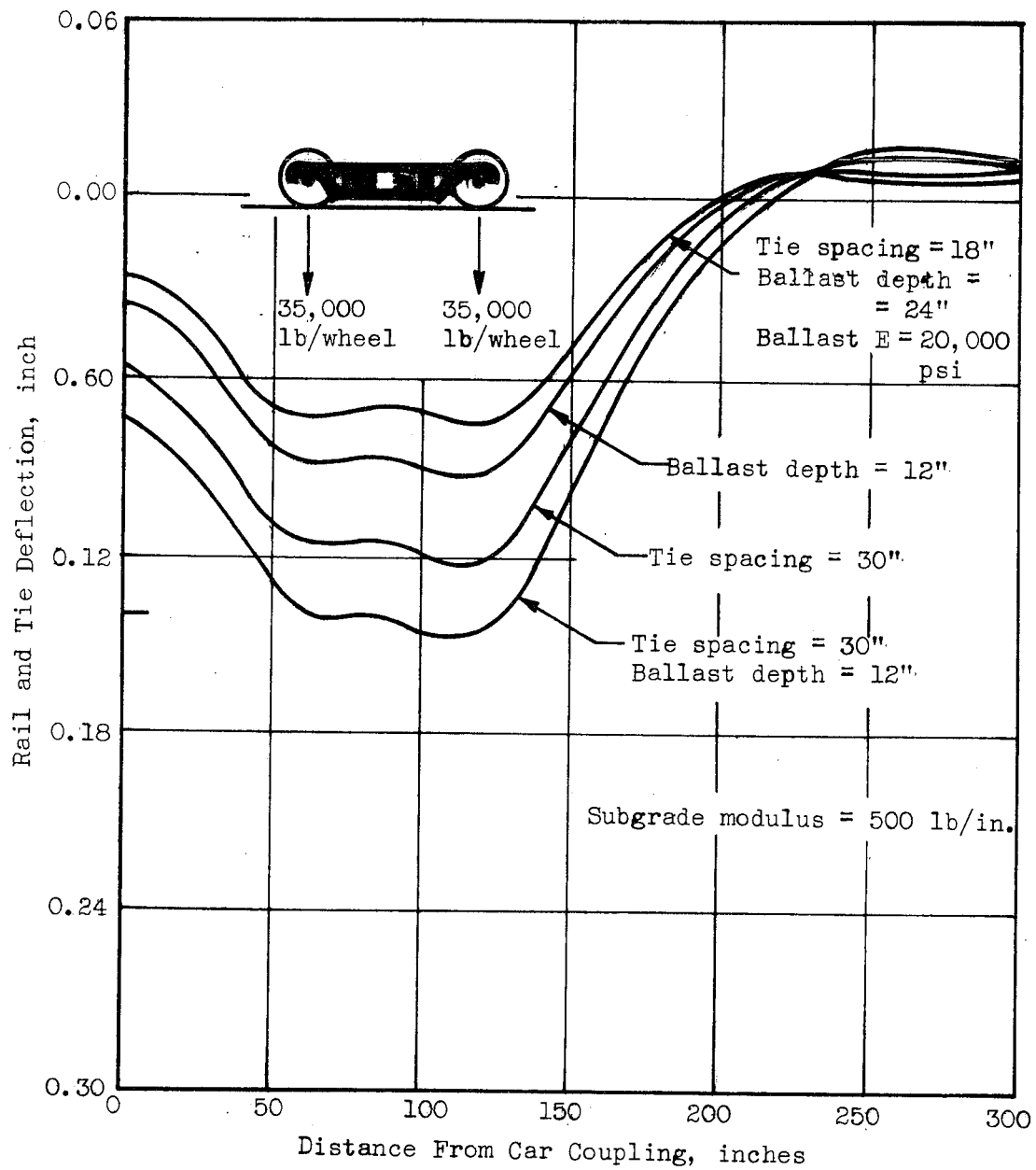
FIGURE 9. TRACK DEFLECTIONS FOR WOOD-TIE STRUCTURES
WITH HIGH SUBGRADE MODULUS

TABLE 3. AVERAGE RESPONSE OF CONVENTIONAL TRACK TO STATIC LOADS*

	Track Modulus, lb/in./in.	Rail Deflection, inches	Peak Rail Stress, psi	Tie Bearing Pressure, psi	Subgrade Pressure, psi
Wood Tie Track (K_o = 100 lb/in.^{3})	1687	0.306	12,213	47.6	13.7
Wood Tie Track (K_o = 500 lb/in.^{3})	5760	0.098	8,831	53.5	15.4
Concrete Tie Track (K_o = 100 lb/in.^{3})	2314	0.225	11,206	28.3	10.2
Concrete Tie Track (K_o = 500 lb/in.^{3})	8178	0.071	8,116	32.3	11.6

* 35,000 lb wheel loads, 136 lb rail, 6 ft axle spacing

These results brought out two important points. The first is the difficulty in defining (the response of) conventional track, since this is a function of so many variables, one of which varies with time and weather (the subgrade modulus). Therefore, to make valid comparisons of different types of track structure, care must be taken to define the terms of the comparison.

The second point is that, because of the closer axle spacing on the freight car truck (6 feet instead of 8.5 feet on the passenger car), in almost all cases the pressure pulses (or rail deflections) from individual wheels (or axles) merge into more of a single pressure pulse--although there is enough perturbation in the trace to detect individual wheel locations. The lack of individual pulses is most pronounced for the lower soil modulus (K_o = 100 lb/in.^{3}). In surveying the computer results, it was found that of all the variables, changes in the modulus or stiffness of the subgrade had the greatest effect on track response. While values of subgrade modulus of 100 lb/in.^{3} and 500 lb/in.^{3} had been used in all computer runs to date,

covering the complete range to be expected for almost any type of subgrade, it became obvious that an estimate of the modulus in the proposed Santa Fe experimental track roadbed was needed.

To determine a typical value which could be expected for well-prepared compacted fill such as should be used with a track structure, engineers with the State of Ohio Highway Department were contacted. These discussions led to the conclusion that a value of 200 lb/in.[3] was the highest that would be expected, particularly with a lime-stabilized soil such as that in the Santa Fe Kansas territory, and that a typical value would be on the order of 150 lb/in.[3] It was also learned that the modulus of the prepared fill is not measured (for example, using a loaded plate test) prior to building a highway, but rather its value is "inferred" from laboratory soil test data on core samples taken from the initial soil survey. Based on this information, it was concluded that the response of conventional (wood and concrete ties) track on the subgrade with the 100 lb/in.[3] modulus would be the better reference for the Santa Fe installation. Also, future runs were made with modulii in the range of 150-220 lb/in.[3].

At this point, then, it was possible to define certain criteria for advanced track structures for the Santa Fe installation in some detail, based on these studies of the response of conventional track to static loads. The following criteria were considered to be important for increased track stability with the actual values based on the response shown in Table 3.

- Lower direct bearing pressure (less than 30 psi)
- Lower subgrade pressure (less than 10 psi)
- Lower rail bending stresses (less than 11,000 psi)
- One pressure pulse per truck on ballast and subgrade.

The design of track structures meeting these and other criteria is discussed in the later section entitled "Development and Analysis of Advanced Track Structures".

23

Response to Dynamic Loading

No dynamic analyses of conventional track structures were made during Phase I; during Phase II dynamic analyses of conventional tie-type track were made, and these were continued during Phase III, with particular emphasis on the proposed Santa Fe test track installation.

The derivation of the track structure models for analysis of dynamic loading is given in Appendix B. For the dynamic analyses conducted during Phase II, several tie-type track structures were modeled on the analog computer. These included wooden-tie-track with and without rail pads; MR-3 concrete-tie-track with and without rail pads (ties on 21-inch centers); and the Dutch "zig-zag" track design. The lumped parameters defining these structures are shown in Table 4, together with selected computer results. Two types of dynamic analysis were made: steady state frequency response to a sinusoidal rail profile input, and transient response to a 1/4-inch step-down in rail profile. For the steady-state analysis, the total system consisted of that portion (one-half) of a 50-ton Budd rapid-transit railcar body supported by one truck, the truck itself, and that length of a continuous track structure associated with the support of one truck, as shown in Figure 10. The vertical deflection response of the wheel-rail contact point was recorded along with the input rail profile, the wheel-rail force, the car-body acceleration, and the deflections of the car body, axle, and bolster, all taken in the vertical direction.

In the transient analysis, the deflection of a fixed point on the rail in response to passing wheel-rail forces was determined. The system in this case consisted of a model of the track structure alone, and the input consisted of the continuous wheel-rail force multiplied by an influence coefficient function to compensate for the changing distance between the wheel and a point on the track. With this method, full force is applied to the track when the passing wheel is directly over the fixed point of interest, zero force to the track when the wheels are a certain distance away, and a varying fraction of the force during the time the wheel is approaching and then leaving a fixed point on the track. The influence

24

TABLE 4. SUMMARY OF LUMPED PARAMETERS DEFINING TIE-SUPPORTED TRACK STRUCTURES

Rail Load, P_4 = 22,500 pounds

A.R.E.A. 132-pound rail

Crushed Rock Ballast (E_b = 35,000 psi)

Ballast Depth, L = 24 inches

Weak Soil (k_o = 100 psi/in.)

| Structure Parameter (See Figure 7) | 21-Inch Tie Spacing | | | | 30-Inch Tie Spacing | | |
| | Standard Wooden Ties | | MR-3 Concrete Ties | | MR-3 Concrete Ties | | Dutch Zig-Zag |
	Without Pad	With Pad*	Without Pad	With Pad*	Without Pad	With Pad*	Without Pad
Track Structure Overall Spring Rate, k_R (10^3 lb/in.)	228	215	280	263	212	200	168
Equivalent Lumped Mass, m_R (lb-sec^2/in.)	2.20	2.22	2.97	3.05	3.21	3.32	3.73
Natural Frequency of Lumped System, f (cps)	51.2	49.5	48.9	46.8	40.9	39.0	33.7
Average Ballast Pressure Beneath Tie, p_o (psi)	21.1	20.8	13.4	13.0	17.6	17.2	27.0
Average Subgrade Pressure Beneath Ballast, p_L (psi)	4.2	4.2	3.6	3.5	4.7	4.6	5.9
Peak Rail Bending Stress σ_{rail} (psi)	10,000	10,000	8,500	9,300	9,800	10,100	10,600

* Individual pad stiffness = 700,000 lb/in. vertically.

$37,135$ m_c	1/2 car body
k_s C_s	2 suspension springs, dampers
1096 m_b	1 bolster
k_{sp} C_{sp}	1 shock pad
θ 1292 $M_{sf}, (J_{sf})$	1 spider, 2 side frames
k_b C_b	2 bearing sleeves (each side)
4450 m_w	1 axle, 2 wheels, etc.
k_{wr}	Wheel-rail contract
$Z_{(input)}$	Vertical profile input
F_{wr}	Wheel-rail reaction
m_r	Rail mass
k_{rp} C_{rp}	Rail pads and rail
m_B	Beam mass
k_{BS} C_{BS}	Soil and beam
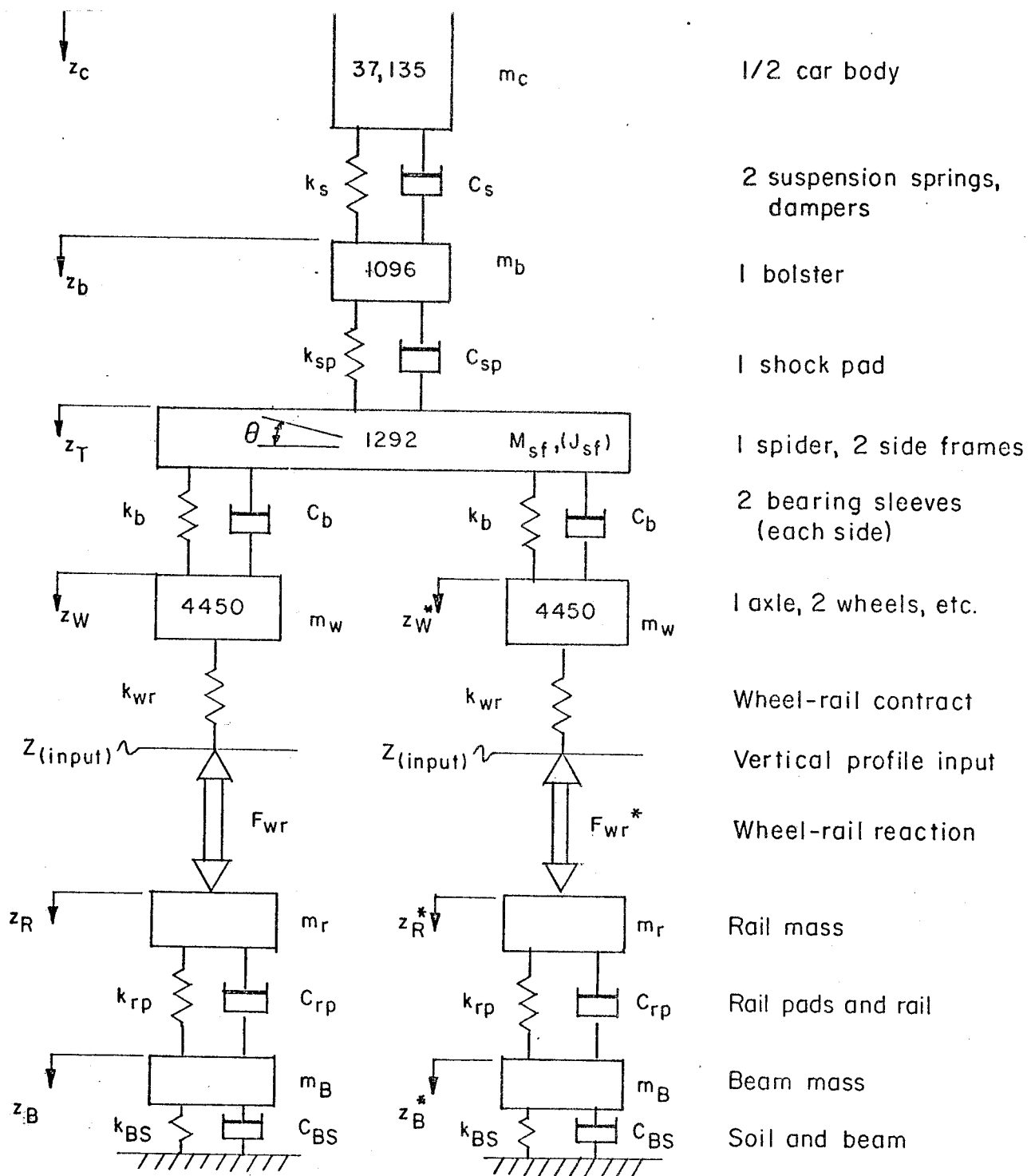
FIGURE 10.   ANALOG COMPUTER MODEL REPRESENTING PORTION OF CAR AND TRACK STRUCTURE ASSOCIATED WITH ONE TRUCK

26

coefficient was obtained from the curves for the static deflection of the continuous rail structures.

Three parameters in these analyses were considered to be particularly important: (1) the car body acceleration--because it is a measure of ride comfort and safety; (2) the wheel-rail force--a measure of the severe localized stresses at wheel and rail surfaces as well as a measure traction and braking potential; and (3) track structure deflection--because this is a measure of basic track stability (which relates to alignment, deterioration, and failure).

Sinusoidal Frequency Response. The results of the steady-state analysis are shown in Figure 11, where peak-to-peak car body acceleration per inch of (peak-to-peak) rail waviness amplitude is plotted versus frequency of input. The dashed lines indicate that the rail waviness amplitude, ε, was decreased because the wheels began to lift off the rail. The first conclusion that can be drawn from this graph is that exchanging concrete ties for wooden ones, or inserting a relatively stiff resilient rail pad, or both, have little effect on the car acceleration resonances resulting from steady-state sinusoidal excitation. However, the Dutch "zig-zag" track with its lower natural frequency, reduced the car body acceleration amplitude by 35 percent.

The second conclusion from the frequency response is that on the Dutch "zig-zag" track the frequency at which wheel lift occurs is almost three times as high as on the other four types of track investigated. Wheel-hop is delayed because the Dutch "zig-zag" track resonance condition (when the wheel forces reach their maximum) occurs at a lower frequency and consequently is a lower amplitude oscillation, low enough that the rail acceleration does not exceed one (1) G, meaning that the wheel force due to weight is not relieved. Practically speaking, this means that a softer, more resilient track (such as the Dutch "zig-zag" design) permits a train to maintain a higher speed over a wavy rail profile while maintaining a more constant level of wheel-rail force, resulting in better tractive,

27
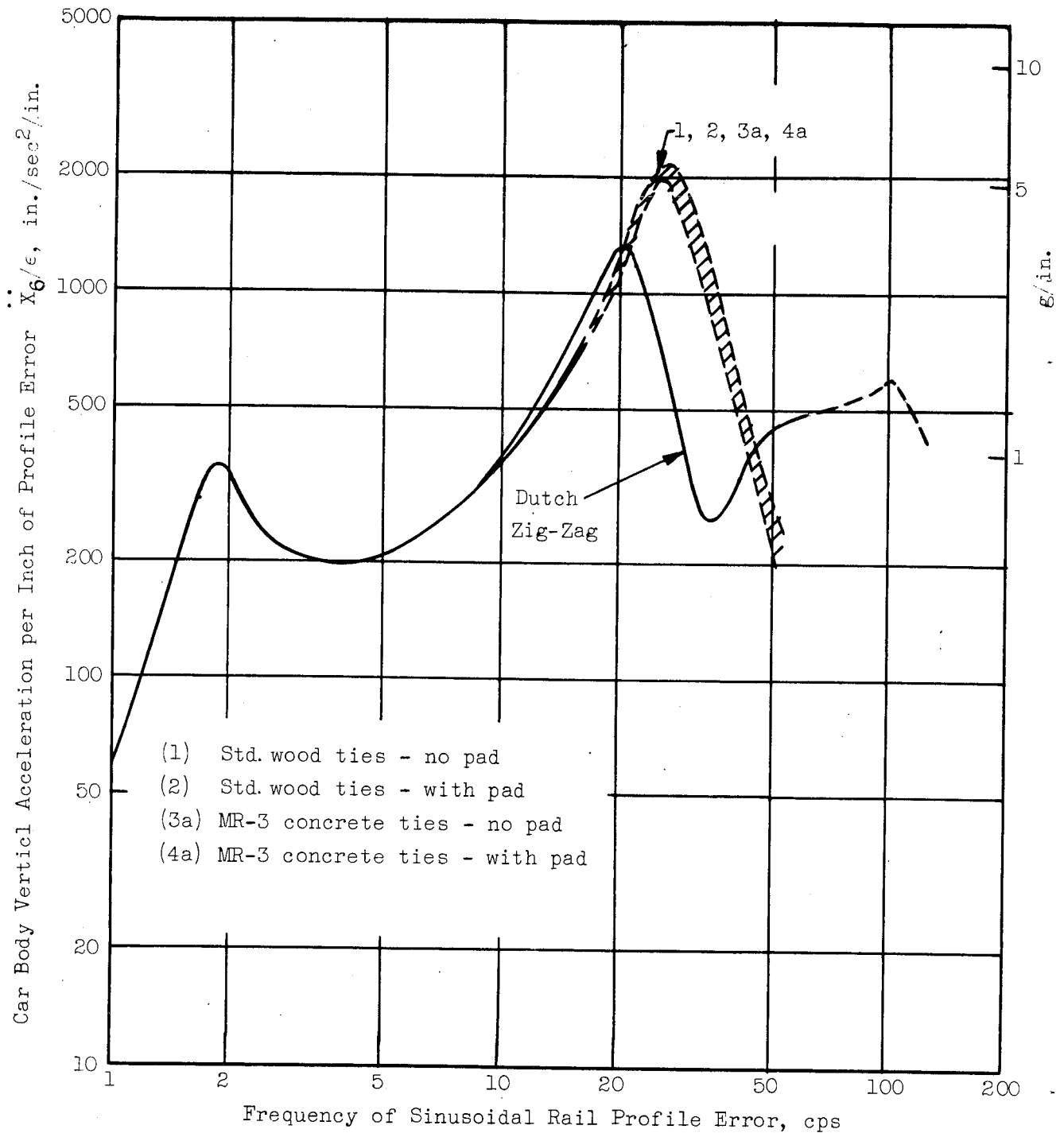
FIGURE 11. CAR BODY VERTICAL ACCELERATION IN RESPONSE TO SINUSOIDAL
RAIL PROFILE INPUT FOR VARIOUS TIE-SUPPORTED TRACK STRUCTURES

braking, and control characteristics. Unfortunately, in the Dutch design, the lower spring rate is obtained by low bearing areas at the expense of high roadbed pressures, rather than by the use of resilient pads.

The dynamic motion of the track structure itself is plotted in Figure 12 as a function of frequency. This can be interpreted as one measure of long-term track stability, since the ballast directly under the ties must move an equal amount; the curve shows the Dutch "zig-zag" ties move more than conventional ties.

Response to Step Inputs. For the mathematical representation of vehicle and roadway commonly used for computer studies, the vehicle is represented by a spring-mass system supported by another spring-mass system representing the roadway, as in Figure 10. The input to the system is usually a displacement representing the vertical profile of the track, highway, or other surface supporting the vehicle.

The wheel-roadway force generated in such a program represents a force traveling at vehicle speed and located at the wheel. For studies of vehicle response, this is a perfectly proper system, giving as it does the continuous force exciting the vehicle.

For a study of the roadway, however, it is obvious that this force is a transient value with respect to any fixed point on the roadway. The force directly over any point reaches a maximum only when the wheel is directly over that point. An important point to consider is that actual field measurements of track structure response must be obtained by applying instrumentation at one or more fixed locations along the track. It is desirable to validate any mathematical representation of the track structure used on the computer by comparing computer data with measured data from stationary (with respect to length along track) locations; the response of a fixed point on the track is, therefore, a desirable output from the computer study.

29
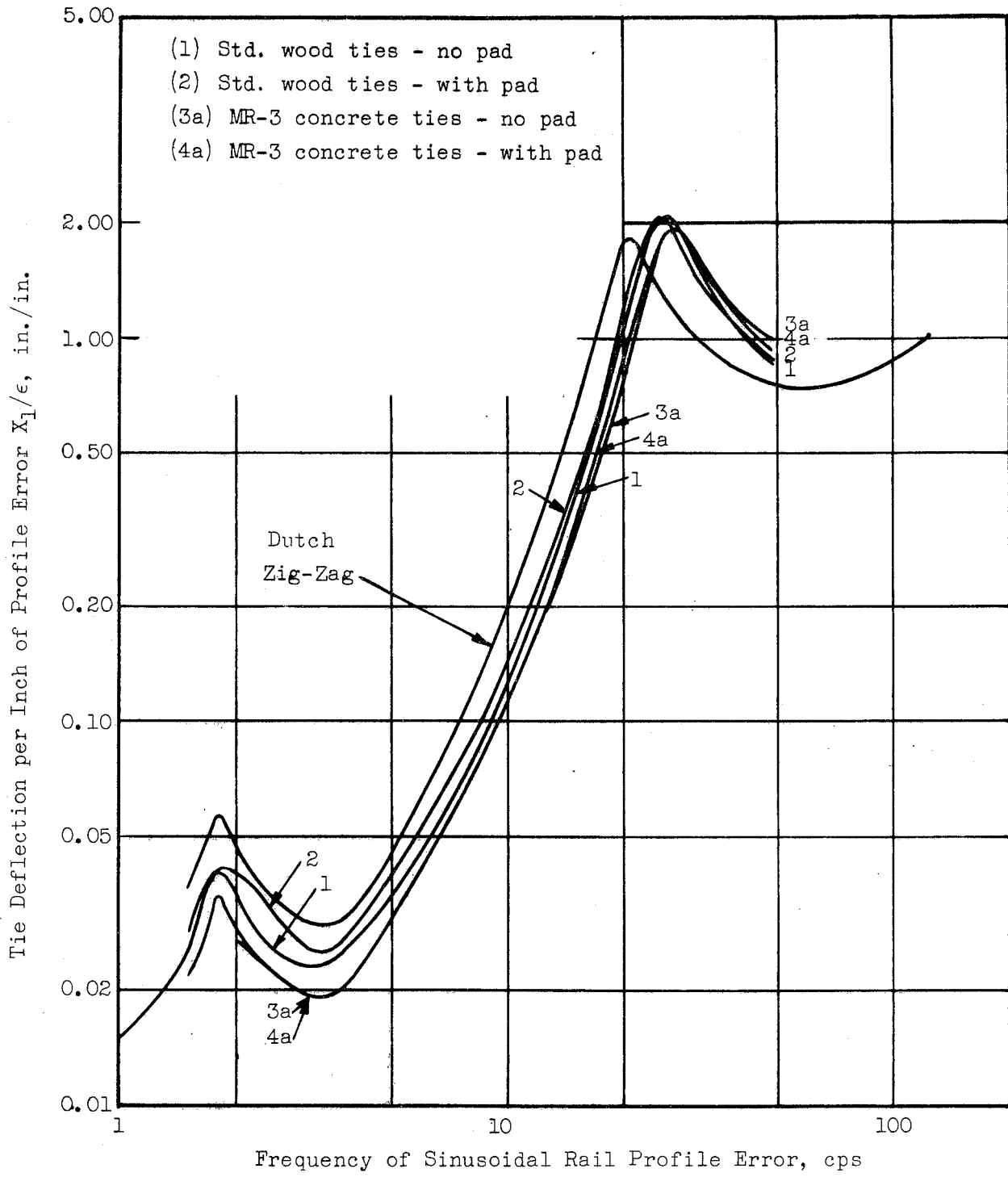
FIGURE 12. TIE DEFLECTION IN RESPONSE TO SINUSOIDAL RAIL PROFILE INPUT FOR VARIOUS TIE-SUPPORTED TRACK STRUCTURE

30

If the roadway were perfectly smooth and free from profile errors and inconsistencies in the subgrade, etc., measurements show that the curve of deflection versus length for static wheel loads would be approximately the same as the curve of deflection versus time taken at any point on the track structure for conventional train speeds. In the first case, a given distance on the abscissa would represent the longitudinal distance between two wheels on the vehicle, while in the second case this distance would represent the time it takes for the vehicle to travel a distance equal to that between the two wheels. There is, of course, some difference between the static and dynamic vertical deflection due to the inertia and damping effects associated with speed (that is, the rate at which the track is displaced vertically by a passing train), but this difference is negligible up to speeds at which the frequency of wheel load application approaches the natural frequency of the track structure. For a truck with an 8-foot wheelbase and a track structure with a natural frequency of 50 cps, this speed would be 273 mph. Therefore, for practical purposes, the static deflection curve can be assumed to represent the dynamic deflection versus time curve for the case where the rails are perfectly straight, the wheels perfectly smooth, and the track structure has perfectly uniform properties along its length.

However, since this case is not one encountered in practice, the question of practical interest is how to generate the deflection versus time trace of a track having realistic profile errors and nonuniform properties along its length.

This can be done by considering the problem as a two-step problem. The first step is to generate the moving wheel-rail force using the conventional representation of vehicle and track, including track profile errors as well as factors such as reduced stiffness at joints, etc. The traveling wheel force generated from this program then can be used as the input to a representation of the track structure itself, using an influence coefficient function to modify the effect of this force on a given point on the rail, according to the distance of this force away from the rail. Obviously, the coefficient is one when the (wheel) force is directly over the fixed point,

31

and drops to zero at some distance away from the point, this value depending on the track structure design.

This procedure was used for the transient analysis of the track structures, except that the wheel-rail force obtained as an input for the vehicle-roadbed simulation was simultaneously multiplied by the influence coefficient and used as the input to the (duplicate) track structure simulation, all done at one time on the analog computer.

For the transient analysis, the car was assumed to encounter a 1/4-inch drop in rail level (such as a severely misaligned joint) as it moved along at 50 mph. Soil modulii of 100 lb/in.^{3} and 500 lb/in.^{3} were used. Typical response data are shown in Figure 13 for concrete-tie and Dutch "zig-zag" structures; selected data are shown in Table 5.

The peak car body acceleration was proportional to the overall track stiffness, being highest for the concrete tie structure (without tie pads) and lowest for the Dutch "zig-zag" track, for both weak and stiff soils. The lowest wheel-rail force was obtained on the unpadded wooden-tie "conventional track" for both weak and stiff soils. The highest wheel-rail force for a weak soil condition was on the Dutch "zig-zag" track, but for a stiff soil condition the concrete tie track had the highest force. Although the Dutch design has a low spring rate, its high mass tends to increase the wheel-rail impact force. With the soft soil, differences in the five structures gave considerably different impact forces, but with the stiffer soils the wheel-rail forces were less sensitive to the differences in the five track structures.

The data for dynamic response showed, in general, the following trends:

(1) For step inputs, the peak impact wheel-rail force increased as overall track stiffness increased

(2) For step inputs, car body accelerations increased as overall track stiffness increased

(3) Tie-ballast peak pressures decreased as overall track stiffness increased

32

Track Profile (input)

Influence coefficient (based on static load deflection)

Car body acceleration — $\ddot{X}_6$

0.1 G

Displacement of fixed point in rail — Y_1

$0.1''$

Displacement of moving point in rail — X_1

$0.1''$

Wheel-rail contact force — F_w

$60,000$ lb

Wheel displacement — X_3

$0.2''$

Car body displacement — X_6

$0.4''$

$0.5''$

0.5
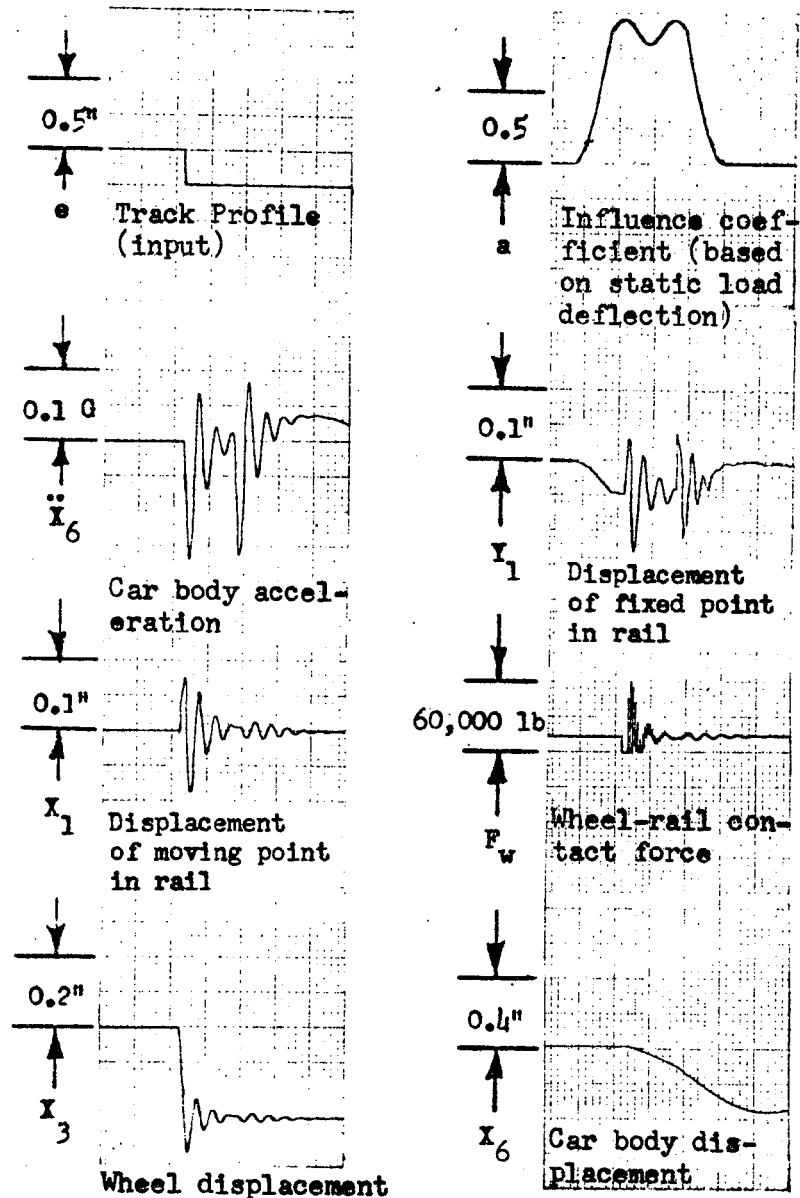
a) MR-3 Concrete Ties, No Pads. Soil Modulus
   $k_0 = 100$ lb/in^3, Speed $= 50$ mph.

FIGURE 13.   RESPONSE OF TWO TIE-TYPE TRACK STRUCTURES
              TO STEP DISCONTINUITY IN TRACK PROFILE

0.5" ⤒⤓ e

Track profile
(input)

0.5 ⤒⤓ a

Influence coef-
ficient

0.1 G ⤒⤓ $\ddot{X}_6$

Car body accel-
eration

Displacement
of fixed point
in rail

0.1" ⤒⤓ Y_1

0.1" ⤒⤓ X_1

Displacement
of moving point
in rail

60,000 lb ⤒⤓ F_w

Wheel-rail con-
tact force

0.2" ⤒⤓ X_3

Wheel displacement

0.4" ⤒⤓ X_6

Car body dis-
placement
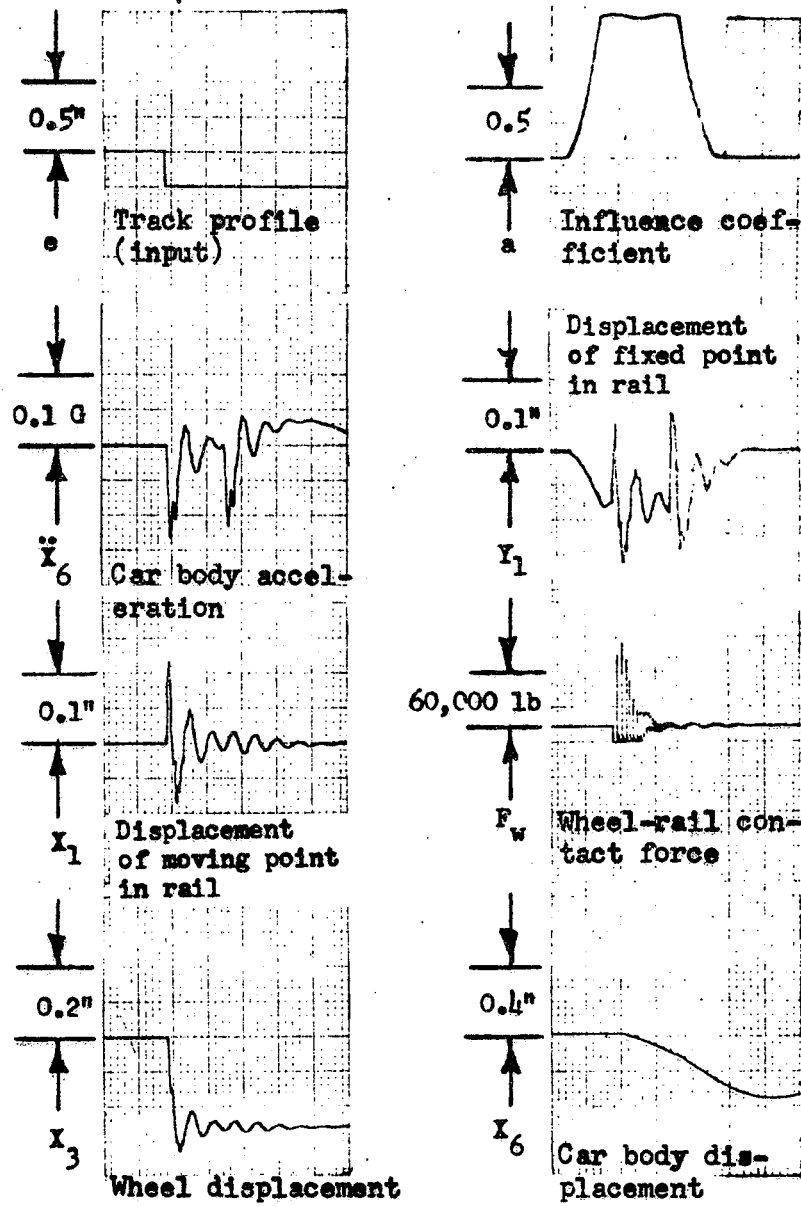
b) Dutch Zig-Zag Structure, Soil Modulus
    $k_o = 100$ lb/in^3, Speed = 50 mph.

FIGURE 13. (CONTINUED)

34

TABLE 5. DYNAMIC RESPONSE OF TRACK STRUCTURES TO 1/4-INCH STEP-TYPE PROFILE INPUTS

Structure (See Table 5 for More Complete Description)	Subgrade Modulus, lb/in.^{3}	Overall Stiffness, lb/in.	Car Body Acceleration, in./sec^2 $\ddot{X}_6$	Wheel Overshoot Displacement, in. X_1	Rail Overshoot Displacement, in. Y_1	Peak Wheel-Rail Force, lb $F_{12}/1000$
Wood Ties @21", No Pad	100	228,000	66.4	0.105	0.102	50.4
Wood Ties @21", Resilient Pad	100	215,000	65.0	0.106	0.111	51.6
MR-3 Ties @21", No Pad	100	280,000	68.0	0.088	0.083	60.0
MR-3 Ties @21", Resilient Pad	100	263,000	65.0	0.088	0.087	60.0
Dutch Zig-Zag	100	168,000	52.8	0.083	0.083	84.6*
Wood Ties @21", No Pad	500	562,000	75.2	0.070	0.053	71.4
MR-3 Ties @21", No Pad	500	700,000	76.0	0.062	0.047	78.0
MR-3 Ties @21", Resilient Pad	500	540,000	74.4	0.068	0.060	78.0
Dutch Zig-Zag	500	422,000	73.6	0.079	0.075	72.0

* On all structures the wheel-rail forces went to zero 2X (bounced twice) except Structure 5 on a soft subgrade, which bounced about 8 times.

(4) For sinusoidal inputs, vehicle-track structure
frequency response did not vary appreciably for
any of the tie-supported structures except the
Dutch "zig-zag" type.

The Dutch "zig-zag" structure proved to be quite an anomaly.
Under static load rail stresses, tie-ballast pressures, and soil pressures
were the highest, while natural frequency and overall spring rate were the
lowest. All of these characteristics can be attributed to the low bearing
area per unit length.

The dynamic response of this structure was also unique, giving a
lower amplitude of vibration with sinusoidal excitation but higher rail dis-
placements and wheel-rail forces for the step-type input. These character-
istics result from the relatively high-mass, low-spring rate characteristics
of this dynamic system. In summary, the Dutch "zig-zag" track structure
appears to offer no advantages.

With respect to the other tie-supported structures, including
variations of tie spacing and use of a stiff resilient pad, dynamic per-
formance differences were minor rather than substantial, with the trends
noted above making the choice of overall track stiffness somewhat of a com-
promise, depending on whether the ballast, wheels and rails, or vehicle are
to be favored.

Dynamic Analysis Related to Computer Program Validation and Santa Fe Installation

Computer Studies

Analyses of conventional track continued during Phase III, with
specific emphasis on the Santa Fe installation and the anticipated valida-
tion runs on the Penn Central high speed track between Washington, D. C.
and New York City. Several basic improvements were incorporated into the
computer program described earlier. One of the changes was the use of the
exact (theoretical) curves, rather than a sinusoidal approximation, for the

36

static rail deflection that was included in the portion of the program for generating the dynamic track deflections at a fixed location along the rail.

Computer analysis was divided into two tasks: (1) generation of response data simulating the DOT test car on the Penn Central high speed track for validation of the computer program, and (2) preliminary analyses of track structures under consideration for the DOT-Santa Fe test track. For the first task the DOT test car was simulated (rather than the heavier Metroliner, which has an entirely different truck design) to allow comparison with controlled test runs to be made in the future. Since little was known of the track vertical profile at the site proposed for trackside measurements, analyses were made for both smooth track and also for a track with joints. A track joint was chosen as a "disturbance function" for computer simulation to provide a response with a reasonably high signal-to-noise ratio. Each track joint was simulated as having both a reduced stiffness and a profile error (a low spot) due to permanent set of the rail by traffic action. For the validation work, computer runs at simulated speeds of 30, 60, 90, 120, and 150 mph were made for the following conditions: (1) smooth track profile, no joint, (2) smooth track profile, joint with 75 percent and 50 percent of nominal track stiffness, (3) joint with 75 percent of nominal track stiffness, profile errors of 0.1, 0.2, and 0.3 inch. These were run on a simulated conventional track structure with an overall stiffness of 221,000 lb/in. per rail, representing a track with 140 lb/yd rail, 7 x 9 x 102-inch wooden ties on 21-inch spacing, 18 inches of ballast with an elastic modulus of 30,000 lb/in.^{2}, and a subgrade modulus of 100 lb/in.^{3}. In addition, runs were made using a stiffer (389,000 lb/in. per rail) track. Both nominal and ballasted car weights were simulated. Curves showing typical response of the vehicle and track structure are presented in Figures 14 and 15, and are discussed further in later sections covering the computer program validation.

For the second task, the evaluation of track structures proposed for future tests on the Santa Fe, a simulation of a 100-ton freight car was used. The basic parameters describing this car were : 72-inch truck

TRACK GEOMETRY ERROR (INPUT)
(75% NOMINAL STIFFNESS)

0.3"

CAR BODY DISPLACEMENT

0.2"

CAR BODY ACCELERATION

0.05G

MAIN SUSPENSION STROKE

0.2"

0.1 SEC.

WHEELS-AXLE ACCELERATION

5G

WHEEL-RAIL FORCE   ZERO

15,000 LB.

RAIL DISPLACEMENT (UNDER FRONT WHEEL)

ZERO

0.05"

RAIL ACCELERATION (UNDER FRONT WHEEL)

50 G

TRACK OVERALL STIFFNESS = 221,000 lb/in
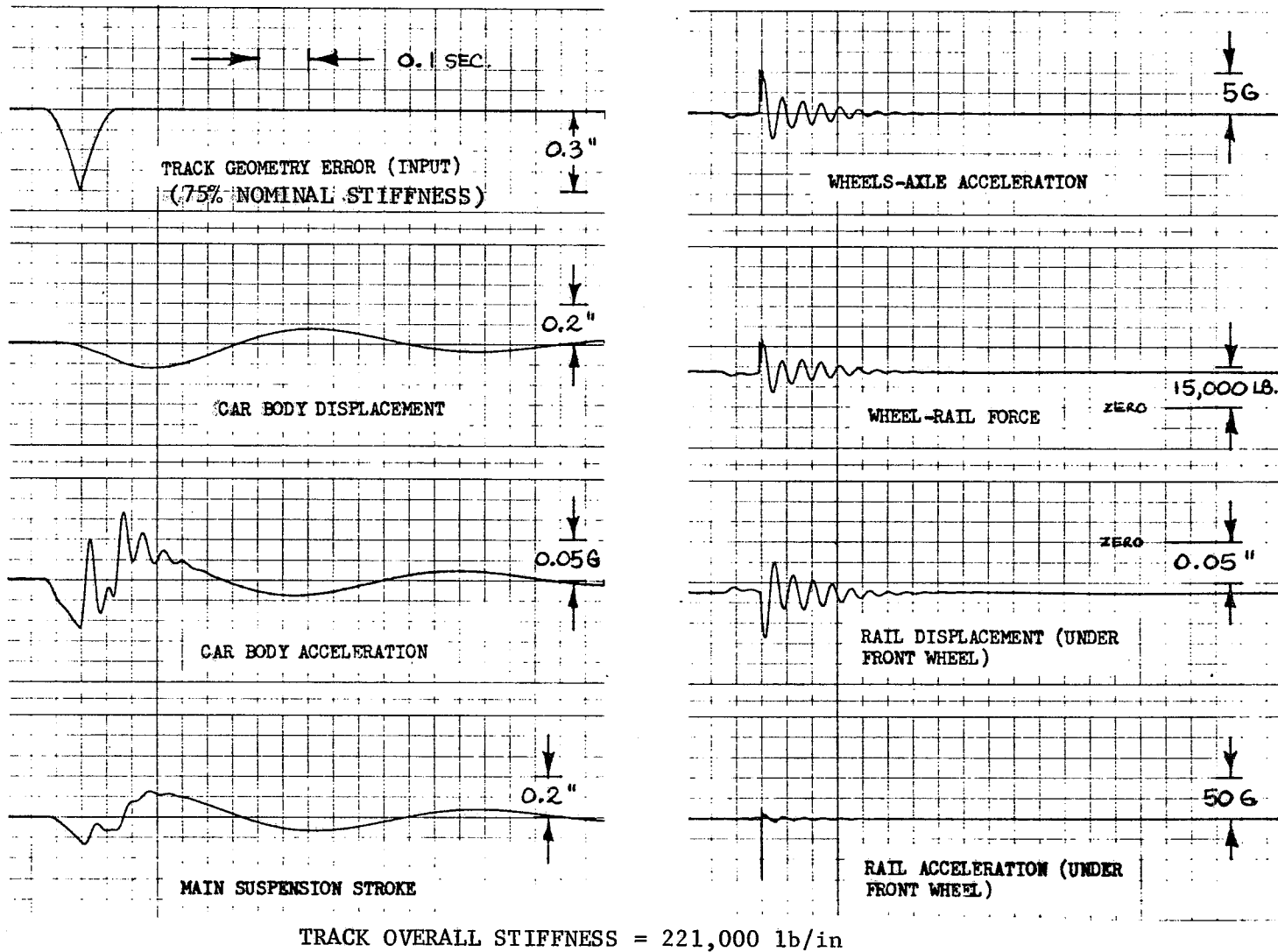
FIGURE 14. ANALOG COMPUTER SIMULATION OF DOT TEST CAR HITTING LOW JOINT
AT 90 MPH ON CONVENTIONAL TRACK STRUCTURE

38

39
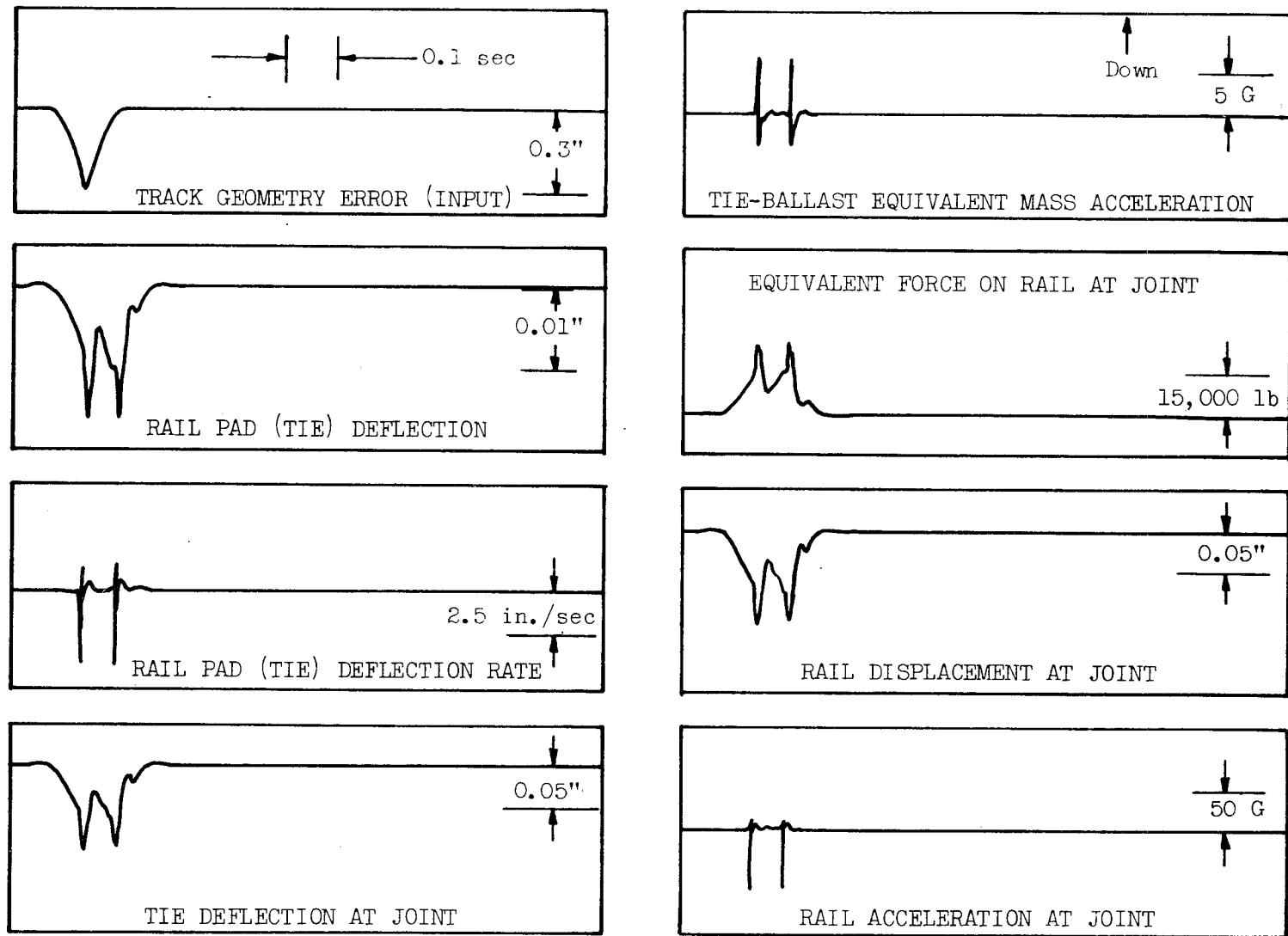
FIGURE 15. ANALOG SIMULATION OF CONVENTIONAL TRACK STRUCTURE (221,000 LB/IN. STIFFNESS) IN RESPONSE TO DOT TEST CAR AT 90 MPH HITTING JOINT IN RAILS WITH 75 PERCENT NOMINAL STIFFNESS, 0.3-INCH GEOMETRIC ERROR

wheelbase, 8640-pound truck unsprung weight, 45,000 lb/in. springs (3-11/16"-travel) per truck, 8000 pounds vertical friction damping per truck, and a static wheel load of approximately 32,500 pounds. For consistency, a rail joint with 75 percent of nominal stiffness and a 0.2-inch profile error was used throughout as a disturbance function.

Tie-type track structures simulated were: (1) conventional wooden-tie structure, (2) conventional wooden tie structure with plastic-impregnated ballast (ballast-brittle), (3) MR-3 concrete tie structure with 21-inch and 30-inch spacing, with rail pads of 200,000, 400,000, and 700,000 lb/in. stiffness.

Characteristics of ballast and subgrade (effective mass and damping) were estimated from recent work by the AAR[5] and others in the field of ballast and soil mechanics. All runs (with the exception of the conventional wooden-tie track structure) assumed a subgrade modulus of 150 $lb/in.^3$ and (in the case of the concrete ties) a 24-inch depth of high-grade ballast.

Several interesting facts were brought out by the results of these runs. First, the "ballast-brittle" caused a slight increase in the vehicle unsprung mass accelerations, and approximately 10 percent increase in the tie accelerations. The other response variables were essentially unchanged. The small changes in response cited above must be attributed to the slight reduction in damping (167 lb-sec/inch rather than 261 lb-sec/inch equivalent viscous damping with conventional ballast; c_{BS} in Figure 10) resulting from the treatment of the ballast, since this was the only change made in the program to represent the treated ballast.

Also of interest were the results for the runs using different rail pad stiffnesses. The wheel-rail impact loads at the joint were almost directly proportional to the rail pad stiffness; at 40 mph the dynamic impact factor increased from 1.068 to 1.095 as the pad stiffness was increased from 200,000 lb/in. to 700,000 lb/in., and at 80 mph the impact factor increased from 1.15 to 1.19 over the same range of pad stiffness.

40

Again, the importance of providing resilience in the stiffer track structures was demonstrated.

Computer runs were made for speeds up to 150 mph for the case of a perfectly smooth track with uniform characteristics. For this condition computer response showed no discernible effect on dynamic loads and deflections of the track with increased speed. As noted earlier, this is to be expected at speeds below about 250 mph.

Validation Measurements Made on the C&O/B&O Railroad

Validation of the computer program was desirable for a number of reasons. First, there are known discrepancies between the classical beam-on-an-elastic-foundation model and an actual railroad track. For example, in the mathematical model, the rail support springs are assumed to be linear and to resist upward as well as downward motions of the rail and ties. In the actual case, there is no resistance to normal uplift motions of the rail, since the spikes are usually loose. Also, preliminary spring rate measurements indicated the roadbed support to be nonlinear rather than linear. Also, in development of the dynamic models, lumped masses, spring rates, and damping values are calculated, but the damping in particular is somewhat questionable in actual track.

The computer runs described previously were made in February of 1969; to validate the computer program, a series of field measurements was made later in the year. Two different tracks were instrumented, and the track structure dynamic response was recorded during the passage of both passenger and freight traffic. For this program, specialized instrumentation was designed and built to measure the following parameters:

    (a) rail vertical acceleration
    (b) rail-tie vertical and angular displacement
    (c) rail-ground absolute displacement

41

(d) tie plate vertical load

(e) ballast-subgrade vertical pressure.

The measurement program consisted of two parts. The first part was conducted on the mainline C&O/B&O track near Columbus, Ohio, in March, 1969, and was basically for checking out the new instrumentation. The second part was conducted in December, 1969, on the high-speed Penn Central track near Washington, D.C., using the DOT research cars to give a series of controlled-speed runs.

Figure 16 shows some of the trackside instrumentation as installed on the C&O/B&O track for checkout. Of particular interest was the special tie plate for measuring vertical load; this unique design employed a standard tie place so that it could be moved to a different location in the track quickly without disturbing the tie on which it was installed.

Traffic on the track consisted mainly of heavy coal trains (northbound) and empty coal trains and time freights (southbound). The "Sportsman", a passenger train, made one round trip per day, usually passing the measurement site at a speed of approximately 80 mph. This mix of traffic enabled a good range of data to be obtained.

Typical track response data is shown in Figure 17. It was interesting to find that the shapes of the tie plate load and rail absolute displacement traces were considerably different; the former showed more distinct pulses for individual wheels than the latter. This indicated a nonlinear roadbed spring rate, as opposed to the linear vertical spring rate used in the computer program and the classical-beam-on-elastic-foundation problems. The presence of a nonlinear spring rate was verified by plotting simultaneous vertical load and displacement values, giving the curve shown in Figure 18. Other significant points about the data were the distinct presence of rail uplift ("wave action") which was evident, and the fact that a flat wheel on an 80 mph train was easily detected by the tie plate load cell, indicating the effectiveness of such instrumentation for monitoring traffic.

42
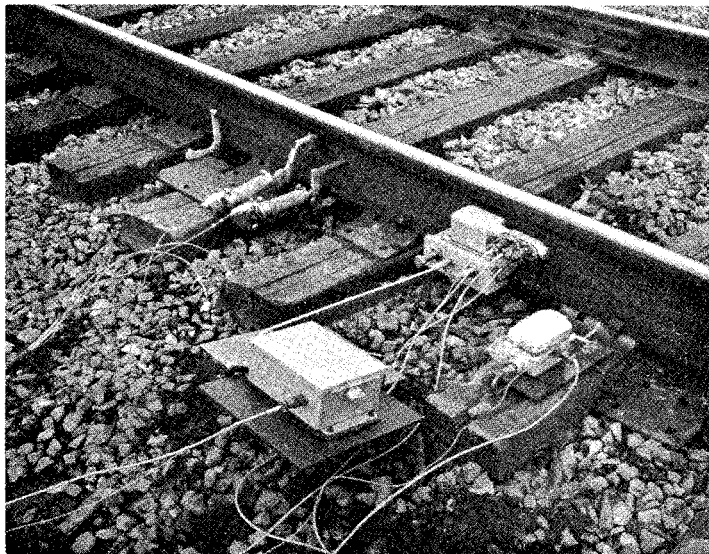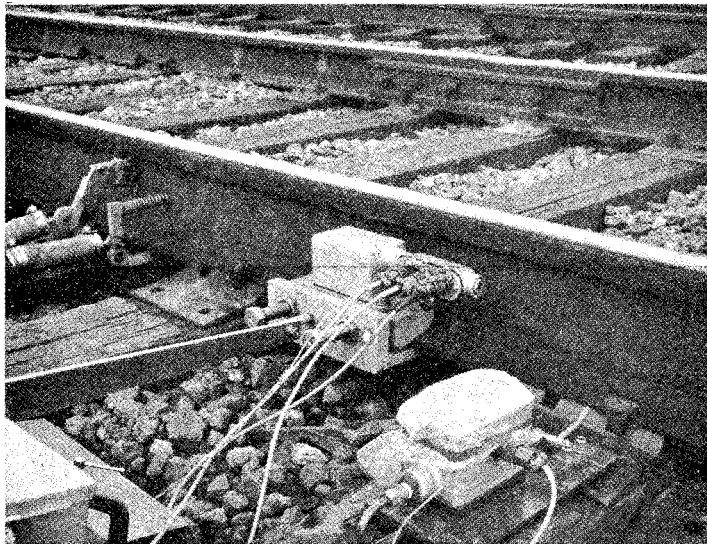
FIGURE 16. TRACKSIDE INSTRUMENTATION

(Rail lateral and vertical displacement transducers, rail vertical,
lateral, and longitudinal acceleration package, rail absolute dis-
placement transducer, and tie plate load transducer.)

43
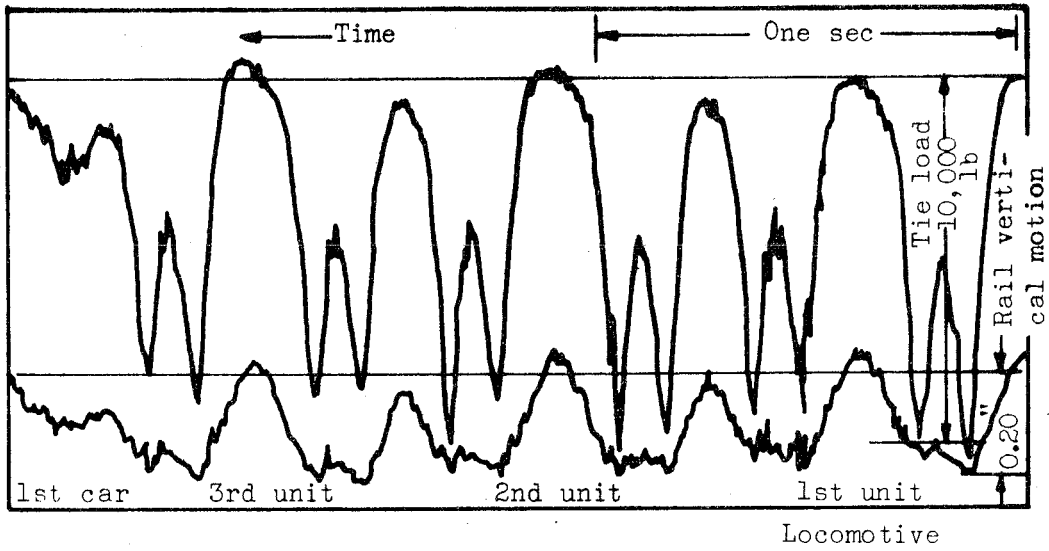
Recordings of tie load and rail vertical motions under three-unit
locomotive (GP-9's) pulling empty hopper cars. Linworth, Ohio,
4-3-69. Speed: 55 mph
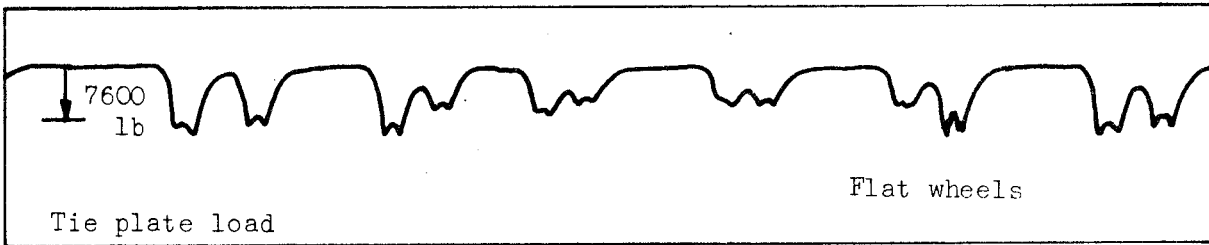
Tie plate load for portion of freight train

FIGURE 17.   TYPICAL TRACES OF TIE PLATE LOAD AND RAIL VERTICAL
MOTION FOR FREIGHT TRAFFIC

44
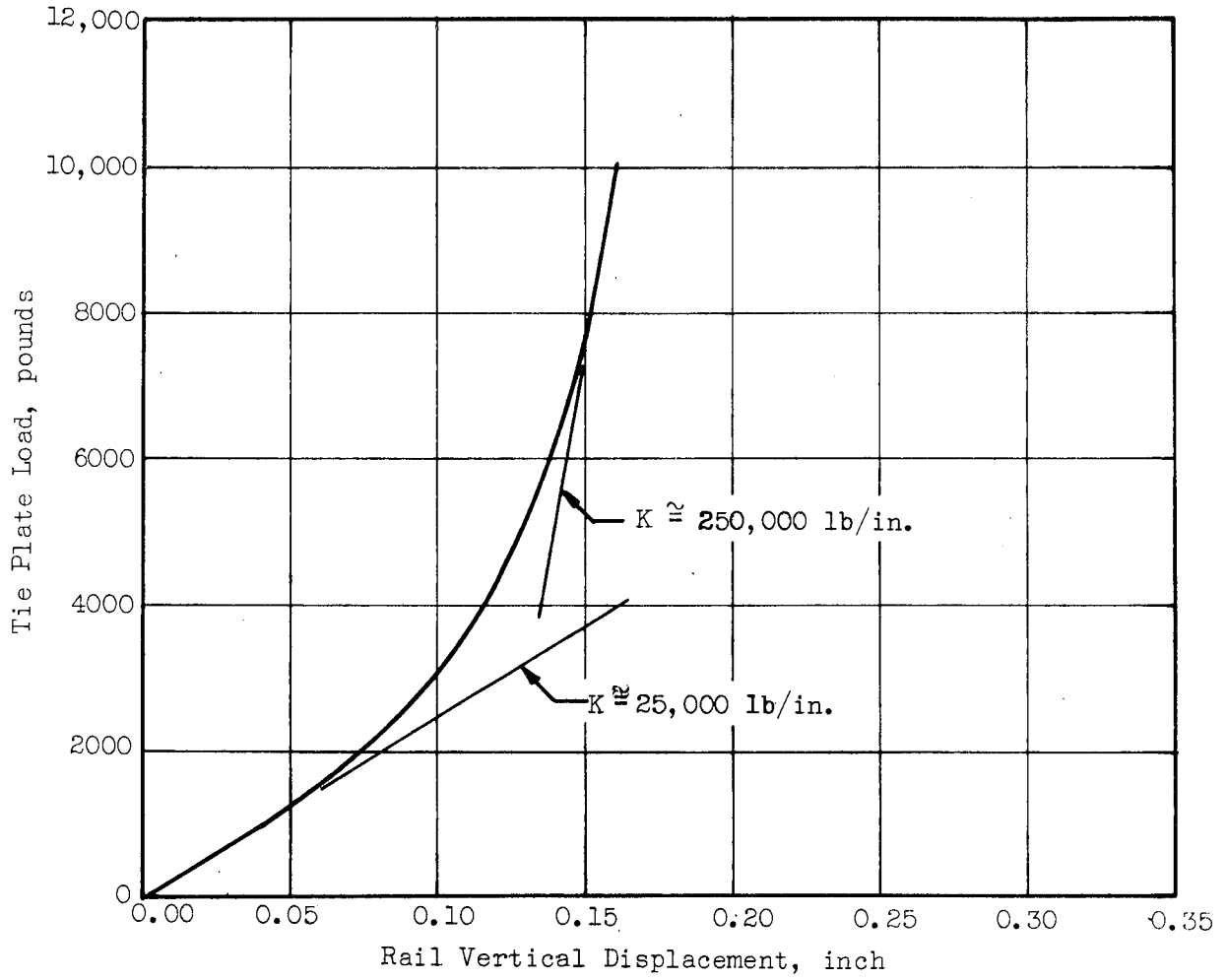
FIGURE 18. PLOT SHOWING NONLINEAR TRACK SPRING RATE MEASURED ON MAINLINE RAILROAD TRACK

45

Validation Measurements Made on the Penn Central High-Speed Track

The Penn Central high-speed track was chosen for the measurements to validate the computer vehicle-track model. Track #3 (continuously-welded rail) at milepost 121.95, immediately north of the Springfield Road crossing, Bowie, Maryland, was the designated site; one reason this location was chosen was because it was the (south) end of a long section of welded rail, providing a location where data could be taken at a rail joint as well as away from the joint. Ideally, a location where two rail joints were directly across from each other was required for validating the computer data, since the computer model was of the so-called "bicycle" type in which motions of the vehicle and track components in a vertical longitudinal plane were described. Inherent in this representation is the assumption that left and right wheels on a given axle are excited simultaneously and identically, so that there is no component of roll motion involved. Because the railroads purposely do not allow two joints to occur side-by-side, no such location was available; the staggered-joint location was chosen as one which would most nearly approach the condition assumed earlier for the computer runs. The stagger between joints on opposite rails was about 3 feet.

A grid of 8 soil pressure cells was buried in the subgrade 3 feet beneath the base of the ties, approximately 30 feet north of the first rail joint (for a southbound train). The location of the pressure cells and all other instrumentation is shown in Figure 19. The pressure cells were installed on December 5, and the first data was recorded just 5 days later. A longer period of track stabilization and consolidation would, of course, have been desirable. Snow and heavy rain thoroughly soaked the subgrade on the 6th and 7th, and again on the 10th. With the prevailing weather conditions and periodic tamping of the ballast by the track crew, the degree of stabilization of the subgrade around these cells could not be accurately judged.

The majority of the data was recorded during the three-day period of December 10--December 12. As can be seen from the data-traffic log in

46
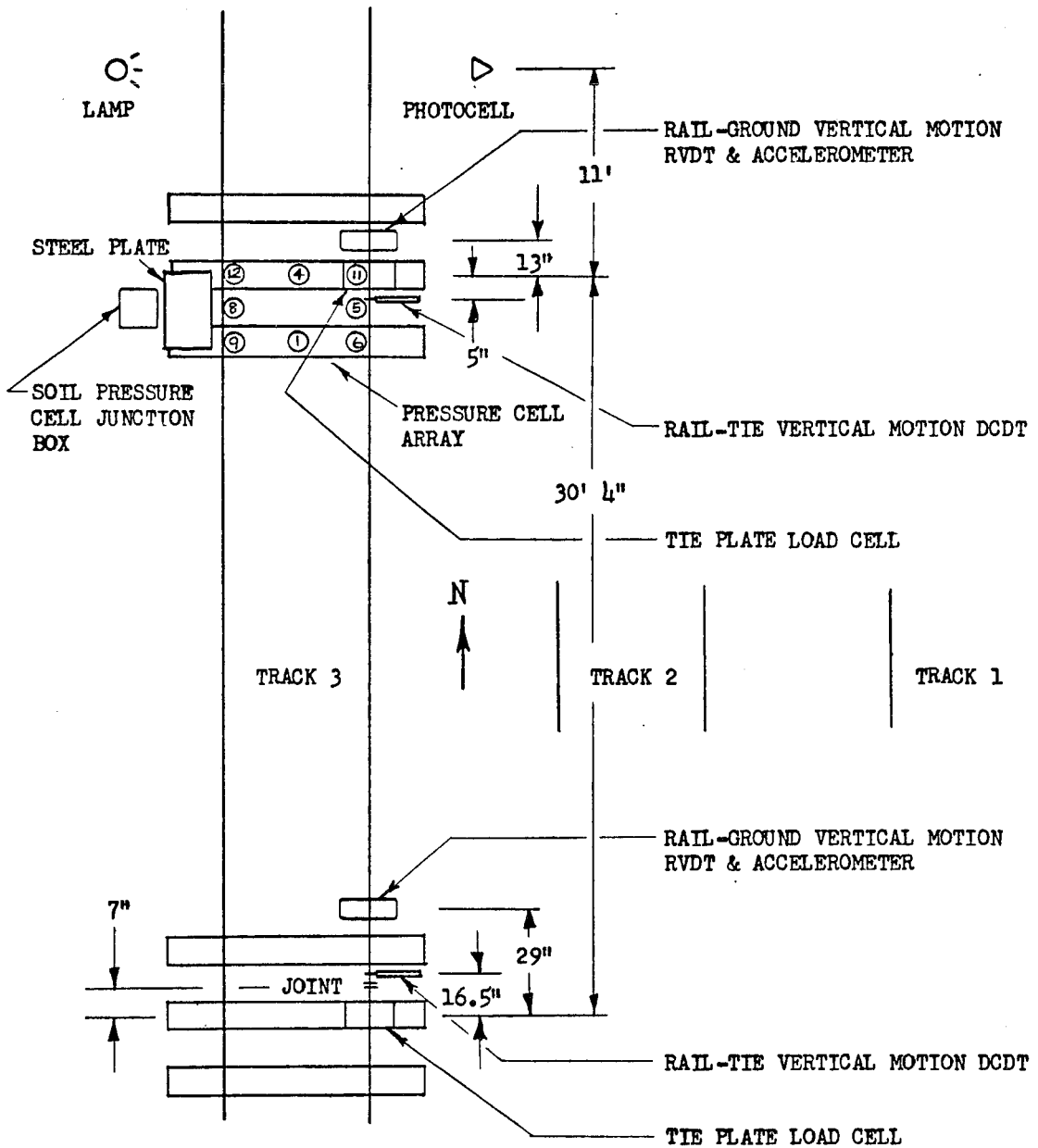
FIGURE 19. LOCATION OF INSTRUMENTATION INSTALLED ON
PENN CENTRAL HIGH SPEED TRACK NEAR BOWIE, MD.

47

Table 6, data was obtained from nearly 50 trains, including not only the controlled speed runs of the DOT research cars, but also regular freight and passenger runs, including Metroliners.

Results of Track Measurements

Selected data from the field measurements are given in the text; additional data are included in Appendix C. A typical CEC recorder trace obtained during the first day of measurements is shown in Figure 20, in which the track response to passage of the DOT test train at 55 miles per hour is given. One interesting deviation from the typical computer response shown in Figure 15 was immediately apparent: due to a joint gap of roughly 5/8" (plus some chamfer, or batter), the tie plate load was instantaneously relieved before the dynamic "spike" load, unlike the sudden increase in load produced by the "gapless" computer model. Also, in the computer simulation, the decay of the joint transient persists for a period of time amounting to several feet of travel along the rail, whereas the actual recorded force pulse died out more quickly, and appeared to be a much higher frequency impulse.

During the first day of tests, a series of five runs was made with the DOT test train at progressively higher speeds (from 8.4 to 67.5 mph) over a time span of 2-1/2 hours. Regular traffic (Metroliners, GG1, and heavy E44 freight locomotives) were interspersed throughout this period. A steady rain beginning 3 to 4 hours prior to the first test train run resulted in a gradual change in track conditions, so that the last two (highest speed) runs resulted in lower tie plate loads and reduced subgrade pressures. This phenomenon can be seen in the abbreviated data for runs on 12-10-69, Table 7. Apparently the tie was tamped such that the tie plate at the joint was supporting very nearly 100 percent of the wheel load on this first day--the load cells managed to survive a shocking 33,100 lb peak load under an E44 locomotive. The tie plate was removed at the end of the day's testing, and when replaced the following day supported a more

48

TABLE 6. RECORD OF TRAFFIC FOR WHICH TRACKSIDE RESPONSE WAS RECORDED

Date	Time	Train Description	Speed	Direction	Run
12/10	9:15 a.m.	Passenger, GG-1 & 5 Cars	78.3	South	1
"	1:30 p.m.	Passenger, GG-1 & 14 Cars	82.6	South	2
"	2:05 p.m.	Passenger, #172	Unkn.	North	3
"	2:13 p.m.	DOT Test Train	8.4	South	4
"	2:25 p.m.	Metroliner	116	South	5
"	2:30 p.m.	Passenger, GG-1 & 6 Cars	77.2	South	6
"	2:38 p.m.	DOT Test Train	27.0	South	7
"	3:00 p.m.	DOT Test Train	38.5	South	8
"	3:25 p.m.	Freight, 2 E44's	46.6	South	9
"	3:48 p.m.	Metroliner, 6 Cars	114	South	10
"	3:50 p.m.	DOT Test Train	54.7	South	11
"	4:38 p.m.	DOT Test Train	67.5	South	12
12/11	11:45 a.m.	DOT Test Train	Slow		13
"	1:12 p.m.	Metroliner	95.8	North	14
"	1:19 p.m.	Passenger, GG-1 & 14 Cars #135	79.5	South	15
"	1:23 p.m.	DOT Test Train	55.6	South	16
"	1:38 p.m.	DOT Test Train	74.6	North	17
"	2:05 p.m.	Passenger, GG-1 & 16 Cars #172	73.3	North	18
"	2:23 p.m.	Metroliner	115	South	19
"	2:35 p.m.	DOT Test Train	88.0	South	20
"	2:37 p.m.	Passenger, GG-1 & 6 Cars	80.9	South	21
"	2:48 p.m.	DOT Test Train	36.3	North	22
"	3:30 p.m.	DOT Test Train	115	South	23
"	3:50 p.m.	Metroliner	114	South	24
"	4:01 p.m.	DOT Test Train	101.5	South	25
"	4:14 p.m.	DOT Test Train	12.4	North	26
"	4:24 p.m.	Freight, 2 E44's, 33 Cars	53.0	South	27
"	4:34 p.m.	Passenger, Blue GG-1, 10 Cars	77.6	South	28
"	4:38 p.m.	DOT Test Train	71.8	South	29
"	4:48 p.m.	DOT Test Train	43.1	North	30
"	5:01 p.m.	DOT Test Train	40.0	South	31
"	5:18 p.m.	DOT Test Train	26.4	North	32
"	5:28 p.m.	DOT Test Train	54.1	South	33
12/12	9:13 a.m.	Passenger, GG-1, 10 Cars	79.5	South	34
"	10:18 a.m.	Metroliner, 6 Cars	115	South	35
"	10:20 a.m.	Passenger, GG-1, 9 Cars	80.4	South	36
"	10:30 a.m.	DOT Test Train	25.1	South	37
"	10:40 a.m.	DOT Test Train	28.6	North	38
"	11:00 a.m.	DOT Test Train	24.3	South	39
"	11:59 a.m.	Passenger, GG-1, 9 Cars #133	77.6	South	40
"	12:29 p.m.	DOT Test Train	13.4	North	41
"	12:38 p.m.	DOT Test Train	86.2	South	42
"	1:21 p.m.	Passenger, GG-1, 16 Cars #135	84.6	South	43
"	1:30 p.m.	Freight, 2 E44's	47.7	South	44
"	1:47 p.m.	DOT Test Train	120.1	South	45
"	2:03 p.m.	DOT Test Train	44.1	North	46
"	2:15 p.m.	DOT Test Train	55.2	South	47
"	2:55 p.m.	DOT Test Train	125.7	South	48
"	3:30 p.m.	DOT Test Train	54.2	South	49

1.7 psi

p_O = 4.0 psi   SUBGRADE PRESSURE CELL NO. 1

3.5 psi

p_O = 2.9 psi   SUBGRADE PRESSURE CELL NO. 11

7500 lb

NORTH TIE PLATE LOAD
(NO JOINT)

1 sec   Time

15,500 lb

SOUTH TIE PLATE LOAD (JOINT)

0.19 in.

SOUTH RAIL DEFLECTION (ABSOLUTE...JOINT)
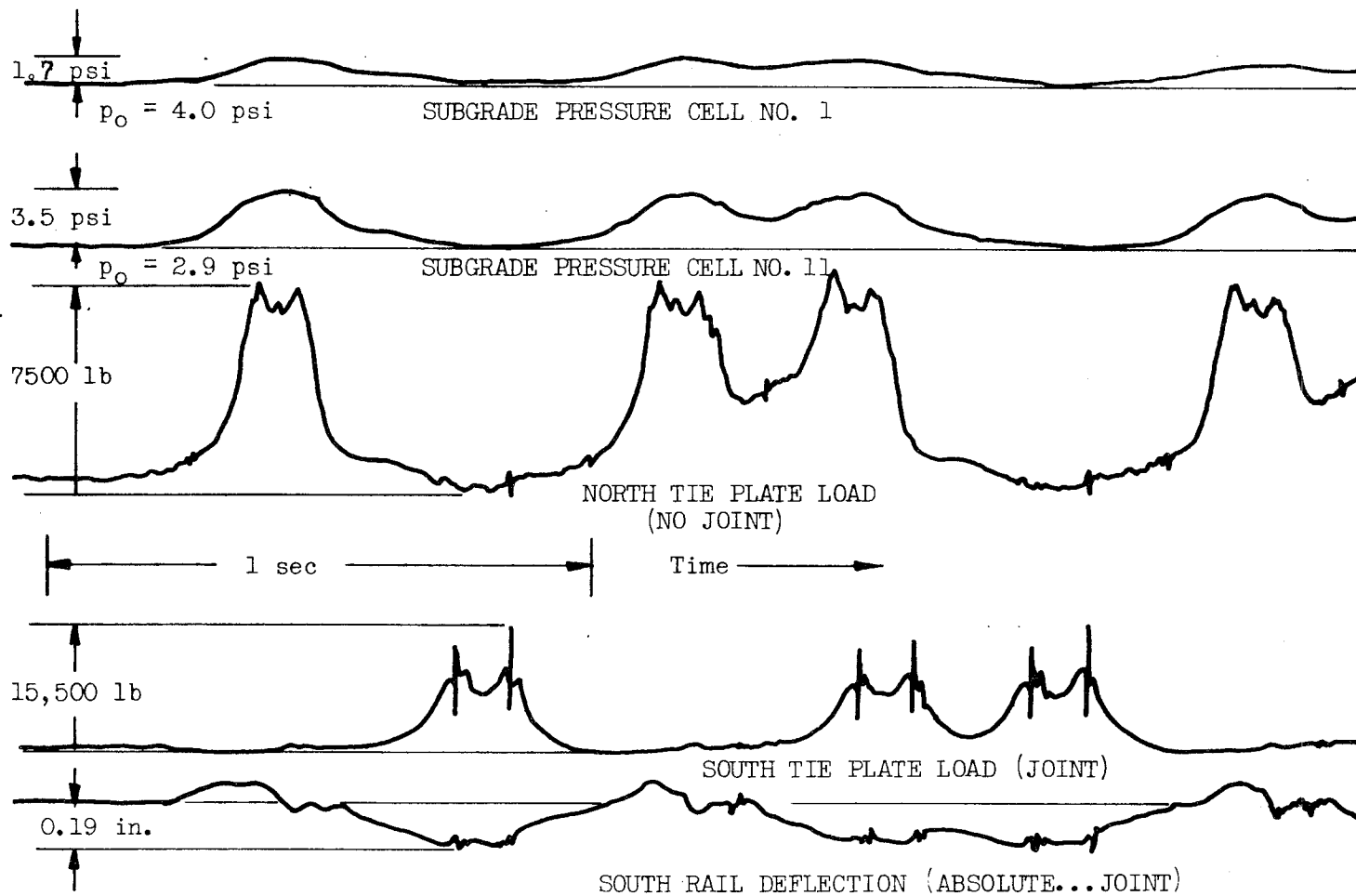
FIGURE 20.   TRACK DYNAMIC RESPONSE TO DEPARTMENT OF TRANSPORTATION TEST TRAIN
AT 55 MPH, PENN CENTRAL TRACK 3 AT M.P. 121.95, BOWIE, MD., 12-10-69

50

TABLE 7.   SUMMARY OF DATA TAKEN DECEMBER 10, 1969

Speed MPH	Run No.	Tie Plate Loads (Joint)		Subgrade Press.* (over static)		Rail Abs. Displ.	
		#2 Peak/ p-p	#15 Peak/ p-p	#8 Peak/ p-p	#11 Peak/ p-p	NRVDT Compress/ Extend	SRVDT Compress/ Extend
82.6 (GG1)	2	>14,500 3,000	30,900 15,200	1.68	4.40 1.40		
116 (Metro)	5	10,950 2,600	22,400 12,600	2.08	5.05 2.24		0.366 (spikes to 0.420) 0.134
8.4 (DOT)	4	8,400	13,300 3,450	1.6	4.8	0.030 0.008	0.210 0.035
77.2 (GG1)	6	14,500 2,250	26,200 16,600	2.48	5.52 1.76		0.285 (spikes to 0.349) 0.116
27.0 (DOT)	7	8,500	14,200 6,900	1.4	3.6	0.035 0.004	0.204 0.058
38.5 (DOT)	8	8,250 1,000	16,900 10,700	1.6	3.6	0.030 0.004	0.192 0.070
46.6 (E44)	9	>14,500 (off scale)	33,100 19,500	2.64	6.87 0.72		0.280 0.088
114 (Metro)	10	11,000 1,800	19,000 13,800	1.75	4.5 0.6	0.068 0.011 (spikes to 0.046)	0.337 (spikes to 0.420) 1.16 (spikes to 0.145)
54.7 (DOT)	11	8,100 1,000	15,600 10,700	1.2	3.2	0.030 0.023	0.195 0.093
67.5 (DOT)	12	7,950 1,100	14,800 10,200	1.2	3.1	0.030 0.011	0.198 (spikes to 0.244) 0.105

* Static pressure: #8 -- 2.49 psig
                     #11 -- 2.88 psig

reasonable 40 percent of the load. (It should be borne in mind that through-out the test period, the track condition was changing in response to action of both the track crew and the rainy weather.)

Tests on the second day provided a wide range of useable data, in terms of speeds and types of traffic; test train runs as high as 115 mph were recorded. A summary of the data is given by Table 8. A plot of tie plate load versus speed (away from the joint) will show that the load increases linearly in the speed range of 15-90 mph, then starts to increase at a higher rate.

From this data the vertical stiffness of the test track was obtained as shown by Figure 21. The track stiffness away from the joint was found to be very nearly linear: a 500-750 lb preload was recorded on the tie plate, and an average 46 percent of the static wheel load was sup-ported by the instrumented tie plate. The overall stiffness of 351,000 to 492,000 lb/in. (calculated by dividing a single wheel load by maximum rail deflection) was significantly higher than the 221,000 lb/in. used in previous computer runs.

At the joint a decidedly nonlinear characteristic was found, with an average stiffness under higher loads (the steeper slope) of 140,000 lb/in., about one-third of the stiffness away from the joint. The use of a 75 percent joint stiffness (166,000 lb/in.) and a "geometric error" of 0.1 to 0.3 inch in the previous computer program was, then, coincidentally quite close to the test conditions measured nearly a year later.

Rail vertical acceleration data using a high frequency-response recording system were obtained on December 12, as well as tie plate load and pressure cell data. For this day's runs both tie plate load cells were located away from the joint, opposite one another on the same tie. The tie plate newly-located under the west rail was found to carry roughly 40-42 percent of the wheel load, slightly less than the 46 percent carried under the east rail. Data from runs on December 12 are given in Table 9. Of particular note are the rail accelerations at the joint, reaching well over 300 g's with the 115 mph Metroliner.

52

TABLE 8. SUMMARY OF DATA TAKEN DECEMBER 11, 1969

Train	Run No.	Speed (MPH)	Time (12/11/69)	Direction	Tie Plate Load No Joint Lb Peak	No Joint Lb P-P	Joint Lb Peak	Joint Lb P-P	Subgrade Pressure Cell #9 Peak	Cell #9 P-P	Cell #11 Peak	Cell #11 P-P	Rail Displacement No Joint Peak	No Joint P-P	Joint Nom.	Joint Spike
DOT Test	13a	slow	11:45 a.m.	N	6,850		5,800				1.77	0.27	0.030		0.250	
" "	26	12.4	4:14 p.m.	N	8,520	315	8,180	3,410	1.24	0.36	1.77	0.23	0.033		0.256	
" "	32	26.4	5:18 p.m.	N	8,470	580	7,670	3,410	1.29	0.40	1.78	0.18	0.038	0.081	0.280	0.315
" "	22	36.3	2:48 p.m.	N	8,630	685	7,340	3,410	1.38	0.29	1.91	0.27	0.048	0.075	0.270	0.310
" "	31	40.0	5:01 p.m.	S	9,000	700	8,800	5,110	1.20	0.09	1.91	0.14	0.048	0.085	0.262	0.310
" "	30	43.1	4:48 p.m.	N	8,670	530	8,700	4,100	1.24	0.31	1.91	0.25	0.049	0.087	0.280	0.321
" "	33	54.1	5:28 p.m.	S	8,840		8,700	6,100	1.15	0.22	1.91	0.27	0.045	0.095	0.268	0.308
" "	16	55.6	1:23 p.m.	S	8,320	1,000	7,850	4,260			2.13	0.50	0.077	0.112	0.290	0.330
" "	29	71.8	4:38 p.m.	S	9,210	1,160	9,050	5,630	1.33	0.31	2.14	0.55	0.053	0.105	0.286	0.370
" "	17	74.6	1:38 p.m.	N	9,480	1,300	8,350	5,300			2.18	0.73	0.075	0.110	0.286	0.342
" "	20	88.0	2:35 p.m.	S	9,590	1,160	10,250	7,000	1.60	0.49	2.05	0.77	0.045	0.098	0.274	0.370
" "	25	101.5	4:01 p.m.	S	9,950	1,350	11,100	8,180	1.60	0.67	2.45	1.00	0.065	0.118	0.274	0.357
" "	23	115	3:30 p.m.	S	10,700		13,300	8,860	1.73	0.71	2.54	1.00	0.056	0.140	0.286	0.357
" "	37	25.1	Next Day 10:30 a.m.	S	7,100	790			1.26	0.30	1.67	0.17	0.043			
Pass. (GG1)	15	79.5	1:19 p.m.	S	17,200	8,900	14,800	8,900			4.22	1.77	0.150	0.130	0.374	0.428
" "	18	73.3	2:05 p.m.	N	15,300	2,900	11,800	5,500	3.33	1.20	4.45	1.59	0.070	0.090	0.327	0.387
" "	21	80.9	2:37 p.m.	S	16,000	8,900	15,700	9,900	2.80	1.56	3.91	2.09	0.135	0.182	0.316	0.411
" "	28	77.6	4:34 p.m.	S	16,300	7,200	15,500	9.050	2.54	1.29	3.73	1.87	0.105	0.140	0.345	0.416
Metroliner	14	95.8	1:12 p.m.	N	11,600	1,840	11,100	7,700			3.76	1.14	0.075	0.115	0.380	0.500
"	19	115	2:23 p.m.	S	13,250	1,850	15,400	10,600	2.22	0.84	3.32	1.32	0.053	0.160	0.298	0.399
"	24	114	3:50 p.m.	S	13,900	3,320	15,200	10.750	2.26	0.93	3.41	1.50	0.068	0.143	0.357	0.435
Freight (E44)	27	53.0	4:24 p.m.	S	18,700	7,900	21,800	15,000	3.11	0.50	4.63	1.00	0.090	0.178	0.335	0.430

(over static pressure)
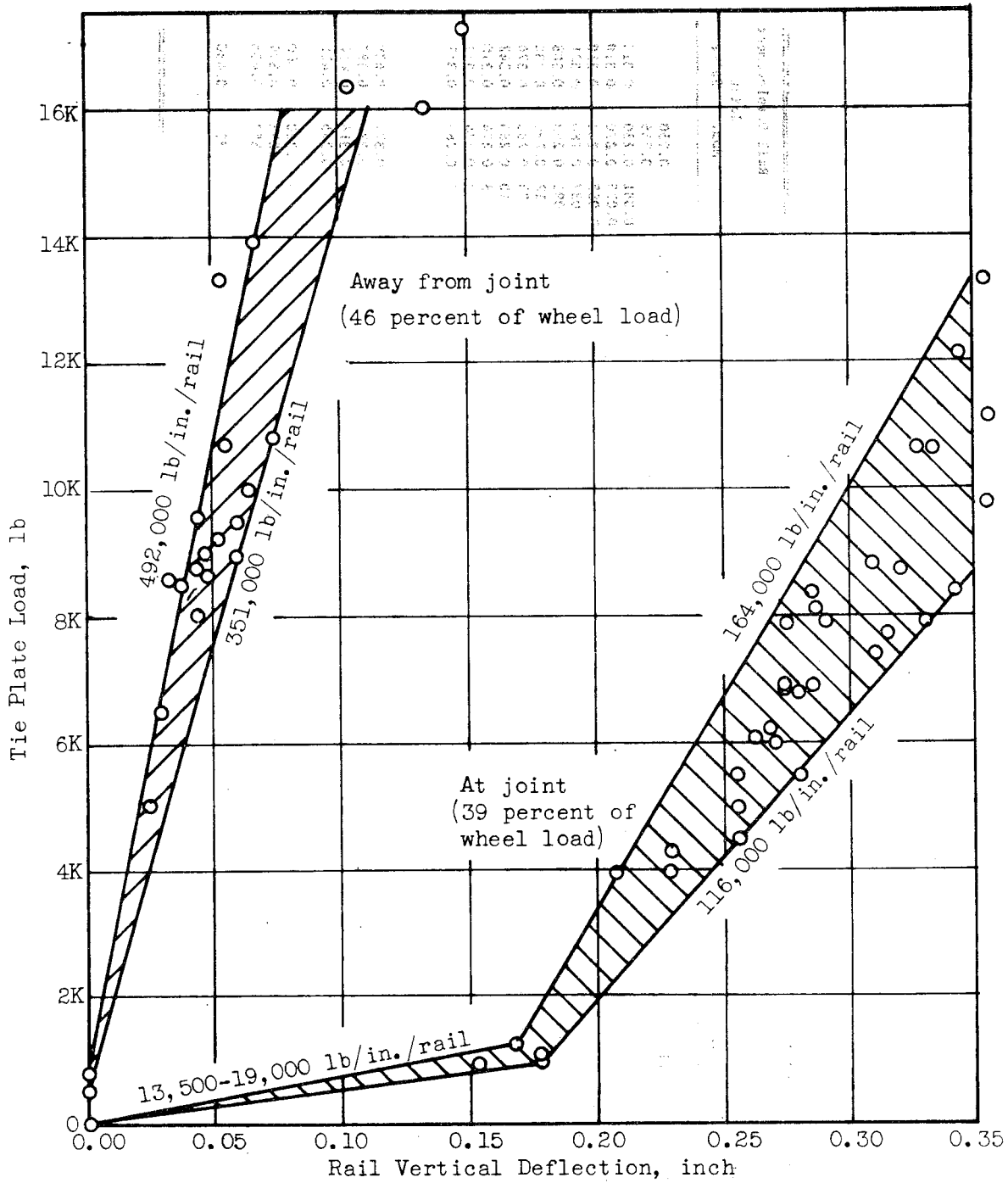
FIGURE 21. MEASURED TRACK SPRING RATE AT A JOINT AND AWAY FROM A JOINT

54

TABLE 9. SUMMARY OF DATA TAKEN DECEMBER 12, 1969

| Speed MPH | Run No. | Tie Plate Loads | | Subgrade Pressures* | | | | Acceleration at Joint | | |
		#2 Peak	#15 Peak	Pressure Cell #9 (over static) Peak	p-p	Pressure Cell #11 (over static) Peak	p-p	p-p	+	-
115 metro	35	10,200	8,900	2.22	0.91	3.04	1.17	590 to 670	310 to 324	280 to 346
80.4 GG1	36	11,400	10,600	2.48	1.52	3.58	1.95	436	171	265
25.1 DOT	37	7,100	5,620	1.26 (1st axle) 1.04 (2nd axle)	0.30	1.67	0.17 max	89 (both axles) (94	24 20	65 74)
77.6 GG1	40	14,300	10,250	2.35	1.43	3.50	1.79	576	228	348
86.2 DOT	42	7,800	6,150	1.26	0.44	1.42 (1st axle) 1.96 (2nd axle)	0.71	369 (1st axle) 331 (2nd axle)	130 121	239 210
13.4 DOT	41	6,900	5,800	0.91 (1st axle) 1.26 (2nd axle)	0.39	1.62	0.21	41 (both axles)	15	26
44.1 DOT	46	7,250	5,970	0.96 (1st axle) 1.22 (2nd axle)	0.39	1.74	0.25	212 (1st axle) 177 (2nd axle)	88 59	124 118
55.2 DOT	47	7,260	6,140	1.31 (1st axle) 1.13 (2nd axle)	0.31	1.75	0.27	304 (1st axle) 274 (2nd axle)	98 59	206 215

* Static pressure: #9 -- 2.43 psig
                     #11 -- undetermined

Tie plate galvo 2 -- east rail
    "   "   " 15 -- west rail

Comparison of Predicted Response with Measured Response

The purpose of the field measurements was to validate the computer programs for predicting vehicle-track response, and/or to indicate areas where refinements or changes to the programs were needed. Although there were many differences in the conditions of the comparison (for example, rail joint in one rail only), a good idea of the degree of correlation was obtained.

Considering first the case where no rail joint was present, the question of roadbed spring rate was paramount. The measurements on the C&O/B&O (judged to be a well-maintained track) showed that the spring rate was nonlinear, with a value of 250,000 lb/in. for a tie plate load of around 8000 pounds. On the other hand, the Penn Central track away from the joint gave a more linear spring rate, with an average value of approximately 400,000 lb/in. These facts, combined with the fact that the spring rate at the Penn Central joint was very nonlinear, led to the conclusion that "looseness" in the track such as rail-tie plate and tie-ballast clearances produced the nonlinear effect; once these clearances are taken out the basic roadbed spring rate is more nearly linear. However, the degree of nonlinearity may be different for each tie. In fact, for both mainline tracks it was noted that the traces of tie plate load were not symmetrical about a vertical centerline. This could be caused by the presence of damping or of different spring rates on either side of the particular tie that was instrumented. A check of the data showed the latter to be true; runs were made in both directions and the data showed the same side was always softer. This illustrates the difficulty in defining a standard or uniform track with which to validate computer results.

Another point of validation concerns the subgrade pressures: the presence of individual pulses for the longer wheelbase cars was confirmed, and the data indicated the pressure profiles were not changed appreciably as the speed increased from 15 mph to 135 mph. While ideally

all of the pressure cells would show nearly identical readings, the actual range of dynamic pressures for the DOT car was from around 1.0 to 2.5 psi, once again illustrating the nonuniformity of a conventional track. (Whether or not the outputs become closer as the roadbed stabilizes remains to be seen.) For the 10,000-pound tie plate load measured, the subgrade pressure calculated by the 20° pyramid method is 6.4 psi at a depth of 3 feet, so the quantitative correlation is not particularly good. If a 30° angle is assumed, the calculated pressure is reduced to 3.2 psi, much closer to the measured value.

One final point here concerns roadbed damping. With the computer simultation of the smooth track, the degree of damping in the structure was low enough that the peak wheel-rail (or tie plate) load was essentially unchanged with speed. The measured loads, on the other hand, showed a very gradual but definite increase with speed. Unfortunately, the DOT research car equipped to measure track profile was not available at the time the runs were made, but it is believed that it was the imperfect track profile, rather than the presence of more damping than was simulated, that caused the wheel-rail load to increase with speed.

Considering response now at the rail joint, a comparison of computed and measured response is shown in Table 10. In this table the computer data for the runs with a "geometric error" of 0.2 inch are compared with the field data. A good comparison between peak wheel loads is found, but the measured "spikes" or impulse loads are much higher, in spite of the fact that both "computer rails" had joints side-by-side. As mentioned before, the comparison of data traces showed that the gap in the actual rail changed the response qualitatively as well as quantitatively. The inclusion of the rail gap is relatively easy to do in the computer program, and would improve the simulation; the "negative spike" will be introduced and computed accelerations will be increased. However, to increase the frequency of the force transient to correspond with measurements, it may also be necessary to decrease the effective mass of the rail.

The computer traces (see Figure 15) of the simulated "standard" track at a fixed point during passage of one truck of the model DOT test car showed two distinct frequencies: a higher-frequency response seen in the force and acceleration traces (160-170 Hertz) and a lower-frequency response

57

TABLE 10. COMPARISON OF COMPUTED AND MEASURED TRACK RESPONSE DATA

	Speed	Tie Plate Load Lb Peak	Lb P-P	Wheel Load* Lb Peak	Lb P-P	Displacement In. Nom	Max "Spike"	Rail Acceleration, G +	-
Computer	30			16,800	2,700	0.278			
Test	26.4	7,670	3,410	16,700	7,410	0.280	0.315		
Computer	60			20,400	4,850	0.289			
Test	55.6	7,850	4,260	17,100	9,270	0.290	0.330		
Computer	90			22,700	7,800	0.299			
Test	88.0	10,250	7,000	22,300	15,200	0.274	0.370		
Computer	120			24,300	11,800	0.310			
Test	115	13,300	8,860	28,900	18,900	0.286	0.357		
Computer	30							3.7	17
Test	25.1							24	65
Computer	60							12	34
Test	55.2							98	206
Computer	90							12	49
Test	86.2							130	239
Computer	120							13	67
Test	120.1							290	335

* Assuming tie plate supports 46 percent of wheel load.

58

(26 Hz). The higher frequency results from the rail effective mass oscillating on the tie stiffness, while the lower frequency represents the sum of the unsprung masses (test car truck, rail, and ballast effective masses) oscillating on the overall track spring rate. An even higher frequency (roughly 800 Hz) was present, but not evident due to the slow chart speed: this represents the "contact resonance" of the rail mass on the wheel-rail contact stiffness.

In examining the test traces, the 26 Hz was found to be quite distinct in subgrade pressures and occasionally in rail absolute displacement. A pot pourri of higher frequencies were generated by the test train, varying in distinctness from run to run. The more prominent frequency bands noted were: 25-30 Hz, 50-70 Hz, 100-130 Hz, 150-170 Hz, 250-260 Hz, 450-500 Hz, and (with the high chart speed) 800 Hz. The actual track structure appears to be non-linear enough to generate harmonics and subharmonics, depending on the type of excitation.

In summary, the field measurements indicated definite areas in which refinements could be made to improve the computer simulations. On the other hand, they also revealed the degree of nonuniformity that exists on conventional tie-type track--even between two adjacent locations on a given track. Therefore, it appears that the errors in simulation are no greater than the degree of nonuniformity of a conventional track. As is true in many cases, then, the computer programs should be viewed not as sources of data which will compare quantitatively with measured data with an accuracy of a few percent, but as analytical tools for studying various track designs and the effects of changes in the many parameters involved in a conventional track structure. For these purposes, the computer simulations are considered to be very suitable.

Development and Analysis of Nonconventional Track Structures

In the previous section of this report, research relating to conventional tie-type track was described. These studies, including computer analyses validated by data from trackside measurements obtained at speeds up to 120 mph, fulfilled the basic objectives of (1) furthering the understanding of conventional tie-type track, particularly its dynamic response at high speeds, and (2) providing a bench mark, or reference, for evaluating concepts for advanced track structures.

Throughout the entire track structure program, particular emphasis was placed on the tie-ballast interface, regarding this as the area having the most potential for improving track stability. Therefore, the "pressure signature" of the tie on the ballast was considered most carefully. As predicted by calculations (Figure 1) and verified by the field measurements (Figure 17), individual pressure or load pulses may or may not be transmitted into the roadbed each time an axle passes over, depending on the specific vehicle and track parameters--particularly the axle spacing and the subgrade modulus. Therefore, for vehicles with larger axle spacings, including most locomotives and passenger cars, there is one definite pressure pulse per axle; this was noted even in the signals from the subgrade pressure cells located in the ballast 3 feet below the base of the ties (see Figure C-1). For freight car trucks with wheelbases on the order of 5-1/2 to 6 feet, the individual pulses usually do not occur, depending on the roadbed modulus.

Following the basic approach that an "advanced" track structure is one that will be more stable because of reductions in pressure at the critical ballast area, early in Phase I it was realized that the number of pressure pulses exerted on the subgrade, as well as the magnitude of the pressure pulse, was an important parameter. It was further postulated that if the track structure could be made stiff enough that a single pressure pulse were developed beneath a truck (two axles) instead of beneath each individual axle, a doubling of the speed of the train--for example, from 80 miles an hour to 160 miles an hour--could occur without an increase in the number of pressure pulses transmitted into the subgrade. These requirements--

60

that is, reducing the magnitude of the pressure transmitted into the ballast/subgrade, and reducing the number of pressure pulses developed on the ballast/subgrade support--were considered to be the key requirements for a more stable track.

Considering first the basic requirements of reducing ballast/subgrade pressures, this requirement can, of course, be met with conventional track construction by increasing the bearing area of the ties, decreasing the tie spacing, or both. (Unfortunately, with the advent of the concrete tie which has a larger bearing area, tie spacing has been increased in order to keep the cost consistent with that of wood tie construction, with the net result that in many installations the bearing pressures are not reduced and track stability is not improved.)

On the other hand, the requirements of reducing the number of pressure pulses can be met only by providing a track structure with substantially increased bending stiffness along its length, requiring some type of continuous longitudinal rail support. Thus, the intuitive thought of replacing the lateral ties in conventional track by a continuous slab or longitudinal beam-type structure became a necessity in order to meet these stability criteria.

Attention then was devoted to the development of a design criterion for continuous longitudinal beam or slab-type track structures, based on tie-type track as a reference. Included in this development was the restriction that the pressure between wheels on one truck could not be less than that directly under a wheel--another way of saying that individual pressure pulses per wheel were eliminated. This design criterion was based on the settlement rate of soil under dynamic loading--unfortunately a subject about which little is known. The development of this design criterion is fully described in Appendix D, taken from Reference 1. A parameter called the Soil Deterioration Factor (SDF) was defined, and the SDF was then calculated for beams and slabs of various sizes and stiffnesses, giving a quantitative measure of stability. For example, Figure 22 shows the bearing pressure versus time curves calculated for five different track structures carrying a 100,000 pound car

61

I. (160 mph)

$EI = 8550(10)^7$
$lb\text{-}in^2$
$W = 14.0$ in/rail

II. (160 mph)

$EI = 4500(10)^7$
$lb\text{-}in^2$
$W = 21.5$ in/rail

III. (160 mph)

$EI = 8850(10)^7$
$lb\text{-}in^2$
$W = 43$ in/rail

IV. (160 mph)

$EI = 4500(10)^7$
$lb\text{-}in^2$
$W = 43$ in/rail

CONVENTIONAL TRACK
STRUCTURE (53.3 mph)

100 lb/yd.
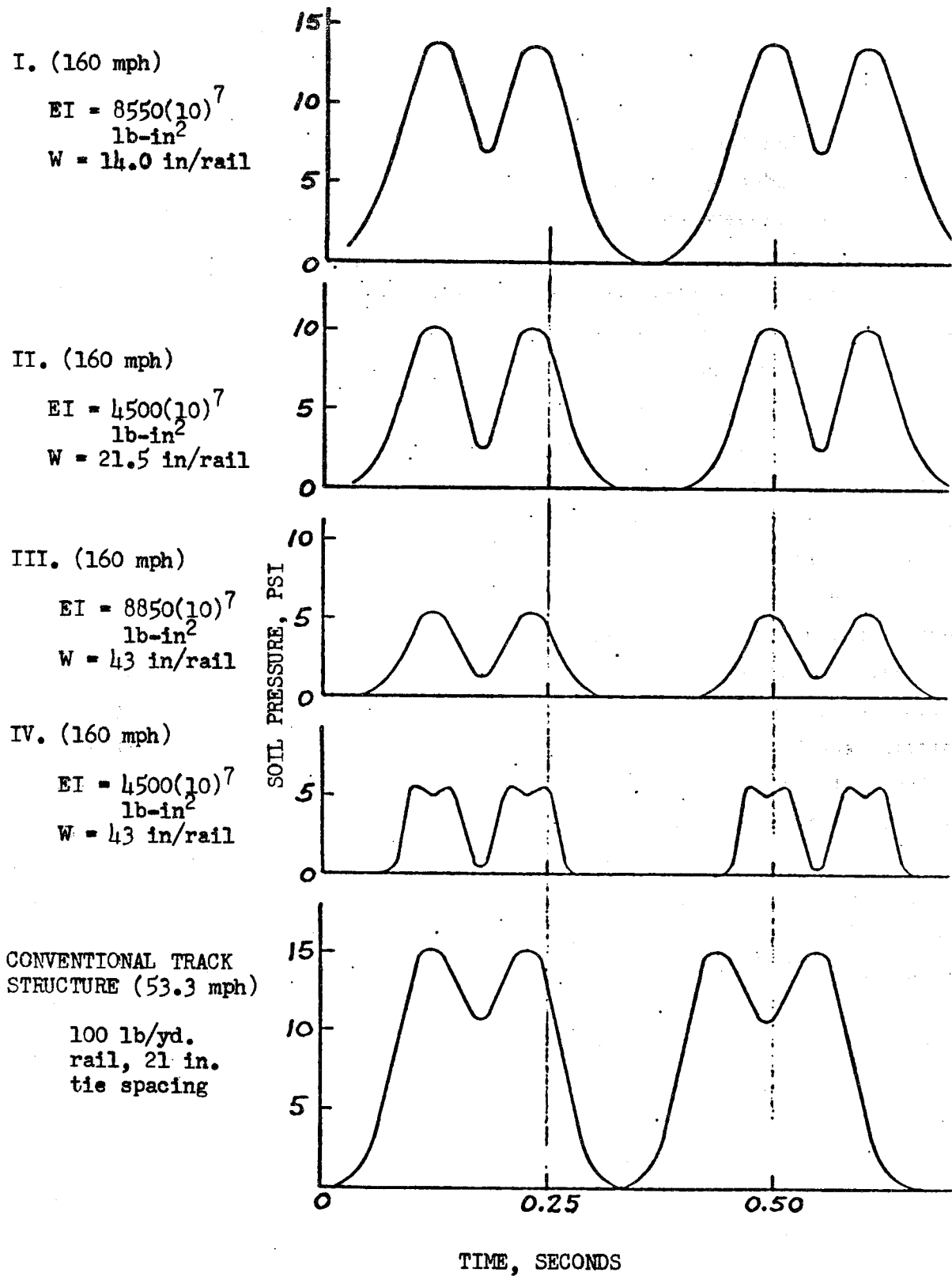rail, 21 in.
tie spacing

SOIL PRESSURE, PSI

TIME, SECONDS

FIGURE 22. SOIL PRESSURE-TIME CURVES FOR TRACK STRUCTURES OF
DIFFERENT WIDTHS AND RIGIDITY (SOIL MODULUS $k_o =$
500 lb/in^3)

62

(based on the Budd-built Silverliner passenger cars). The SDF's calculated for structures I, II, and III were the same, and were equal to that calculated for "typical" conventional track. However, the speeds were different, being 53 mph for the conventional track and 160 mph for the others. In other words, this indicated that structures I, II, and III would provide the same stability with trains running at 160 mph as would the conventional track with trains running at 53 mph. (Structure IV was "disqualified" because of the presence of an individual pressure pulse per wheel.)

Development of Longitudinal Beam and Slab-Type Track Structures

Examination of the structures shown in Figure 22 will reveal that all of them are quite massive and have a high bending stiffness. The next step in the Phase I concept study was to consider the various types of continuous longitudinal type track support structures which might be used, in an attempt to translate the design criteria into the most practical structures. On one extreme a relatively wide but shallow slab structure (very analogous to a modern highway or runway) was considered, while on the other extreme a structure having two individual narrow but deep continuous beams--one beneath each rail--was considered. Many designs within these extremes have been proposed, and while a detailed cost analysis was not within the scope of the limited concept study, a simplified cost analysis was made in an attempt to determine the most economical structure within the wide range of limits mentioned above.

For any of these structures, the engineering materials which were considered to be appropriate for the application were steel and concrete. Relative costs were calculated, considering such factors as the amount of excavation and the volumes of material required to build track structures ranging in design from slabs to deep, narrow beams, but with bending stiffness kept constant. The conclusion of this limited cost study was that an intermediate structure consisting of two beams having roughly square cross-sections would be the most economical to construct.

63

Further engineering analyses of the range of structures showed that while the deep, narrow beams provide the stiffness required to reduce the number of pressure pulses transmitted into the soil--in fact, one pressure pulse per two trucks of adjacent cars can be obtained with this type of structure--the bearing area of two deep but narrow (say 6 inches) beams resulted in an overall bearing pressure higher than that obtained with conventional tie-type construction. On the other hand, a wide slab which was relatively shallow (say 6 inches) met the requirement of reduced pressure magnitude, but was not necessarily stiff enough to eliminate the individual pressure pulse per wheel unless uneconomical amounts of steel reinforcement were used.

Based on these considerations, further design optimization of the twin-beam type structure was carried out, considering the trade-off between the cost of the steel reinforcement and concrete, in an effort to define the most economical design for a cast-in-place reinforced concrete twin-beam structure that would meet the stiffness criterion.

As with most engineering problems, there are often conflicting design requirements which in the end must be compromised in the most practical manner to obtain a final design. The track structure was no exception, for the stiff beam-type structure which was required to reduce ballast/subgrade pressures and thereby improve stability was not necessarily desirable from the standpoint of wheel-rail loads and vehicle ride. This was the subject of a dynamic analysis which was performed concurrently with the static analysis; this is described in a later section of the report.

Based on the considerations just discussed, at the end of Phase I four longitudinal beam and slab-type structures were recommended for further consideration; the two preferred ones are shown in Figures 23 and 24. Rough cost estimates indicated that the costs would range from $250,000 to $300,000 per single track mile, exclusive of rails and fasteners. Thus, at the end of the Phase I study, a good understanding of the design requirements had been gained, specific criteria governing the design of longitudinal beam or

64

Reinforced concrete cross-tie (20-ft intervals)

Cast-in-place rail attachments

23.3"

Reinforcing rods

Longitudinal reinforced concrete beams (EI = 4500 x 10^7 lb-in.^{2}/beam)

21.5"

65
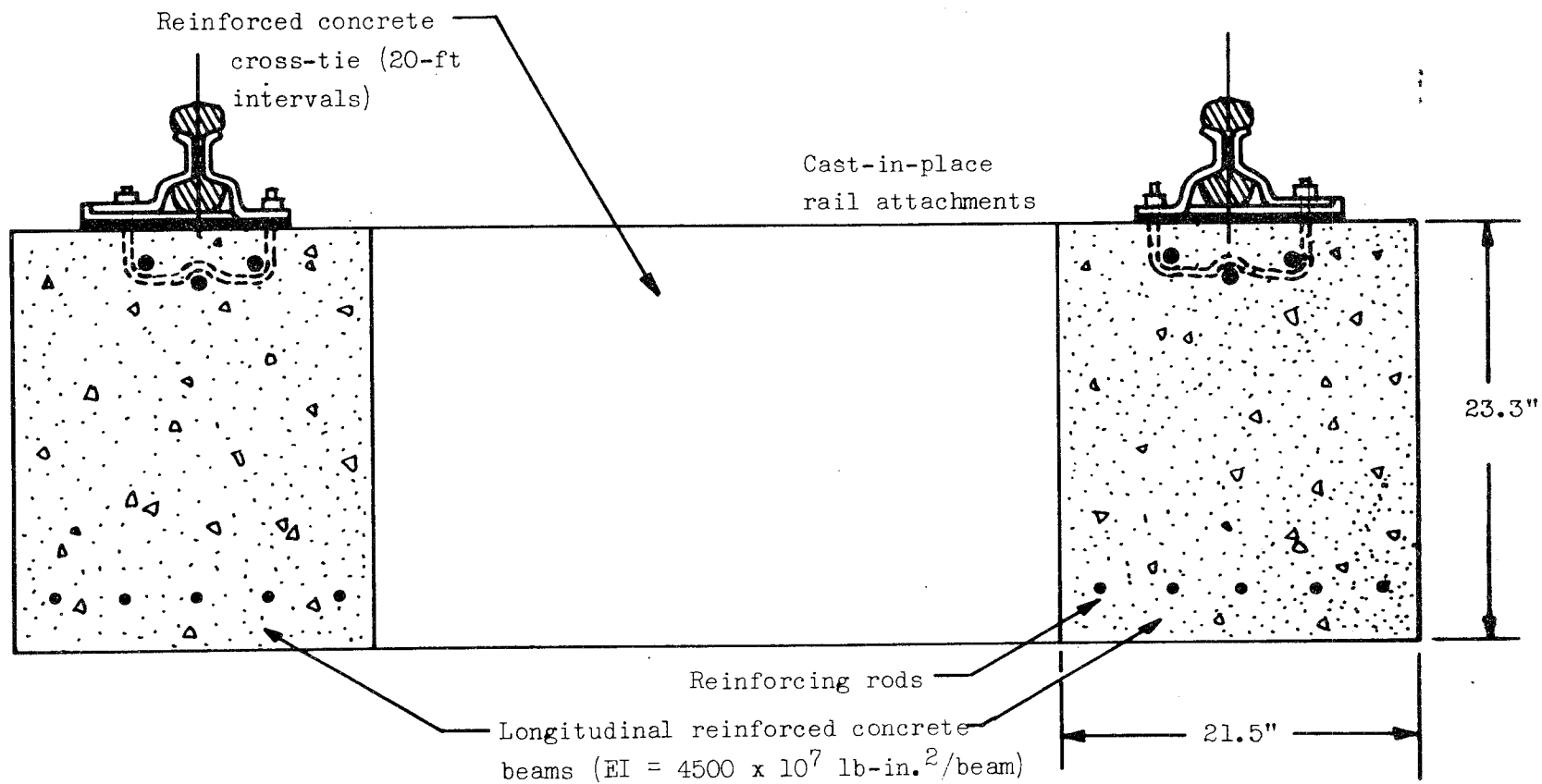
FIGURE 23. TWIN REINFORCED CONCRETE BEAMS WITH DOUBLE-HEADED RAILS

Reinforced concrete slab

Neoprene

Drain hole

WIRAND* concrete

24"

42"

Reinforcing rods

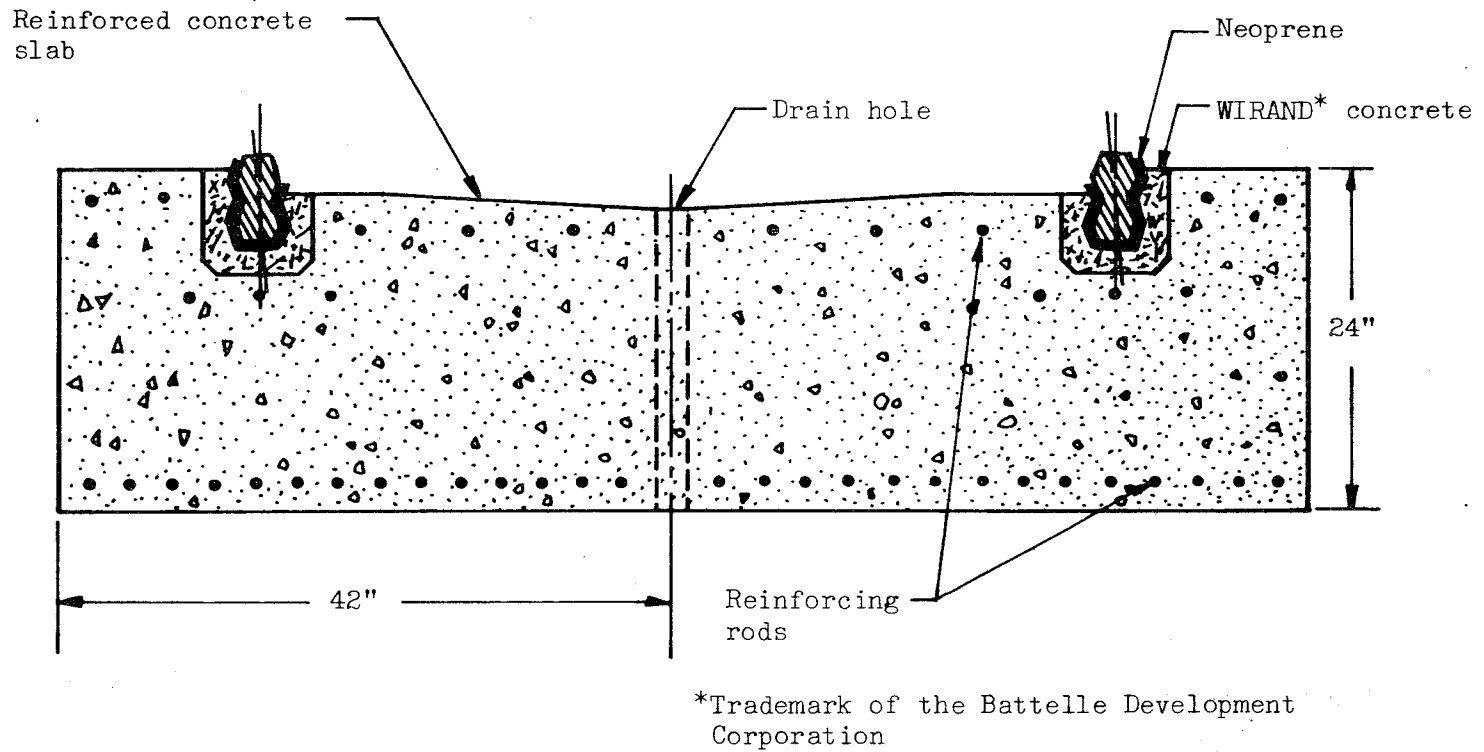*Trademark of the Battelle Development Corporation

FIGURE 24.   REINFORCED-CONCRETE SLAB TRACK STRUCTURE USING NEOPRENE-ENCAPSULATED RAIL

slab-type structures had been developed, the effect of resilience in the fasteners had been defined, and four specific structures were suggested as possibilities for serious consideration for further analysis and eventual installation.

Phase II of the research covered the period from October, 1967 to March, 1968, and was directed at a comparative analysis of eight other track structures, five of which were conventional or semi-conventional, and three of which were specific nonconventional designs suggested by others. No effort was devoted to the refinement of the basic structures recommended earlier.

Work on Phase III of the project started in November, 1968, and shortly after this, DOT and the Santa Fe Railroad announced the possibility of proceeding with a cooperative experimental track installation somewhere west of the Mississippi. Intensive analysis of the longitudinal beam and slab structures was then renewed, with the emphasis shifted from the high-speed passenger application in the Northeast Corridor presumed up to that time, to application in a heavy freight railroad in the west or southwest.

Although the longitudinal beam-slab concepts developed during Phase I showed great promise technically, economically they were considered to be too expensive. Attention was, therefore, devoted to the tradeoff between bending stiffness (EI) and cost. Both the cost and the bending stiffness are, of course, directly related to the amount of steel and concrete used in the structures, and it was decided that a careful study of the implications of using smaller (therefore cheaper) and more flexible beams and slabs was needed.

Response to Static Wheel Loads

At the start of Phase III, a digital computer program was written to facilitate the static analysis of the nonconventional track structures. In this program, a longitudinal track structure was represented as a continuous beam (rail) on a continuous uniform support (resilient fasteners) in turn resting on another continuous beam (support beam or slab) resting on

67

another continuous uniform support (roadbed). Inputs to the program were the rail EI, fastener spacing and resilience, beam EI and width, subgrade modulus, wheel spacing, and wheel vertical load. Outputs from the program included rail deflection and bending moment (convertible to stress), fastener deflections and loads, beam deflections and bending moment, and subgrade deflection and bearing pressure. The program assumed linear spring characteristics for roadbed and fasteners.

A series of runs were made with this program to determine the static load-deflection characteristics of slab and beam-type structures having a wide range of geometries and bending stiffnesses. The range of geometries that were included are shown in Figure 25, together with a plot of the bearing pressure as a function of distance along the track (with Station 0 representing the coupler, and axle loads at Stations 54 and 126). These results quickly illustrated the fact that all structures except the deep narrow beams had bearing pressures lower than conventional track, while the narrow beams had much higher bearing pressures. A direct computer output plot for a 12 inch deep slab is shown in Figure 26, while Table 11 shows a summary of the results of the computer runs. The bending stiffnesses for the various cross-sections were calculated on the assumption that the concrete was resisting both tension as well as compression. Therefore, they represented either prestressed beams or cast-in-place steel-reinforced beams.

Note that the upper curve in Figure 26 is the beam deflection, while the lower curve is the rail deflection. The vertical differences between the two curves represent the resilient fastener deflection. By multiplying the maximum difference in deflection by the fastener spring rate, the maximum fastener load can be obtained. For the particular case shown, the maximum fastener load was 18,200 pounds, or just over half the 35,000 pound wheel load.

The results of these computer runs showed several interesting facts. First of all, for even the most flexible slabs (6 inches deep), individual wheel pulses in the bearing pressure were not obtained with the
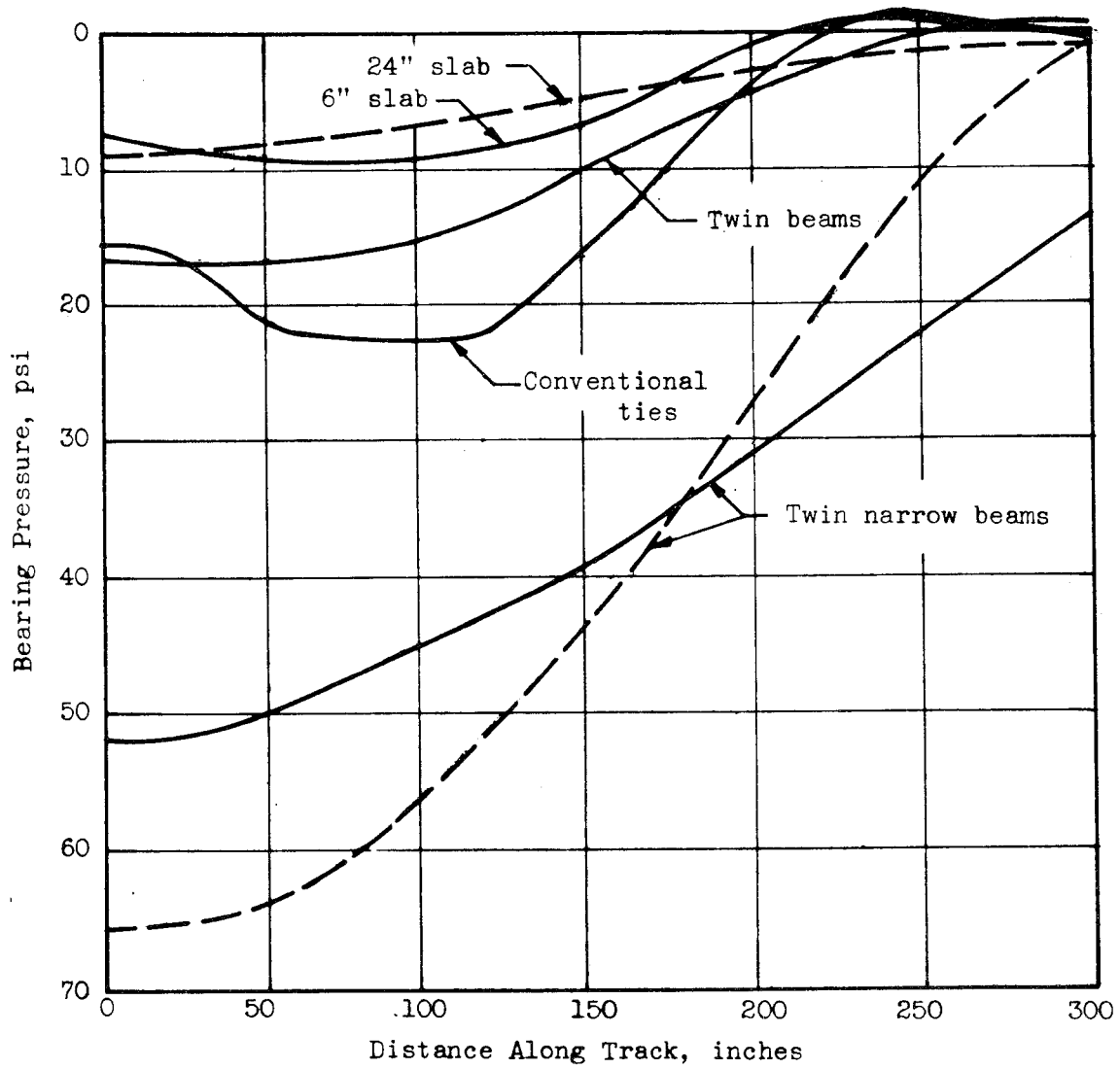
68
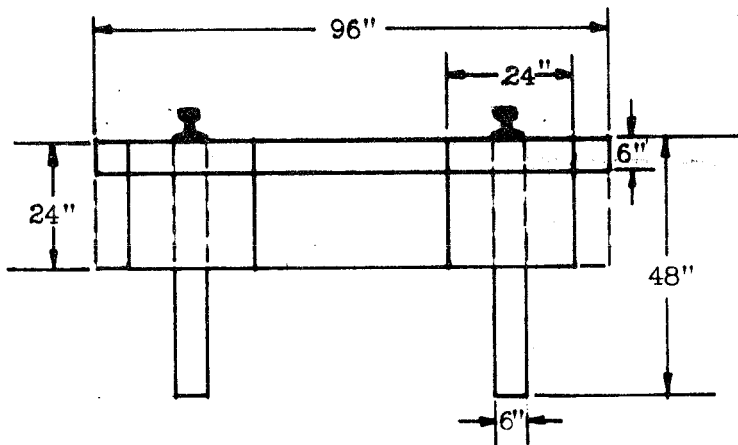
FIGURE 25. COMPARISON OF BEARING PRESSURES OF TRACK STRUCTURE

69
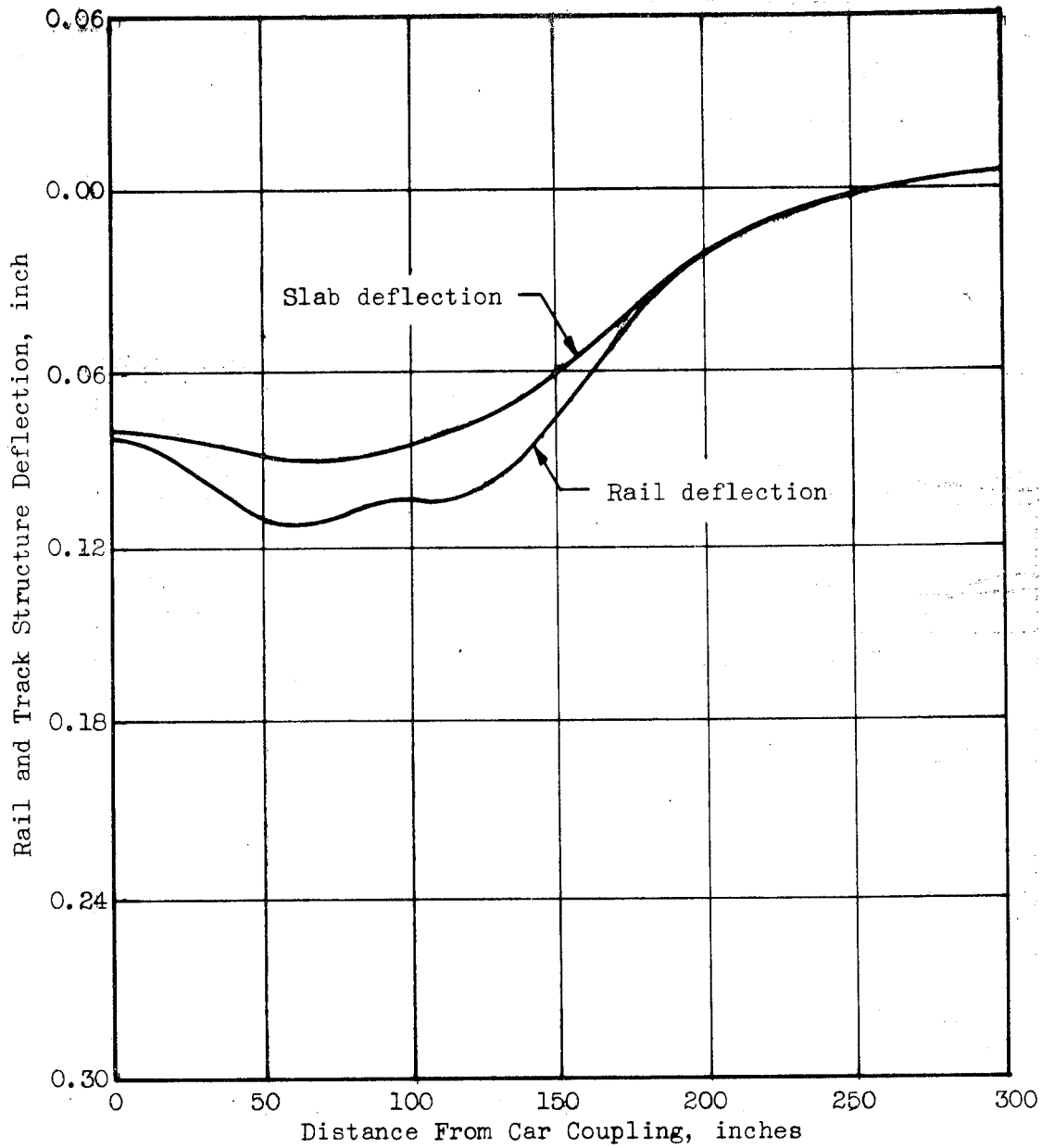
FIGURE 26.   RAIL AND SLAB DEFLECTIONS FOR A 12 INCH DEEP
REINFORCED CONCRETE SLAB TRACK STRUCTURE

70

TABLE 11.   RESPONSE OF REINFORCED CONCRETE SLAB AND BEAM-TYPE
STRUCTURES TO STATIC VERTICAL LOADS*

Slab Beam Depth, inches	EI (One Slab or Two Beams) lb-in.^{2}	Rail Deflection, inches	Peak Rail Stress, psi	Slab or Beam Deflection, inches	Slab or Beam Stress, psi	Slab or Beam Bearing Pressure, psi
Case I - 8-ft Slab, K_o = 100 lb/in.^{3}, Fastener Spacing = 30 in.						
6	516 x 10^7	0.117	11,150	0.099	2,340	9.9
12	4,140 x 10^7	0.113	9,940	0.088	1,940	8.8
18	13,380 x 10^7	0.111	9,400	0.085	1,520	8.5
24	32,240 x 10^7	0.107	9,260	0.083	1,250	8.3
Case II - 8-ft Slab, K_o = 100 lb/in.^{3}, Fastener Spacing = 18 in.						
6	516 x 10^7	0.111	10,650	0.099	2,610	9.9
12	4,140 x 10^7	0.106	9,260	0.088	2,000	8.8
18	13,380 x 10^7	0.103	8,680	0.085	1,550	8.5
24	33,240 x 10^7	0.099	8,550	0.083	1,240	8.3
Case III - 8-ft Slab, K_o = 500 lb/in.^{3}, Fastener Spacing = 30 in.						
6	516 x 10^7	0.047	9,600	0.022	1,025	10.85
18	13,380 x 10^7	0.044	9,150	0.018	800	9.15
Case IV - Twin Beams, 2-ft Wide, K_o = 100 lb/in.^{3}, Fastener Spacing = 30 in.						
15.1	4,140 x 10^7	0.199	10,300	0.172	3,190	17.2
22.7	13,380 x 10^7	0.190	9,650	0.168	2,640	16.8
Case V - Twin Beams, 6-in. Wide, K_o = 100 lb/in.^{3}, Fastener Spacing = 30 in.						
24	4,140 x 10^7	0.671	11,650	0.661	9,580	66.1
36	13,380 x 10^7	0.599	10,850	0.590	9,800	59.0
48	33,240 x 10^7	0.523	10,300	0.521	8,800	52.0

* 35,000 lb wheel loads, 136 lb rail, 6 ft axle spacing

71

6 foot freight car axle spacing. Note that in Figure 26 the rail deflection shows the individual pulses, but the slab deflection does not. Even for the longer 8-1/2 foot passenger car wheelbase, all but the most flexible slab showed just one pulse. On the basis of the soil pressure pulse criterion, then, any of the structures would be acceptable except the shallow slab 6 inches deep. The deep beams, 6 inches wide, were unacceptable from the pressure amplitude criterion. Also, bending stresses were 3-4 times higher than with the other structures.

The bearing pressures for the other beams was about 17 psi, and for the slabs--about 9 psi. This compares with approximately 25-30 psi for conventional concrete tie track, so this in itself should give a great increase in stability. An interesting point here is that the bearing pressure is virtually unaffected by the subgrade modulus, being basically a function of bearing area and vehicle weight. The deflection, on the other hand, is nearly proportional to the modulus. Rail stresses ranged from about 11,000 psi down to 9500 psi for the highest stiffness slabs or beams, and were, therefore, somewhat less than conventional track.

Calculations of bending stiffness and material costs were then made for cast-in-place beams and slabs of various geometries, assuming all tension was taken by the steel reinforcing rods, and that equal amounts of reinforcement were used at top and bottom of the beams. The results are shown in Figure 27; they indicate that the cost increases rapidly as increasing amounts of steel reinforcement are used. Therefore, it is more economical to increase the bending stiffness by using more concrete (deeper sections) to allow a given number of reinforcing rods to be spaced further apart. The lower limit on the cross-sectional area of reinforcing required to control cracking is 0.55 percent of the concrete cross-section; this is indicated by the lines so marked in the figure. The bending stresses in the steel and concrete, of course, impose limitations on the minimum amounts used.

Reviewing all the results, it was concluded that bending stiffness values as low as 2000-4000 x 10^7 lb-in.^{2} per track structure might be acceptable. Note that this is considerably lower than the value of 9000 x 10^7 lb-in.^{2} recommended at the end of Phase I. The latter was based on
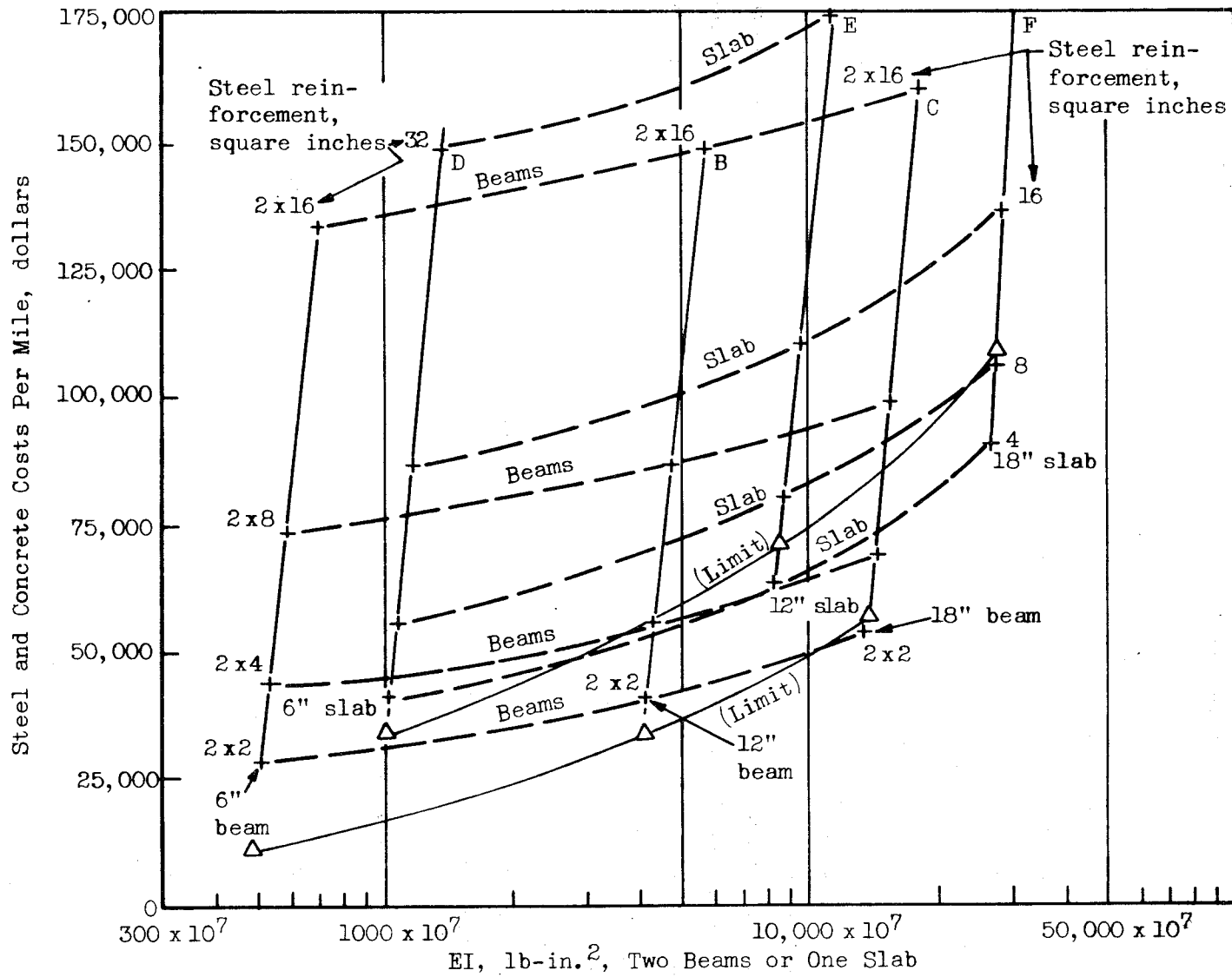
72

FIGURE 27. TRACK STRUCTURE COST AS A FUNCTION OF BENDING STIFFNESS

73

strict adherence to the "pressure-pulse criterion" such that the pressure
between two truck axles could never be less than the pressure at each axle.
The more economical lower-stiffness structures will not meet this criterion
under the wider axle spacings found on passenger cars, but do, in fact, meet
it for freight traffic (excluding the locomotives).

When an estimate of the subgrade modulus expected on the Santa Fe
experimental track (220 lb/in.^{3}) was obtained in the fall of 1969, a final
series of computer runs was made to evaluate the response of the more flexible
structures. A typical output plot is shown in Figure 28 (Run 56), and a
summary of results is shown in Table 12.

Response of Jointed Structures to Static Loading. In the previous
discussions, structures were considered to be continuous longitudinally.
However, even with cast-in-place structures, whether beams or slabs, there
will be joints due either to construction requirements or expansion require-
ments. While joints destroy the continuity of load support, and, therefore,
are considered to be undesirable, it was necessary to determine the effect
of joints in both the beam and slab-type structures, since they are inevitable.
This was done through an analysis of two noncontinuous structures. One of
these structures was a precast twin beam; the second was a jointed concrete
slab track structure. The analysis of these two structures is discussed below.

Analysis of Precast Twin-Beam Structure. Figure 29 shows the
longitudinal twin-beam track structure and the model used to represent it on
the computer. A total of 97 node points and 129 beams were used in order to
obtain an adequate representation (more than two 39-foot beams and three
joints) of the track, including the resilient fasteners and the resilient
soil beneath the structure. Each fastener was represented by a vertical
beam sized to give a vertical spring rate of 750,000 lb/in. each and spaced
at 30-inch intervals to give a resilience of 25,000 lb/in. per inch of
length along the rail. This value was determined earlier from the analog
computer analysis to be an optimum value for a relatively stiff longitudinal-
beam type structure, based on wheel-rail dynamic forces resulting from track
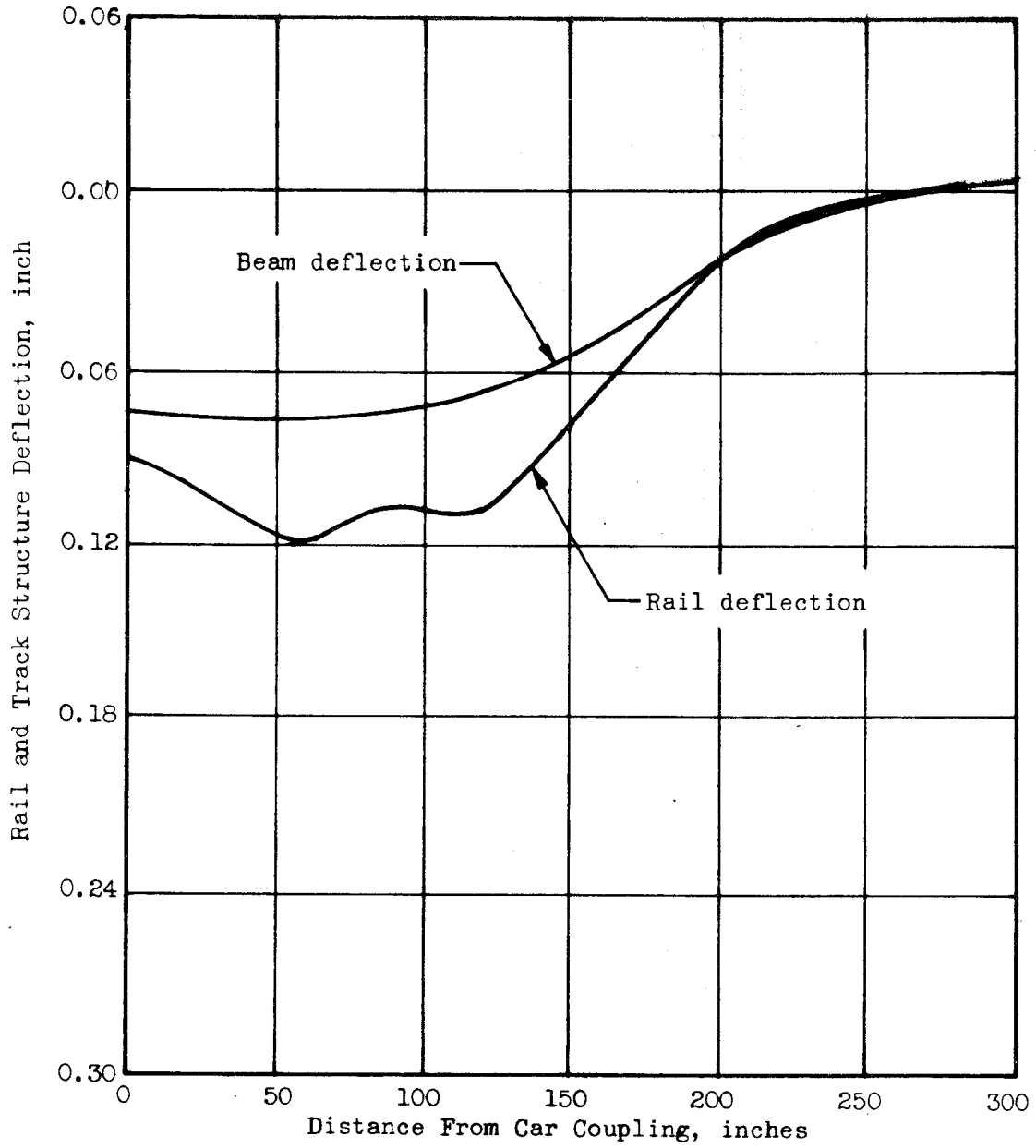
FIGURE 28.   RAIL AND BEAM DEFLECTIONS FOR TWIN BEAM TRACK STRUCTURE

75

TABLE 12. RESULTS FROM COMPUTER RUNS REPRESENTING SANTA FE TRACK STRUCTURES

			Input Data*							Output Data	
Computer Run	Maximum Beam or Slab Positive Bending Moment, in.-lbs	Bearing Width, inch W	Bending Stiffness, lb/in.^{2} (2 beams or 1 slab) EI_2	Fastener Spacing, inches l_t	Fastener Stiffness lb/in. K_f	Stiffness Per Unit Length (K_f/l_t) K_1, psi	Soil Subgrade Reaction lb/in.^{3} K_{o1}	Soil Modulus psi K_2	Max Fastener Deflection, inches	Max Fastener Load, pounds	% of Wheel Load
51	286,000	2(24)	$2,000 \times 10^7$	18	400,000	22,200	100	2400	.025	10,000	28.6%
52	286,000	"	$4,000 \times 10^7$	18	"	"	220	5280	.028	11,200	32.0
53	282,000	"	"	24	"	16,670	"	"	.035	14,000	40.0
54	278,000	"	"	30	"	13,320	"	"	.043	17,200	49.2
55	274,000	"	"	18	200,000	11,100	"	"	.050	10,000	28.6
56	260,000	"	"	30	"	6,670	"	"	.077	15,400	44.0
57	211,000	"	$2,000 \times 10^7$	18	400,000	22,200	"	"	.027	10,800	30.9
58	202,000	"	"	30	"	13,320	"	"	.042	16,800	48.0
59	151,000	2(48)	"	24	"	16,670	"	10,560	.035	14,000	40.0
60	212,000	"	$4,000 \times 10^7$	24	"	"	"	"	.036	14,400	41.2

* Wheel Loads = 35,000 lb, Wheel Spacing = 6 ft, Rail = 136 lb/yd

22,500 lb.   22,500 lb. ⎤
                          ⎥ Loading Case Two
22,500 lb▼ 22,500 lb. ⎤
                          ⎥ Loading Case One

Fastener
Spaced Every
30 Inches

132-lb. rail

39-ft. Concrete
Beam

Subgrade   Joint

(a) Longitudinal Beam Track Structure

Beams Representing Rail

Node Point

Beams Representing Fasteners

Beams Representing Soil

Beams Representing Concrete Beam
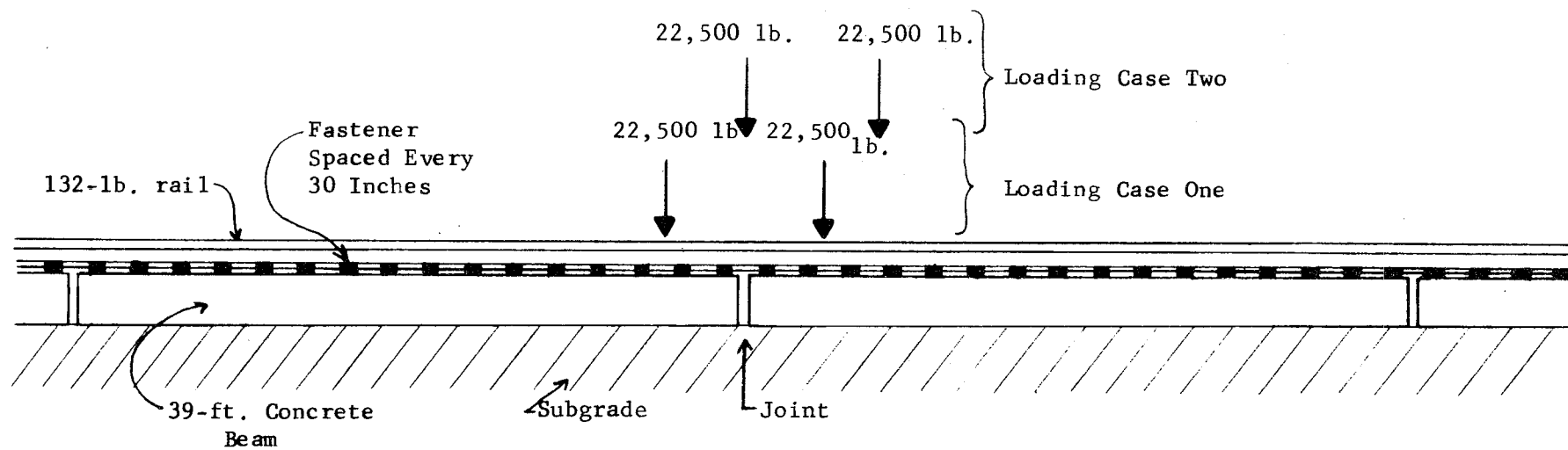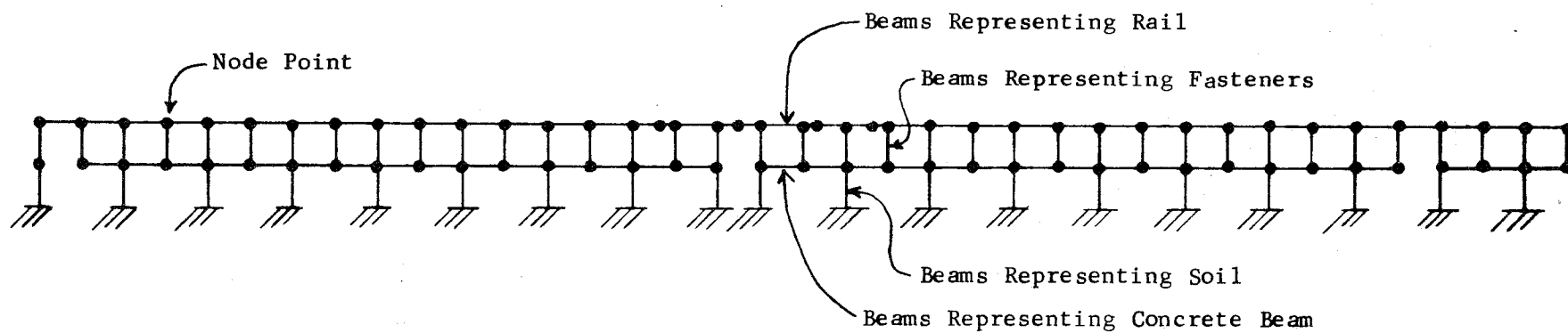
(b) Digital Computer Model of Track Structure

FIGURE 29.   REPRESENTATION OF TWIN LONGITUDINAL BEAM STRUCTURE ON DIGITAL COMPUTER

profile irregularities. The bending rigidity of the vertical beams representing the fasteners was deliberately made small to allow complete angular and longitudinal freedom between the rail and the concrete support beam. It was determined by hand calculation that the vertical beams used to represent the soil could be placed at intervals of 60 inches without significantly affecting the accuracy. These beams were then sized to represent two different soils. The two soils were assumed to have bulk moduli of 100 lb/in.^{3} and 500 lb/in.^{3}, respectively, and these values in conjunction with the 24-inch wide beam gave foundation stiffness of 2400 and 12,000 lb/in. per inch of length along the beam, respectively. A 132-pound rail was used, and a concrete beam having an area of 305 in.^{2} and an area moment of inertia of 6860 in.^{4} (EI = 4116 x 10^7 lb-in.^{2} total for two beams).

Two loading cases were investigated, as shown in Figure 29. In each case, the loads imposed by one four-wheel truck (two loaded axles) were used. The first case considered the truck axles straddling the joint, and the second considered one axle of the truck directly over the joint. It was considered that these two cases bracketed the range of variables. Wheel loads were 22,500 pounds.

The four deflection curves resulting from the two soils and the two loading cases are shown in Figures 30a and 30b. The deflection of the concrete beam is the same as the deflection of the supporting soil beneath the beam, and is, therefore, proportional to the bearing pressure exerted on the soil. The difference between the rail and beam deflection represents the deflection of the resilient rail fasteners.

The stiffness of the overall track structure was only slightly lower at the joint, as indicated by the maximum deflection of the rail when a wheel load was applied directly above the joint. The curves also showed that wheel loads near one joint in the beam did not significantly affect the deflections or pressures at the adjacent joints.

Figure 30c shows the deflection curve for an identical but continuous track structure for the same wheel loading used on the noncontinuous
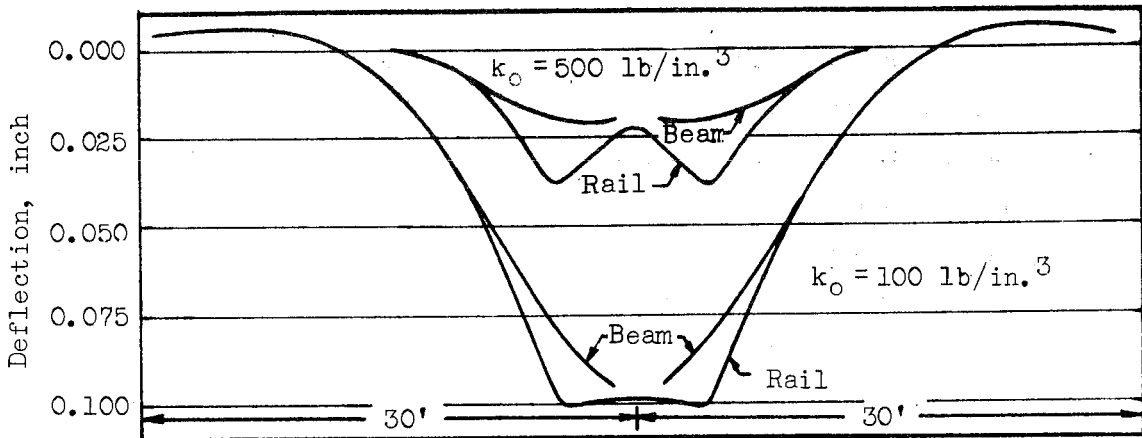
(a)   Jointed Structure; Loading Case One – Wheels Straddling Joint
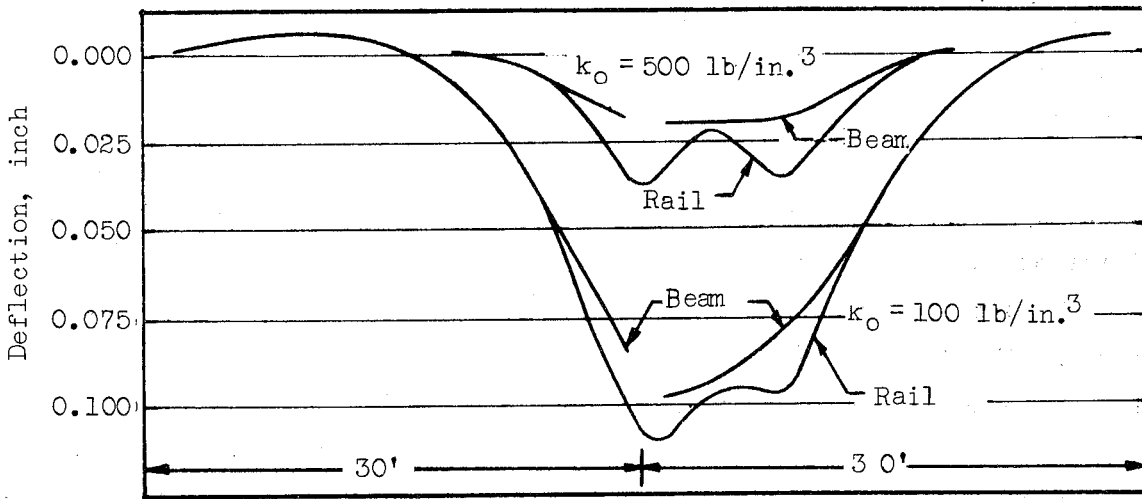
(b)   Jointed Structure; Loading Case Two – One Wheel Over Joint
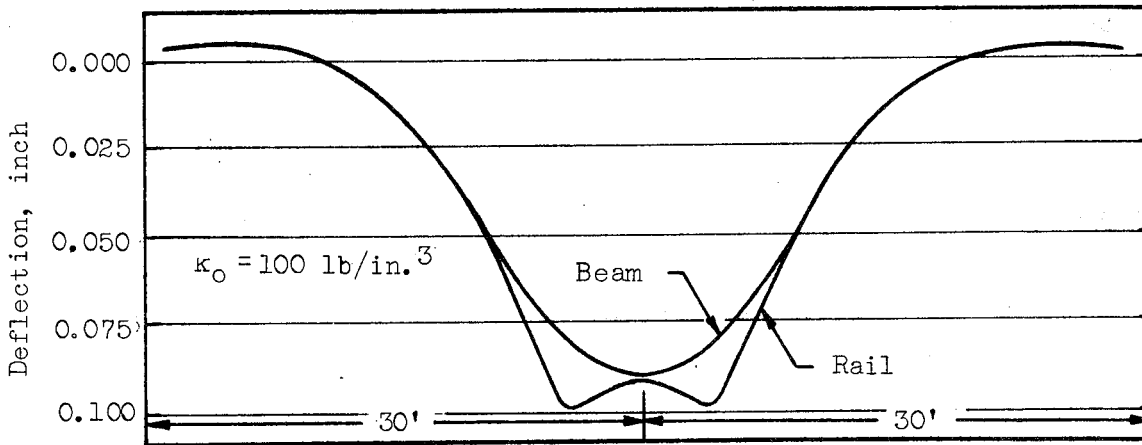
(c)   Continuous Track Structure

FIGURE 30.   RAIL AND BEAM DEFLECTION FOR LONGITUDINAL BEAM TRACK STRUCTURES WITH AND WITHOUT JOINTS (I_{RAIL} = 88.6 in.^{4}, I_{BEAM} = 6,860 in.^{4}, K_{PADS} = 25,000 lb/in.^{2}, WHEEL LOAD = 22,500 lb)

79

structure. Only one soil modulus was considered for this continuous structure, namely, 100 lb/in.^{3}, and the two separate loading cases discussed above result in identical deflection curves for the continuous structure; therefore, only one case is shown in the figure. Comparing this curve with that of the noncontinuous structure in Figures 30a and 30b shows the effects of a joint in the longitudinal beam. This was evidenced by the fact that the deflection of the beam with the joint was only slightly greater than the deflection of the continuous beam (about 11 percent greater). There will, of course, be a "soil stress-concentration factor" at the joints, particularly for the case shown in Figure 30b where a considerable amount of vertical shear is present at the soil in the vicinity of the joint. A shear tie at the joint would eliminate this relative deflection, which is expected to be aggravated by repeated dynamic loading.

The peak bending stress in the rail occurs when the axle is directly over the joint. This was calculated to be 6280 psi for the soil having a modulus of subgrade reaction of 100 lb per cubic inch.

The peak bending stress in the concrete beam occurs when the axle straddles the joint, and assuming a 1000 psi precompression in the concrete, the total peak compressive stresses was calculated to be 1330 psi.

Note that these values are for passenger-car loading, and not for the more severe freight car loadings used later when the Santa Fe track was proposed. A good approximation of the response can be obtained by multiplying by the ratio of wheel loads, 1.55 (35,000/22,500), since the program was linear.

Analysis of Nonreinforced Jointed Concrete Slab Track Structure.
The proposed slab-type track structure used 11 ft 8 in.-long reinforced concrete slabs 9 feet wide and 18 inches thick. The slabs were to be supported on a prepared granular base graded to provide adequate drainage. The rails were to be attached to the slabs with rail fasteners using resilient

rail pads spaced 35 inches apart. The joints between the concrete slabs were designed to transmit shear but have no bending stiffness.

A finite-element stiffness matrix computer program (similar to that shown in Figure 32) was used to determine maximum deflections, stresses, and soil pressures for a 6 foot truck wheelbase with wheel loads of 35,000 pounds. The computer model included six of the slab sections and an equal length of 136-pound rail to represent a continuous track structure. A modulus of 200 lb/in.^{3} was assumed for the prepared subgrade, and a stiffness of 750,000 lb/in. was assumed for the resilient rail pad.

A total of 85 node points and 107 beam elements was used for this analysis. The rail pads and the prepared subgrade were represented by vertical beams sized to have the required axial stiffness but with negligible bending stiffness. The bending and axial stiffness of the elements representing the rail and the concrete slabs were determined from the physical dimensions. Because the concrete slabs were relatively thick, shear deflections were also included. Calculations were made with the truck centered over a joint with one wheel on each of the adjacent slabs (symmetrical loading) and with the truck entirely on one slab with a wheel very close to the joint (asymmetrical loading).

Plots of the output data indicated that the high stiffness of the slabs distributed the wheel loads so that only one pressure peak was transmitted to the subgrade for each truck. To determine the importance of shear restraint at the joints, runs were made with the same loadings but without any shear tie at the joints. Maximum deflections were not changed significantly by eliminating shear ties; however, there was considerable relative motion between slabs at the joints, as shown in Figure 31.

Therefore, the use of shear ties at the slab joints (as proposed by PCA) appeared necessary to eliminate the large relative motion between the slab ends. However, even with shear ties, the lack of bending rigidity at the joints caused a 16 percent variation between the track stiffness at the middle of the slab and at the slab joint. This would produce the same
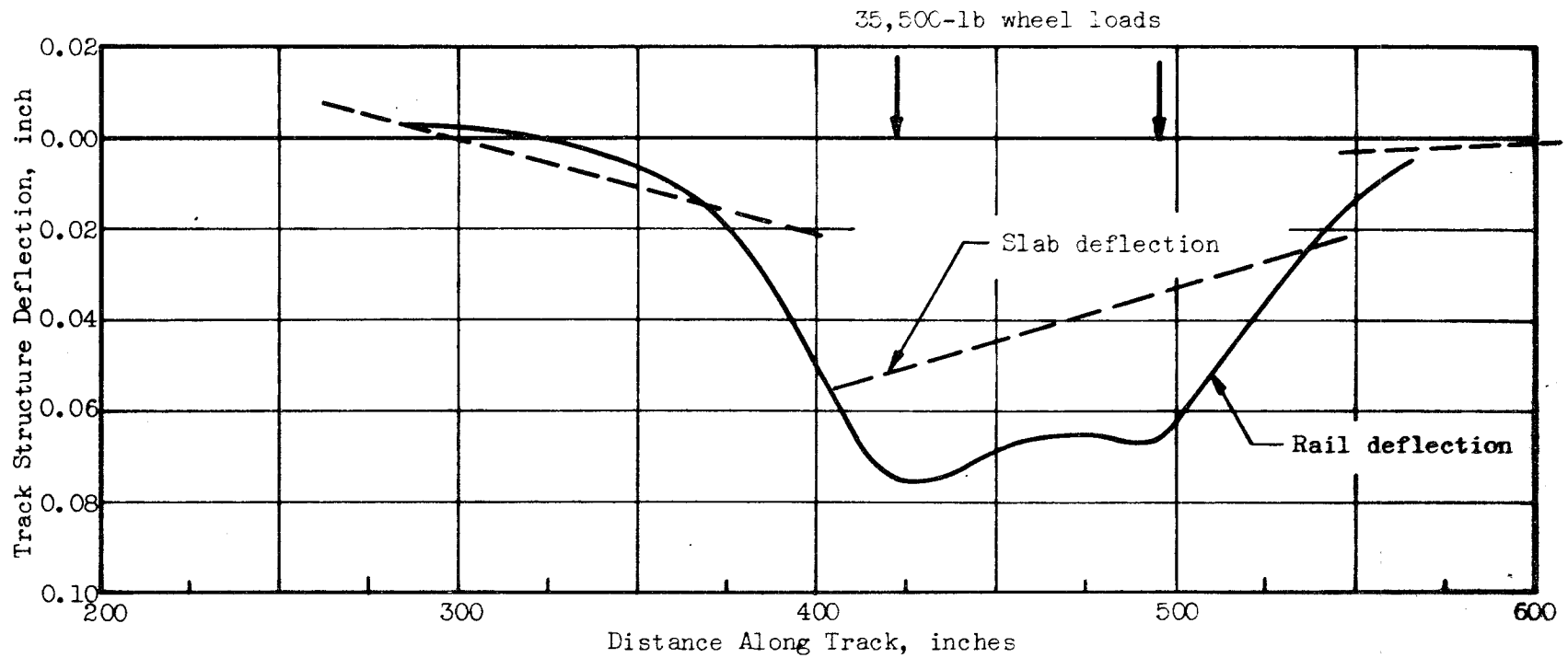
81

FIGURE 31. JOINTED CONCRETE SLAB TRACK STRUCTURE DEFLECTION FOR
SYMMETRICAL LOADING WITH NO SHEAR TIES AT JOINTS

effect as a sinusoidal vertical track profile error, causing undesirable
train vibrations. With the short slabs, at a train speed of 80 mph the
vertical excitation would be at 10 cps, which could excite secondary reso-
nances in car suspensions. Lower train speeds would produce lower frequency
excitation, resulting in a magnification of the track profile error when the
excitation frequency coincided with the primary resonant frequency of the
suspension system. However, the actual displacements are small because this
type of track is very stiff; for freight car service the vibrations might
not be significant.

Consideration of the results of the analyses of two typical track
structures--twin beam and slab--led to the conclusion that the shearing
action on the subgrade (or bearing material) was not consistent with the
basic objective of optimizing the subgrade "pressure signature". The effect
of continued dynamic loading would tend to accelerate the undesirable action
at the joints; also, the rapid force reversal on the fasteners is undesirable.
Therefore, in the preliminary performance specifications for the track struc-
tures, joints having shear restraints were specified. Joints of this type
are common in pavements[6] and appear to be justified from the standpoint of
long-term stability and lowered maintenance requirements.

Analysis of Asphalt Concrete Track Structures. The asphalt concrete
track structure selected for analysis consisted of a continuous asphalt con-
crete roadbed. This design concept proposed was quite similar to the type of
asphalt track structure that has been evaluated on the Japanese National
Railway[7]. Figure 32 shows the track structure with the asphalt roadbed and
the rail fastened to the roadbed but supported on resilient pads. The dimen-
sions shown were recommended by the Asphalt Institute as approximate sizes
for their proposed roadbed for the Santa Fe evaluation study.

Figure 32a shows the loading condition from two trucks of adjacent
cars. The cars were sufficiently long so that track deflections at the rear
truck of a car were independent of the deflections caused by the front truck
of the same car. The 6-foot truck wheelbase and 9-foot separation between
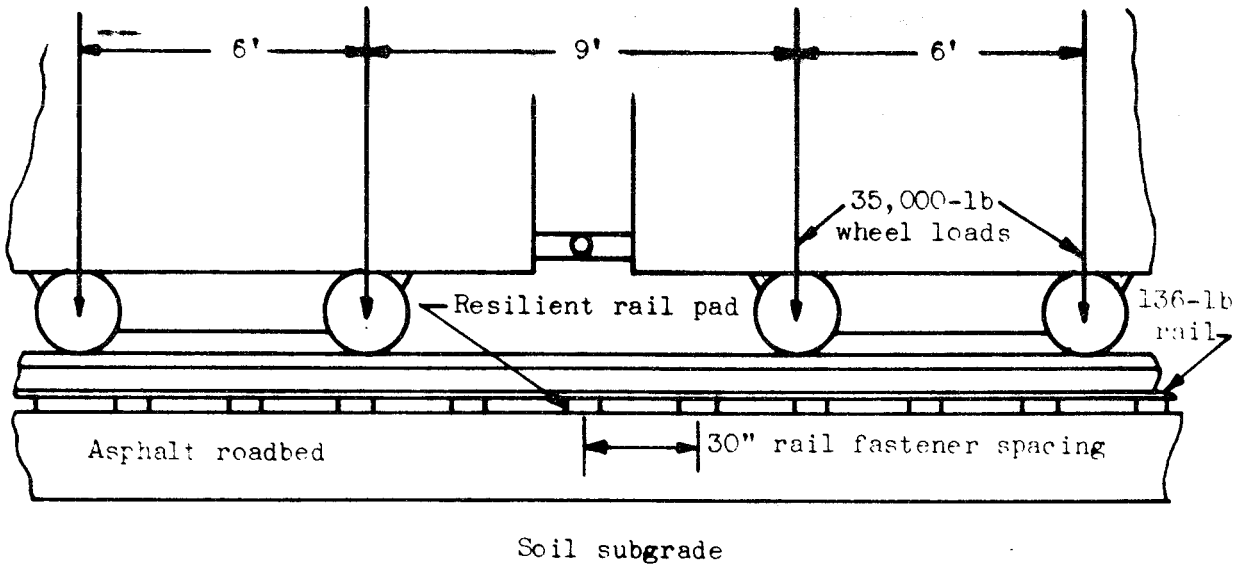
a. Side View of Asphalt Concrete Track Structure with
Freight Car Loading
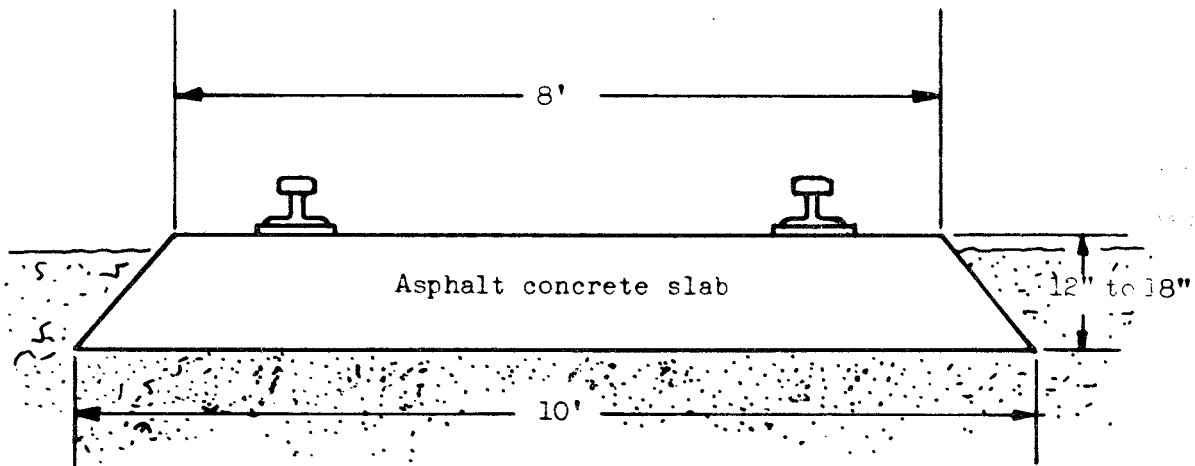
b. End View of Asphalt Concrete Track Structure

FIGURE 32. ASPHALT CONCRETE TRACK STRUCTURE AND LOADING
CONDITIONS USED FOR STATIC LOAD ANALYSIS

trucks of adjacent cars was representative of the expected traffic on the Santa Fe evaluation track. The wheel loads of 35,000 pounds represented only the evenly distributed static car weights, and did not include any factor for dynamic effects from speed, car rolling, or track irregularities. However, all of the static analysis was linear, so that a dynamic load factor could be readily included to determine the changes in track stresses and deflections from those calculated using the static wheel loads.

The static analysis of the asphalt track structure again was made by using a digital computer program to calculate the stresses and deflections of both the rail and roadbed. The model of the track structure used in this program was similar to that described previously. The rail size was 136 pounds per yard, and rail pads were spaced 30 inches apart. Values of asphalt modulus of 0.25×10^6 and 2.5×10^6 psi for temperatures of about 100 F and 30 F, respectively, were used for this analysis.[8] Values of the modulus of soil subgrade reaction of 100 lb/in.^{3} and 500 lb/in.^{3} were used in initial calculations to include the maximum possible soil variation. However, in a final set of calculations an average soil modulus of 150 lb/in.^{3} was assumed to approximate a prepared roadbed subgrade condition.

Figure 33 shows a typical computer plot of both the rail deflection and the asphalt roadbed deflection. The graph only shows the deflection under one truck, starting from the car coupling, because the loading from the two adjacent trucks are symmetrical with respect to the car coupling. Note that while the rail deflection shows peak deflections in the vicinity of each of the wheel loads, the asphalt roadbed shows only a single peak deflection for the truck. All of the asphalt roadbed configurations considered in this analysis with the exception of a 12-inch thick roadbed on 500 lb/in.^{3} soil, effectively distributed the loads so that the soil subgrade was subjected to only one pressure pulse per truck. As mentioned previously, this was considered to be an important factor in reducing the rate of soil settlement under a track structure.

Table 13 summarizes all of the analysis results for the asphalt track structure. Figures 34 and 35 show the influence of asphalt thickness
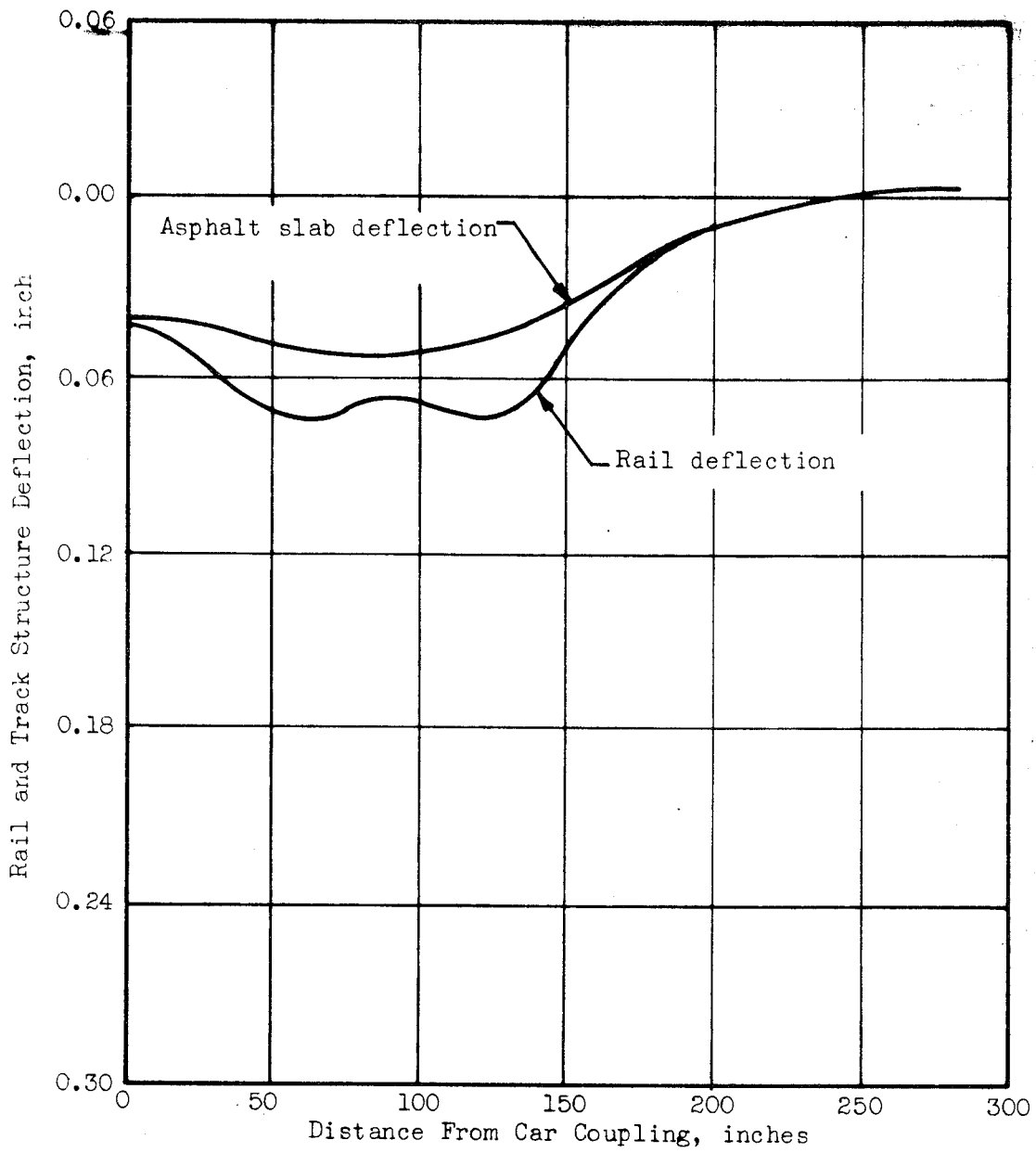
85

FIGURE 33.   TYPICAL COMPUTER PLOT OF STATIC DEFLECTIONS OF
THE RAIL AND ASPHALT ROADBED

86

TABLE 13. RESPONSE OF ASPHALT TRACK STRUCTURE TO STATIC VERTICAL LOADS

| Asphalt Thickness, inch	Asphalt Temperature, °F	Maximum Rail Deflection, inch	Maximum Rail Stress, psi	Maximum Asphalt Deflection, inch	Maximum Asphalt Bending Stress, psi	Maximum Soil Pressure, psi	Maximum Rail Seat Load, lb	Effective Track Modulus, psi	Track Stiffness* (10^5 lb/in.)
Soil: 100 lb/in³., Rail Pad: 700,000 lb/in.									
12	100	0.101	10,950	0.082	46.2	8.2	$\left(\begin{array}{c}18,000\\ \pm\ 500\end{array}\right)$	5,300	4.03
12	30	0.097	9,850	0.072	154.0	7.2		6,790	4.86
18	100	0.098	10,400	0.078	39.3	7.8	"	5,900	4.38
18	30	0.095	9,350	0.069	112.3	6.9	"	8,300	5.65
Soil: 500 lb/in³., Rail Pad: 700,000 lb/in.									
12	100	0.043	9,530	0.018	20.6	8.8	$\left(\begin{array}{c}18,000\\ \pm\ 500\end{array}\right)$	13,900	8.33
12	30	0.042	9,280	0.017	83.8	8.3		14,900	8.76
18	100	0.043	9,400	0.017	20.2	8.7	"	14,400	8.55
18	30	0.041	9,150	0.015	58.7	7.5	"	17,600	9.46
Soil: 150 lb/in³., Rail Pad: 700,000 lb/in.									
12	100	0.079	10,460	0.056	39.0	8.4	$\left(\begin{array}{c}18,000\\ \pm\ 500\end{array}\right)$	7,070	5.0
12	30	0.074	9,480	0.050	129.0	7.5		8,700	5.84
15	100	0.077	10,200	0.055	37.5	8.3	"	7,320	5.15
15	30	0.073	9,170	0.047	111.0	7.1	"	9,500	6.25
18	100	0.076	10,000	0.054	34.8	8.1	"	7,780	5.38
18	30	0.072	8,970	0.046	95.7	6.9	"	10,200	6.61
Soil: 150 lb/in³., Rail Pad: 350,000 lb/in.									
12	100	0.098	11,500	0.056	31.7	8.4	$\left(\begin{array}{c}16,200\\ \pm\ 500\end{array}\right)$	5,360	4.07
12	30	0.094	10,800	0.049	118.7	7.4		6,070	4.48
15	100	0.097	11,330	0.055	30.8	8.3	"	5,550	4.17
15	30	0.093	10,540	0.047	105.2	7.1	"	6,550	4.73
18	100	0.096	11,180	0.053	28.8	8.0	"	5,730	4.27
18	30	0.093	10,380	0.046	92.2	6.9	"	6,950	4.94

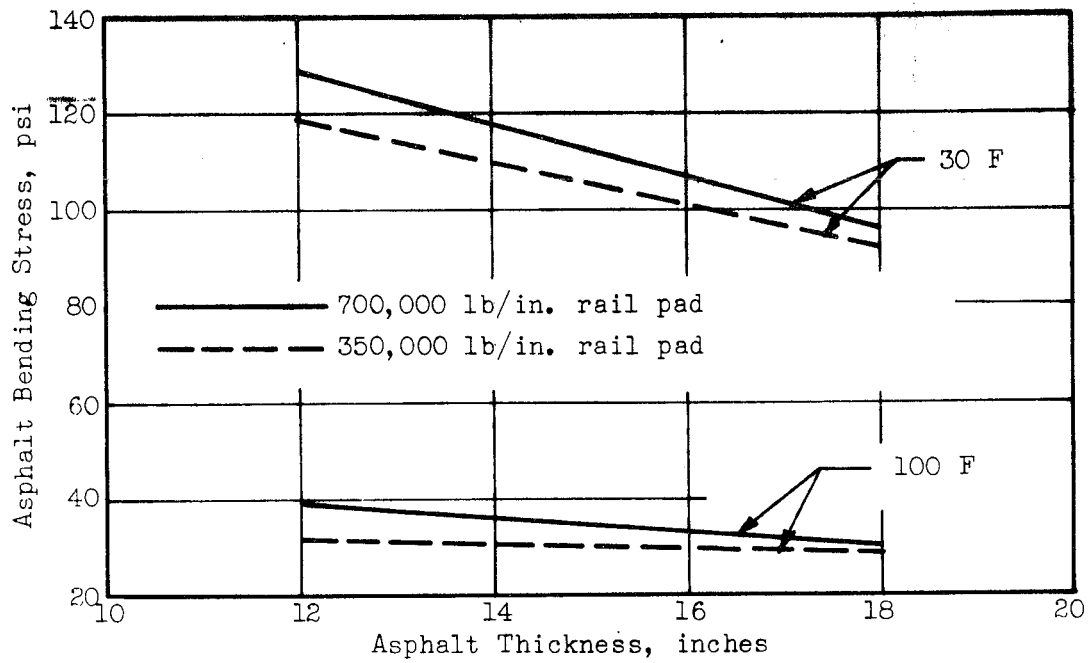* Total stiffness for single vertical load on rail
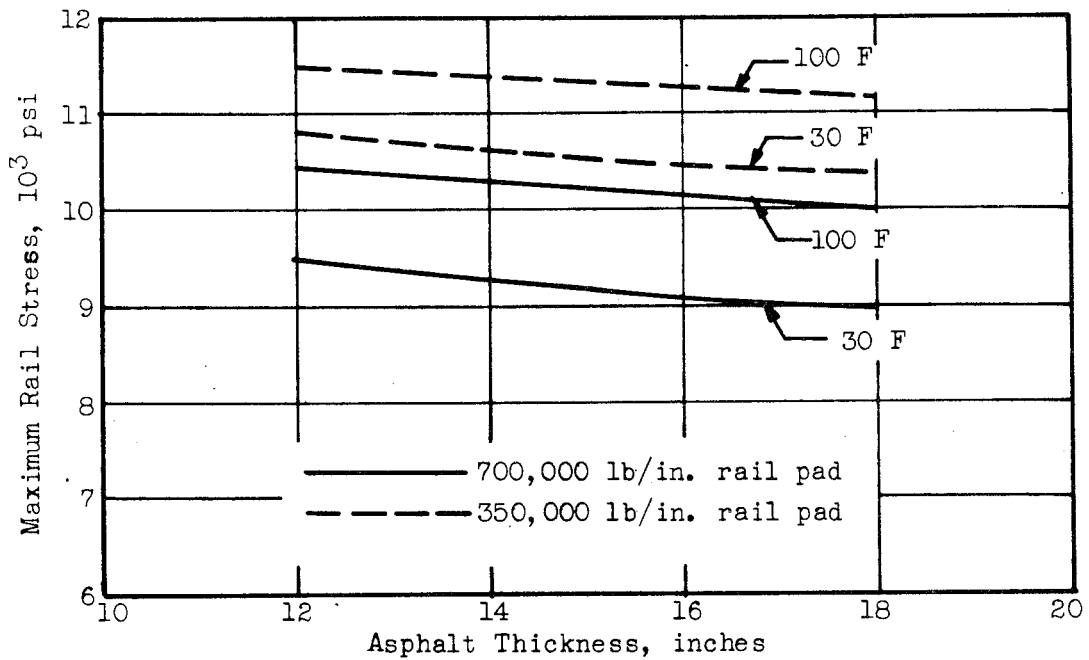
FIGURE 34. RESPONSE OF ASPHALT CONCRETE SLAB TRACK STRUCTURES
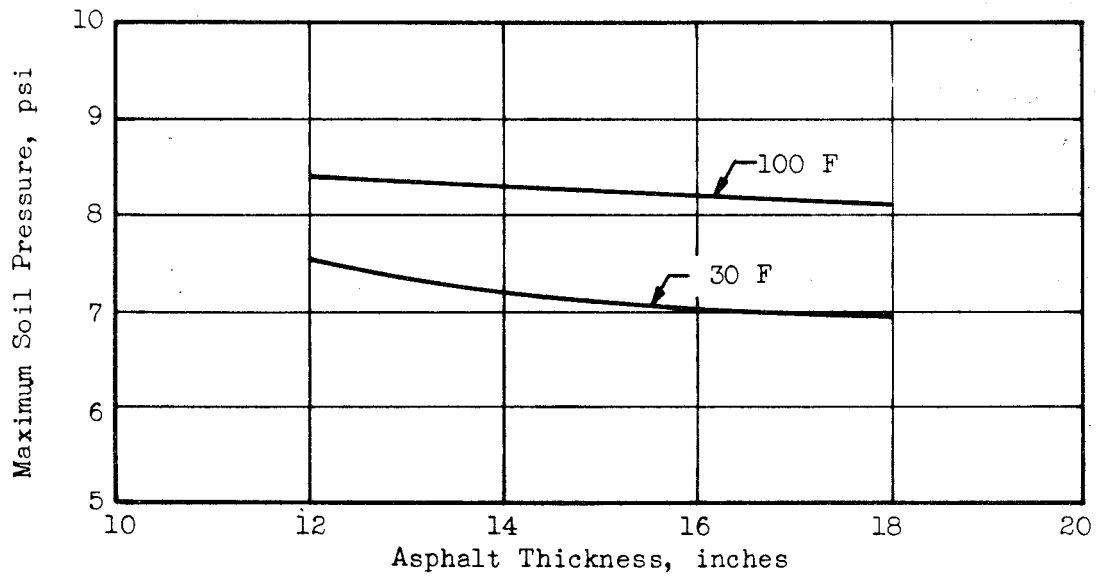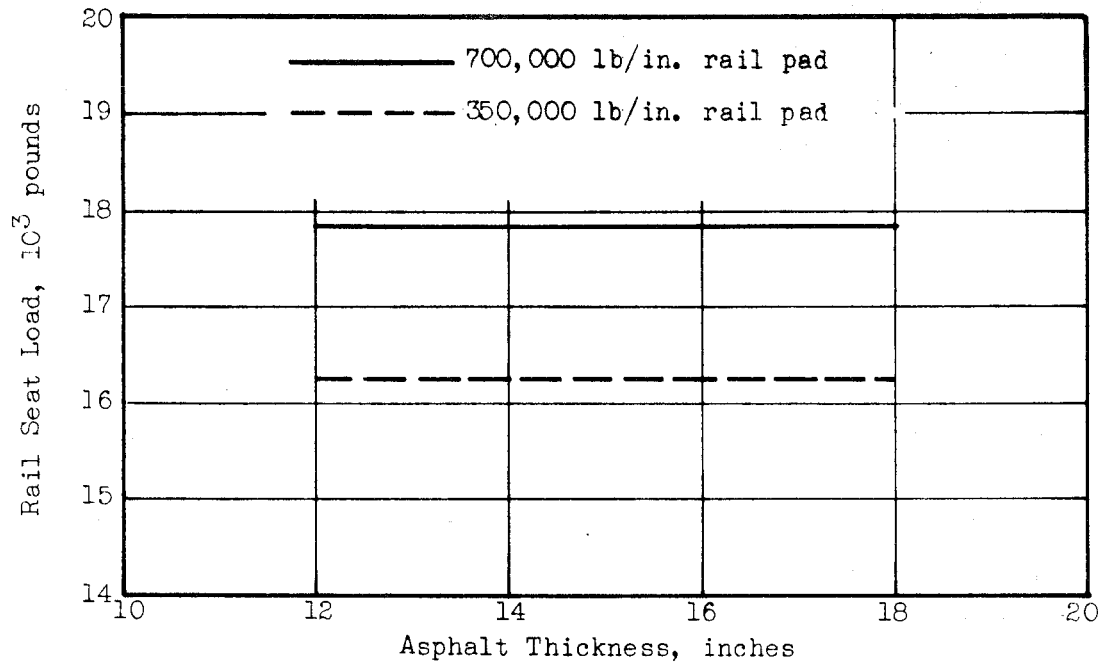
FIGURE 35.   RESPONSE OF ASPHALT CONCRETE SLAB TRACK STRUCTURES

89

on rail and roadbed bending stresses, rail seat loads, and soil pressure for an average soil modulus of 150 lb/in.^{3}. As expected, both the rail and the roadbed bending stresses were reduced by increasing the roadbed thickness; however, the approximately 10:1 change in elastic modulus of the asphalt for a temperature range of 30 F to 100 F had a much greater effect on the roadbed stresses than the thickness changes. It was also significant that rail seat loads were virtually independent of any change in the roadbed structure. The rail seat loads were only affected by changes in the rail pad stiffness or spacing (assumed constant at 30 inches for this analysis). Rail seat loads will be a particularly important design parameter, as a suitable attachment between the rail fastener and the asphalt roadbed must minimize local stresses and maintain a rigid connection between the fastener and the roadbed. The maximum soil pressures shown in Figure 35b indicate that even the 12-inch thick roadbed adequately distributed the wheel loads.

From these results it appeared that a 12-inch thick asphalt roadbed was adequate, and that little advantage was gained by increasing the thickness. However, this conclusion was based on the assumption that the bending stresses shown in Table 13 could be tolerated at the indicated temperatures. Asphalt is a complex material, and limits on bending stress are not readily available and are difficult to determine. Present highway and runway design procedures make use of extensive experience and empirical relations to determine pavement thickness and do not use bending stress predictions--at least in any recognizable manner.

The Japanese National Railway tested three configurations of continuous asphalt roadbed[7] and compared the results with a control section of conventional ballast. The asphalt sections were all 12 inches thick and varied only in the composition of the asphalt. Both the asphalt and ballast control sections used concrete ties spaced 24 inches apart; deflection and stress measurements indicated the effective modulus of all of these sections was about the same, from 2850 to 3450 psi. Vibrations produced by impacting the rail also indicated there was little difference in the dynamic response

of the asphalt and ballast roadbeds. However, there was a significant difference in track settlement under repeated loading. The ballast control section settled five times as much as the best asphalt section and more than two times as much as the worst asphalt section. These results indicate that a primary advantage of an asphalt roadbed is that the bending stiffness (which cannot be obtained from ballast) significantly reduces subgrade pressures, thereby increasing track stability by reducing settlement.

An important point of concern is the long-term stability of the material itself--an area in which asphalt concrete would be expected to have a disadvantage relative to conventional concrete. On the other hand, asphalt concrete is cheaper than Portland Cement concrete; the relationships of these two factors were not predicted by the computer analyses developed in this project.

Analysis of Wirand Concrete Track Structure. The analysis of a Wirand* track structure was originally included within the scope of the Phase III contract. This track structure, as described in Reference 9, was to consist of two deep but narrow beams--one beneath each rail--formed by a special pressurized-slurry method to eliminate the use of forms. Presumably the use of Wirand (a concrete having tensile as well as compressive strength by virtue of being reinforced throughout with finely chopped steel wire) in this structure would eliminate the need for locating reinforcing rods in the trenches--perhaps a necessity for the proposed construction method. However, the results of analyses discussed earlier indicated that bearing pressures were excessive (although shear on the sides of the beams was neglected), and at the suggestion of DOT, no further analysis of Wirand track structures was made.

---

* Registered Trademark of Battelle Development Corporation.

<u>Response of Twin Beam Track Structures to Lateral Loads</u>. While
the track structure response to vertical loads was of prime importance,
lateral response characteristics were also considered, since substantial
lateral loads are generated by the passage of trains and by changes of
temperature in the absence of trains. The lateral loads are particularly
important in the case of twin beam type structures where lateral gage beams
must be placed along the longitudinal beams at regular intervals to maintain
gage of the track structure.

To establish design specifications for the gage beams and for the
torsional-lateral characteristics of longitudinal beams, a digital computer
program was developed to relate factors such as beam strength and spacing
to the gage spread of the track under load. A representative portion of
the track and the computer models used to represent it are shown in Figure
36. In this representation, one beam was considered fixed in space while
the other beam (shown in the figure) moved laterally and torsionally in
response to the lateral loads applied at the rail head. The lateral dis-
placements calculated as outputs, then, represented the spread in gage, rather
than the actual track alignment. For these calculations it was assumed that
the beam was embedded in soil having a modulus of 150 lb/in.^{3}. Four lateral
wheel loads of 14,000 pounds each were applied to 136 pound rail, at spacings
representing the axles of the end trucks of two adjacent cars. Using assumed
lateral gage beam spacings of 12-1/2 or 25 feet, the gage spread was calcu-
lated for various stiffness of both the longitudinal and the lateral beams.

A summary of these results is shown in Table 14, and typical output
data is shown in Figure 37, which shows that the gage spread is reduced from
value of 0.118 inch with no lateral beams to about 0.078 inch with "weak"
gage beams at 25 foot intervals. A more detailed description of this
analysis is given in Appendix E.

Based on these results, it was concluded that under the assumed
loading it would not be difficult to keep the gage spread within allowable
limits on the twin beam structures, and in the performance specifications
a gage beam spacing of 25 feet was specified, of sufficient stiffness to
keep bending stresses in the beam itself within allowable limits.
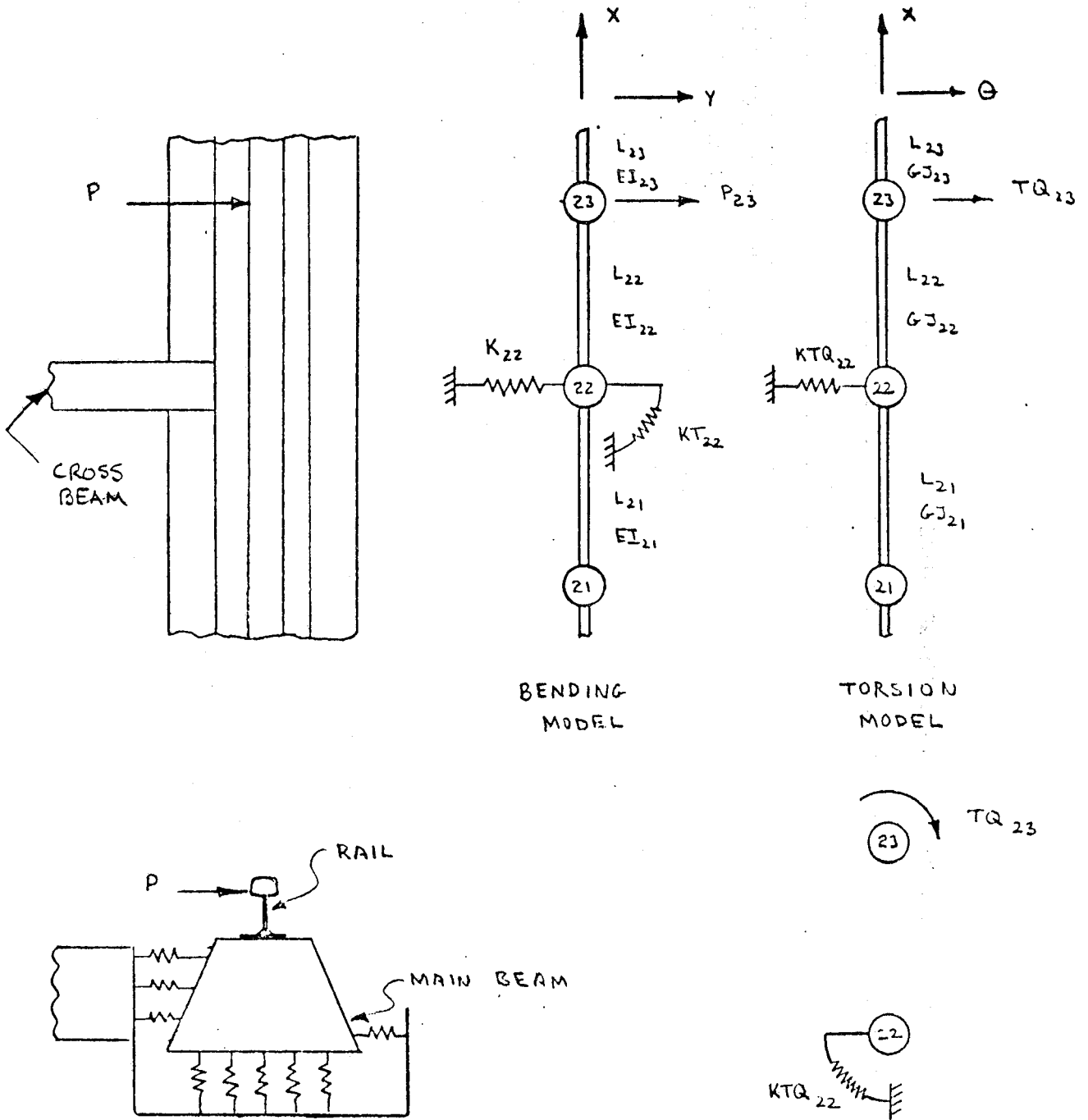
FIGURE 36. TRACK STRUCTURE MODEL USED TO DETERMINE
RESPONSE TO LATERAL LOADS

93

TABLE 14. SUMMARY OF GAGE SPREAD CALCULATIONS

Input Data			Output Data					
Cross-Beam Properties			Gage Spread					
			25-Foot Spacing of Gage Beams			12.5-Foot Spacing of Gage Beams		
K, (lb/in.)	KT, (lb-in./rad)	KTQ, (lb-in./rad)	Bending, (in.)	Torsion, (in.)	Total, (in.)	Bending, (in.)	Torsion, (in.)	Total, (in.)
0	0	0	0.0607	0.0580	0.1187	0.0607	0.0580	0.1187
0.5×10^6	0	0	0.0536	0.0580	0.1070	0.0391	0.0580	0.0960
1.0×10^6	0	0	0.0526	0.0577	0.1051	0.0337	0.0577	0.0903
1.0×10^6	0.266×10^9	0.38×10^9	0.0526	0.0265	0.0791	0.0310	0.0165	0.0475
1.0×10^6	0.532×10^9	0.76×10^9	0.0526	0.0237	0.0763	0.0299	0.0131	0.0430
1.0×10^6	0.798×10^9	1.14×10^9	0.0526	0.0226	0.0752	0.0294	0.0119	0.0413
1.0×10^6	1.065×10^9	1.52×10^9	0.0526	0.0221	0.0747	0.0290	0.0112	0.0402
1.5×10^6	0	0	0.0526	0.0580	0.1044	0.0312	0.0580	0.0880
3.0×10^6	0	0	0.0523	0.0580	0.1035	0.0282	0.0580	0.0845

FIGURE 37. TOTAL GAGE SPREAD OF TWIN BEAM TRACK STRUCTURE WITH CROSS BEAMS SPACED AT 25-FOOT INTERVALS

Response of Nonconventional Track Structures to Dynamic Loading

During Phase I, an important part of the conceptual study was a computer analysis of the effects of resilience between the rails and the relatively stiff longitudinal beam and slab-type structures. The computer model of the vehicle was identical to that described earlier in the section on conventional track, and a lumped param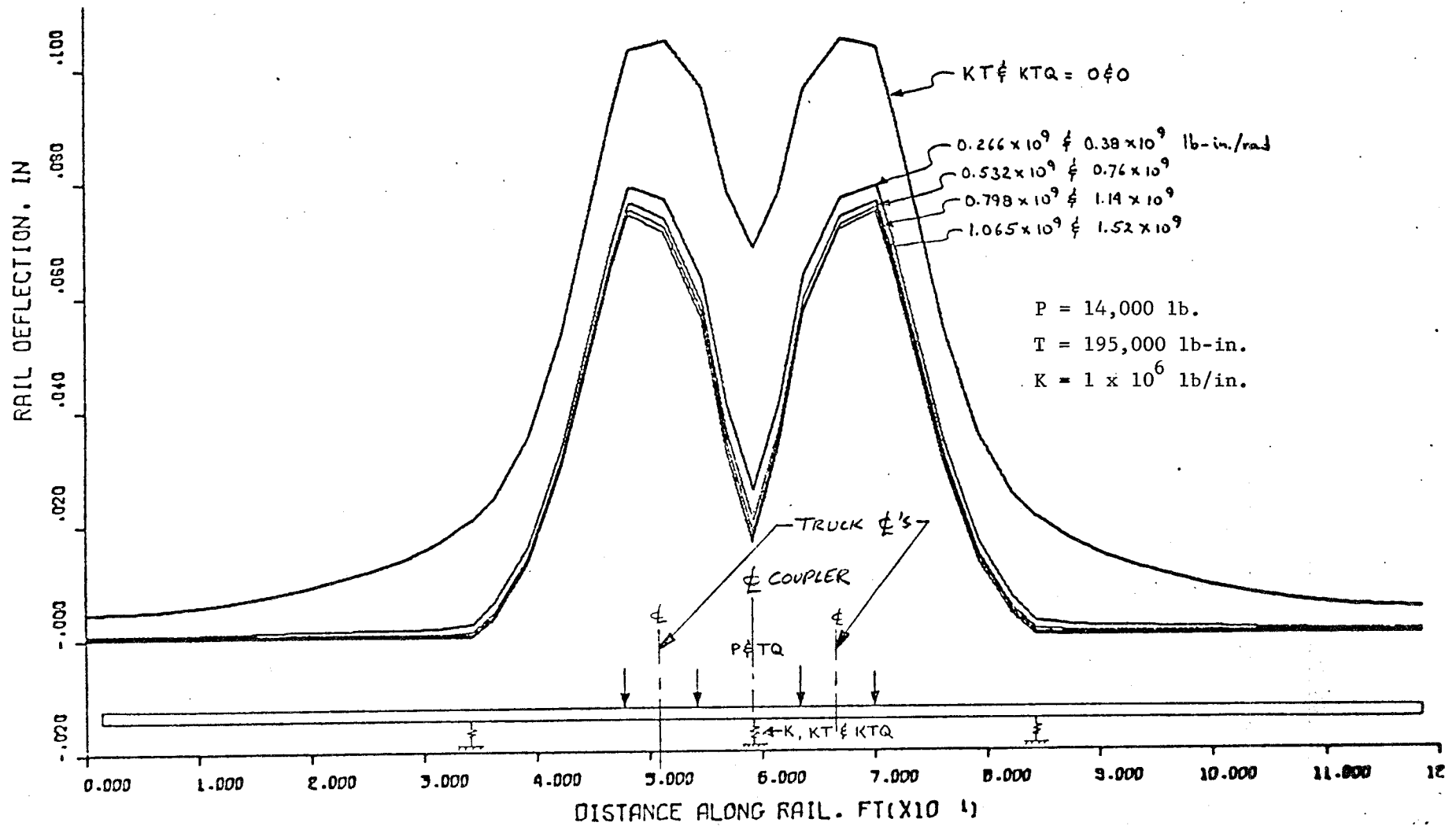eter simulation of the various track structures was developed (see Appendix B). The program simulated relatively light passenger cars (100,000 pounds) travelling on relatively stiff beam and slab-type structures. A series of computer runs was made, with the basic objective being to determine the effects of resilience (in the fasteners) between the rail and the track structures. One of the most significant results was the fact that impact loads between the wheel and rail for a step-type track profile input decreased appreciably as the rail pad stiffness was decreased. From this it was concluded that there was an advantage to be gained by deliberately introducing a resilient member between the rail and its support, in terms of significant reductions in wheel-rail dynamic forces generated as a result of (inevitable) wheel or track irregularities. For the structures being considered at that time, it was found that a stiffness on the order of 25,000 lb/in./in. of longitudinal length per rail was reasonable. In practical terms, this would represent, for example, fasteners having a vertical stiffness of 500,000 lb/in. spaced at 20-inch intervals. Further details of this analysis are given in Reference 1.

During Phase II, dynamic analysis was limited to conventional-type track structures. During Phase III, however, the effects of dynamic loadings on longitudinal beam and slab structures was continued, with particular emphasis on the proposed Santa Fe test track installation. Therefore, a simulation of a 100-ton freight car typical of traffic to be expected there was used. For consistency with the dynamic analyses of conventional track conducted concurrently, a rail joint with 75 percent of nominal stiffness and a 0.2-inch profile error was used as a disturbance function for these runs.

Nonconventional track structures evaluated were (1) concrete slabs with EI values ranging from 4140 x 10^7 lb-in.^{2} to 13380 x 10^7 lb-in.^{2} with three pad stiffnesses, and (2) concrete twin beam structures also with these values of bending rigidity and pad stiffness. All runs were made using a subgrade modulus of 150 lb/in.^{3} beneath the beams or slabs.

Results of this analysis are shown in Figures 38 and 39. In Figure 38, the dynamic response of various structures is shown for the case of the 100-ton car going over a joint at 80 mph. In Figure 39, peak wheel-rail impact loads are plotted as functions of pad stiffness and speed.

These results show that the wheel-rail force for the beam and slab structures has a frequency range of 80-90 cps, rather than the 40 cps for the concrete ties, although the rail pad stiffness is the same in all cases. The oscillatory nature of the wheel-rail force indicates the need for higher damping in the rail pads used on the stiffer structures, although the overall disturbance time period is about the same as for concrete ties. The results also show that the wheel-rail force is fairly insensitive to changes in beam and slab stiffness, and can be controlled more by changing the resilient pad characteristics.

Also shown is the significant decrease in deflection and acceleration of the beams or slabs compared to the concrete ties, tending to deteriorate the underlying roadbed less rapidly.

In summary, the dynamic analyses indicated the importance of resilient pad design for controlling the wheel-rail impact forces, and showed that the highest values of beam and slab bending stiffness could not be justified in terms of improvements in dynamic response.

Rail Fastener Analyses

An integral part of all three phases of the project was the analysis of rail fasteners, particularly for the nonconventional track structures. The results of the fastener studies during Phases I and II are reported in References 1 and 2. During Phase III, further analyses were

5 G

0.1 SEC

WHEELS-AXLE VERTICAL ACCELERATION

30,000 LB

ZERO

WHEEL-RAIL VERTICAL FORCE

0.1"

TIE (BEAM) DEFLECTION

CONCRETE TIES,
30" SPACING

SLAB, LOW EI

SLAB, HIGH EI

TWIN BEAM,
LOW EI

TWIN BEAM,
HIGH EI
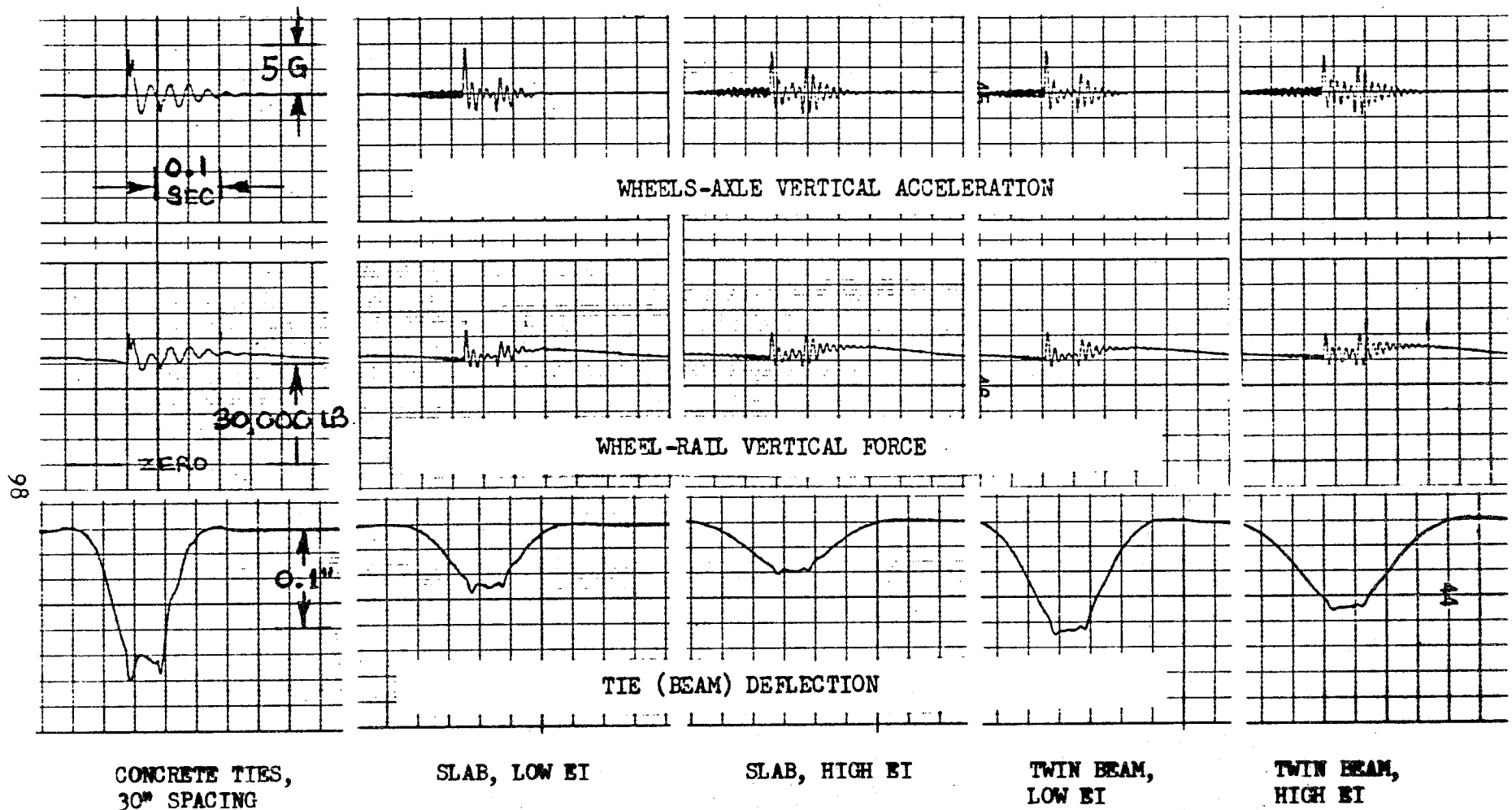
FIGURE 38. SIMULATION OF 100-TON FREIGHT CAR PASSING OVER RAIL JOINT AT 80 MPH.
GEOMETRIC ERROR = 0.2 IN., 75% NOMINAL STIFFNESS. 700,000 LB/IN
PAD STIFFNESS ON 30-INCH SPACING

Graph axes:
- Y-axis: PER CENT INCREASE IN WHEEL-RAIL FORCE (0 to 20+)
- X-axis: RAIL PAD STIFFNESS, LB/IN (0 to 800K)

Legend:
◇ SLAB, LOW EI
⊡ TWIN BEAM, LOW EI
⊙ CONCRETE TIES, 30" SPACING
▽ SLAB, HIGH EI
△ TWIN BEAM, HIGH EI

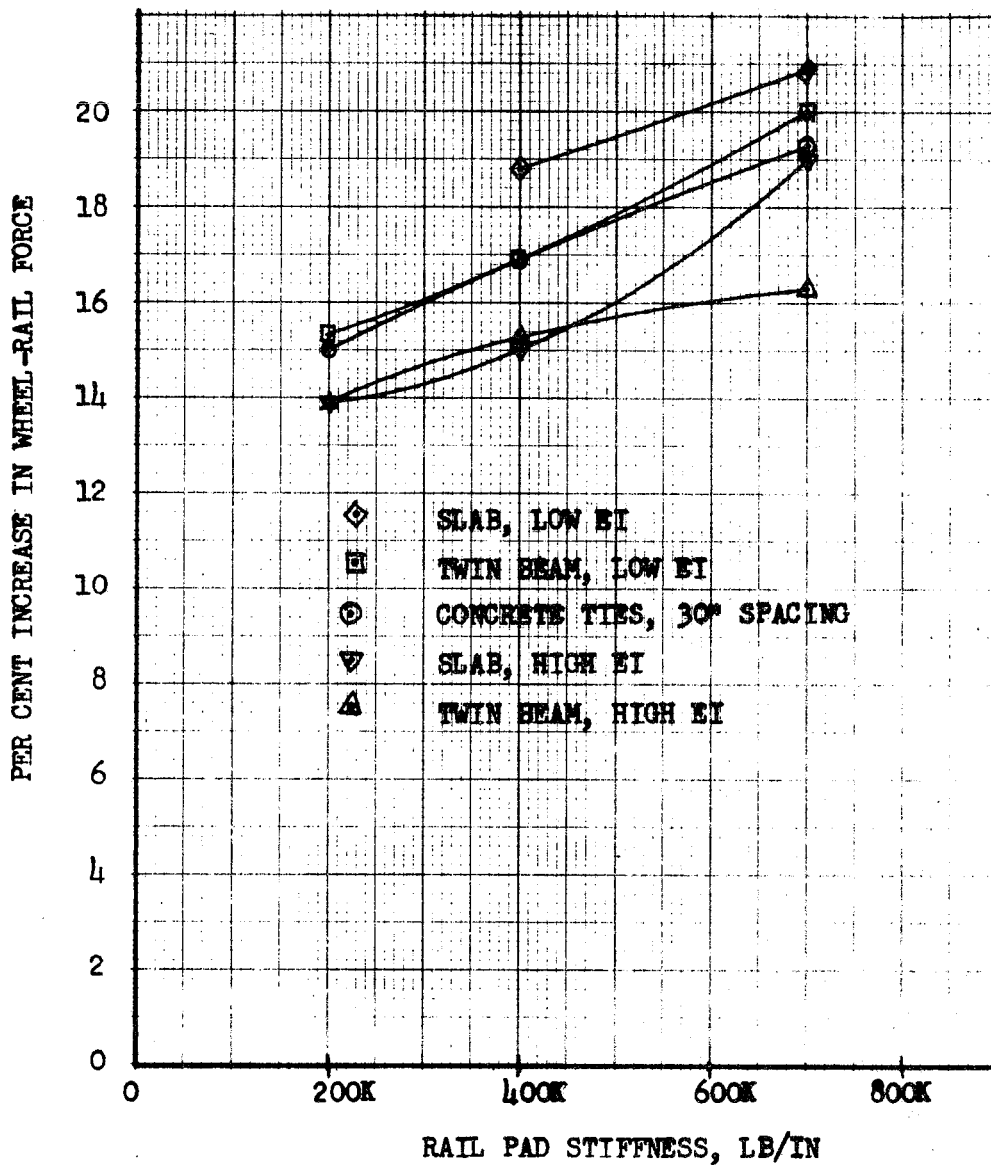FIGURE 39.   INCREASE IN PEAK DYNAMIC WHEEL-RAIL FORCE (OVER
STATIC) VERSUS RAIL PAD STIFFNESS FOR SIMULATED
100-TON FREIGHT CAR HITTING RAIL JOINT AT 80 MPH.
0.2-INCH GEOMETRIC ERROR, 75% NOMINAL STIFFNESS

99

made, and the results were incorporated into a set of performance-type
specifications for the rail fasteners. These specifications, together
with a discussion of all aspects of the specifications, are included as
Appendix E of this report.

Track Structure Costs

In the final analysis, it is the cost that determines whether an
improved track structure will be adopted. Unfortunately, the nonconventional
"advanced" track structures will be more expensive initially than conventional
tie-type track, even though maintenance costs are expected to be much lower.
Costs which are discussed here, however, are the estimated construction costs.

Costs were specifically considered during Phases I and III of the
project. During Phase I, relative costs for beams and slabs of different
geometries were calculated as part of the optimization of the various designs
for continuous beams and slabs. The results of this analysis (see Reference
1) indicated that twin beams having roughly square cross-sections would be
most economical, although slabs had the possibility of more mechanized con-
struction methods, with the potential for reducing costs. In the Phase I
final report, then, four beam and slab-type track structures were recommended;
the estimated costs were from $254,000 to $309,000 per single track mile,
exclusive of rails and fasteners, and from $385,000 to $514,000 per single
track mile, complete.

Admittedly these costs were high, the basic reason being the large
amounts of steel and concrete required for structures stiff enough to meet
the design criterion of one pressure pulse per truck. Therefore, considerable
effort during Phase III was devoted to this subject, realizing that the best
structure will not be adopted if it is too expensive.

Just prior to Phase III, a number of task groups were formed by
DOT to consolidate thinking on the entire Northeast Corridor Program, and
one of these groups considered specifically the subject of guideway costs.
Discrepancies between unit costs used by various investigators were resolved

100

during a series of meetings. As a result, three important unit costs used to calculate costs in Phase I were reduced. It was agreed that the cost of concrete should be $32/yd^3 rather than $50/yd, and that the cost of "placing, removing, and cleaning" forms should be $0.70/ft^2 instead of $1.17/ft^2, and that the cost of elastomer in the rail fasteners should be reduced from $1.20/lb to $0.50/lb. Using these values, the calculated cost of the original twin beam structure was reduced from $254,000 to $200,000 per single track mile, exclusive of rail and fasteners.

Using the revised unit costs, during Phase III the costs of various reinforced concrete track structures were calculated, together with their bending stiffness EI, assuming cast-in-place structures with the concrete taking no tension. The results were shown earlier in Figure 27. That figure showed that increasing the amounts of steel to increase bending stiffness raises cost sharply without corresponding increases in stiffness. Considering now the range of bending stiffness to fall between 2000×10^7 lb-in.^{2} and 9000×10^7 lb-in.^{2}, and $70,000 to be the maximum material cost, three boundaries can be drawn. The fourth boundary, forming the bottom of the area of interest, connects points where the area of steel reinforcing is equal to 0.55 percent of the concrete cross-sectional area, a number quoted as being desirable to control cracking in reinforced concrete structures.[10] The possible range of track structures fall within this area, and include twin beam structures with depths from 9-15 inches, and slabs with depths of 8-12 inches. The amount of steel reinforcement ranges from less than 4 in.^{2} to over 12 in.^{2}.

The material required for the lateral beams in the twin beam structures was not included in the figures, and would increase the material costs by about 10 percent.

Examination of the figure indicates that a slab about 9 inches deep with about 5 in.^{2} of steel reinforcement would have a bending stiffness of 5000×10^7 lb-in.^{2}, and a material cost of around $60,000 per track mile. The total estimated cost for such a structure is as follows:

Excavation and Backfill ($2.50/rail-ft)	$26,400
Forms, Chairs, Spacers, etc.	8,200
Steel-Reinforced Concrete Slab Materials (Installed)	60,000
Fastener Inserts	16,900
Fasteners at $10 apiece, 30-inch spacing (Material Only)	42,000
Rail at 140 lb/yd, $150/ton, (Material Only)	37,000
Fastener and Rail Installation	50,000
	$240,500/track-mile
Contractor's Profit and Contingency (15%)	36,500
	$277,000

It is interesting to note that during the track structure cost meetings mentioned earlier, a number of $200,000/track mile was accepted as a realistic cost for a new installation of conventional track, and also that the fastener material cost is a sizeable portion of the cost. While standard rail was assumed for the Santa Fe installation, smaller rail sections should be considered in other applications of the stiffer track structures[1].

Track Structure Performance Specifications for DOT-Santa Fe Test Track

In considering the overall question of how best to support the rail, the general conclusion of all of the analyses was that continuous longitudinal support is ideal, and that the stability this type of support is determined by two factors—the bearing area, and the bending stiffness. Increased bearing area decreases the magnitude of pressures transmitted into the roadbed, while increased bending stiffness decreases the number of pressure pulses transmitted into the roadbed. Steel-reinforced concrete was chosen as the most economical and suitable material to use. In view of the

102

fact that newly-poured concrete requires a period of weeks to reach maximum strength, and that in some installations where existing track is replaced by nonconventional track it may be necessary to place the new track into operation in a few days, the need for precast as well as cast-in-place concrete structures became evident. The general types of track structures was thus reduced to four: precast slabs, precast beams, cast-in-place slabs, and cast-in-place beams. The precast slab was eliminated from further consideration by DOT, leaving three types of nonconventional track structures to be evaluated in the Santa Fe installation.

Considering first the question of bearing area, the use of slabs and beams automatically gives an approximate 2:1 range in bearing area. Using type MR concrete ties at 30-inch spacing for conventional track, the use of two beams 2 feet wide and a slab 8 feet wide gives a progression of 2.2, 4.0, and 8.0 sq/ft per foot of track length, with the same approximate range of bearing pressures under static wheel loads.

Considering now the bending stiffness, it was considered that specifying the same value for both beams and slabs with their different bearing areas was necessary to isolate the effect of bearing area as a variable. Also, the requirement for the same stiffness achieved by three different designs and two types of construction should give the most insight into costs--that is, the relative costs of obtaining a given stiffness by different designs and construction methods can be obtained.

The next important consideration was the joints in the beams and slabs. With no experience on which to base the design, the field installation should be particularly enlightening in this respect. Because joints are considered undesirable from a maintenance standpoint, a minimum number of joints was specified.

The performance specifications for the three types of structures are given in Appendices G, H, and I.

REFERENCES

1. Meacham, H. C., Voorhees, J. E., Eggert, G. J., Enright, J. J., Fondriest, F. F., and Smith, R. E., "Study of New Track Structure Designs", Research Report from Battelle Memorial Institute to United States Department of Transportation (August 20, 1968).

2. Meacham, H. C., Voorhees, J. E., Eggert, G. J., and Enright, J. J., "Study of New Track Structure Designs, Phase II", Research Report from Battelle Memorial Institute to United States Department of Transportation (February 28, 1969).

3. Timoshenko, S. P., "Method of Analysis of Statical and Dynamical Stresses in Rail", The Collected Papers of Stephen P. Timoshenko, McGraw-Hill Book Co., 1953, pp 422-435.

4. Hetenyi, M., Beams on Elastic Foundation, The University of Michigan Press, 1946, pp 27-30.

5. Letter Report to Kenneth Lawson, U. S. Department of Transportation-- Office of High Speed Ground Transportation, from Association of American Railroads (October 23, 1968).

6. Yoder, E. J., Principles of Pavement Design, John Wiley & Sons, Inc., New York (1959).

7. Washino, Y., Satoh, Y., Miyama, J., and Yamamoto, J., "Experiments on Railway Track with Asphalt Ballast", Report from Japanese National Railways translated by and available from The Asphalt Institute, College Park, Maryland.

8. Kallas, B. F., and Riley, J. C., "Mechanical Properties of Asphalt Pavement Materials" Research Report 67-1, January, 1967, The Asphalt Institute, College Park, Maryland.

9. Bhatia, Gurbachan S., Romualdi, James P., Thiers, Gerald R., "Study of New Track Structure Designs", Report from U. S. Department of Transportation, Office of High Speed Ground Transportation to Carnegie-Mellon University (March, 1968).

10. Construction News, November 14, 1968, "Slab Trials Could Herald Rail Track Revolution".

APPENDIX A

DEVELOPMENT OF MODEL USED FOR COMPUTER ANALYSIS
OF CONVENTIONAL TRACK STRUCTURES WITH STATIC LOADING

APPENDIX A

DEVELOPMENT OF MODEL USED FOR COMPUTER ANALYSIS
OF CONVENTIONAL TRACK STRUCTURES WITH STATIC LOADING

This analysis of conventional track structure makes extensive use of the classical beam on elastic foundation theory that was originally developed to calculate stresses and deflections of railroad track. In this theory the rail deflection y for a single wheel load P at a distance x from the wheel is

$$y = P/K_r \; \epsilon^{-\beta x}(\cos \beta x + \sin \beta x) \; , \qquad (A-1)$$

and the bending moment in the rail is

$$M = \frac{-P}{4\beta} \epsilon^{-\beta x}(\cos \beta x - \sin \beta x) \; , \qquad (A-2)$$

where K_r is the rail stiffness for a single point load given by

$$K_r = \frac{2K}{\beta} \; , \qquad (A-3)$$

$$\beta = \left(\frac{K}{4EI}\right)^{1/4} \; , \qquad (A-4)$$

and K is an overall foundation modulus representing a continuous elastic support under the rail, which has a bending stiffness per unit length, EI. Measurements of rail deflections and rail stresses on railroad track have confirmed that errors using this model are negligible as long as the ties supporting the rail are spaced closely enough so that the rail's deflection wave spans at least eight ties (a condition which is satisfied for all conventional track structures). Because this is a linear theory, deflections and stresses from multiple wheel loads can be obtained by superposition.

However, for a detailed analysis of conventional track, it is necessary to be able to calculate the overall foundation modulus K using parameters for particular track configurations such as tie size and spacing, ballast depth, soil properties, etc. For this reason, the rail supports were considered as vertical springs of stiffness k at each tie and the foundation modulus is then related to the tie spacing ℓ_t by

$$K = k/\ell_t \quad .$$

(A-5)

This spring rate k at each tie is the series equivalent of the spring rate of a resilient rail pad k_p (if any) and half of the spring rate of the ballast-soil foundation k_{bs} beneath the tie

$$\frac{1}{k} = \frac{1}{k_p} + \frac{1}{k_{bs}/2} \quad .$$

(A-6)

The reason for halving the ballast-soil spring rate is that there actually is a continuity of the deflection of the ballast and soil between adjacent loaded ties. This continuity is not accounted for in the fundamental assumption of an elastic foundation and experiments indicate that each of the ties supporting a loaded rail is approximately twice as flexible as when it is loaded alone.*

The ballast-soil spring rate k_{bs} used in Equation (A-6) can be determined from the series equivalent of the ballast stiffness k_b and the soil stiffness k_s by

$$\frac{1}{k_{bs}} = \frac{1}{k_b} + \frac{1}{k_s} \quad .$$

(A-7)

From the theory of elasticity, the effective stiffness of the ballast depends upon the area and shape of the loading area of the tie, the distribution of the loading pressure, and the elastic properties of the

---

* Hetenyi, M., "Beams on Elastic Foundation", U. of Michigan Press, 1946, pp 27-30.

A-2

ballast. When the pressure is evenly distributed over the loading area, the surface stress is uniform but the deflection is not, and the spring rate must be calculated on the basis of an average deflection. This is called "flexible" plate loading in the literature. "Rigid" plate loading yields a uniform surface deflection but the surface stresses are theoretically infinite at the plate edges so this is not a totally realistic model. However, by comparing the theoretical aspects of several models it has been found that a more simplified model can be used to obtain substantially the same results as the more complex models based on the theory of elasticity.

This simplified model assumes both a uniform deflection and a uniform pressure distribution at every depth in an imaginery pyramid spreading downward through the ballast. By the assumptions for this "pyramid" model, the material outside the pyramid is not stressed at all and the material inside is only under vertical compression. Consequently, Poisson's ratio effects are replaced by the "angle of internal friction", a familiar property in soil mechanics that indicates the inclination of the sides of the pyramid to the vertical and thus determines the degree to which the load is distributed as it is transferred downward.

Using the above assumptions, the ballast stiffness for the pyramid model is

$$k_b = \frac{C(\ell - w)\, E_b}{\ell_n\left[\dfrac{\ell}{w}\left(\dfrac{w + CL}{\ell + CL}\right)\right]} \quad , \qquad (A-8)$$

where

E_b = Young's modulus for ballast, psi

ℓ, w = length and width of rectangular loading area ($\ell > w$), inches

L = ballast depth

$C = 2 \tan \alpha$, α = angle of internal friction (20 degrees assumed for ballast) .

A-3

Because the soil section of the pyramid of uniform pressure is assumed to spread out indefinitely, the pyramids beneath neighboring ties would overlap. The overlapping would couple the adjacent soil pyramids, but since the coupling effect has already been included once by halving k_{bs} in Equation (A-6), the soil representation was modified to give an equation for soil stiffness k_s,

$$k_s = k_o A_L = k_o \ (\ell + CL)(w + CL) \quad , \tag{A-9}$$

where k_o is the subgrade modulus of the soil and A_L is the load bearing area at the base of the ballast pyramid at depth L.

Using these models for the ballast and soil, the pressure on the ballast P_b is determined by

$$P_b = \frac{ky}{A_o} \quad , \tag{A-10}$$

and the pressure on the soil P_s is

$$P_s = \frac{P_b A_o}{A_L} \quad , \tag{A-11}$$

where the spring rate at each tie point, k, is obtained from Equation (A-6), and A_o is the effective bearing area of the tie given by

$$A_o = \ell w \quad . \tag{A-12}$$

Recalling the assumed uniform pressure distribution used for the pyramid model, these pressures must be interpreted as average pressures over the loading area so that the actual pressure distribution can be expected to differ somewhat from these predicted averages.

APPENDIX B

DEVELOPMENT OF LUMPED PARAMETER MODEL USED FOR
ANALYSIS OF TRACK STRUCTURES WITH DYNAMIC LOADING

APPENDIX B

DEVELOPMENT OF LUMPED PARAMETER MODEL USED FOR
ANALYSIS OF TRACK STRUCTURES WITH DYNAMIC LOADING

The accepted theory for the vertical deflection of rails is based
on the assumption that the rail can be considered as an elastic beam con-
tinuously supported by an elastic foundation. The static deflection of the
rail is given in the text.

The deflection of the rail under traffic, however, is not a static
problem. For one thing, the point of application of any wheel-load moves
along the rail at the speed of the train, and for another, the magnitude of
the force felt by the rail may be time-varying (due to dynamic unbalance in
the wheels and/or surface irregularities such as flat spots on the wheels and
joints in the rails).

The dynamic response of the rail to a single unbalanced wheel load
moving at constant velocity, V, along a conventional track was investigated
first by considering the two limiting cases of the problem, which are

   (1) The applied force is stationary (V = 0) but the magnitude
        of the force is varying harmonically with time at some
        frequency, f

   (2) The applied force has a constant magnitude, but it is
        moving along the rail at some velocity, V.

There are two ratios that determine the degree to which each of
these limiting dynamic cases causes a significant difference between the
dynamic response and the static response of the system. For limiting case
(1) it is the ratio of the forcing frequency, f, to the natural frequency,
f_o, of the loaded rail and roadbed. For limiting case (2) it is the ratio
of the train speed, V, to the so-called critical velocity, V_c, of the rail
and roadbed. If f/f_o is small the effect of imbalance may be neglected; if
it is nearly one, then the effects of imbalance are significant and the fact

that the wheels are rotating will affect the response of the rails and must be taken into account. If V/V_c is small then the effect of train velocity is negligible; if it is nearly one then the fact that the train is moving will affect the response of the rails and must be taken into account.

The relative magnitudes of these two ratios indicate the degree to which the limiting cases of (1) and (2) are interdependent. If the ratios are nearly the same the coupling is a maximum and the response of the system cannot be approximated by either limiting case.

Considering limiting case (1) first, the natural frequency of the rail and roadbed, which is the frequency that could be most excited by a stationary harmonic force applied directly to the rail, is given in Reference (19) as

$$f_o = (K/M_r)^{1/2}/2\pi, \text{ cps} \quad , \qquad (B-1)$$

where

$$K = \text{foundation modulus, psi}$$
$$= \text{stiffness per unit length}$$
$$M_r = \text{mass of rail per unit length, lb-sec}^2/\text{in.}^2 \quad .$$

If the harmonic force is due to wheel imbalance, then the forcing frequency is given by

$$f = V/R2\pi, \text{ cps} \quad , \qquad (B-2)$$

where

$$V = \text{velocity of the train, in./sec}$$
$$R = \text{radius of train wheel, in.}$$

B-2

Choosing the following typical physical parameters for conventional track with 140-pound rail,

$$\text{Rail:} \quad M_r = 0.0101 \text{ lb-sec}^2/\text{in.}^2$$
$$\text{Roadbed:} \quad K = 1500 \text{ lb/in.}^2$$
$$\text{Train:} \quad R = 18 \text{ in.}$$
$$V = 160 \text{ mph}$$

results in

$$f_o = 61.3 \text{ cps}$$
$$f = 24.9 \text{ cps}$$
$$f/f_o = 0.406 \quad .$$

Considering limiting case (2), the so-called critical velocity, V_c, of the rail and roadbed is a property of the system similar to the natural frequency, f_o. It is defined as the lowest velocity at which a free wave will propagate along the rail, and given in References (19), (20), and (21) by the relation

$$V_c = 2\pi f_o / \beta \quad . \tag{B-3}$$

For the same conventional track with 140-pound steel rail,

$$EI = 2.87 \times 10^9 \text{ lb-in.}^2 \quad ,$$

$$\beta = (K/4EI)^{1/4} = 1.9 \times 10^{-2} \text{ in.}^{-1} \quad ,$$

from which

$$V_c = 2.027 \times 10^4 \text{ in./sec} = 1152 \text{ mph,}$$

$$V/V_c = 160/1152 = 0.139 \quad .$$

B-3

The fact that $f/f_o = 0.406$ is important because although the frequency ratio is small, it is not quite negligible and, therefore, unbalanced rotating wheels will have some magnifying effect on the forces and deflection of the system. There are two important qualifications to the significance of this conclusion, however. First, the system that it pertains to is the rail and roadbed alone without the large mass of the train resting on it. When this large mass is added to the small rail mass per unit length, M_r, in Equation (15), a second and lower natural frequency of the system is introduced, giving an f/f_o ratio greater than 0.406. Secondly, there is surely some damping in the system which, when taken into account, decreases the magnitude of the effect of the rotating unbalance. In fact, for the smallest amount of damping, the one-degree-of-freedom system with $f/f_o = 0.406$ will experience dynamic contact forces and deflections less than 17 percent greater than their static counterparts.

The fact that $V/V_c = 0.139$ indicates that for a train speed of 160 mph the dynamic case is not significantly different from the static case. This conclusion was verified experimentally by Birmann[3] in his investigations.

Lumped Parameter Model of Track Structure. Because the velocity effects can be neglected, it is not necessary to consider the solution of the wave equations for the prediction of track response. For this study of dynamic characteristics, it was concluded that the track could be adequately represented by a single-degree-of-freedom system with a lumped stiffness, k_r, and an effective rail length, L_r, which will give an effective lumped mass corresponding to the natural frequency of the distributed system.

The values of L_r and m_r are determined by writing Equation (15) in the form

$$2\pi f_o = \left[\frac{KL_r}{ML_r}\right]^{1/2} = \left[\frac{k_r}{m_r}\right]^{1/2} \quad , \tag{B-4}$$

B-4

and rewriting Equation (2) in the form

$$k_r = \frac{P}{y(0)} = \frac{2K}{\beta} \quad , \qquad \text{(B-5)}$$

which gives the lumped system parameters

$$L_r = 2/\beta, \text{ in.} \quad , \qquad \text{(B-6)}$$

$$m_r = M_r L_r, \text{ lb sec}^2/\text{in.} \quad , \qquad \text{(B-7)}$$

$$k_r = K L_r, \text{ lb/in.} \qquad \text{(B-8)}$$

Figure 10 shows a longitudinal beam type of track structure with two wheels and the corresponding lumped-parameter model of this system. The model for a conventional tie-type track structure is the same, with different values for the masses and spring rates.

For inputs, or forcing functions, track irregularities are represented by a time function, $\epsilon(t)$, corresponding to spatial variation and train speed so that

$$z_{wr} = z_r + \epsilon(t)$$

$$\qquad \text{(B-9)}$$

$$z^*_{wr} = z_r + \epsilon(t-t_o) \quad .$$

All displacements, z and z^*, are measured relative to static equilibrium positions. Consideration of wheel-lift requires auxiliary equations to calculate the contact force between wheel and rail, and a switching circuit to transfer to modified equations for the lift-off period when the calculated contact force indicates that the total load between wheel and rail, including static weight, is zero.

Although both mass and damping of the rail beam and soil, m_{RBS} and C_{RBS} have been included in the model, they can both be neglected so

B-5

long as the frequencies of interest are less than about 0.3 f_0. Soil (and ballast) damping, C_{RBS}, is an elusive quantity, but if the damping ratio for the single-degree-of-freedom system is no more than 0.2, the damping can be neglected for all frequencies below about 0.6 f_0 with little loss in accuracy.

Effects on Model of Additional Wheels. Deflection curves show that if the wheel separation distance, L, is greater than $L_r = 2/\beta$, the coupling between the rail deflections under the different wheels can be neglected. For the nominal track data used herein, this gives an L_r = 8.77 feet. Note that this is the effective rail length used to calculate the dynamic mass, so that if the wheel separation distance is just equal to 8.77 feet, it is easy to visualize the section of rail between the wheels divided equally, both mathematically and physically.

When the wheel separation distance is less than L_r, the response of the two wheels will be coupled through the rail deflections.

Resilient Rail Pad. The model used for a track system containing a resilient rail pad was the double mass-spring system depicted in Figure 10 . The lumped mass of the rail, m_r, and the spring rate of the rail-pad system, k_{rp}, were determined as described above for a single beam (the rail) on a continuous elastic foundation (the rubber pad). The lumped mass of the beam structure and soil roadbed, m_B, and its spring rate, k_{BS}, were determined in the same way, by assuming that this beam structure also acts as a beam on a continuous elastic foundation (the soil).

APPENDIX C

DATA FROM TRACK RESPONSE MEASUREMENTS ON
PENN CENTRAL HIGH-SPEED TRACK
December 10-12, 1969
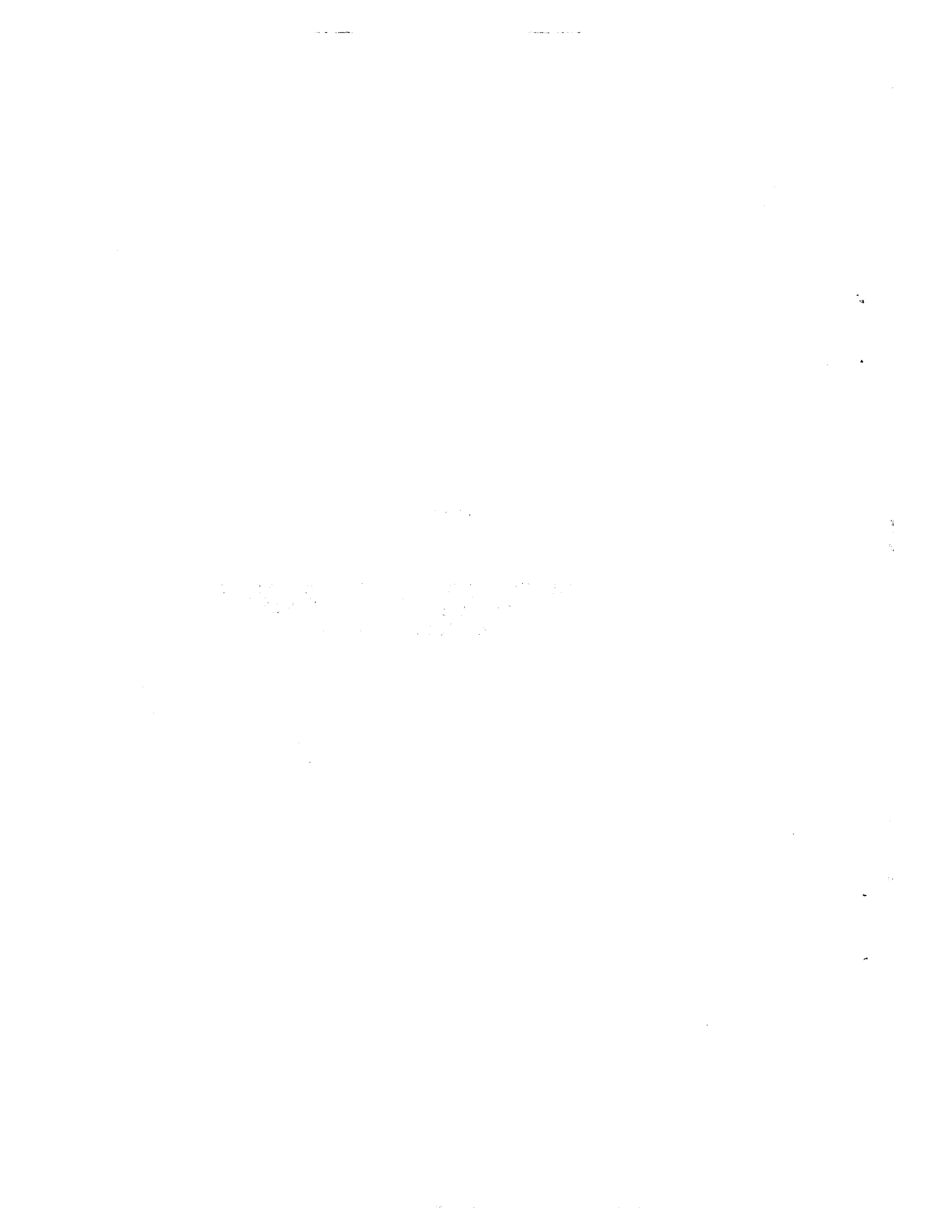
APPENDIX C

DATA FROM TRACK RESPONSE MEASUREMENTS ON PENN CENTRAL HIGH-SPEED TRACK
December 10-12, 1969

Traces representative of data obtained from track response measurements are presented in this appendix. Sixteen channels of data were recorded on a Consolidated Electrodynamics Corporation (CEC) System D galvonometer recording system: 2 tie plate loads, 8 subgrade pressures, 4 vertical motions, and 2 vertical accelerations. In addition, seven channels of data were recorded on FM tape: 2 tie plate loads, 2 vertical motions, 2 subgrade pressures, and one vertical acceleration.

The two tie plate load cells, using miniature strain-gage load washers installed in standard tie plates, were used in conjunction with the CEC Type 124 light-beam oscillograph with galvonometers having a frequency response flat to 600 Hz. Motion transducers, because of mechanical linkages, were limited in frequency response to roughly 100 Hz. Rail accelerations were recorded with a Kistler Type 802A piezoelectric accelerometer in conjunction with a Kistler Type 568 charge amplifier and CEC Type 326 galvonometers with frequency response flat to 3000 Hz.

Traces in Figures C-1 through C-6 were re-recorded from the FM tape on a Brush Mark 220 pen recorder having a frequency response flat to approximately 100 Hz. Impulsive response (tie plate loads as wheels hit the joint, for example) is consequently attenuated in these traces. Values tabulated in the report were taken from the original light-sensitive CEC recordings, which have superior frequency response, but cannot be reproduced easily. A typical CEC recording is shown in Figure C-7: the data traces of interest have been laboriously traced over with pencil in order to retain and reproduce the data in the presence of ultraviolet light.
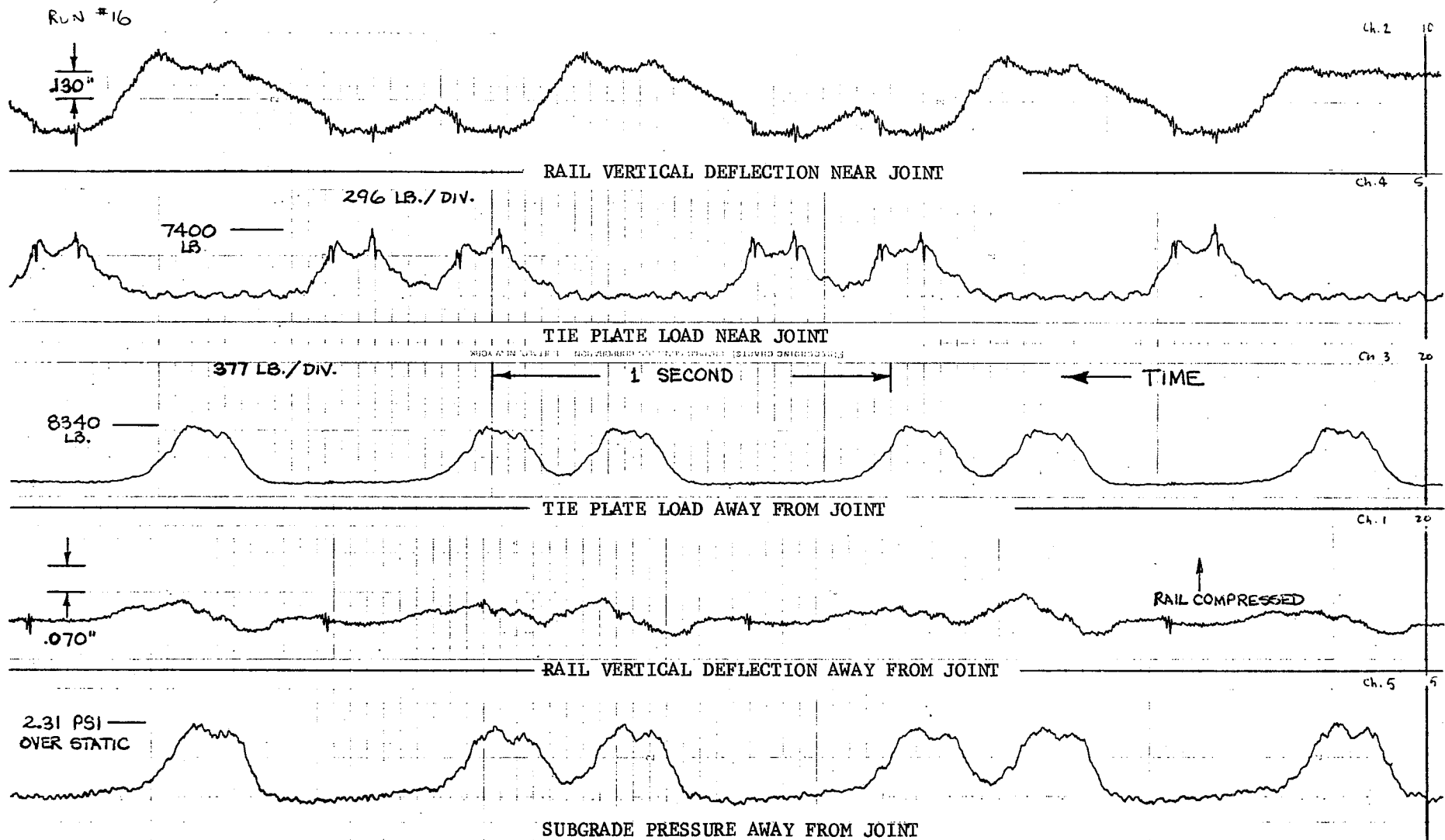
RUN #16

.130"

RAIL VERTICAL DEFLECTION NEAR JOINT

Ch.2   10

296 LB./DIV.

7400 LB

TIE PLATE LOAD NEAR JOINT

Ch.4   5

377 LB./DIV.

8340 LB.

1 SECOND   TIME

TIE PLATE LOAD AWAY FROM JOINT

Ch.3   20

.070"

RAIL COMPRESSED

RAIL VERTICAL DEFLECTION AWAY FROM JOINT

Ch.1   20

2.31 PSI
OVER STATIC

SUBGRADE PRESSURE AWAY FROM JOINT
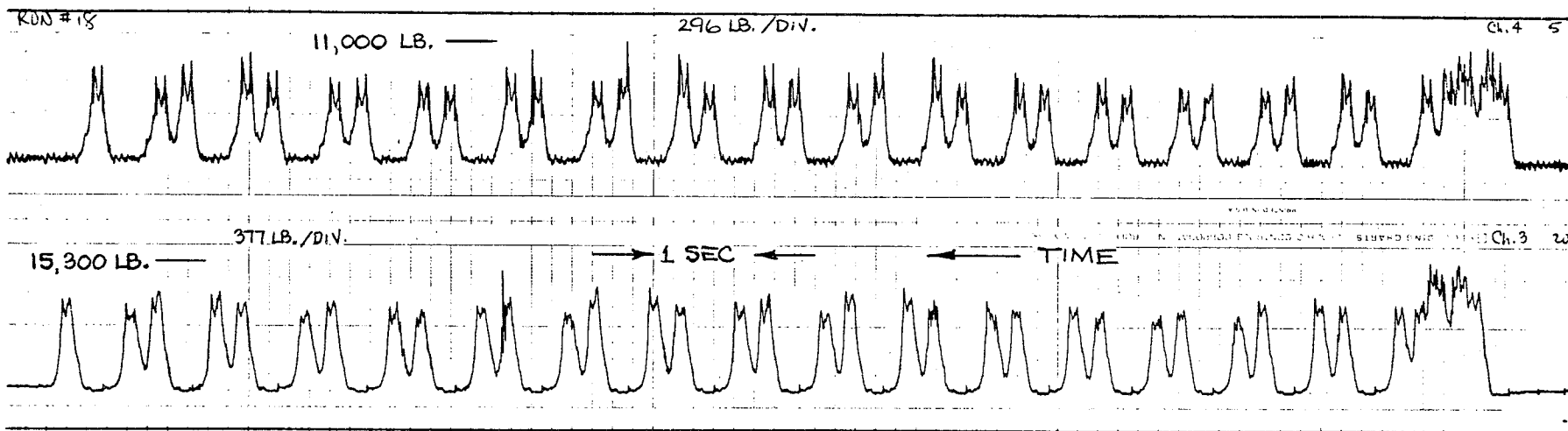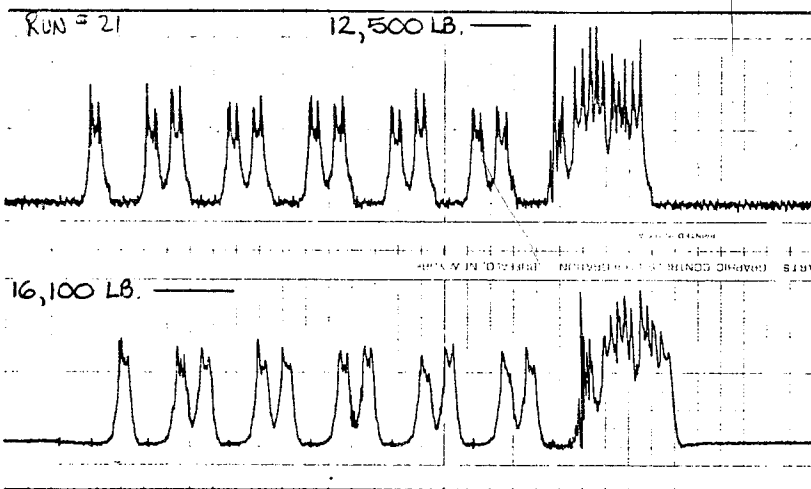
Ch.5   5

FIGURE C-1.   TRACK RESPONSE TO DOT TEST TRAIN SOUTH AT 55.6 MPH,
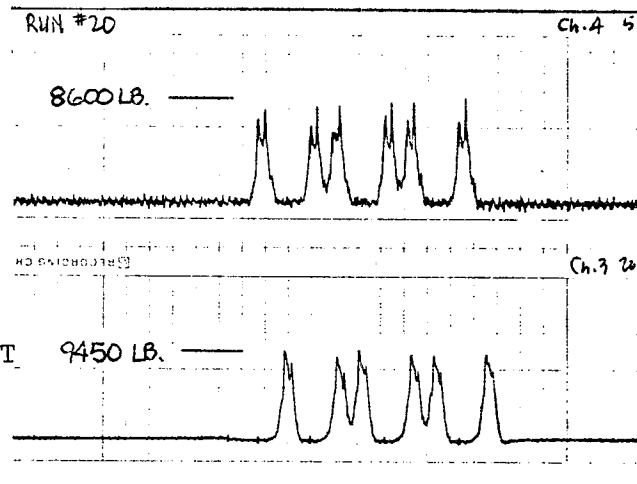   BOWIE, MARYLAND, 12-11-69.

a) NORTHBOUND PASSENGER TRAIN # 172, GG-1 WITH 16 CARS; 73.3 mph. 12-11-69

CH. 4 -- TIE PLATE
LOAD NEAR JOINT

CH. 3 -- TIE PLATE
LOAD AWAY FROM JOINT

b) PASSENGER TRAIN SOUTH, GG-1 WITH 6 CARS;
    80.9 mph. 12-11-69
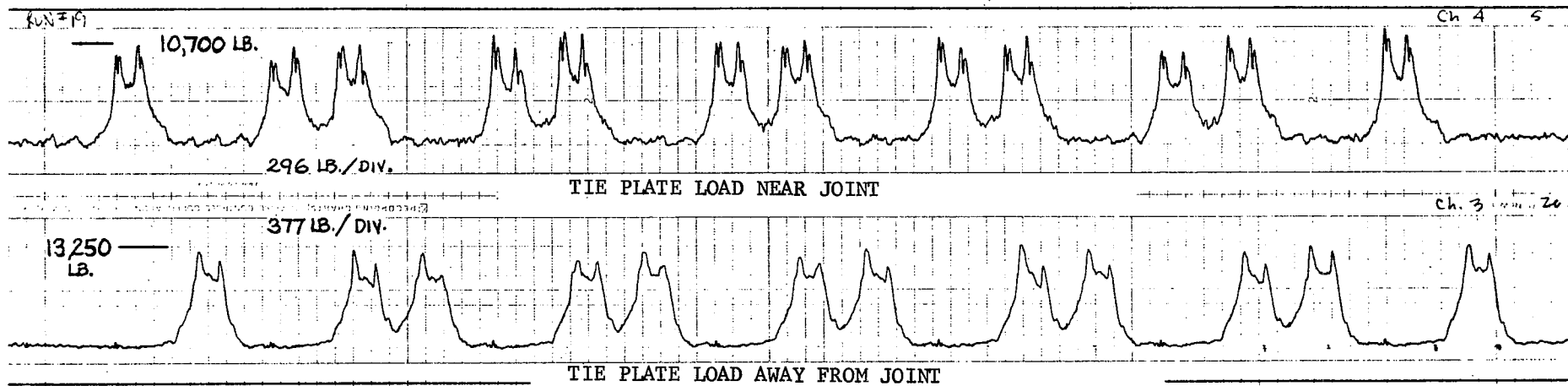
c) DOT TEST TRAIN SOUTH, 88.0 mph.
    12-11-69

FIGURE C-2. RECORDINGS OF TIE PLATE LOADS UNDER
             MISCELLANEOUS TRAFFIC.

RUN #10

.044"

RAIL COMPRESSED
(DOWN)

← 1 SECOND →

← TIME

RAIL VERTICAL DEFLECTION AWAY FROM JOINT

397 LB/DIV.

11,900
LB.

TIE PLATE LOAD AWAY FROM JOINT
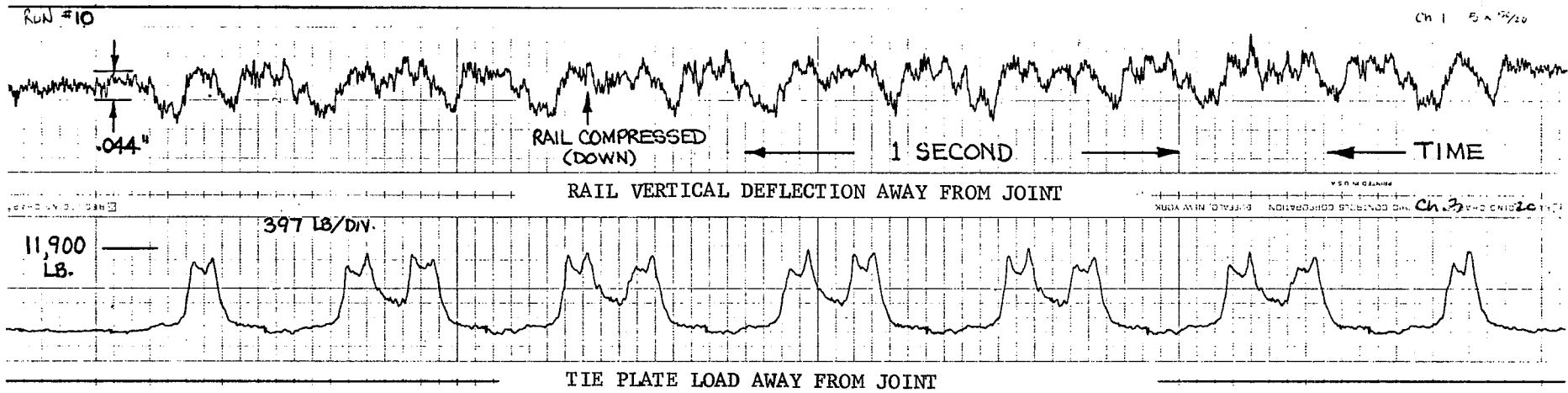
a) METROLINER SOUTH AT 114 MPH, 12-10-69.

RUN #9

10,700 LB.

296 LB./DIV.

TIE PLATE LOAD NEAR JOINT

377 LB./DIV.

13,250
LB.

TIE PLATE LOAD AWAY FROM JOINT

b) METROLINER SOUTH AT 115 MPH, 12-11-69

FIGURE C-3. TRACK RESPONSE TO HIGH-SPEED METROLINER TRAFFIC,
PENN-CENTRAL TRACK NO. 3, BOWIE, MARYLAND.

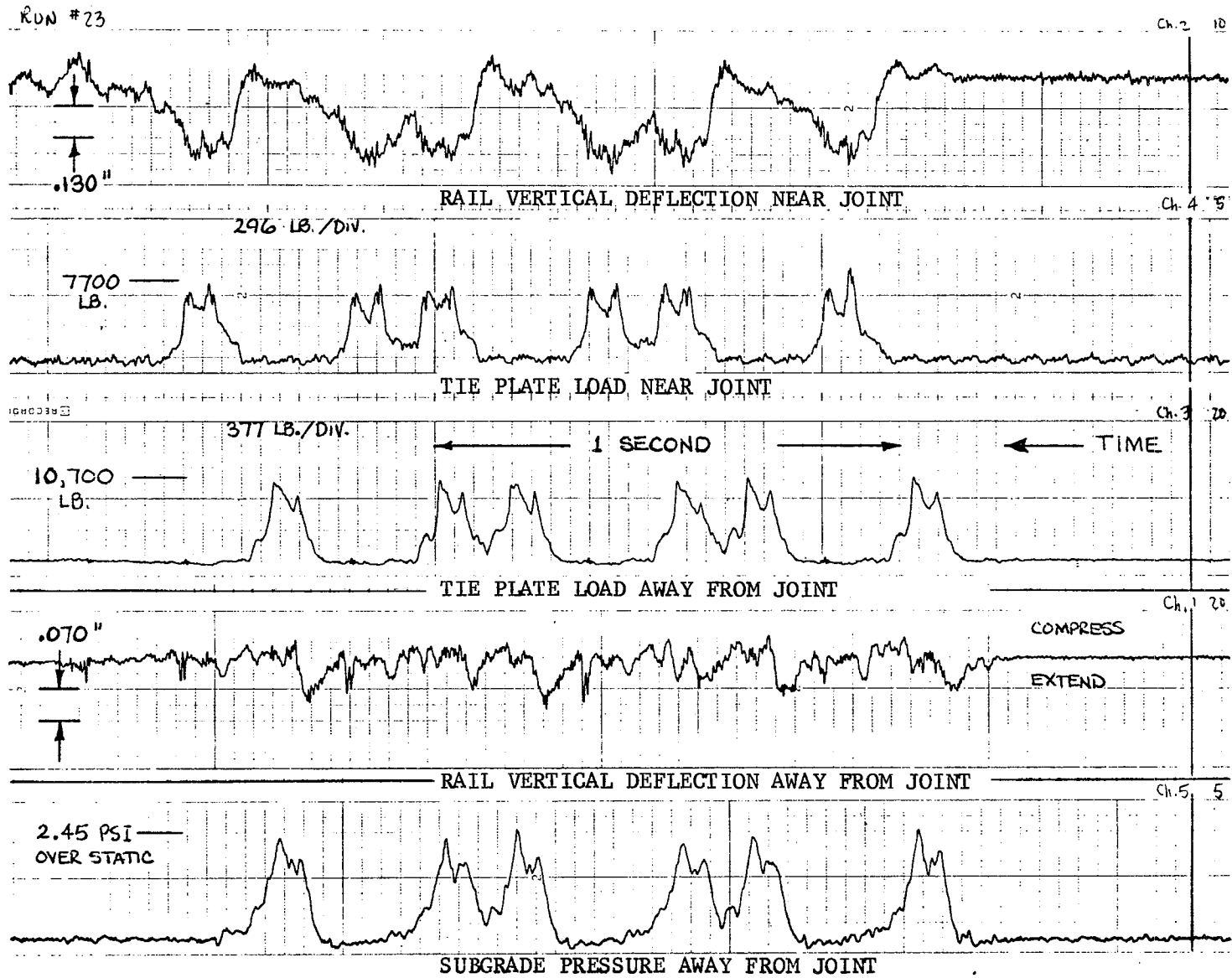RUN #23

FIGURE C-4. TRACK RESPONSE TO DOT TEST TRAIN SOUTH AT 115 MPH,
BOWIE, MARYLAND, 12-11-69

RUN #27

.260"

592 LB./DIV.

RAIL VERTICAL DEFLECTION NEAR JOINT

Ch.2 10

Ch.4 10

21,400 LB

TIE PLATE LOAD NEAR JOINT

377 LB./DIV.

18,700 LB.

1 SEC

TIME

Ch.3 20

TIE PLATE LOAD AWAY FROM JOINT

.140"

RAIL COMPRESSED

Ch.1 20

RAIL VERTICAL DEFLECTION AWAY FROM JOINT

Ch.5 10
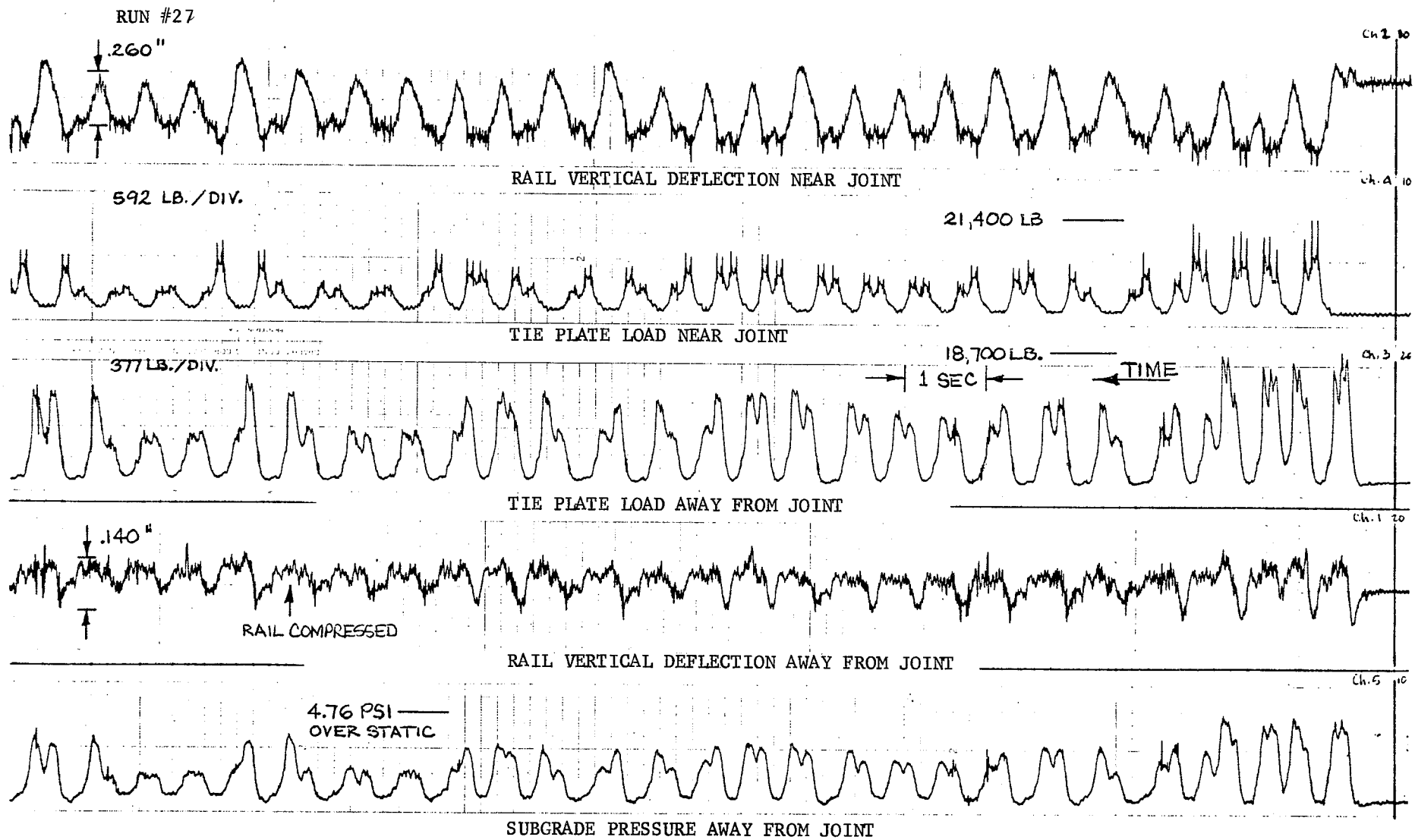
4.76 PSI
OVER STATIC

SUBGRADE PRESSURE AWAY FROM JOINT

FIGURE C-5. TRACK RESPONSE TO SOUTHBOUND FAST FREIGHT, 2 E44 ELECTRIC
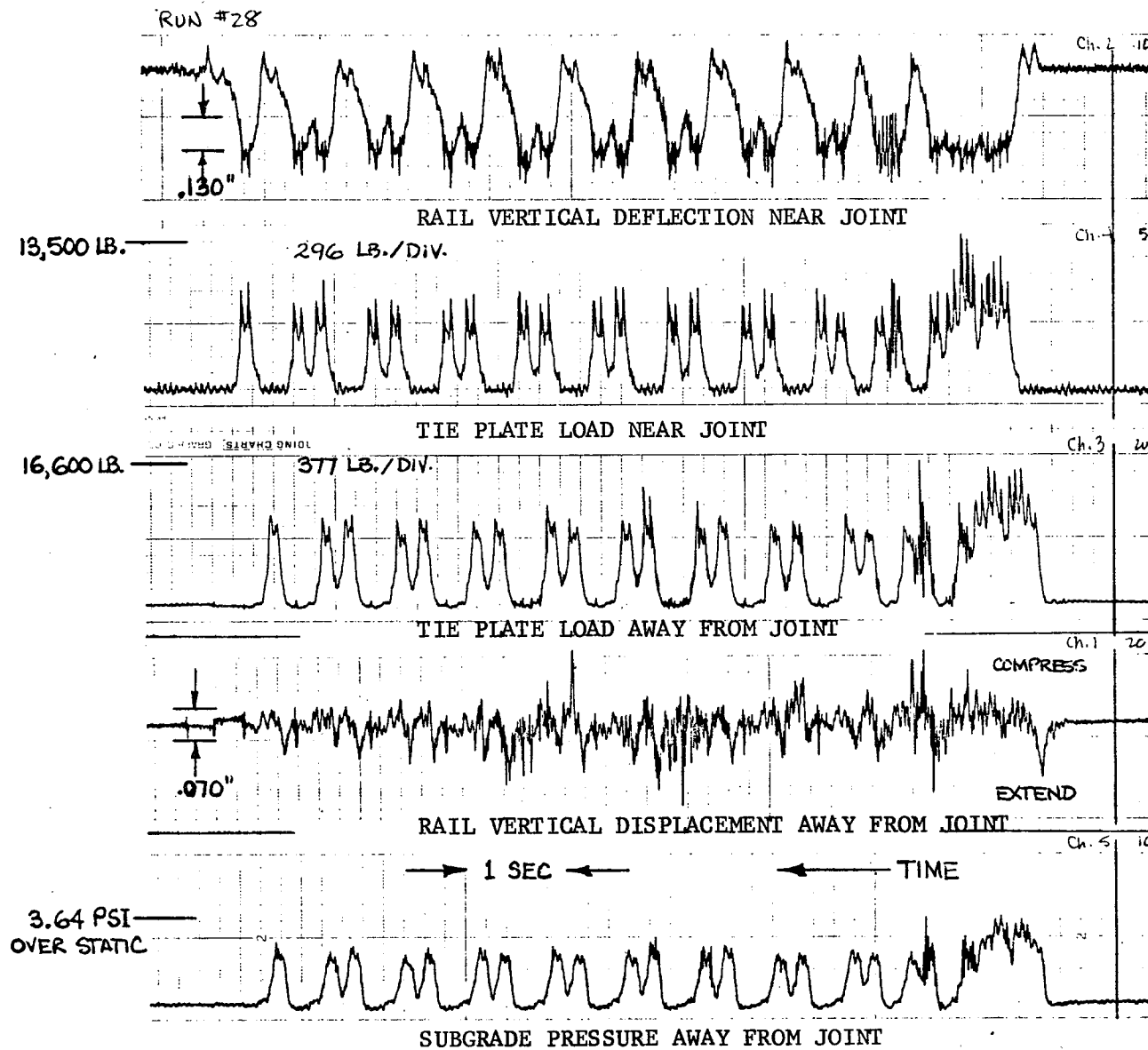LOCOMOTIVES, 33 CARS OF MIXED FREIGHT, 53.0 MPH. BOWIE,
MARYLAND, 12-11-69

RUN #28

RAIL VERTICAL DEFLECTION NEAR JOINT

.130"

13,500 LB.

296 LB./DIV.

Ch. 4   5

TIE PLATE LOAD NEAR JOINT

16,600 LB.

377 LB./DIV.

Ch. 3   w

TIE PLATE LOAD AWAY FROM JOINT

Ch. 1   20

COMPRESS

.070"

EXTEND

RAIL VERTICAL DISPLACEMENT AWAY FROM JOINT

Ch. 5   10

1 SEC   TIME

3.64 PSI
OVER STATIC

SUBGRADE PRESSURE AWAY FROM JOINT

FIGURE C-6.   TRACK RESPONSE TO SOUTHBOUND PASSENGER TRAIN AT 77.6 MPH:
THE "BLUE" GG-1 WITH 6 CARS; BOWIE, MARYLAND, 12-11-69

RAIL DISPLACEMENT
AT JOINT

.29"

0

TIE PLATE LOAD AT JOINT   15
0

8450#   6550#

13

.06"

RAIL DISPL. AWAY FROM JOINT

TIE PLATE LOAD AWAY FROM JOINT
0

8300#

#12
#11
SUBGRADE
PRESSURES
2.0 PSI
#8
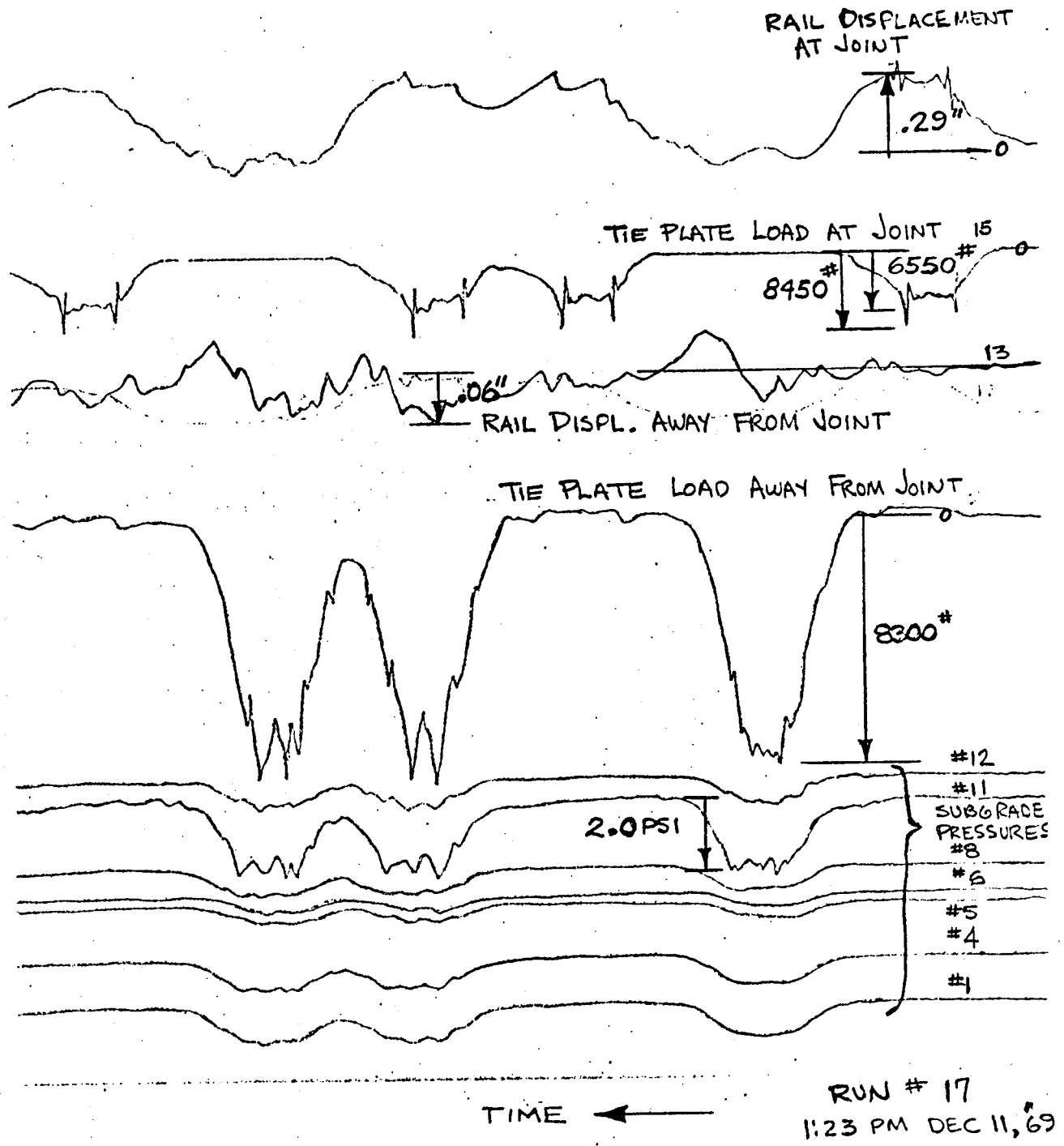#6
#5
#4
#1

TIME ←

RUN # 17
1:23 PM DEC 11, 69

FIGURE C-7.   TRACK RESPONSE TO DOT TEST TRAIN SOUTH
AT 74.6 MPH, 12-10-69.   TYPICAL CEC GALVO-
NOMETER RECORDING.

APPENDIX D

DESIGN CRITERION FOR TRACK STRUCTURES
FOR HIGH-SPEED TRAINS BASED ON
ALLOWABLE TIME-VARYING SOIL PRESSURES

APPENDIX D

DESIGN CRITERION FOR TRACK STRUCTURES
FOR HIGH-SPEED TRAINS BASED ON
ALLOWABLE TIME-VARYING SOIL PRESSURES

Based on this analysis of conventional track structures and
dynamic soil characteristics, a design criterion was evolved from the basic
objective of imposing the least hardship on the soil supporting the track
structure. This can be done by keeping the amplitudes and frequencies of
pressures transmitted to the soil as low as practical.

This basic objective can be met by using longitudinal beams to
distribute the wheel loads over a large area of soil and thereby decrease
both the amplitude and frequency of the bearing pressure on the soil. The
extent to which a longitudinal beam does this is dependent on its bending
rigidity, on its width resting on the soil, and on the resilience of the
soil ("modulus of subgrade reaction"). A relationship between these
parameters and the time-varying pressure on the soil beneath the beam was
developed, and this relationship expanded into a design criterion, a
detailed discussion of which follows. The criterion has been used to design
and analyze longitudinal beam-type track structures.

The development of this design criterion enabled track structures
of greatly differing design to be compared on a quantitative basis. After
sizing the designs to meet the design criterion, they were compared on a
cost basis, since in the final analysis the cost-performance balance will
determine the selection of an improved track structure.

Different track structures, using longitudinal beams to support
the rails, can have similar pressure-time curves. As shown in Figure D-1,
a deep, narrow structure has high bending rigidity and distributes the wheel
loads longitudinally over a large area, whereas a shallow, wide structure
distributes the loads over a large width. The resultant two pressure-time
curves are similar, with the peak pressure the same in both cases. The goal
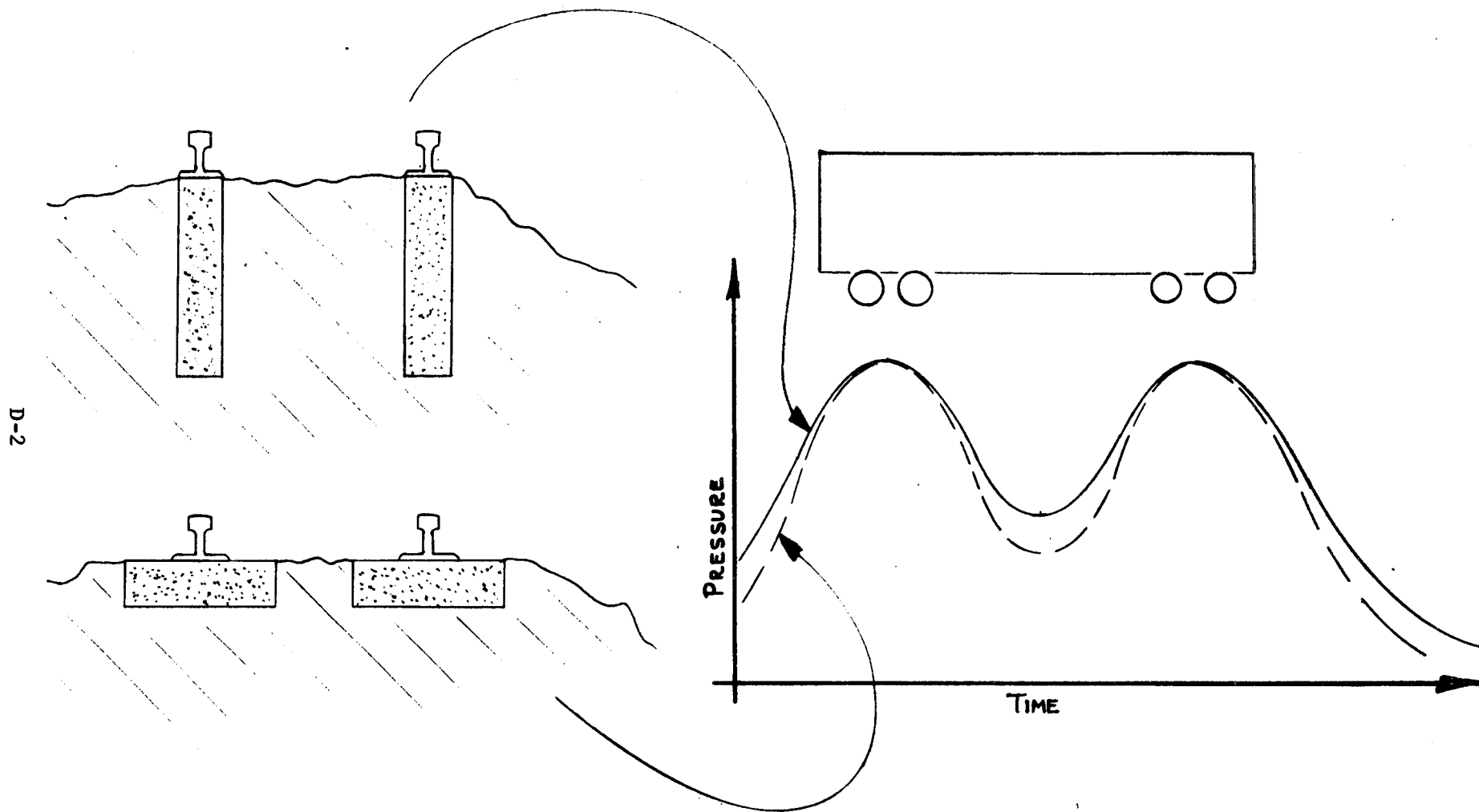of generating only one pressure pulse per truck, rather than two, can be

FIGURE D-1. TWO DIFFERENT TRACK STRUCTURES WHICH YIELD SIMILAR SOIL PRESSURE-TIME CURVES

attained with either design by making the track structure sufficiently
rigid.

Predicting Settlement Rate of Soil

The first step in the development of the design criterion was to
derive a quantitative relationship between the imposed cyclic pressures and
the settlement of the soil; the settlement rate of the soil was the parameter
that was used to compare different pressure-time curves. Ideally, the
settlement rate under the track structure can be predicted if the pressure-
time curve is analyzed as to its frequency content and pressure amplitude at
each frequency, and if the settlement rate curve (Figure D-2) is well known
for the soil of interest. In practical terms, however, this is unrealistic,
and for this reason mathematical approximations were made of both the
pressure-time curve and the settlement rate curve.

Approximate Pressure-Time Curve

The pressure-time curve can be closely approximated by:

$$p(t) \approx p_1 \cos 2\pi f_1 t + p_2 \cos 2\pi f_2 t + p_2 \qquad (1)$$

where

$$f_1 = 1/\tau_1$$

$$f_2 = 1/\tau_2.$$

τ_1 and τ_2 are the periods of the two most important cycles, as shown in
Figure D-3, and are constants for a given wheel spacing and train speed.
p_1 and p_2 are the amplitudes of these two pressure cycles and are constants
(for a given track structure) chosen such that $p(t)$ passes through points
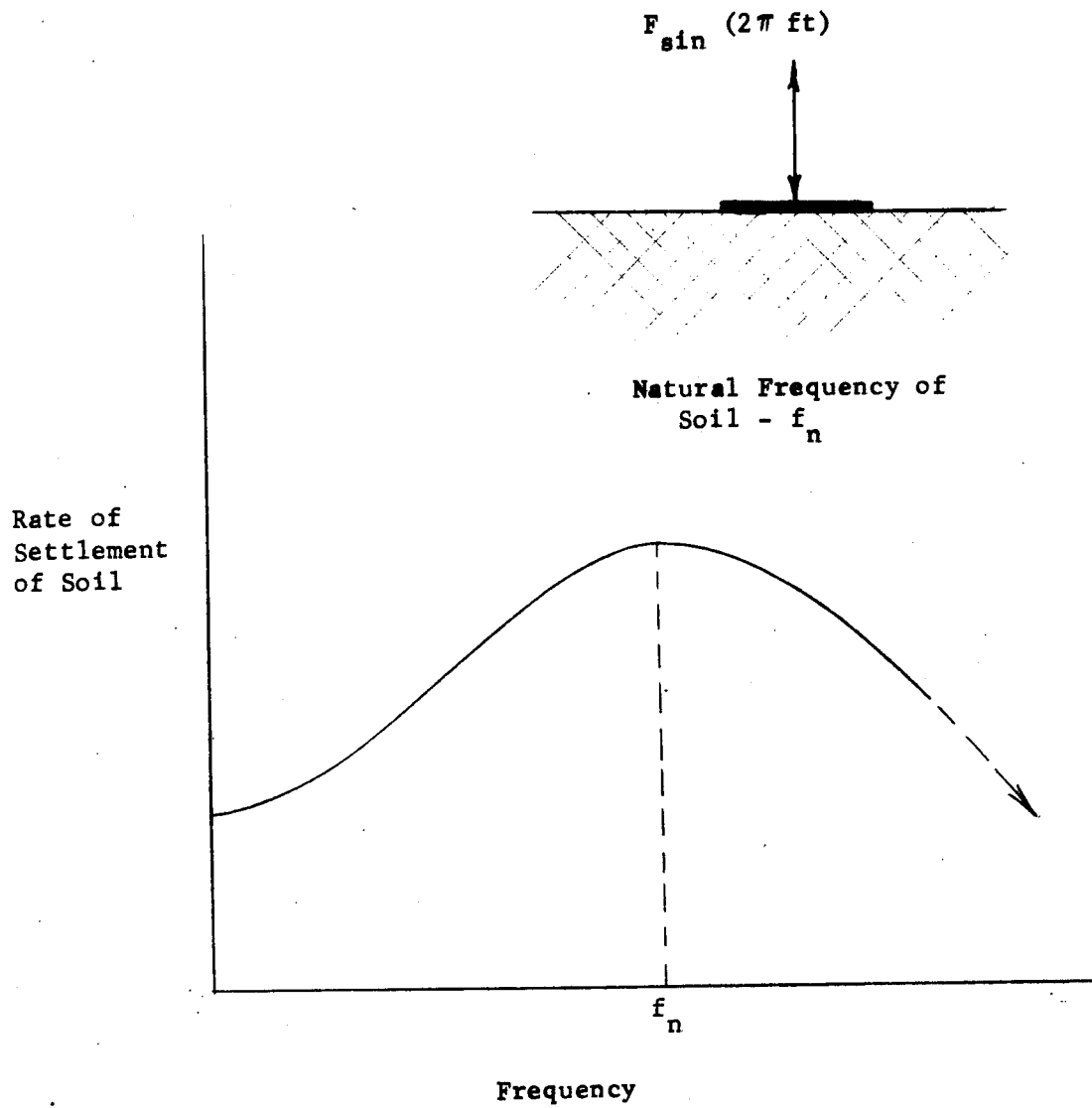MT and BC in Figure D-3.

$F_{sin} (2\pi ft)$

Natural Frequency of
Soil - f_n

Rate of
Settlement
of Soil

f_n

Frequency

FIGURE D-2. RATE OF SETTLEMENT OF SOIL AS A FUNCTION OF THE APPLIED
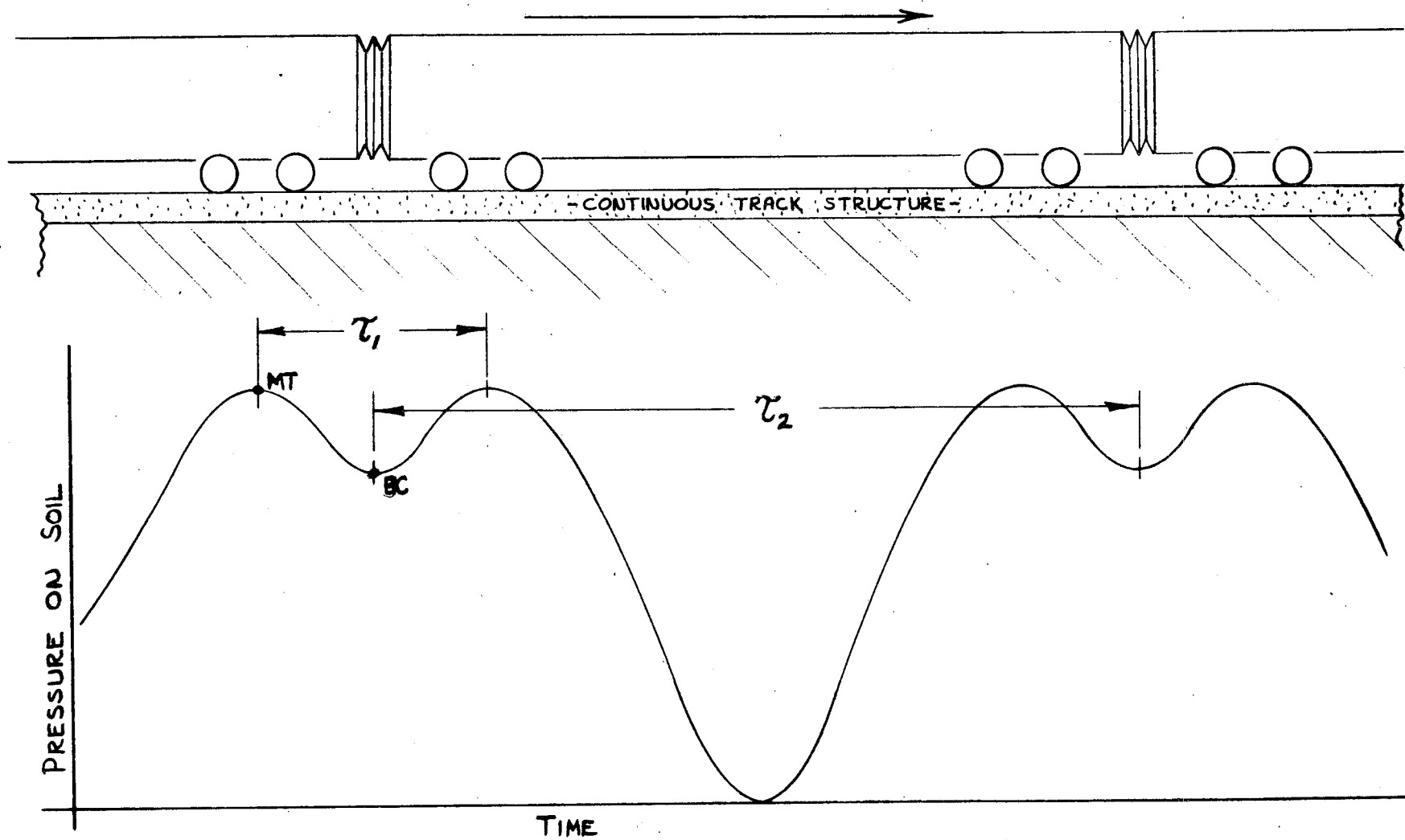FREQUENCY OF A CONSTANT MAGNITUDE PRESSURE

D-4

FIGURE D-3. PRESSURE-TIME CURVE EXPERIENCED BY SOIL BENEATH A FAIRLY RIGID TRACK STRUCTURE
(NO PRESSURE FLUCTUATIONS FOR INDIVIDUAL WHEELS)

This approximation contains the two most important frequencies in the pressure-time curve (f_1 and f_2) and their respective amplitudes p_1 and p_2. The accuracy of this approximation is shown in Figure D-4, which compares a typical pressure-time curve with its approximate curve. Greater accuracy could, of course, be obtained by increasing the number of terms in the expression.

Approximate Settlement Rate

With the approximation of the pressure-time curve as described above, the total settlement of the soil becomes dependent only on the values of p_1, p_2, f_1, and f_2. Earlier it was mentioned that new track structures for high-speed use should be designed so that there is no soil pressure fluctuation for each wheel, so that both f_1 and f_2 would be below f_n, the natural frequency of the soil, for the Budd car traveling at 160 mph. Therefore, only the left half of the settlement rate curve of Figure D-2 need be approximated in order to evaluate the effects of f_1 and f_2.

The settlement rate curve can be approximated as:

$$s = (\mu - 1)(\text{pressure amplitude}) \tag{2}$$

where μ = magnification factor for a single-degree-of-freedom system

$$= \frac{1}{1-r^2} \text{ (for zero damping)}$$

r = ratio of the forcing frequency to the natural frequency of the soil

$$= f/f_n \ .$$

For a pressure varying sinusoidally at one frequency (as shown in Figure D-2), (μ-1) can be calculated and thus the rate of settlement can be predicted.
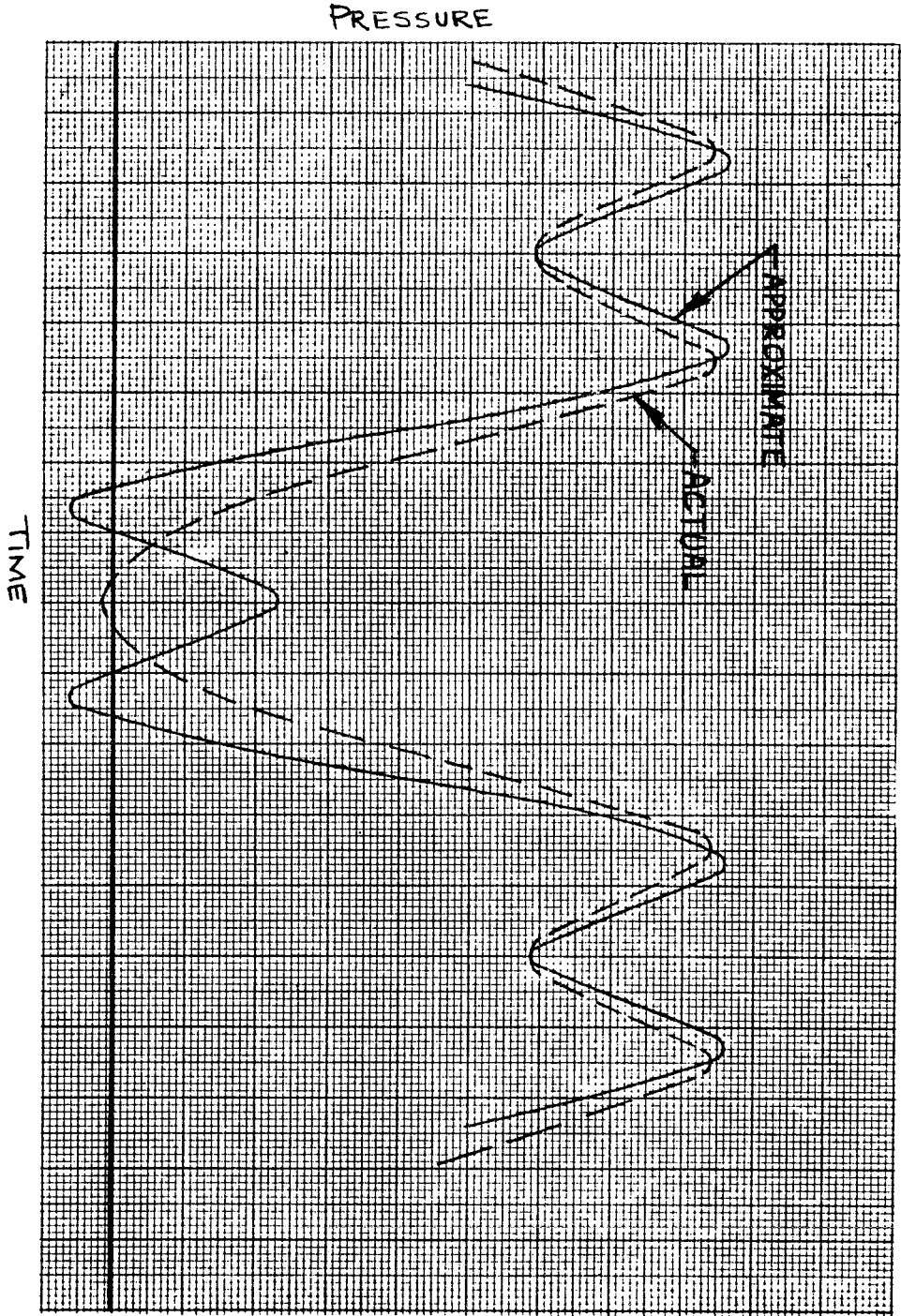
D-6

PRESSURE

TIME

APPROXIMATE

ACTUAL

FIGURE D-4. APPROXIMATE AND ACTUAL PRESSURE-TIME CURVE

The assumption of zero damping is not critical for values of forcing frequency that are less than about one-half of the natural frequency (which is the case in point), because the magnification factors for these frequencies do not change significantly with added damping.

With these two approximations, an estimate of the total effect of the time-varying pressure on the settlement of the soil can be made. This has been done, and a Soil Deterioration Factor (SDF) has been defined as the sum of settlement rates at the frequencies f_1 and f_2.

$$SDF = s_1 + s_2 \tag{3}$$

$$SDF = |p_1| \, (\mu_1 - 1) + |p_2| \, (\mu_2 - 1) \tag{4}$$

$$SDF = |p_1| \, [r_1^2/(1 - r_1^2)] + |p_2| \, [r_2^2/(1 - r_2^2)] \tag{5}$$

This one number (SDF) can now be used to quantitatively compare the severity of the soil loading and, in turn, it can be used to compare two different track structures on the basis of soil loading. This method of comparison is especially useful in that it can be used to compare different track structures which carry different speed trains. For example, a track structure carrying a train at 160 mph can be designed to have the same amount of soil deterioration as a conventional track carrying the same train at 53.3 mph by equating the Soil Deterioration Factors based on the pressure-time curves for the two cases.

Reference System

To provide reference against which to compare advanced high-speed track structures, a conventional rail-tie-ballast track was chosen. To simplify the calculations and to obtain the least error in the approximations, the reference car and speed were chosen to be the Budd car traveling at

53.3 mph. One reason for using this speed as a reference was that at 53.3 mph, f_1 = 9.2 cps, which is the same as that obtained with the Budd car at 160 mph under a structure rigid enough so that individual wheels do not cause individual pressure fluctuations. Also, this speed was believed to be one which well-built conventional track can withstand without requiring a large amount of maintenance.

A reference soil was chosen which has a natural frequency of 20 cps. It was believed that this value was a reasonably conservative value, and it was used for all calculations.

The pressure-time curve for this reference system was shown in Figure D-5, and is approximated by Equation (1) where f_1 and f_2 are 9.2 cps and 3.07 cps, respectively. By setting

$$p(t_1) = 15.1 = p_1 \cos 2\pi \ (9.2) \ t_1 + p_2 \cos 2\pi \ (3.07) \ t_1 + p_2 \tag{6}$$

and

$$p(t_2) = 10.4 = p_1 \cos 2\pi \ (9.2) \ t_2 + p_2 \cos 2\pi \ (3.07) \ t_2 + p_2 \tag{7}$$

and solving the two equations simultaneously, it is found that

$$p_1 = 4.20 \text{ psi}$$

and

$$p_2 = 7.30 \text{ psi}$$

The Soil Deterioration Factor can now be calculated as

$$\text{SDF} = 4.20 \ [(9.2/20)^2/(1 - (9.2/20)^2)] + 7.30 \ [(3.07/20)^2/(1 - (3.07/20)^2)]$$

$$\text{SDF} = 1.31.$$

This, then, is the value which was used as a reference, based on the specific case of the Budd car traveling over a conventional track structure
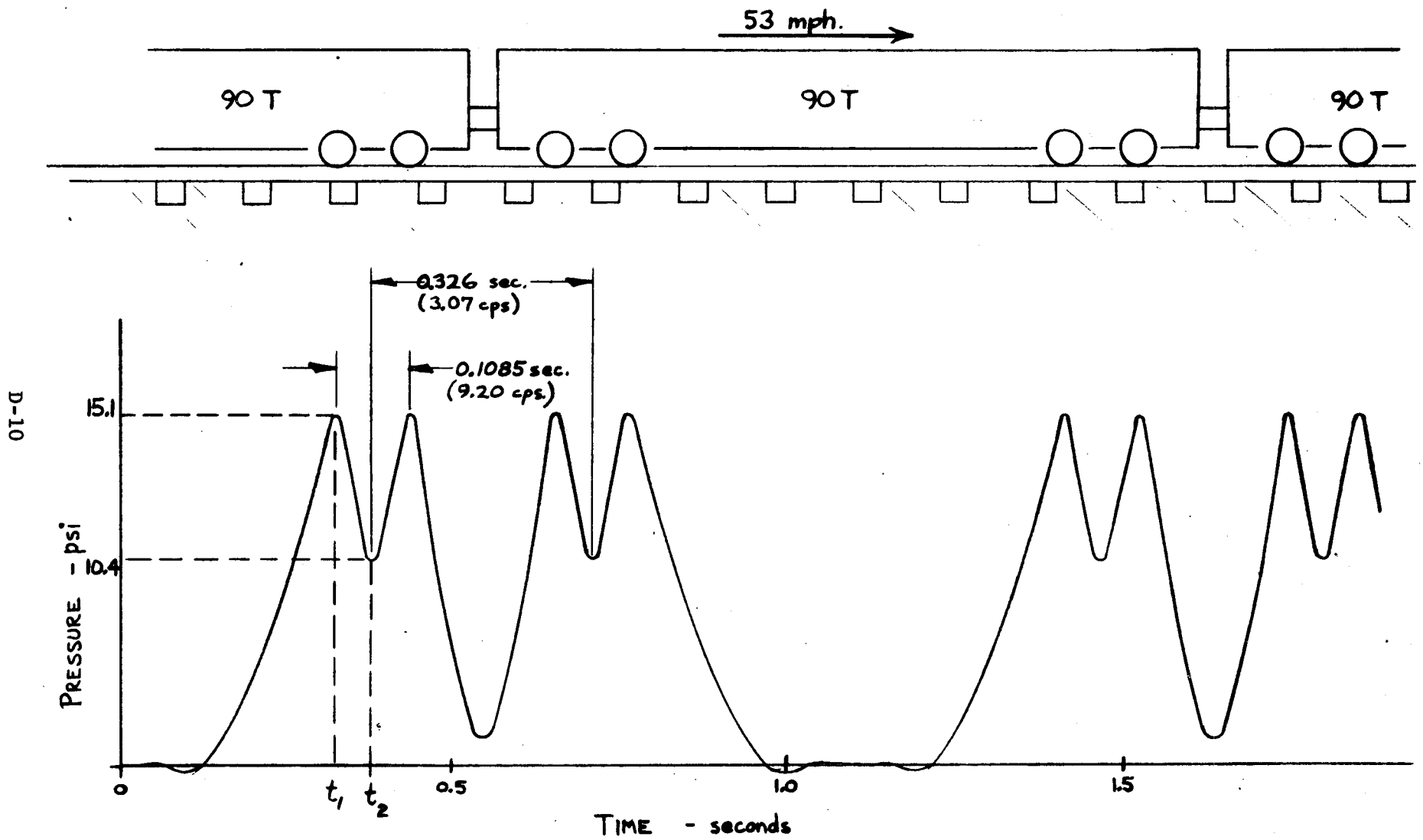
FIGURE D-5. TYPICAL PRESSURE-TIME CURVE FOR PRESSURE DIRECTLY
UNDER A TIE OR A CONVENTIONAL TRACK STRUCTURE

at approximately 50 mph. Deterioration of the soil increases as the SDF becomes larger; advanced track structure designs were based on meeting or exceeding (lower SDF) this criterion at a train speed of 160 mph.

In general, the SDF depends on the pressure-time curve which, for a continuous beam-type structure, depends on the following:

(1) The bending rigidity of the track structure (EI)

(2) The width of the structure that rests on the soil (W)

(3) The modulus of the soil (k_o)

(4) The car weight

(5) The wheel spacing of the car

(6) The train speed.

The interrelationship of the first four of these factors is shown in Figure D-6 for the Budd car's wheel spacing. Each curve represents the static pressure at a different point under the train-loaded track structure (or, for a particular train speed, each curve represents a different point on the pressure-time curve). A close examination of this curve is important. Note that for a given wheel load, and track structure width, each of the curves becomes a plot of soil pressure (proportional to deflection) versus soil stiffness per unit length and rail bending stiffness. A decrease in soil stiffness has the same effect as an increase in rail stiffness. To satisfy the criterion of seeing only one pressure pulse per truck, the portion of the curves to the left of $(K/EI)^{1/4}$ = 0.025 must be used. To the right of this point, the pressure at mid-truck (MT) drops below that at the wheels (IA and OA) meaning that two pressure pulses per truck would be generated, rather than one.

The design criterion, then, is composed of two restrictions which EI/k_o and W must meet:

(1) $$SDF = f(EI/k_o, W) \leq 1.31.$$

This means that the deterioration to the soil will be no worse at 160 mph than it is for conventional track carrying a 53.3 mph train.
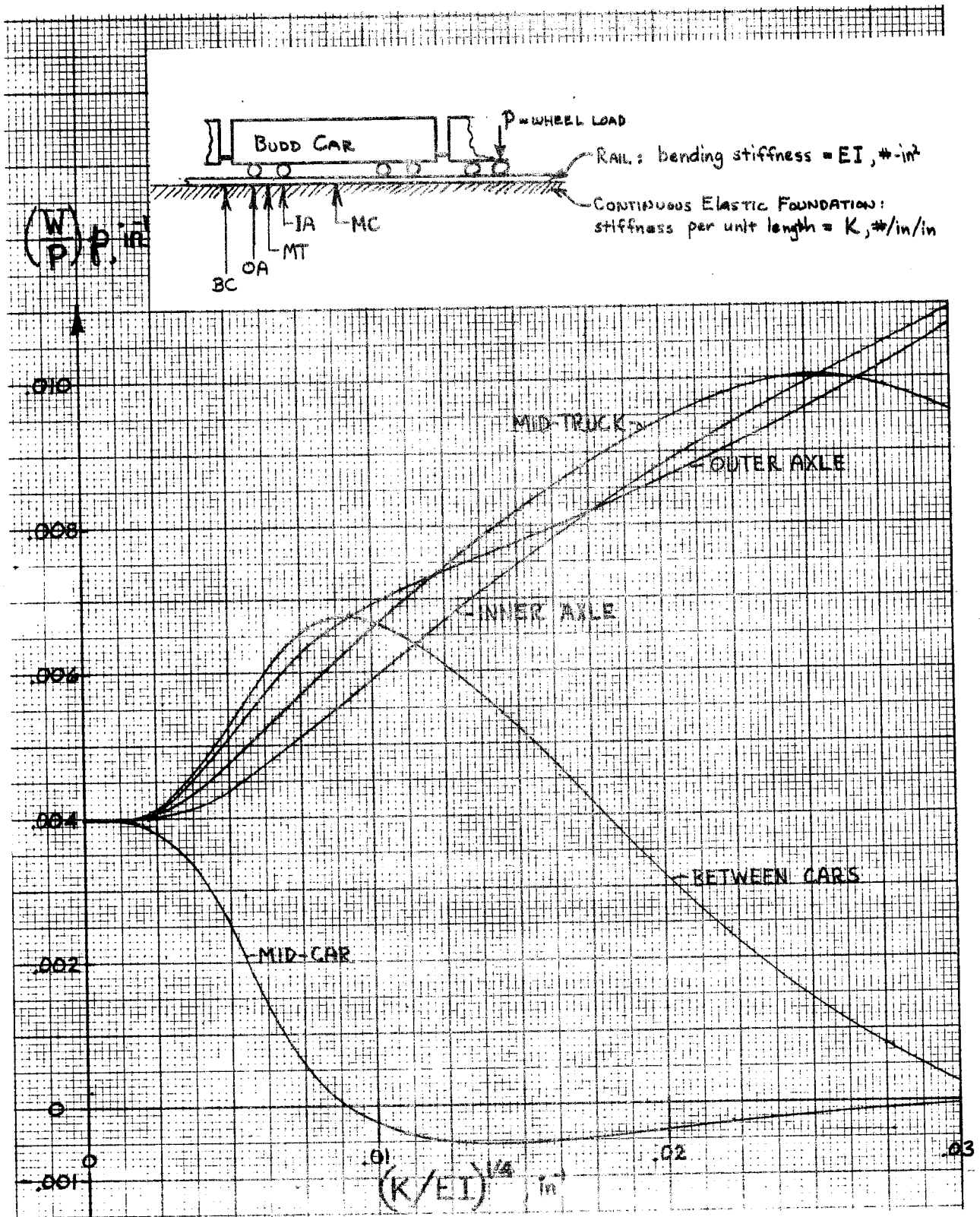
FIGURE D-6. VARIATION OF STATIC SOIL PRESSURE UNDER DIFFERENT POINTS OF BUDD CAR WITH RELATIVE STIFFNESS OF RAIL AND ELASTIC FOUNDATION

(2) EI/k_o and W

must be such that individual wheel pressures are not experienced by the soil From Figure D-6, if

$$(K/EI)^{1/4} \leq 0.022 \qquad (8)$$

this requirement is conservatively satisfied, this reduces to

$$\frac{k_o W}{I_{steel}} \leq 7.3 \ lb/in.^6 \qquad (9)$$

These two restrictions on EI/k_o and W are shown in Figure D-7. For points above the line, the criterion is satisfied; for points below the line it is not satisfied.

Points I, II, and III on the curve represent track structures (discussed in the next section) which satisfy the criterion, and point IV represents a track structure which does not satisfy the criterion because the point falls below the line. The pressure-time curves for these four track structures carrying the Budd car at 160 mph are shown in Figure D-8. For these curves, a conservative value of $k_o = 500 \ lb/in.^3$ was used. (A conservative value of k_o is a relatively large one, because the pressure on the soil increases as k_o increases.) The pressure-time curve for conventional track carrying the Budd car at 53.3 mph shown in Figure D-5 is repeated in Figure D-8 for comparison purposes.

The structures represented by points I, II, and III have similar pressure-time curves because they all meet the criterion. Structure IV does not meet the criterion because of the high-frequency fluctuation caused by individual wheel pressures. This high frequency is expected to rapidly deteriorate the soil, causing the track to quickly lose its alignment.

Thus, the curve of Figure D-7 identifies almost all longitudinal beam-type track structures and classifies them on the basis of the design
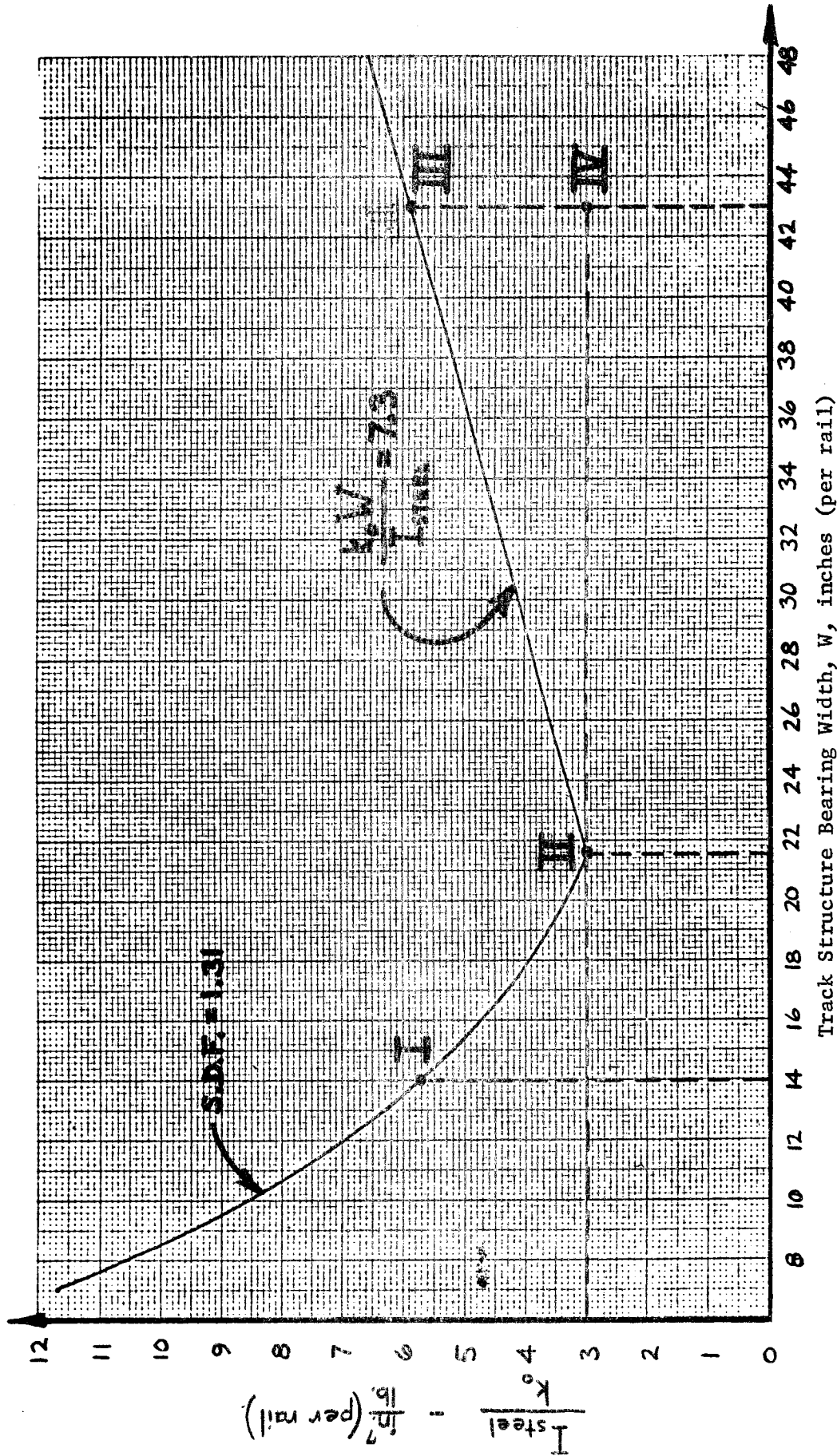
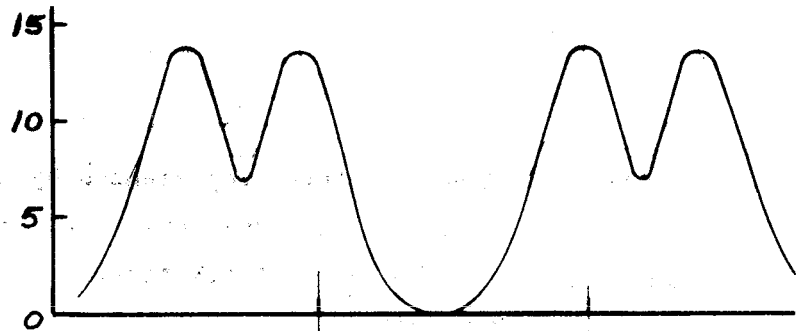Track Structure Bearing Width, W, inches (per rail)

$\frac{I_{steel}}{k_o}$ — $\frac{in^7}{lb}$ (per rail)

S.D.F.=1.31

$\frac{L}{M.W.}$=.73

I

II

III

IV

FIGURE D-7. DESIGN CRITERION CURVE FOR SIZING TRACK STRUCTURE
ON THE BASIS OF TIME-VARYING SOIL PRESSURE

I. (160 mph)

I_{steel} = 2850 in.^{4}

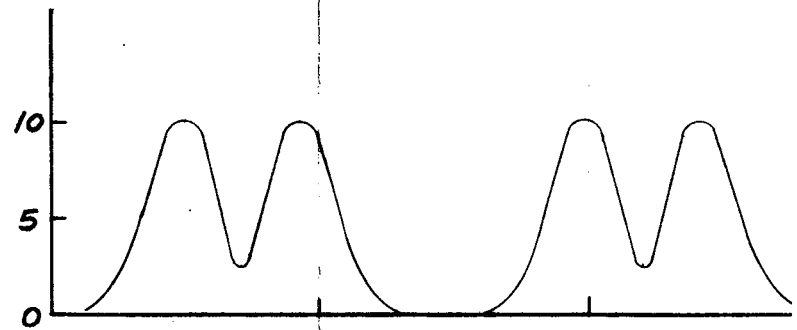W   = 14 in./rail

II. (160 mph)

I_{steel} = 1500 in.^{4}

W   = 21.5 in./rail

III. (160 mph)

I_{steel} = 2950 in.^{4}

W   = 43 in./rail
       (86-inch slab)
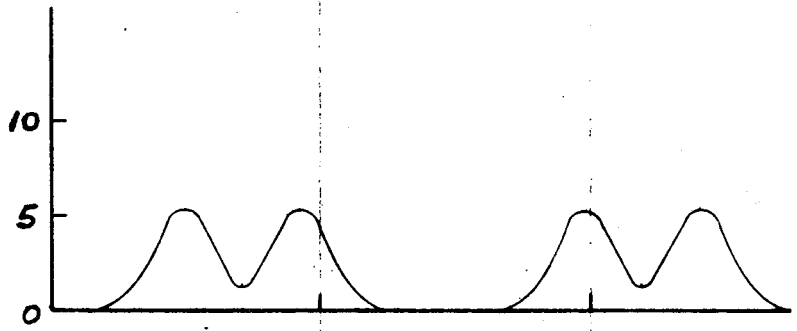
IV. (160 mph)

I_{steel} = 1500 in.^{4}

W   = 43 in./rail
       (86-inch slab)
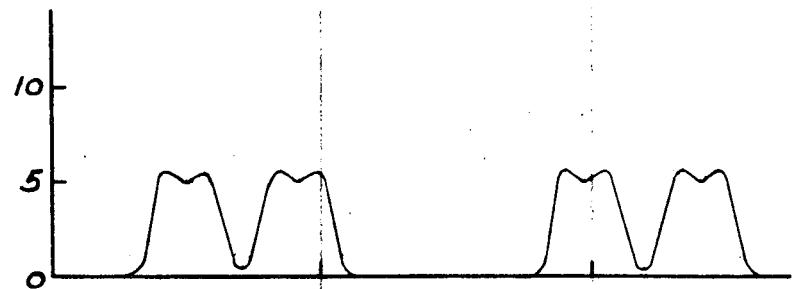
CONVENTIONAL TRACK
STRUCTURE (53.3 mph)

   (100 lb. rail,
    21 in. tie center-to
    center spacing)
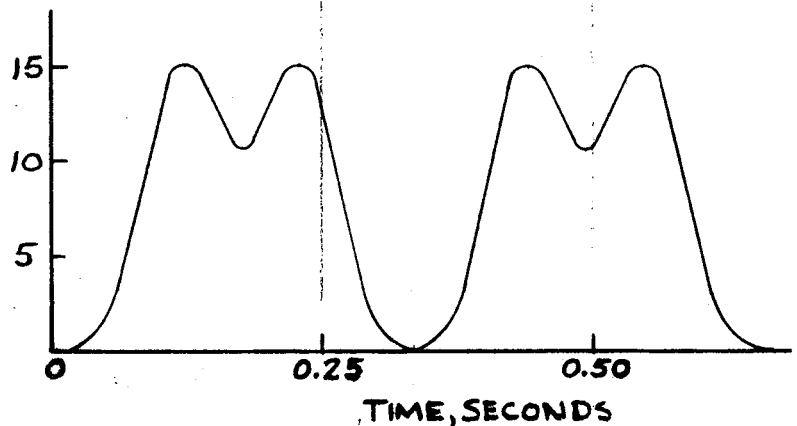
FIGURE D-8. SOIL-PRESSURE-TIME CURVES FOR TRACK STRUCTURES OF DIFFERENT
            WIDTHS AND RIGIDITY (SOIL MODULUS, k_o = 500 LB/IN.^{3})

D-15

criterion. The structures represented by the line all meet the criterion of producing one soil pressure pulse per truck, and thus the final selection of an "optimum" track structure can be based on other considerations, such as cost.

APPENDIX E

GAGE SPREAD OF TWIN REINFORCED
CONCRETE BEAM TRACK STRUCTURE

APPENDIX E

GAGE SPREAD OF TWIN REINFORCED
CONCRETE BEAM TRACK STRUCTURE

TRACK STRUCTURE MODELING

An existing nonuniform-beam digital computer program was modified
to calculate the static deflection of a beam subjected to both bending and
torsion loads. The program was used to solve the bending and torsion problems
independently of each other. The total deflection of any point was therefore
obtained by adding the two deflection components.

The models used for the computer analysis are shown in Figures E-1
and E-2. Basically the static deflection analysis of a continuous beam was
initiated by breaking up the beam into N stations. Beam sections between
stations were considered to be uniform, and the stiffness properties for
any section were taken as the mean values of the nonuniform beam over that
section. Each station could be supported by linear lateral, bending and
torsional springs. In addition, each station could be subjected to lateral
and torsional loads.

A representative portion of track and the computer models used
to represent it are shown in Figure E-3. The effect of the lateral load
applied at the top of the rail was represented by a lateral and torsional
load acting on (for example) Station 23 of the bending and torsional models,
respectively. The effect of the cross-tie beam was represented by three
springs attached to (for example) Station 22. The three springs represented
the lateral and bending restraints that the cross-beam exerted on the main
beam. The effect of the soil restraint was included, and is discussed later.
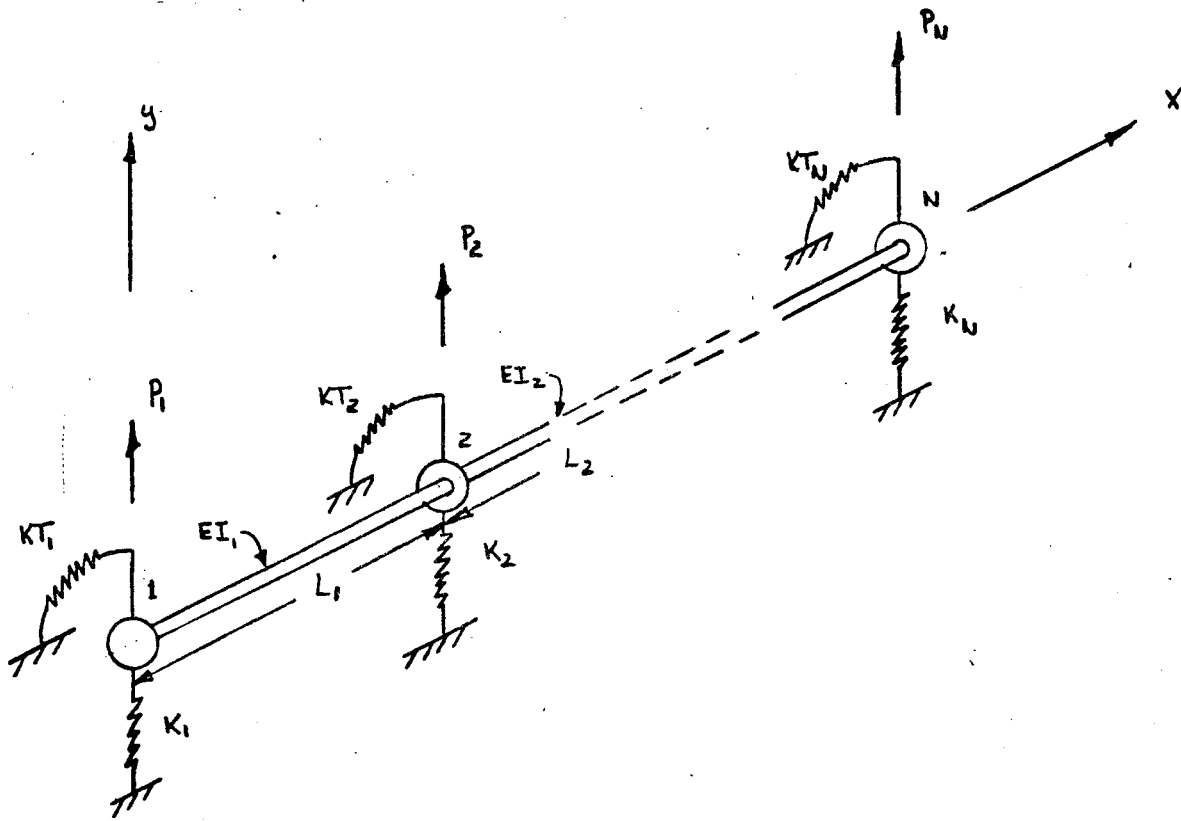
N = STATION NUMBER

L_N = LENGTH BETWEEN STATIONS, IN.

EI = FLEXURAL STIFFNESS BETWEEN STATIONS, LB-IN^2

P = LATERAL LOAD, LB.

K_N = LATERAL SPRING RATE, LB/IN

KT = BENDING SPRING RATE, LB-IN/RAD

FIGURE E-1. BEAM BENDING MODEL

E2
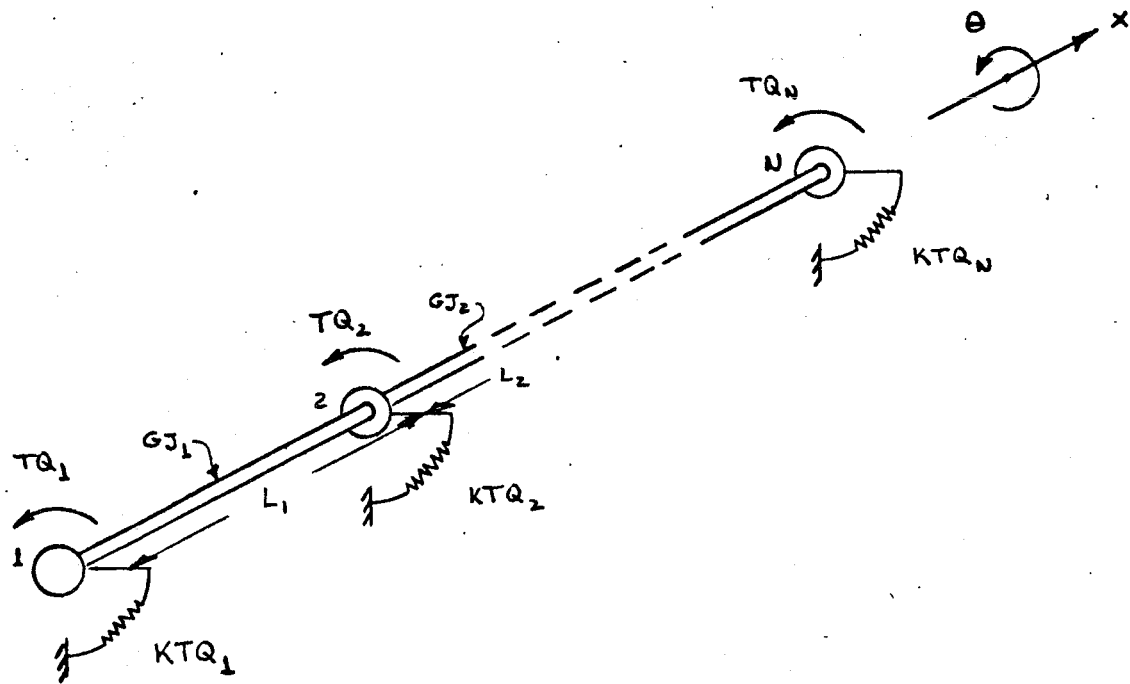
N = STATION NUMBER

L_N = LENGTH BETWEEN STATIONS, IN.

GJ = TORSIONAL STIFFNESS BETWEEN STATIONS, LB-IN^2

TQ = TORSIONAL LOAD, LB-IN.

KTQ = TORSIONAL SPRING RATE, LB-IN/RAD.

FIGURE E-2.   BEAM TORSION MODEL

P

CROSS
BEAM

L_{23}
EI_{23}
P_{23}

K_{22}
22
KT_{22}

L_{22}
EI_{22}

L_{21}
EI_{21}

21

BENDING
MODEL

L_{23}
GJ_{23}
TQ_{23}

KTQ_{22}
22

L_{22}
GJ_{22}

L_{21}
GJ_{21}

21

TORSION
MODEL

TQ_{23}
23

22
KTQ_{22}
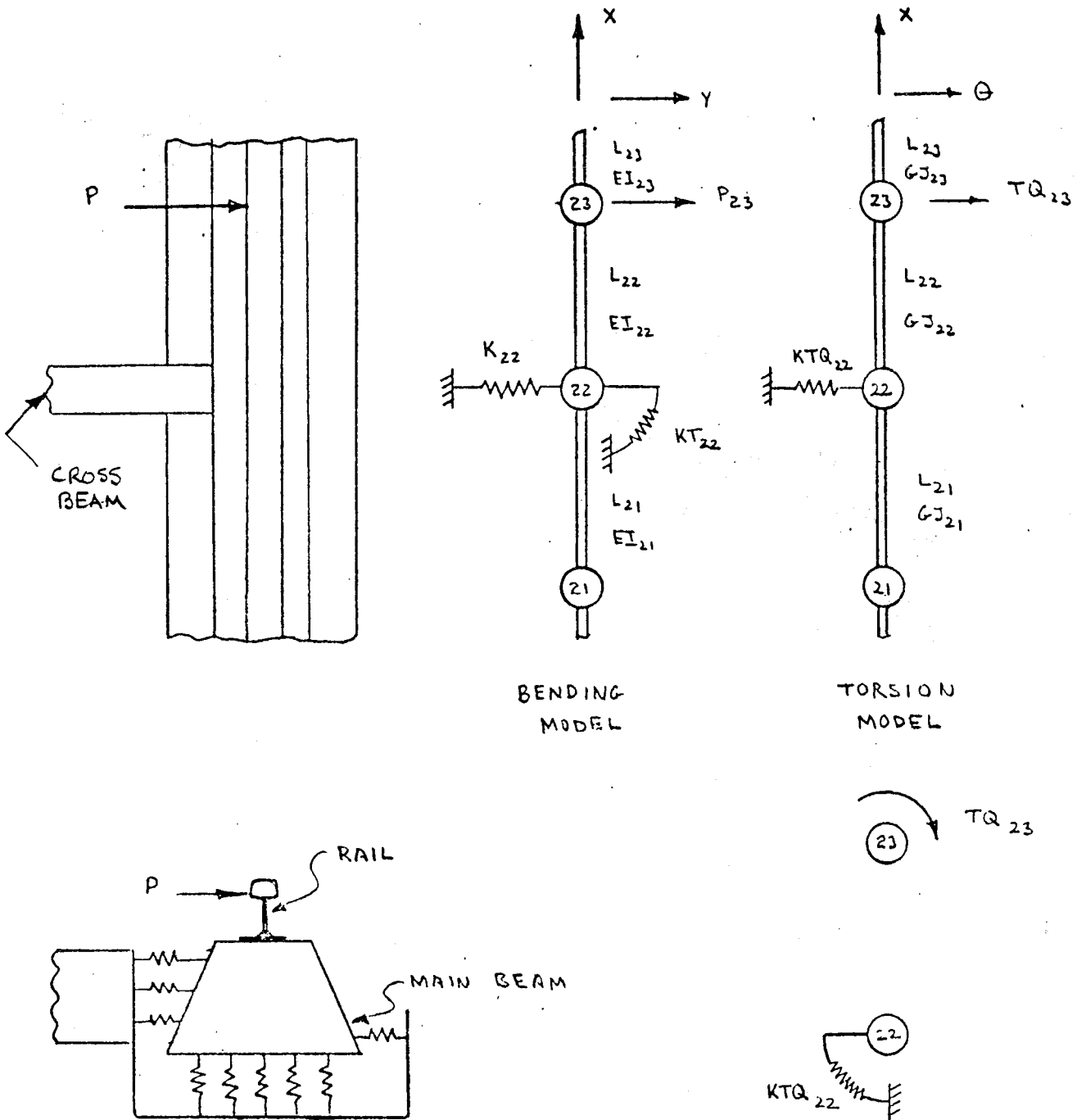
P
RAIL
MAIN BEAM

FIGURE E-3. PARTIAL TRACK STRUCTURE MODEL.

CALCULATION OF GAGE SPREAD

     The reinforced concrete beam cross-section that was used to analyze gage spread is shown in Figure E-4. The beam section was trapezoidal, 16 and 24 inches wide at the top and bottom, respectively, and 18 inches deep. The steel reinforcement rods were one inch in diameter and were located 2-1/2 inches from the top and bottom surfaces. The stiffness properties around a vertical and horizontal axis were 9.6×10^9 and 13.7×10^9 lb-in.^{2}, respectively, while the torsional rigidity was 11.65×10^9 lb-in.^{2}.

     It was assumed that the beam was embedded in soil (or other material) having a modulus of 150 lb/in.^{3}, as shown in Figure E-5. The restraining effects of the soil on the beam were represented by equivalent lateral and torsional springs, as shown in the figure.

     The lateral gage beam members were treated as beams having spring rates calculated by the equations shown in Figure E-6.

     The above parameters were combined to create a model of the rail and rail support beam for studying the effects of lateral wheel loads on gage spread, as shown in Figure E-7.

     It was assumed that four lateral wheel loads of 14,000 pounds each were applied to a 136-pound rail. The wheel loads were represented by 14,000-pound lateral loads and 195,000-lb-in. torques applied to the beam, as shown in Figure E-7. The actual rail support beam was represented by a 120-foot-long beam section which was adequate to simulate the entire rail for the loading conditions considered--that is, wheel loads from the two end trucks on adjacent cars.

     For analysis purposes it was also assumed that the gage beams would be used either at 25 or 12.5-foot intervals. The effects of expansion joints located every 50 feet were also considered. However, the stiffness properties of the dowelled sections were not reduced by more than 50 percent, which for all practical purposes did not increase the gage spread.
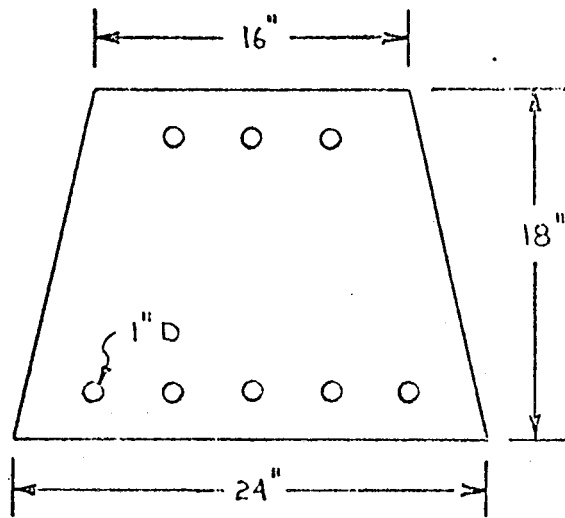
FIGURE E-4.   REINFORCED CONCRETE BEAM
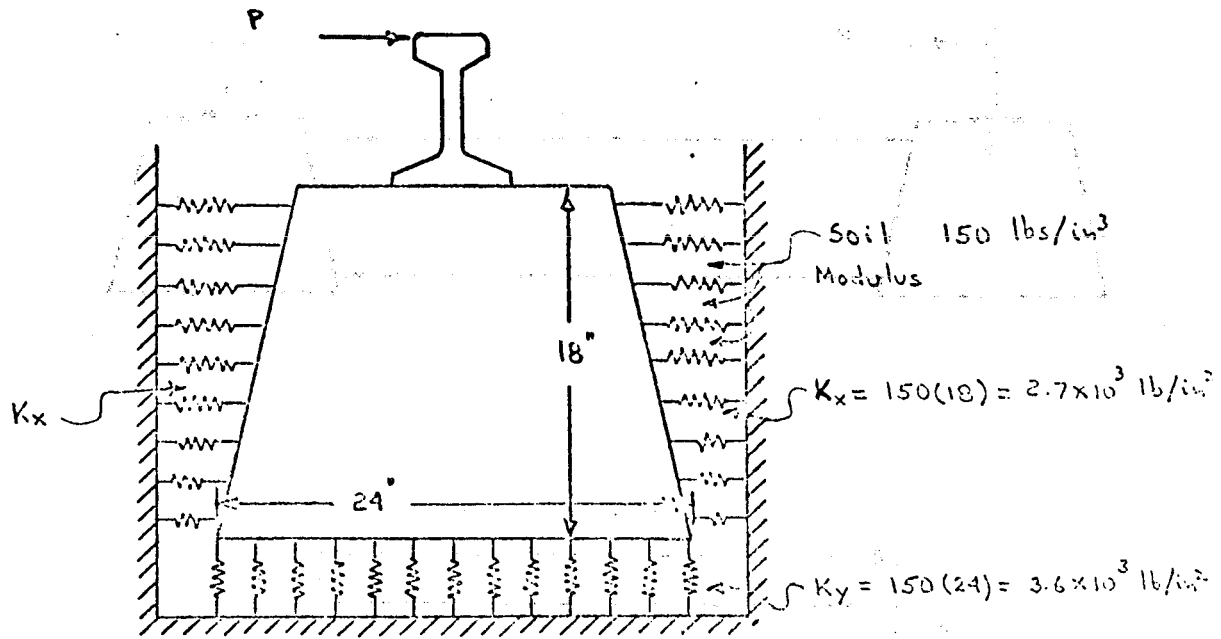
$$K = K_x = 2.7 \times 10^3 \; lb/in^2$$

$$KTQ = 2K_x \frac{(18)^2}{12} + K_y \frac{(24)^2}{12} = 3.19 \times 10^5 \; lb\text{-}in/rad/in$$
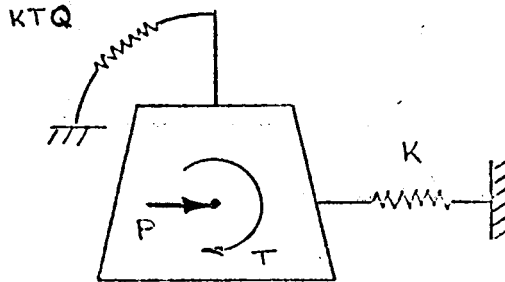
FIGURE E-5. MODELING OF SOIL EFFECTS ON BEAM
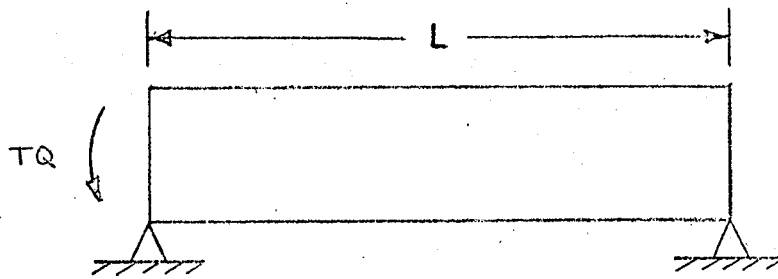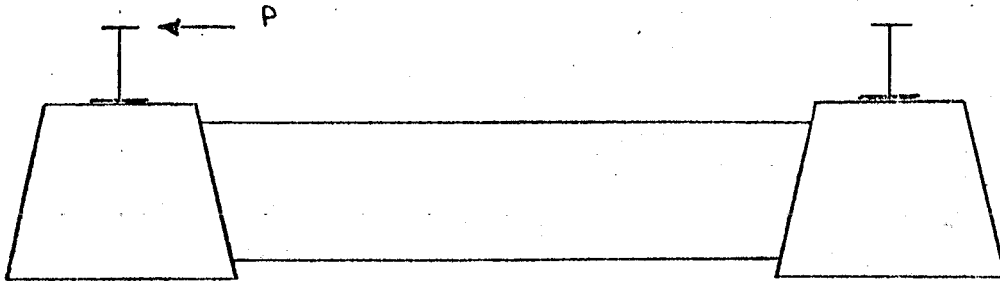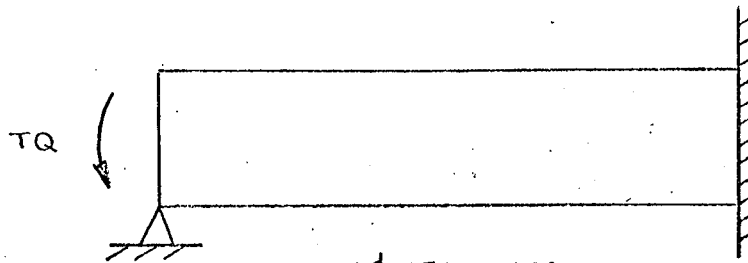
FIGURE E-6. CROSS BEAM SPRING RATE CALCULATIONS

Lateral & Torsional Loads

6' 9' 6'

K, KT, KTQ
(CROSS BEAM
SPRINGS)

12.5' 12.5' 12.5' 12.5'

Lateral & Torsional
Soil Springs

(PLAN VIEW)
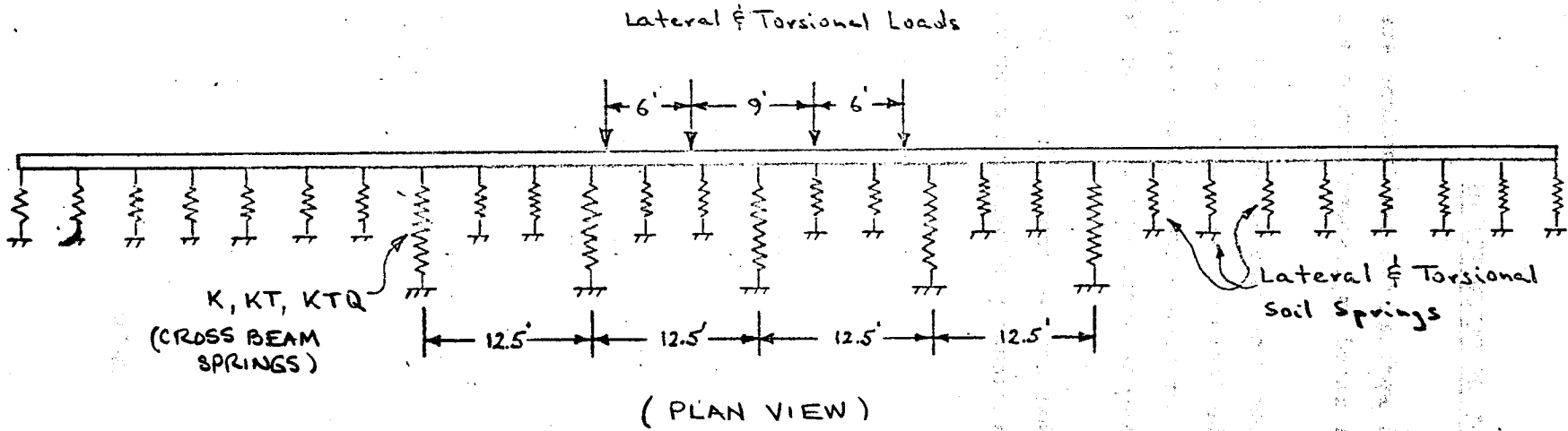
FIGURE E-7. COMPLETE TRACK STRUCTURE MODEL

RESULTS OF CALCULATIONS

The results of several spring rate combinations are summarized in Table E-1. Several computer-generated gage spread curves are shown in Figures E-8 through E-13.

The results indicate that the gage spread will not exceed 0.119 inch even without any cross-ties. The introduction and cross-tie spring rates at either 25 or 12.5-foot spacings can reduce the gage spread significantly. For example, with 12.5-foot cross-tie spacings the gage spread can be reduced to 0.040 inches.

The main conclusion that can be reached from these results is that gage spread should not be a significant problem with concrete beam rail supports.

TABLE E-1. SUMMARY OF GAGE SPREAD CALCULATIONS

| K, (lb/in.) | KT, (lb-in./rad) | KTQ, (lb-in./rad) | Gage Spread | | | | | |
| | | | 25-Foot Spacing of Cross-Beam | | | 12.5-Foot Spacing of Cross-Beam | | |
			Bending, (in.)	Torsion, (in.)	Tot., (in.)	Bending, (in.)	Torsion, (in.)	Tot., (in.)
0	0	0	0.0607	0.0580	0.1187	0.0607	0.058	0.1187
0.5×10^6	0	0	0.0536	0.0580	0.1070	0.0391	0.0580	0.0960
1.0×10^6	0	0	0.0526	0.0577	0.1051	0.0337	0.0577	0.0903
1.0×10^6	0.266×10^9	0.38×10^9	0.0526	0.0265	0.0791	0.0310	0.0165	0.0475
1.0×10^6	0.532×10^9	0.76×10^9	0.0526	0.0237	0.0763	0.0299	0.0131	0.0430
1.0×10^6	0.798×10^9	1.14×10^9	0.0526	0.0226	0.0752	0.0294	0.0119	0.0413
1.0×10^6	1.065×10^9	1.52×10^9	0.0526	0.0221	0.0747	0.0290	0.0112	0.0402
1.5×10^6	0	0	0.0526	0.0580	0.1044	0.0312	0.0580	0.0880
3.0×10^6	0	0	0.0523	0.0580	0.1035	0.0282	0.0580	0.0845

FIGURE E-8.   GAGE SPREAD DUE TO BENDING, CROSS BEAMS SPACED
AT 25 FEET.

FIGURE E-9. GAGE SPREAD DUE TO TORSION, CROSS BEAMS SPACED AT 25 FEET.

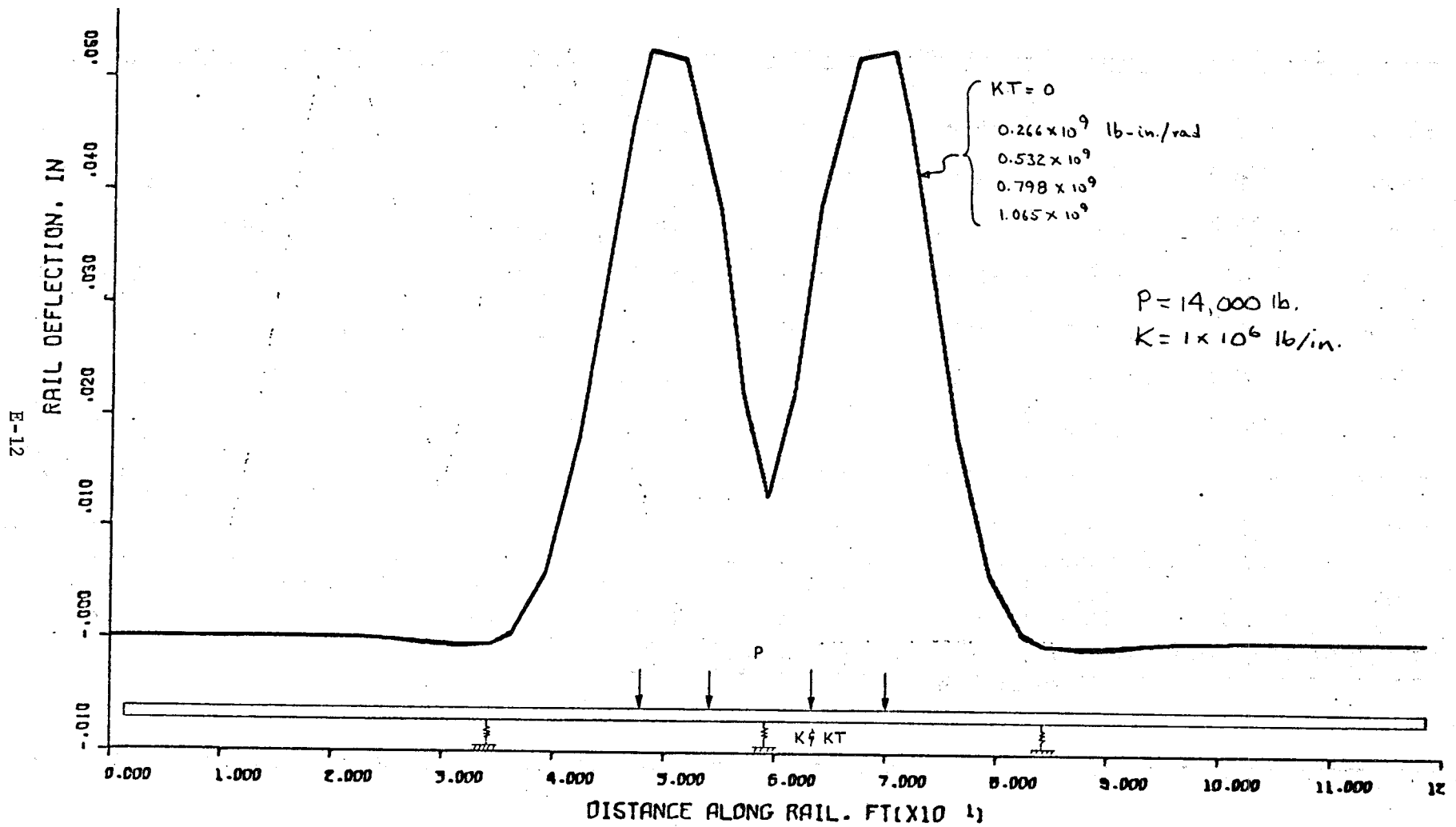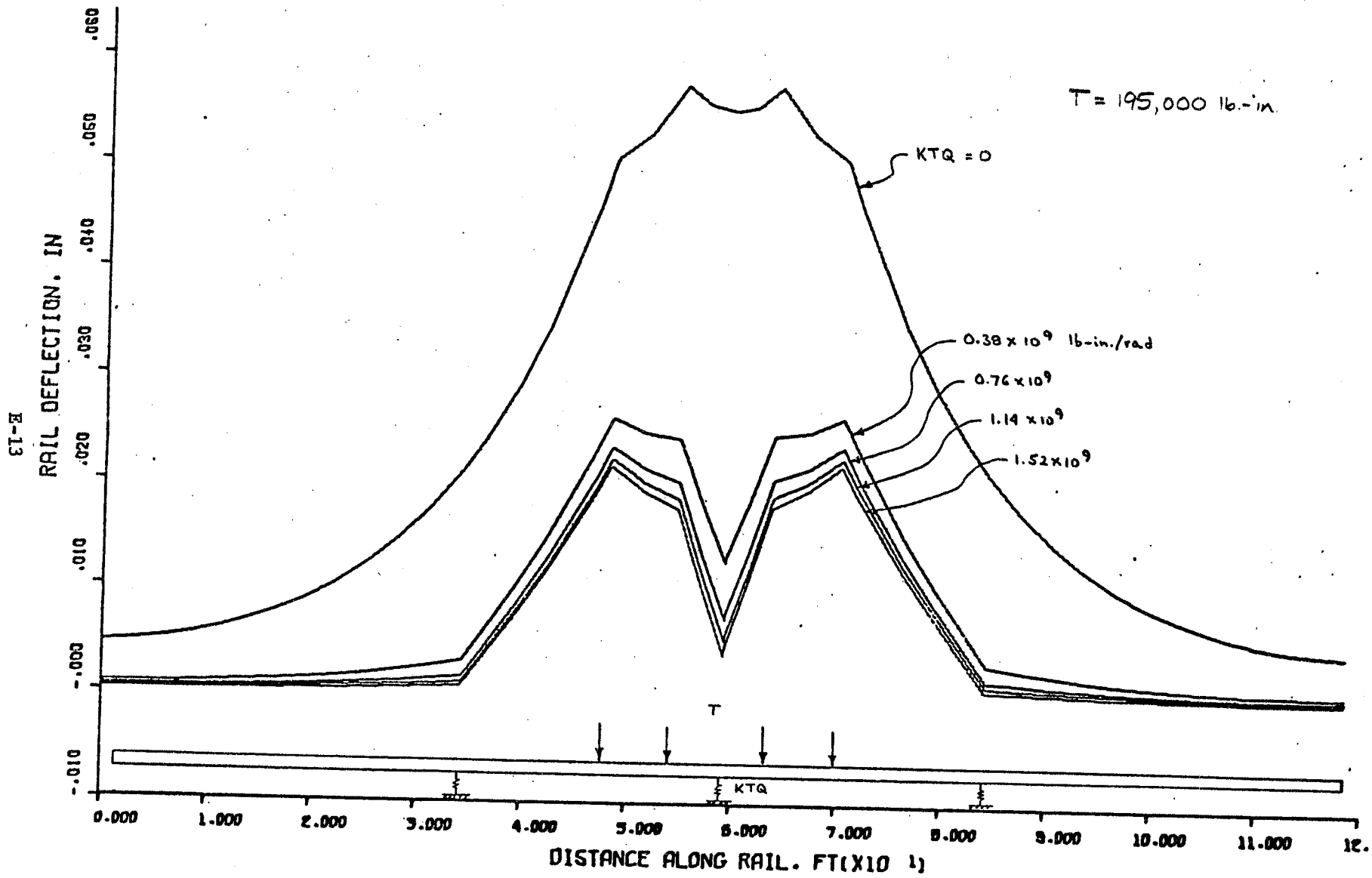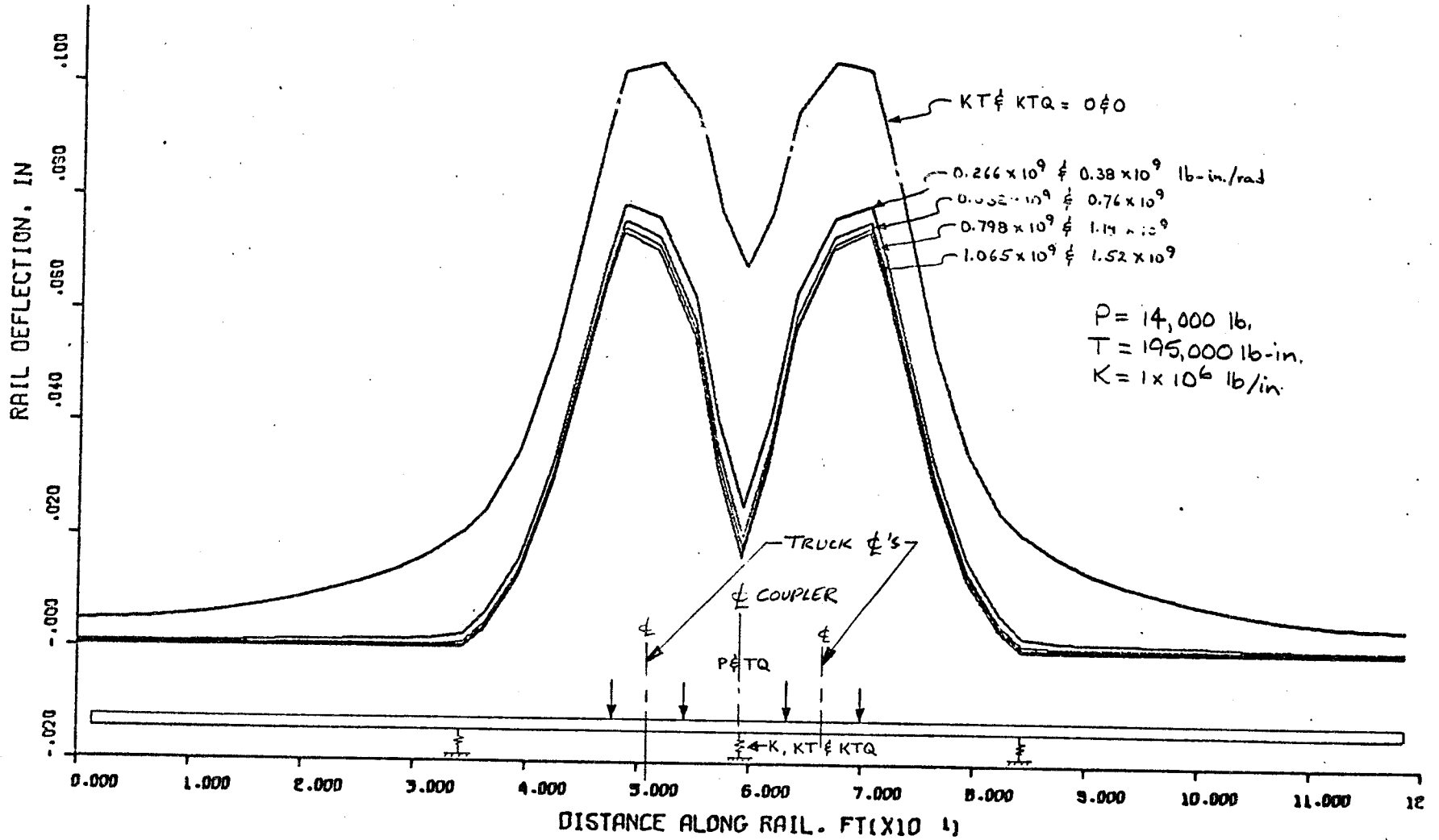FIGURE E-10. TOTAL GAGE SPREAD, CROSS BEAMS SPACED AT 25 FEET
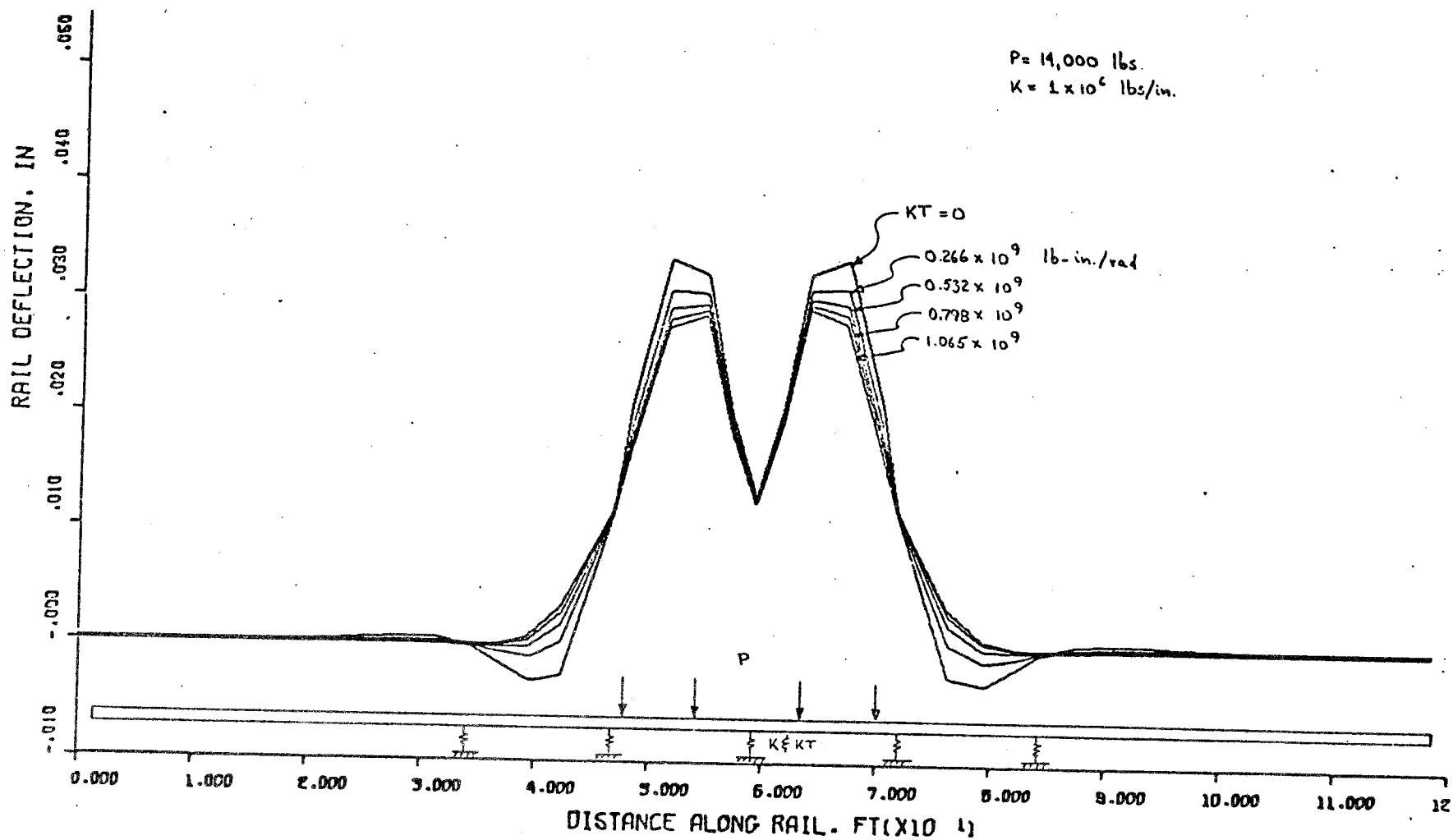
FIGURE E-11.   GAGE SPREAD DUE TO BENDING, CROSS BEAMS SPACED AT 12.5 FEET
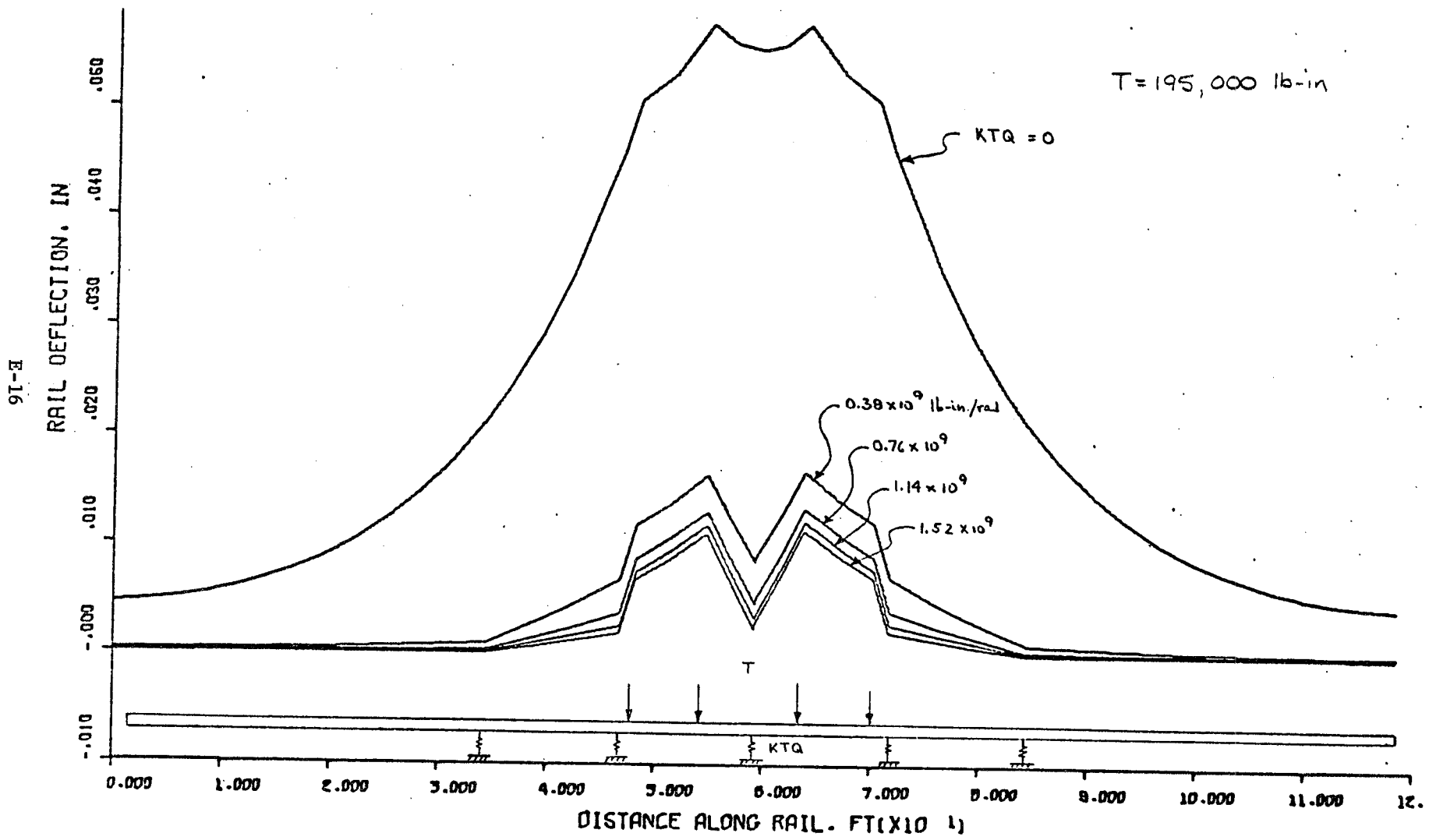
FIGURE E-12. GAGE SPREAD DUE TO TORSION, CROSS BEAMS SPACED AT 12.5 FEET
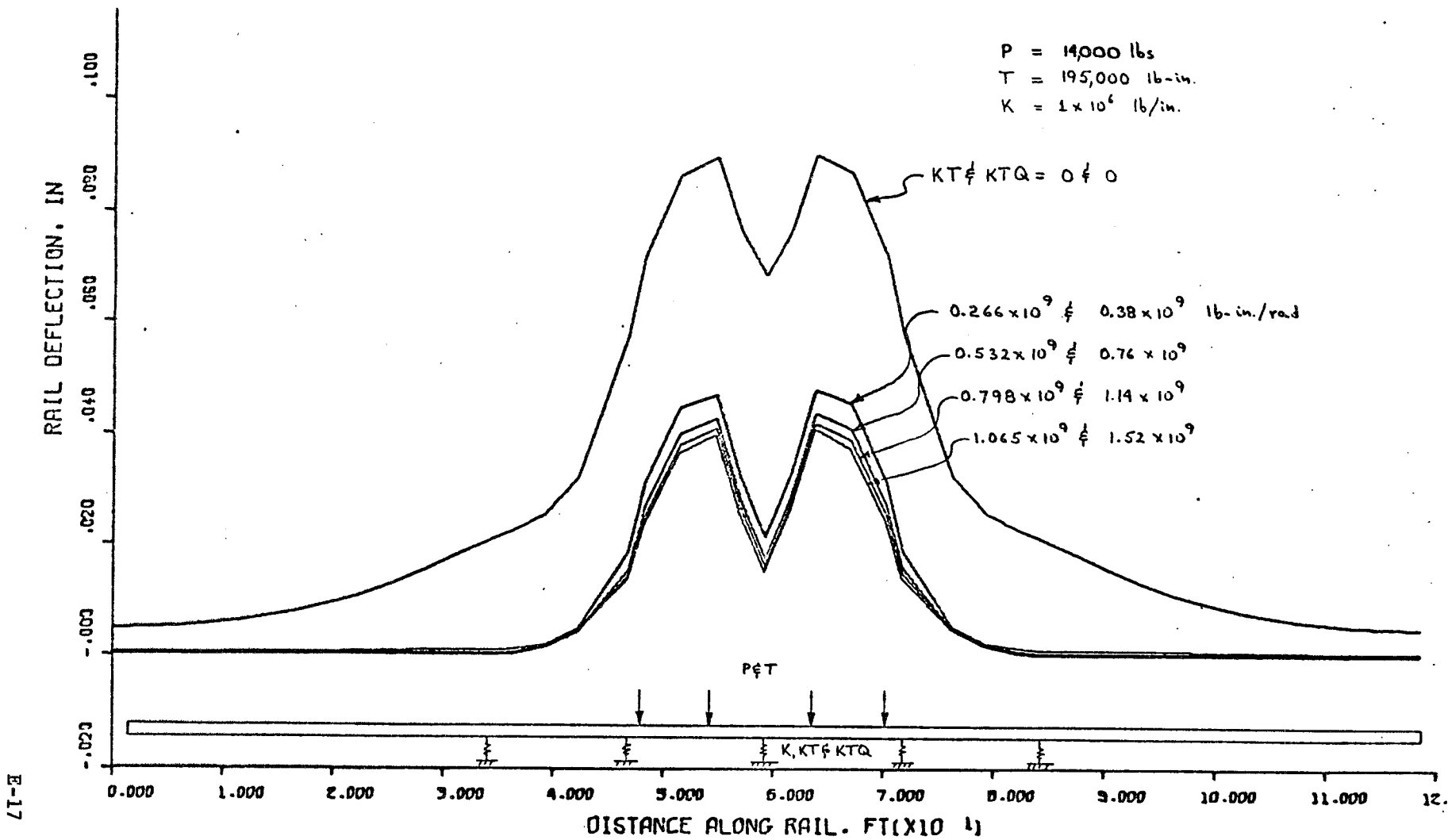
FIGURE E-13. TOTAL GAGE SPREAD, CROSS BEAMS SPACED AT 12.5 FEET

APPENDIX F

RAIL FASTENER PERFORMANCE SPECIFICATIONS

APPENDIX F

RAIL FASTENER PERFORMANCE SPECIFICATIONS

The following specifications have been prepared to aid in the selection of rail fasteners for reinforced concrete longitudinal beam and slab-type track structures for the DOT-Santa Fe test track at Aikman, Kansas.

1.0 Basic Design Requirements

1.1 Rail fasteners will be used with standard 136-pound rail, continuously welded. The term rail fastener shall include all hardware necessary to attach the rail to a reinforced concrete beam or slab fitted with two projecting studs (or female inserts) to attach each fastener. The spacing of these studs or inserts will depend on the fastener, but the lateral separation of the two studs or inserts (opposite or diagonal from each other) must be between 9 and 15-1/2 inches.

1.2 The installation, adjustment, and replacement of the rail fasteners shall be capable of being accomplished easily by one or two men with hand tools.

1.3 The dimension of the rail fastener base measured lontitudinally along the rail shall not be less than 5 inches, nor greater than 10 inches.

1.4 The dimension of the rail fastener base measured laterally relative to the rail shall not exceed 16 inches.

1.5 The vertical distance from the bearing surface of the fastener to the bottom surface of the rail as installed in the fastener shall be minimized, and shall not exceed 2 inches, exclusive of shims for vertical adjustment.

1.6 The rail fastener shall be capable of being adjusted laterally through a range of plus or minus one inch in

1/8-inch increments. A positive lateral lock not dependent on friction shall be provided as a part of the adjustment feature. A shoulder or other positive stop shall be provided to restrict the change in the lateral position of the rail to a maximum of 1-1/4 inches in the event of failure or loosening of the lateral clamping device. Any shims or special devices required for lateral adjustment shall be supplied by the fastener manufacturer and shall be considered to be part of the rail fastener. Shims, if used, shall be positively retained other than by friction.

1.7 The rail fastener shall be capable of being adjusted vertically through a range of plus or minus one inch in 1/8-inch increments by the use of some type of shims, with a final adjustment no coarser than 1/16-inch being provided. The shims shall have a bearing area approximately equal to that of (the rail on the fastener or) the fastener on the beam or slab surface (depending on the shim design) and shall be retained in a positive manner not dependent on friction. A direct vertical force path from the base of the rail to the beam or slab shall be provided at all times. Any shims required for vertical adjustment shall be supplied by the fastener manufacturer and shall be considered to be part of the rail fastener. A design is preferred in which it is possible to install the shims with a minimum vertical movement of the rail. Shims shall be positively retained other than by friction. The number of fasteners needing vertical adjustment, and the extent of these adjustments, will not be known until after the track has been in operation for some period of time.

1.8 An elastomeric pad or other element shall be incorporated into the fastener to provide the load-deflection characteristics specified in 2.1. Positive retention of the

elastomeric element, not relying on friction, shall be provided to prevent shifting of the elastomeric element in the lontitudinal and lateral directions.

1.9 The fastener could provide for the conventional 1:40* cant of the rail relative to the top horizontal surface of the beams or slabs on which they will be mounted.

1.10 The rail fastener shall electrically insulate the rail from the beam or slab to which it is attached. (The two attachment bolts or studs are considered to be parts of the beam or slab.) An electrical impedance of at least 2000 ohms per fastener must be provided, in a frequency range from DC to 10 k Hz with an applied voltage of 50 volts a.c. This impedance shall be measured between the rail and each attachment stud projecting from the beam or slab surface, with the fastener attached in the prescribed manner, and under both wet and dry conditions.

1.11 The design of the fastener must be such that it can withstand high frequency, low amplitude, vibrations of the rail relative to the supporting beam or slab. For design purposes, a sinusoidal vertical rail motion having a peak-to-peak amplitude of 0.008 inches at a frequency of 700 cps shall be used, and calculations shall be made to determine the fatigue life and variation in clamping force of those elements affected by this vibration.

2.0 <u>Static Tests</u>. The following test measurements shall be made at room temperature to determine rail fastener load-deflection characteristics and ability to survive maximum loads.

* The specification of cant provided by the fastener will depend on final design of the track structure and availability of fasteners with cant.

2.1 <u>Vertical Load Application</u>. Apply a vertical load downward on the center of the rail head and increase the load in increments of 5000 pounds until a maximum load of 40,000 pounds is reached. Record the vertical deflection of the rail head at each load increment and plot the results on a graph. The vertical spring rate determined from the average slope of the load-deflection curve between 15,000 and 25,000 pounds must be between 200,000 and 400,000 lb/in. The rail deflection at 20,000 pounds load must be between 0.050 and 0.125 inch. After the maximum load is removed, the rail head must return to within $\pm$ 0.010 inch of its original unloaded position and there must be no visible breaking or yielding of any fastener components.

Apply a vertical lifting load at the center of the rail head and increase the load in increments of 500 pounds until a maximum load of 3000 pounds is reached. Record the deflection at each load increment. The maximum deflection for the lifting load must be within $\pm$ 25 percent of the maximum deflection for a 3000-pound downward vertical load as determined from the load-deflection graph.

2.2 <u>Vertical and Lateral Load Application</u>. Apply combined vertical and lateral loads to the head of the rail (gage side) until maximum loads of 20,000 pounds vertical and 12,000 pounds lateral are reached. ("Vertical" and "lateral" are references relative to the rail as installed in a track rather than in the test machine.) The loads may be applied with one or two actuators, providing the rail is free to move naturally under the influence of the combined loads. If one actuator is used, the required loading is 23,300 pounds ·at an angle of 31° from vertical. Record the vertical and lateral deflection of the rail at each lateral load increment of 2000 pounds and plot the results. The

maximum lateral deflection of the rail head must not
exceed 0.125 inch.

Apply combined vertical and lateral loads to the
head of the rail (gage side) until maximum loads of 30,000
pounds vertical and 30,000 pounds lateral load are reached.
The maximum lateral deflection of the rail head must not
exceed 0.30 inch. After the lateral load is removed, the
rail head must return to within $\pm$ 0.050 inch of its
original position and there must be no visible breaking or
yielding of any fastener components.

Repeat the application of the 20,000 pound
vertical load and 12,000 pound lateral load. The maximum
lateral deflection must be within $\pm$ 20 percent of the
maximum deflection recorded originally for this loading
condition.

2.3 <u>Longitudinal Load Application</u>. Apply a longitudinal load
on the rail web or base and increase the load in increments
of 500 pounds until the longitudinal deflection of the rail
reaches 0.25 inch. At each load increment hold the load
constant until the rail deflection stabilizes and record the
maximum deflection. Plot these results on a graph. The
fastener must maintain a load between 3000 and 5000 pounds
at 0.25 inch deflection. During this test, the rail end
must be supported on a roller or other frictionless support
at the proper elevation to prevent the lontitudinal load from
binding the rail in the fastener.

2.4 <u>Longitudinal and Vertical Load Application</u>. With a vertical
downward load of 20,000 pounds applied to the rail head,
apply longitudinal load in increments of 1000 pounds until a
maximum load of 5000 pounds is reached. During this test
the vertical load must be applied in such a way that it does

not restrain longitudinal motion of the rail. Release the load in 1000-pound increments. At each load increment record the lontitudinal deflection. Plot the results on a graph. At completion of this test, with all load removed, the rail must return to within 0.010 inch of its original longitudinal position.

3.0 <u>Dynamic Load Durability Test</u>. The following two tests shall be performed to determine the durability of the fastener under cyclic loading based on tangent track installation. During these two tests the preload on those fastener elements clamping the rail (e.g., elastomeric pads, metal clips, etc.) must be sufficient to prevent loss of contact of any of these elements with the rail.

   3.1 <u>Vertical Cyclic Load</u>. Apply a cyclic vertical load to the rail head. Each cycle shall consist of 20,000 pounds downward force followed by 2000 pounds uplift force. Apply this load pattern for a total of 2 million cycles at a frequency not exceeding 10 cycles per second. Failure of the fastener, or any of its components, must not occur.

   3.2 <u>Vertical and Lateral Cyclic Load</u>. Apply a 20,000-pound downward load to the rail at an angle of 10 degrees ($\pm$ 1°) from the rail "vertical" centerline on the field side, followed by a 23,000-pound downward load at an angle of 31 degrees from the rail "vertical" centerline on the gage side. These loads shall be applied alternately for a total of two million cycles (two load applications, one at each of the two angles, constitute one cycle) at a frequency not to exceed 10 cycles per second. Failure of the fastener, or any of its components, must not occur.

4.0 <u>Static Tests After Durability Tests</u>. The following tests will be performed to demonstrate fastener performance after the durability test is completed.

4.1 <u>Vertical Load Application.</u> Repeat the vertical load test
described in Section 2.1. The vertical spring rate and
deflection at 20,000 pounds must be within ± 25 percent of
those recorded for a 20,000-pound load in Section 2.1.

The maximum deflection for a 3000-pound lifting
load must be within ± 25 percent of the deflection recorded
for the 3000-pound lifting load in Section 2.1.

4.2 <u>Vertical and Lateral Load Application.</u> Apply loads as
described in the second paragraph of Section 2.2 until
maximum load of 30,000 pounds vertical and 30,000 pounds
lateral load are reached. Deflections must be within ± 25
percent of those specified in Section 2.2, and there must be
no visible breaking or yielding of any fastener components.

4.3 <u>Longitudinal Load Application.</u> Repeat the longitudinal load
test described in Section 2.3. The fastener must maintain a
load between 3000 and 5000 pounds at 0.25 inch deflections,
and the loss of longitudinal load must not exceed 25 percent
of the original longitudinal restraint.

4.4 <u>Longitudinal and Vertical Load Application.</u> Repeat the test
described in Section 2.4. At completion of this test, the
rail must return to within 0.020 inch of its original
longitudinal position.

* * * * * * * * *

The tests described in Articles 2.0 through 4.4 shall be performed
by the fastener supplier/or by an agency approved by the OHSGT project
officer, in a manner approved by the project officer. In case the supplier
is unable to conduct these tests, the OHSGT may elect to conduct same,
depending on the apparent merit of the fastener in question.

The OHSGT project officer shall have the final jurisdiction in
questions concerning interpretation of results or test procedures, and final
selection of rail fasteners.
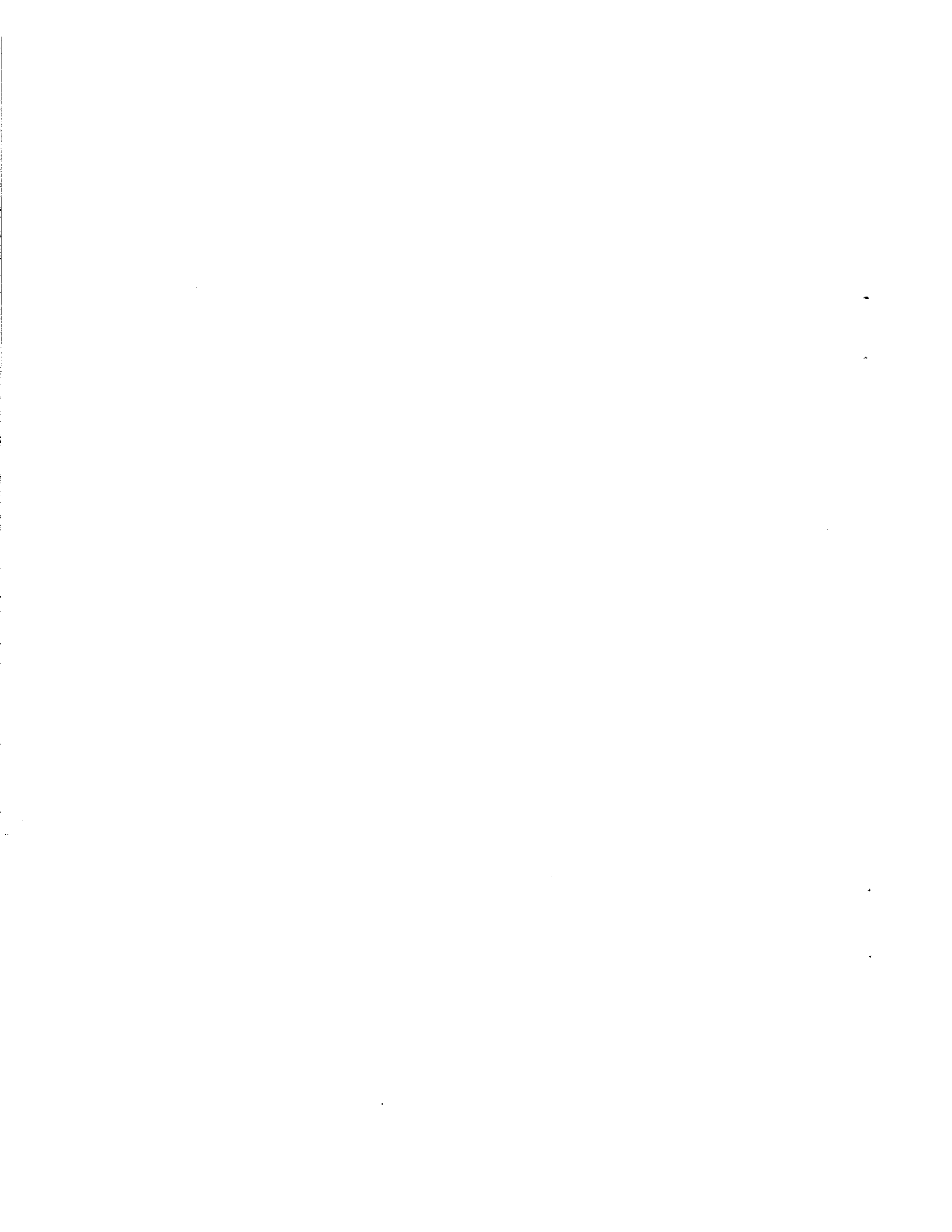
APPENDIX G

<u>PERFORMANCE SPECIFICATIONS FOR CAST-IN-PLACE</u>
<u>REINFORCED CONCRETE SLAB TRACK STRUCTURE</u>
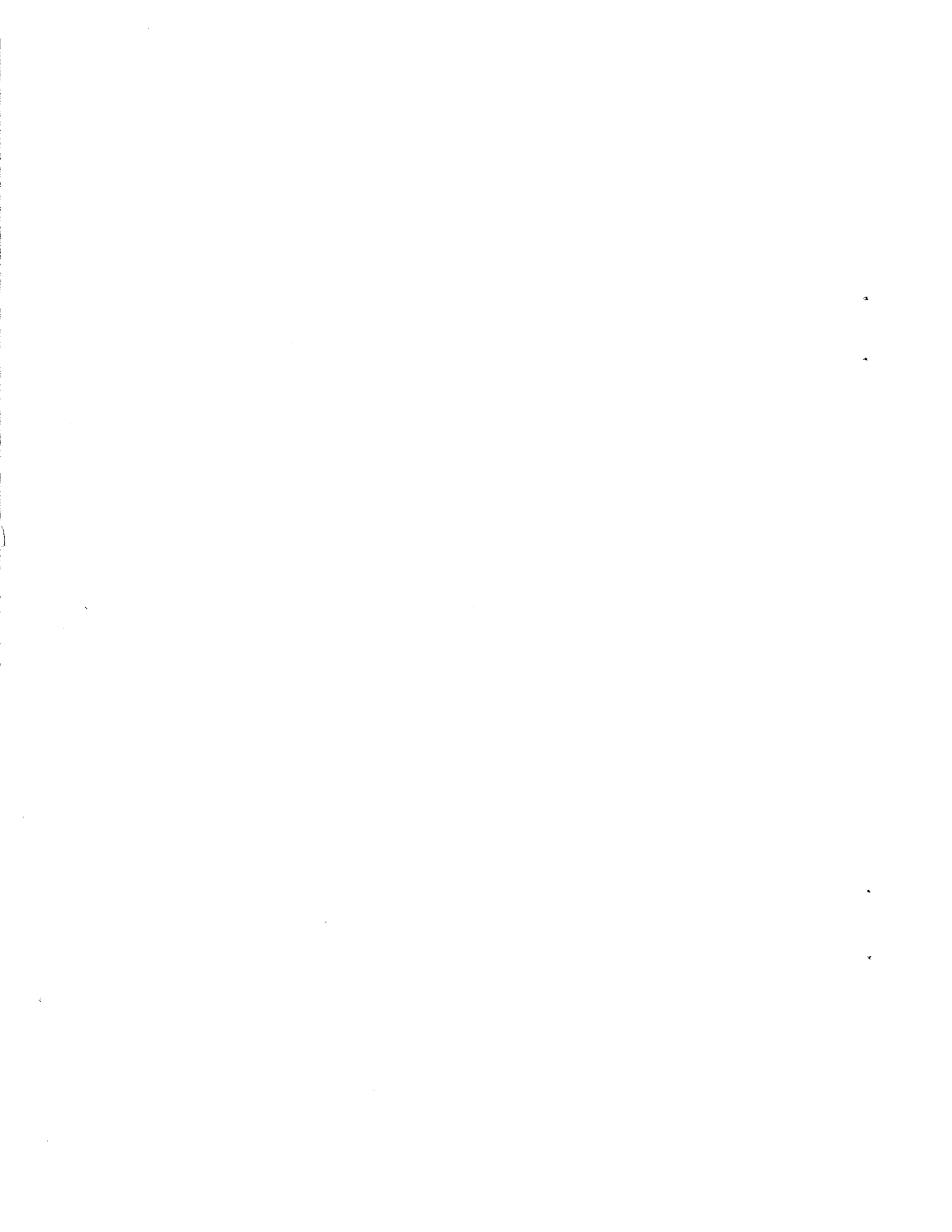
TRACK STRUCTURE SPECIFICATIONS

Cast-in-Place Reinforced Concrete Slab

1.0 <u>General Description</u>. The cast-in-place reinforced concrete slab
track structure is envisioned as being very similar to conven-
tional "rigid" type concrete highways and runways, being a simple
slab of approximately rectangular cross-section. The main dif-
ference is that a deeper slab together with a greater amount of
reinforcing steel is required to obtain the desired bending
stiffness, and this heavier reinforcement will also minimize
the spread of cracks caused by the applied loads. The complete
track structure actually includes four components: rail, rail
fasteners, concrete beams, and the subgrade or other continuous
support beneath the beams. These components are described briefly
below.

1.1 <u>Rail</u>. Continuously-welded C.F.&I. 136-pound rail will be
used, having a moment of inertia of 94.9 in.^{4} resisting
bending due to vertical loads applied by the wheels.

1.2 <u>Rail Fasteners</u>. Rail fasteners will be used to support the
rail at 30-inch intervals along the length of the slab.
Each fastener will provide a vertical static spring rate of
200,000 to 400,000 lb/in., and will also provide an adjust-
ment capability of $\pm$ 1 inch vertically and laterally of the
rail relative to the slab to compensate for misalignment and
wear.

1.3 <u>Cast-in-Place Reinforced Concrete Slab</u>. The slab shall be
basically of simple rectangular cross-section, with a width
of 8 feet and a depth of at least 12 inches. Reinforcement
in the form of continuous longitudinal steel rods near the
top and bottom surfaces of the slab will be required to
provide the specified bending stiffness. Lateral reinforce-
ment will be required at intervals corresponding to the rail

fastener spacing to absorb the loads transmitted into the slab at the rail fastener attachment points.

The total length of the cast-in-place concrete slab track structure will be approximately 800 feet. The detailed structural and geometric requirements of the slab are given in the following portions of these specifications.

1.4 <u>Subgrade Support</u>. The track structure will be continuously supported by a compacted subgrade having a 4 to 6 inch layer of ballast, crusher run, or other similar permeable material as its top layer, providing drainage directly beneath the slab. The modulus of subgrade reaction shall be assumed to fall within the range of 150 to 200 lb/in.^{3}.

2.0 <u>Design Loads</u>.

2.1 <u>Vertical Loads</u>. Traffic over the experimental track structures will be that of the existing Santa Fe mainline track. This traffic is almost entirely mixed freight, having a wide variation in axle loading and spacing. However, for design purposes, locomotive axle loads of 38 tons (38,000 pounds per wheel) can be assumed, and freight car axle loadings of 35 tons (35,000 pounds per wheel) shall be considered typical. These loads are based on the static weights; dynamic wheel loads will be higher, depending on a number of factors. For design purposes, a maximum impact factor of 2.0 shall be used.

The stiffness of the rail and the use of resilient rail fasteners between the rails and supporting structure will distribute the vertical wheel loads longitudinally over several rail fasteners, so that the maximum load transmitted by an individual rail fastener normally will be no more than 60 percent of the wheel load. For example, the maximum vertical load transmitted into the structure by an individual rail fastener will be on the order of 40,000 pounds when the actual wheel-rail load is 70,000 pounds.

2.2 <u>Lateral Loads</u>. The lateral wheel-rail loads are known with
much less certainty than the vertical loads, since the
generation of lateral loads is a function of relative wheel-
rail alignment on tangent track. However, for design pur-
poses, it can be assumed that maximum lateral loads normally
will not exceed 0.4 times the vertical loads, but that on
infrequent occasions lateral loads equal to 0.6 times the
vertical loads can occur.

The lateral load transmitted into the supporting
structure by any individual rail fastener can be assumed,
for design purposes, to be equal to 0.9 times the lateral
wheel-rail load. Maximum lateral loads on the rail will be
those caused by wheel flange contact, and therefore will be
in the direction away from the track centerline.

2.3 <u>Load Distribution</u>. The distribution of loaded axles along
the length of the track will be a function of the particular
train consist. However, for design purposes, typical axle
spacings of 8 feet for locomotives and 6 feet for freight
car trucks can be assumed.

3.0 <u>Allowable Stresses</u>. Stresses in the steel and concrete shall be
calculated for each particular beam design, using the design in-
formation given above. These stresses must meet the requirements
of present codes covering the particular type of construction--
particularly such things as the AASHO (American Association of
State Highway Officials) specifications covering allowable Unit
Stresses, ACI (American Concrete Institute) Specification 318,
and pertinent ASTM (American Society for Testing Materials)
specifications.

4.0 Structural and Geometric Requirements

4.1 Slabs.

4.1.1 Bending Stiffness.

The longitudinal bending stiffness (EI) of the slab about the neutral axis of the slab lateral cross-section shall be at least 4000×10^7 lb-in.^{2}. In calculating this stiffness the tensile strength of the concrete shall be assumed to be zero.

4.1.2 Top Surface.

The top surface of the slab shall be such that runoff water from rain or snow melt shall be dispersed as locally (continuous along the length) as possible. Simple shallow center peaking can accomplish this.

In addition, the top surface shall provide proper bearing surfaces for the rail fasteners which will be spaced at 30-inch intervals along the length of the slab. Although future rail fastener designs and construction techniques may include provision for the 1:40 conventional inward rail cant in the fastener itself, and for inclusion of attachment inserts or studs anchored solidly into the slab reinforcement as an integral part of the slab, deference to conventional practice and rail fastener design requires that an inward cant of 1:40 be cast into the rail fastener bearing areas of the slabs. (Note that the slopes of the bearing areas will be opposed to that required generally for drainage.)

Each fastener bearing surface shall incorporate two (or more) female inserts, the tops of which will be flush with the bearing seat and which will be anchored in the concrete by means of projections integral with the insert. It is not expected that an effort will be made to attach these fasteners to the

reinforcing steel (other than for positioning during installation).

4.1.3 <u>Fastener Inserts</u>. The precise configuration of the rail fastener is not known at this time. It will be identified prior to completion of final structural design. This much may be reasonably assumed: that in all cases the fasteners will present a continuously flat base plate to the concrete bearing area and that in no case is this plate likely to be less than 5 inches by 9 inches. There will be a fairly stiff elastomeric material between the base of the fastener and the concrete. Rail gage to be standard 56.5 inches.

Two inserts, into which fastener hold down bolts can be threaded, are required. These inserts will occur, one on each side of the running rail, at a nominal spacing of between 9 inches and 15.5 inches apart--either diagonally placed or opposed.

It is hoped that design work can proceed during the interval in which the process of fastener selection is underway and that the requisite descriptive information can be provided early enough to avoid compromise of steady work progress.

The design and accurate placement of the fastener attachment hardware incorporated into the slab is considered to be the most demanding aspect of the cast-in-place slab construction. The following methods of obtaining the required end result--that is, two inserts descending vertically from the top surface of the slab at each rail fastener location, are envisioned as possibilities:

(a) Locate female inserts accurately prior to casting the slab, such that after casting the tops of the inserts are flush with the

slab surface and the surface around the inserts is smooth and flat, providing a satisfactory bearing area for the rail fastener base plate.

(b) Locate inserts accurately above the surface just after casting the slab, and vibrate or otherwise insert these members into the slab while still maintaining a smooth and flat surface around them providing a satisfactory bearing area for the rail fastener base plate.

(c) Drill holes into the slab surface after it has partially hardened, and press inserts into the holes such that projecting studs can then be installed.

These or other methods of construction are all acceptable, provided that the final insert assembly is positioned accurately and meets the strength requirement as determined from the fastener identification study.

Although the relatively short lengths of test track which will be constructed may result in hand-forming of slabs and hand placement of inserts, preference will be given to designs in which the placement of fastener attachment hardware is adaptable for use with more mechanized construction techniques, particularly slip-form paving.

4.1.4 Steel Reinforcement. Longitudinal steel reinforcing bars shall be used near the top and bottom of the slab to aid in obtaining the required bending stiffness and to retard cracking. This reinforcement shall be at least 0.55 percent of the slab cross-sectional area.

4.1.4a   Positioning of Reinforcing Steel. The rein-
forcement rods near the top surface may be
arranged so that the majority of the rein-
forcement lies in two bands lying beneath the
rails (and rail fasteners), these bands being
approximately 1-1/2 feet wide and 5 feet apart
on centerlines. A similar arrangement of the
reinforcement rods near the bottom surface can
be used, but is not necessary. It may be
desirable to locate longitudinal rods at the
top such that the two rows of fastener inserts
(one on each side of the rail) can be fastened
directly to the reinforcing rods.

Lateral reinforcing rods can be
placed near the top of the beam (and preferably
at bottom and sides, also) and shall be tied
into the longitudinal rods at intervals of 30
inches at locations corresponding to the rail
fastener locations. Other reinforcement com-
monly used to complement the longitudinal rein-
forcing rods should be used.

No reinforcement steel may be placed
closer than one inch to an outer surface of
the slab, with the exception of "chairs" or
other elements needed to locate and support
the steel during the pouring operation, or
elements specifically associated with transfer
of rail fastener loads into the slab.

4.1.5   Bottom Surface. The bottom surface of the slab will
lie directly on the layer of ballast, crusher run, or
other similar material providing drainage beneath the
slab. One of the advantages of the cast-in-place
construction technique is the good bond which can be

obtained between concrete and the supporting material, and it is important that such a bond be obtained to transfer the high vertical and shearing loads effectively into the subgrade. Construction techniques shall be designed with this in mind. To prevent the deterioration of the slab by chemical action on the steel and concrete, the amount of steel extending into the bottom surface shall be minimized.

4.2 <u>Joints</u>. In general, joints cost money initially and are a potential source of trouble throughout the life of a structure, often requiring costly maintenance. Therefore, while some joints will be required in a cast-in-place slab track structure, their number should be minimized consistent with good design practice. Unfortunately, even in relatively well established engineering fields of highway and runway design and construction, there is a wide variation in philosophy and practice regarding not only the spacing of joints, but their design as well. In general, there is agreement that the greater the amount of steel reinforcement the fewer the number of joints required, since the steel withstands tensile as well as compressive loads. Since the reinforced concrete slab track structure described in these specifications will be relatively highly reinforced to provide the required bending stiffness, it follows that the number of joints required will be a minimum. To determine what this minimum is, however, the joint spacing is to be varied in the test track section, and the tendency of the various sections to crack will be monitored throughout the test program. Based on a section 800 feet in length, the lengths of continuous slab between joints shall be 200, 50, 50, 100, and 400 feet from southwest to northeast. This last 400 foot segment to be continuously reinforced.

Joints between the longitudinal slab sections shall be of the expansion type, allowing longitudinal motions of adjacent slabs to occur with temperature changes.

However, it is desirable to provide the same stiffness at the joint as away from it in order to eliminate "soft" points in the slab. This requirement can be approached by using a shear connection in conjunction with a larger bearing area at the joint. That is, starting several feet away from the joint the slab width shall start to increase, reaching its greatest width at the joint. It is suggested that this flare in width be linear, starting 8 feet from the joint, and increasing such that the slab width is 10 feet at the joint, or is of such width as determined from design calculations to be required to maintain the constant vertical spring rate.

4.2.1 <u>Joint Clearance</u>. With the exception of the joint at the interior (southwest) end of the 400 foot slab, the joint clearance at the completion of construction shall be 0.75 inches based on a temperature of 70 F. The joint clearance between the interior end of the 400 foot slab and the adjoining 100 foot slab shall be 1.5 inches. In all cases, joint fillers shall be used to prevent infiltration of water or other foreign material into the joint.

APPENDIX H

<u>PERFORMANCE SPECIFICATIONS FOR CAST-IN-PLACE</u>
<u>REINFORCED CONCRETE TWIN-BEAM TRACK STRUCTURE</u>

APPENDIX H

PERFORMANCE SPECIFICATIONS FOR CAST-IN-PLACE REINFORCED CONCRETE TWIN-BEAM TRACK STRUCTURE

TRACK STRUCTURE SPECIFICATIONS

Cast-in-Place Twin Reinforced Concrete Beams

1.0 <u>General Description</u>. The general type of beam structure
which is anticipated will include two beams--of generally
rectangular or trapezoidal cross-section. If trapezoidal
the narrower of the two parallel surfaces shall be the top
surface of the beam. The two longitudinal beams will be
joined at intervals by lateral "gage beams". The complete
track structure actually includes four components; rail,
rail fasteners, concrete beam assembly, and the subgrade
providing continuous support beneath the beams. These
components are described briefly below.

   1.1 <u>Rail</u>. Continuously-welded C.F.&I 136-pound rail will
be used, having a moment of inertia of 94.9 in.^{4}
resisting bending due to vertical loads applied by
the wheels.

   1.2 <u>Rail Fasteners</u>. Rail fasteners will be used to
support the rail at 30-inch intervals along the length
of the beams. Each fastener will provide a vertical
static spring rate of 200,000 to 400,000 lb/inch, and
will also provide an adjustment capability of $\pm$ 1 inch
vertically and laterally of the rail relative to the
beam to compensate for misalignment and wear.

   1.3 <u>Cast-in-Place Reinforced Concrete Beams</u>. The cast-in-
place twin-beam structure will consist of two
longitudinal beams joined at 25 -foot intervals by
lateral "gage beams" to maintain lateral spacing. The
longitudinal beams shall be of trapezoidal or rectan-
gular cross-section--depending on the economics of
of construction--with each of the beams having a

bottom width of 24 inches and a depth of between 12 and 18 inches. Reinforcement in the form of continuous lontitudinal steel rods near the top and bottom surfaces of the beam will be required to provide the specified bending stiffness.

1.4 Subgrade Support. The track structure will be continuously supported by a compacted subgrade having 4 to 6 inch layer of ballast, crusher run, or other similar permeable material as its top layer, providing drainage directly beneath the beam. The modulus of subgrade reaction of the prepared roadbed shall be assumed to fall within the range of 150 to 200 $lb/in.^3$.

2.0 Design Loads.

2.1 Vertical Loads. Traffic over the experimental track structures will be that of the existing Santa Fe mainline track. This traffic is almost entirely mixed freight, having a wide variation in axle loading and spacing. However, for design purposes, locomotive axle loads of 38 tons (38,000 pounds per wheel) can be assumed, and freight car axle loadings of 35 tons (35,000 pounds per wheel) shall be considered typical. These loads are based on the static weights; dynamic wheel loads will be higher, depending on a number of factors. For design purposes, a maximum impact factor of 2.0 shall be used.

The stiffness of the rail and the use of resilient rail fasteners between the rails and supporting structure will distribute the vertical wheel loads longitudinally over several rail fasteners, so that the maximum load transmitted by an individual rail fastener normally will be no more than 60 percent of the wheel load. For example, the maximum vertical load

transmitted into the structure by an individual rail
fastener will be on the order of 40,000 pounds when
the actual wheel-rail load is 70,000 pounds.

2.2 <u>Lateral Loads</u>. The lateral wheel-rail loads are known
with much less certainty than the vertical loads, since
the generation of lateral loads is a function of
relative wheel-rail alignment on tangent track. However,
for design purposes, it can be assumed that maximum
lateral loads normally will not exceed 0.4 times the
vertical loads, but that on infrequent occasions
lateral loads equal to 0.6 times the vertical loads can
occur.

The lateral load transmitted into the
supporting structure by any individual rail fastener can
be assumed, for design purposes, to be equal to 0.9
times the lateral wheel-rail load. Maximum lateral
loads on the rail will be those caused by wheel flange
contact, and therefore will be in the direction away
from the track centerline.

2.3 <u>Load Distribution</u>. The distribution of loaded axles
along the length of the track will be a function of the
particular train consist. However, for design purposes,
typical axle spacings of 8 feet for locomotives and 6
feet for freight car trucks can be assumed.

3.0 <u>Allowable Stresses</u>. Stresses in the steel and concrete shall
be calculated for each particular beam design, using the
design information given above. These stresses must meet
the requirements of present codes covering the particular
type of construction--particularly such things as the AASHO
(American Association of State Highway Officials) specifi-
cations covering allowable Unit Stresses, ACI (American Con-
crete Institute) Specification 318, and pertinent ASTM
(American Society for Testing Materials) specifications.

4.0 Structural and Geometric Requirements

4.1 Beams.

4.1.1 Bending Stiffness.

The longitudinal bending stiffness (EI) of each longitudinal beam about the neutral axis of the beam lateral cross-section shall be at least 2000×10^7 lb-in.^{2}. In calculating this stiffness the tensile strength of the concrete shall be assumed to be zero.

4.1.2 Top Surface.

The top furfaces of the longitudinal beams will be nominally flat. The rail fasteners which hold the rail in place will be mounted directly on the two beam surfaces exactly opposite one another. Rail fastener bearing surfaces which supply an inward cant of 1:40 shall be provided. This degree of cant can be continuously cast in the top surface during construction of the beams, if desired. (To the extent that cant is present the cross-sectional configuration will be nontrapezoidal, in a strict sense.)

Each fastener bearing surface shall incorporate two (or more) female inserts, the tops of which will be flush with the bearing seat and which will be anchored in the concrete by means of projections integral with the insert. It is not expected that an effort will be made to attach these fasteners to the reinforcing steel (other than for positioning during installation).

4.1.3 <u>Fastener Inserts</u>. The precise configuration
of the rail fastener is not known at this time.
It will be identified prior to completion of
final structural design. This much may be
reasonably assumed: that in all cases the
fasteners will present a continuously flat
base plate to the concrete bearing area and
that in no case is this plate likely to be less
than 5 inches by 9 inches. There will be a
fairly stiff elastomeric material between the
base of the fastener and the concrete. Rail gage
to be standard 56.5 inches.

Two inserts, into which fastener hold
down bolts can be threaded, are required. These
inserts will occur, one on each side of the
running rail, at a nominal spacing of between
9 inches and 15.5 inches apart--either
diagonally placed or opposed.

It is hoped that design work can pro-
ceed during the interval in which the process
of fastener selection is underway and that the
requisite descriptive information can be
provided early enough to avoid compromise of
steady work progress.

The design and accurate placement of
the fastener attachment hardware incorporated
into the beams is considered to be the most
demanding aspect of the cast-in-place beam
construction. The following methods of
obtaining the required end result--that is, two
inserts descending perpendicular to the top

H-5

surface of the beam at each rail fastener
location, are envisioned as possibilities:

(a) Locate female inserts accurately
prior to casting the beams, such that
after casting the tops of the inserts
are flush with the beam surface and the
surface around the inserts is smooth
and flat, providing a satisfactory
bearing area for the rail fastener
base plate.

(b) Locate inserts accurately above the
surface just after casting the beams,
and vibrate or otherwise insert these
members into the beam while still
maintaining a smooth and flat surface
around them providing a satisfactory
bearing area for the rail fastener base
plate.

(c) Drill holes into the beam surface after
it has partially hardened, and press
inserts into the holes such that pro-
jecting studs can then be installed.

These or other methods of construction
are all acceptable, provided that the final
insert assembly is positioned accurately and
meets the strength requirement as determined
from the fastener identification study.

Although the relatively short lengths
of test track which will be constructed may
result in hand-forming of beams and hand place-
ment of inserts, preference will be given to
designs in which the placement of fastener

attachment hardware is adaptable for use with
more mechanized construction techniques,
particularly slip-form paving.

4.1.4 Steel Reinforcement. Longitudinal steel
reinforcing bars shall be used near the top and
bottom of the beams to aid in obtaining the
required bending stiffness and to retard
cracking. This reinforcement shall be at least
0.55 percent of the beam cross-sectional area.

4.1.4a Positioning of Reinforcing Steel. The rein-
forcement rods near the top surface may be
arranged so that the majority of the rein-
forcement lies in two bands lying beneath the
rails (and rail fasteners), these bands being
approximately 1-1/2 feet wide and 5 feet apart
on centerlines. A similar arrangement of the
reinforcement rods near the bottom surface can
be used, but is not necessary. It may be
desirable to locate longitudinal rods at the
top such that the two rows of fastener inserts
(one on each side of the rail) can be fastened
directly to the reinforcing rods.

Lateral reinforcing rods can be placed
near the top of the slab (and preferably at
bottom and sides, also) and shall be tied into
the longitudinal rods at intervals of 30 inches
at locations corresponding to the rail fastener
locations. Other reinforcement commonly used to
complement the longitudinal reinforcing rods
should be used.

No reinforcement steel may be placed
closer than one inch to an outer surface of the

slab, with the exception of "chairs" or
other elements needed to locate and support
the steel during the pouring operation, or
elements specifically associated with
transfer of rail fastener loads into the
slab.

4.1.5 Bottom Surface. The bottom surface of the beams
will lie directly on the layer of ballast, crusher
run, or other similar material providing drainage
beneath the slab. One of the advantages of the
cast-in-place construction technique is the good
bond which can be obtained between concrete and
the supporting material, and it is important that
such a bond be obtained to transfer the high
vertical and shearing loads effectively into the
subgrade. Construction techniques shall be
designed with this in mind. To prevent the
deterioration of the slab by chemical action on
the steel and concrete, the amount of steel
extending into the bottom surface shall be
minimized.

4.2 Joints. In general, joints cost money initially and
are a potential source of trouble throughout the life
of a structure, often requiring costly maintenance.
Therefore, while some joints will be required in a cast-
in-place beam track structure, their number should be
minimized consistent with good design practice.
Unfortunately, even in relatively well established
engineering fields of highway and runway design and
construction, there is a wide variation in philosophy
and practice regarding not only the spacing of joints,
but their design as well. In general, there is agree-
ment that the greater the amount of steel reinforcement

the fewer the number of joints required, since the steel withstands tensile as well as compressive loads. Since the reinforced concrete beam track structure described in these specifications will be relatively highly reinforced to provide the required bending stiffness, it follows that the number of joints required will be a minimum. To determine what this minimum is, however, the joint spacing is to be varied in the test track section, and the tendency of the various sections to crack will be monitored throughout the test program. Based on a section 800 feet in length, the lengths of continuous beam between joints shall be 200, 50, 50, 100, and 400 feet from southwest to northeast. This last 400 foot segment to be continuously reinforced.

Joints between the longitudinal beam sections shall be of the expansion type, allowing longitudinal motions of adjacent beams to occur with temperature changes.

However, it is desirable to provide the same stiffness at the joint as away from it in order to eliminate "soft" points in the beams. This requirement can be approached by using a shear connection in conjunction with a larger bearing area at the joint. That is, starting several feet away from the joint the beam width shall start to increase, reaching its greatest width at the joint. It is suggested that this flare in width be linear, starting 8 feet from the joint, and increasing such that the beam width is 3 feet at the joint, or is of such width as determined from design calculations to be required to maintain the constant vertical spring rate.

4.2.1 _Joint Clearance._ With the exception of the joint at the interior (wouthwest) end of the 400 foot beams, the joint clearance at the completion of construction shall be 0.75 inches based on a temperature of 70 F. The joint clearance between the interior end of the 400 foot beams and the adjoining 100 foot beams shall be 1.5 inches. In all cases, joint fillers shall be used to prevent infiltration of water or other foreign material into the joint.

4.3 _Gage Beams._ At equal intervals along the length of the longitudinal beams, lateral connectors known as "gage beams" shall be used to maintain the proper lateral distance between longitudinal beams. The suggested maximum longitudinal spacing of gage beam centerlines is 25 feet. The design of the gage beams shall be such as to provide the required tensile strength in the lateral direction, while minimizing any change in the bending stiffness in the longitudinal direction. This is to prevent the occurrence of vertical "hard spots" along the length of the track structure which could create undesirable resonance in the train-track structure under traffic.

To prevent such hard spots, the effective bearing area of the gage beams and their dimensions in the longitudinal direction of the track structure must be minimized. No portions of the bottom of the gage beams shall extend below the bottom of the longitudinal beams, and the area of the bottom surface of the gage beams shall not exceed one square foot per beam.

The preferable method of construction of the gage beams is to cast them in place simultaneously with casting of the longitudinal beams, tying the reinforcing

rods of the gage beams into that of the longitudinal
beams. If hand forming is used, this presents no
problem, but with slip forming techniques, this may be
impractical. Therefore, the gage beams can be installed
later if their attachment to the longitudinal beam is
such that an integral structure results. The gage beams
may be constructed of steel or concrete and steel.

The gage beams must withstand the vertical
and lateral loads given in Section 2.0 (Design Loads)
without developing stresses in excess of those specified
in Section 4.0 (Allowable Stresses).

A highly desirable feature of the design
would be the provision by the gage beams of restraint
of torsional moment in the rail supporting beams. The
designer should be well aware of the fact that he is
working with an experimental, train-support concept,
unlike any existing for the loads, isolated and
cumulative, and train speeds (70 mph maximum) contem-
plated during the life of this project. An outward
rolling of the rails and beams under load would be
unsatisfactory as a gradual, long-term effect and,
conceivably, catastrophic as a sudden occurrence. The
exercise of design innovation, consistent with good
practice and reasonable cost, in the approach of this
particular problem, and the whole project area included
in this definition of scope as well, is encouraged. In
making available this required torsional restraint,
the designer should bear in mind the earlier discussion
concerning "hard spots" at the gage beam locations.
Ideally, the rolling vehicle wheel will not sense the
pressure of gage beam junctions with the longitudinal
beams.

APPENDIX I

PERFORMANCE SPECIFICATIONS FOR PRECAST TWIN
REINFORCED CONCRETE BEAM TRACK STRUCTURE

PERFORMANCE SPECIFICATIONS FOR PRECAST TWIN REINFORCED CONCRETE BEAM TRACK STRUCTURE

TRACK STRUCTURE SPECIFICATIONS

Precast Twin Reinforced Concrete Beams

1.0 General Description. The precast twin reinforced concrete beam
track structure basically will consist of two longitudinal beams--
one beneath each rail--joined together at intervals by lateral
gage beams to maintain the proper gage. A prestressed method of
construction is preferred for the longitudinal beams, providing
the most efficient structure in terms of material usage and mini-
mizing weight. The complete track structure will actually consist
of four components: rail, rail fasteners, concrete beams, and the
subgrade or other continuous support beneath the beams. These
components are described briefly below.

1.1 Rail. Continuously-welded C.F.&I. 136-pound rail will be
used, having a moment of inertia of 94.9 $in.^4$ resisting
bending due to vertical loads applied by the wheels.

1.2 Rail Fasteners. Rail fasteners will be used to support the
rail at 30-inch intervals along the length of the slab.
Each fastener will provide a vertical static spring rate of
200,000 to 400,000 lb/in., and will also provide an adjust-
ment capability of ± 1 inch vertically and laterally of the
rail relative to the slab to compensate for misalignment and
wear.

1.3 <u>Precast Twin Reinforced Concrete Beams</u>. The longitudinal beams shall be basically rectangular or trapezoidal in cross-section, each having a width of 24 inches at the base, and a width between 18 and 24 inches at the top surface. The depth of the beams shall be between 12 and 18 inches. Reinforcement in the form of continuous longitudinal steel rods near the top and bottom surfaces of the slab will be required to provide the specified bending stiffness. Lateral reinforcement will be required at intervals corresponding to the rail fastener spacing to absorb the loads transmitted into the slab at the rail fastener attachment points. The beams shall be cast in lengths not to exceed 50 feet.

1.4 <u>Subgrade Support</u>. The track structure will be continuously supported by a compacted subgrade having a 4 to 6 inch layer of ballast, crusher run, or other similar permeable material as its top layer, providing drainage directly beneath the slab. The modulus of subgrade reaction shall be assumed to fall within the range of 150 to 200 lb/in.^{3}.

2.0 <u>Design Loads</u>.

2.1 <u>Vertical Loads</u>. Traffic over the experimental track structures will be that of the existing Santa Fe mainline track. This traffic is a most entirely mixed freight, having a wide variation in axle loading and spacing. However, for design purposes, locomotive axle loads of 38 tons (38,000 pounds per wheel) can be assumed, and freight car axle loadings of 35 tons (35,000 pounds per wheel) shall be considered typical. These loads are based on the static weights; dynamic wheel loads will be higher, depending on a number of factors. For design purposes, a maximum impact factor of 2.0 shall be used.

I-2

The stiffness of the rail and the use of resilient rail fasteners between the rails and supporting structure will distribute the vertical wheel loads longitudinally over several rail fasteners, so that the maximum load transmitted by an individual rail fastener normally will be no more than 60 percent of the wheel load. For example, the maximum vertical load transmitted into the structure by an individual rail fastener will be on the order of 40,000 pounds when the actual wheel-rail load is 70,000 pounds.

2.2 Lateral Loads. The lateral wheel-rail loads are known with much less certainty than the vertical loads, since the generation of lateral loads is a function of relative wheel-rail alignment on tangent track. However, for design purposes, it can be assumed that maximum lateral loads normally will not exceed 0.4 times the vertical loads, but that on infrequent occasions lateral loads equal to 0.6 times the vertical loads can occur.

The lateral load transmitted into the supporting structure by any individual rail fastener can be assumed, for design purposes, to be equal to 0.9 times the lateral wheel-rail load. Maximum lateral loads on the rail will be those caused by wheel flange contact, and therefore will be in the direction away from the track centerline.

2.3 Load Distribution. The distribution of loaded axles along the length of the track will be a function of the particular train consist. However, for design purposes, typical axle spacings of 8 feet for locomotives and 6 feet for freight car trucks can be assumed.

3.0 Allowable Stresses. Stresses in the steel and concrete shall be calculated for each particular beam design, using the design

information given above. These stresses must meet the requirements of present codes covering the particular type of construction--particularly such things as the AASHO (American Association of State Highway Officials) specifications covering allowable Unit Stresses, ACI (American Concrete Institute) Specification 318, and pertinent ASTM (American Society for Testing Materials) specifications.

4.0 <u>Structural and Geometric Requirements</u>.

4.1 <u>Longitudinal Beams</u>.

4.1.1 <u>Bending Stiffness</u>. The longitudinal bending stiffness (EI) of each of the longitudinal beams about the neutral axis of the beam lateral cross-section shall be at least 2000×10^7 lb-in.^{2}.

4.1.2 <u>Top Surface</u>. The top surface of the beams will provide the support for the rail fasteners which hold the rail in place. These fasteners will be located at 30-inch intervals along the length of the beam, and each fastener will be connected to the beam by two bolts spaced opposite or diagonally to each other at a nominal lateral spacing of 12-inches. The rails shall be canted inward at an angle of 1:40 (conventional practice), and to accommodate the fasteners a fastener bearing surface the full width of the beams shall be provided at the 30-inch longitudinal spacing. These surfaces shall be at an angle of 1:40 to provide proper rail cant, and shall have a dimension of at least 6-inches in the longitudinal dimension. Considering a longitudinal strip along the top of the beam 8-inches wide (corresponding to that area of the beam directly beneath the base of the rail as installed), within this area no portion of the top surface of the beam shall extend more than 1/2-inch above the

fastener bearing surfaces. No portion of the
remainder of the top surface of the beams shall
extend more than 1-1/2 inches above the highest
point on the fastener bearing surface. (This pro-
vision is made to allow the fasteners to be somewhat
recessed into the top of the beam to afford some
protection against damage from derailed cars.)

4.1.3 Fastener Inserts. To provide for the attachment of
the rail fasteners to the beams, female inserts shall
be located in the beams with their tops flush with the
fastener bearing furface. Two inserts will be
required for each rail fastener, with the spacing
matching that of the particular rail fastener design
(which will not be known until the specific fastener
design has been chosen). The inserts must be threaded
to accept 3/4-inch diameter threaded studs, and must
be of such design that they do not pull out of the
beams, or cause cracking, under the design loads given
in Section 2.0. (The precast method of construction
facilitates the design and placement of these inserts,
and the beam designer should exploit this fact to
provide a superior insert arrangement.)

4.1.4 Steel Reinforcement. Longitudinal steel reinforcing
bars shall be used near the top and bottom of the beams
to aid in obtaining the required bending stiffness and
to retard cracking. This reinforcement shall be at
least 0.55 percent of the beam cross-sectional area.

4.1.4a Positioning of Reinforcing Steel. The reinforcement
rods near the top surface may be arranged so that the
majority of the reinforcement lies in two bands lying
beneath the rails (and rail fasteners), these bands
being approximately 1-1/2 feet wide and 5 feet apart

on centerlines. A similar arrangement of the rein-
forcement rods near the bottom surface can be used,
but is not necessary. It may be desirable to locate
lontitudinal rods at the top such that the two rows of
fastener inserts (one on each side of the rail) can
be fastened directly to the reinforcing rods.

Lateral reinforcing rods can be placed near
the top of the slab (and preferably at bottom and
sides, also) and shall be tied into the longitudinal
rods at intervals of 30 inches at locations corres-
ponding to the rail fastener locations. Other rein-
forcement commonly used to complement the longitudinal
reinforcing rods should be used.

No reinforcement steel may be placed closer
than one inch to an outer surface of the slab, with
the exception of "chairs" or other elements needed to
locate and support the steel during the casting
operation, or elements specifically associated with
transfer of rail fastener loads into the slab.

4.1.5   <u>Bottom Surface</u>. The bottom surface of the beams shall
be ridged, corrugated, waffled, sawtoothed, or similarly
designed so as to provide resistance to longitudinal
and lateral motion of the track structure when
installed and resting on a layer of ballast, crusher
run, or other similar material providing drainage.
The lower surface should be designed accordingly, with
a course-enough pattern to insure reasonable bearing
on such materials. The depth of the "texturing" of
the bottom surfaces should not exceed 2 inches, and
the bearing area resisting longitudinal motion should
be roughly three times that resisting lateral motion,
due to the lateral restraint provided by the sides of
the beams.

4.2 Joints. Since, the maximum length of the precast sections of longitudinal beams is 50 feet, some type of joint will occur at least every fifty feet. However, it is not necessary that each of these joints be an expansion joint; it is planned that expansion joints will occur only at intervals of 100, 400, 200, 50, and 50 feet along the 800 foot length of precast beam track structure. At all other joints, then, it is preferable to join the precast beam sections together in a manner that will provide bending moment restraint. This can be done by joining reinforcing rods in adjacent beam sections together, both at the top and bottom of the beams. If this is not feasible, joints providing shear restraint should be used at all locations.

4.2.1 Joint Clearance. With the exception of the joints at both ends of the 400 foot beams, the joint clearance at the other expansion joints at the completion of construction shall be 3/4-inch, assuming a temperature of 70° F. The joint clearance at both ends of the 400-foot section shall be 1-1/2 inches. Joint fillers shall be used to prevent infiltration of water, subgrade, or other foreign material into the joint.

4.3 Gage Beams. At equal intervals along the length of the longitudinal beams, lateral connectors known as "gage beams" shall be used to maintain the proper lateral distance between longitudinal beams. The suggested maximum longitudinal spacing of gage beam centerlines is 25 feet. The design of the gage beams shall be such as to provide the required tensile strength in the lateral direction, while minimizing any change in the bending stiffness in the longitudinal direction. This is to prevent the occurrence of vertical "hard spots" along the length of the track structure which

I-7

could create undesirable resonance in the train-track structure under traffic.

To prevent such hard spots, the effective bearing area of the gage beams and their dimensions in the longitudinal direction of the track structure must be minimized. No portions of the bottom of the gage beams shall extend below the bottom of the longitudinal beams, and the area of the bottom surface of the gage beams shall not exceed one square foot per beam.

The gage beams may be constructed of steel or concrete and steel. The gage beams must withstand the vertical and lateral loads given in Section 2.0 (Design Loads) without developing stresses in excess of those specified in Section 4.0 (Allowable Stresses).

A highly desirable feature of the design would be the provision by the gage beams of restraint of torsional moment in the rail supporting beams. The designer should be well aware of the fact that he is working with an experimental, train-support concept, untried for the loads, isolated and cumulative, and train speeds (70 mph maximum) contemplated during the life of this project. An outward rolling of the rails and beams under load would be unsatisfactory as a gradual, long-term effect and, conceivably, catastrophic as a sudden occurrence. The exercise of design innovation, consistent with good practice and reasonable cost, in the approach to this particular problem, and the whole project area included in this definition of scope as well, is encouraged. In making available this required torsional restraint, the designer should bear in mind the earlier discussion concerning "hard spots" at the gage beam location. Ideally, the rolling vehicle wheel will not sense the pressure of gage beam junctions with the longitudinal beams.